The Characterisation of Foaming in Suspension Cultures of *Morinda citrifolia*.

A thesis submitted to Dublin City University

for the degree of Masters of Science

by

Winifred (Úna) Cusack, BSc

August 1998

Under the direction of

Dr P M Kieran

Head of School Professor Richard O' Kennedy

School of Biological Sciences

Dublin City University

I hereby certify that this material, which I now submit for assessment on the programme of study leading to the award of Masters of Science is entirely my own work and has not been taken from work of others, save and to the extent that such work has been citied and acknowledged within the text of my work.

Signed: Winfred (Lisa) Grace I.D. No.: 94971198

Date: 11th September 1998

TABLE OF CONTENTS

ACKNOWLEDGMENTS

I would like to express my appreciation to the following people

Dr Patricia Kieran for her continuous support and guidance throughout my postgraduate years at DCU

The Department of Chemical Engineering, UCD

Dr Graham Wilson, Department of Botany, UCD, for providing the cultures of *Morinda citrifolia*

Brian Corcoran and Ben Austen for their technical assistance and patience

The postgraduates of the Biochemical Engineering Research Group for their moral support and company, Miriam O' Shea, Donal O' Shea, Tony McCarty and Audrey McNulty

All fellow postgraduates, for their companionship and advice especially Eamon, Andrew, Maria and Vivienne

A special thanks to friends Olivia, Orla, Sinead, Daragh and Joanne for the many years of laughter and for their unlimited moral support during my time at DCU

To my parents for their love, encouragement and understanding

ABSTRACT

The characterisation of foaming in plant cell cultures was investigated using *Morinda citrifolia*, as a test organism Suspensions were cultivated in 250 ml shake flasks, over the course of 21 day batch growth cycles, and were characterised in terms of biomass concentration, conductivity, morphology, pH and metabolite production (extracellular proteins and extracellular polysaccharides (ECP)) The rheological and surface tension profiles of the cell-free broths were assessed, with a view to understanding the influence of these characteristics on foaming behaviour A bubble column, to investigate the foaming potential of cell-free broths, was designed and validated A preliminary study was performed, to monitor the ability of a silicone antifoam to suppress foaming and to investigate its influence on culture growth and productivity

Image analysis-based morphological studies showed that the distributions of chains and cells in these suspensions are log-normal A linear relationship was identified between conductivity and biomass concentration, expressed in terms of fresh weight and cell number, however, this relationship was only apparent up to the stationary phase, for dry weight measurements Metabolite production was strongly growth-associated The viscosity of the broth was found to increase with culture age and was successfully correlated with ECP production Surface tension was observed to reach a minimum during the early stages of the growth cycle and to remain relatively stable for the remainder of the growth cycle These variations were attributed to extracellular proteins

Foaminess characterisation studies in both cell-free broths and in model systems (using BSA and xanthan gum) revealed that foaminess was greatly influenced by proteins, polysaccharides and nature of the suspending fluid Foaminess in medium-based solutions was significantly greater than in comparable aqueous-based solutions The antifoam employed was compatible with this suspension culture, when cultivated in shake flasks and was effective in suppressing foam formation during foaming experiments in the bubble column

NOMENCLATURE

a	Specific interfacial area available for mass transfer
A	Area
bik	Bikerman foaminess (s)
BOD	Biological oxygen demand
BSA	Bovine serum albumin
C	Concentration of solute (mol cm^{-3})
°C	Degrees Celsius
COD	Chemical oxygen demand
DCU	Dublin City University
dim	Dimensionless foaminess (-)
DNA	Deoxyribonucleic acid
DW	Dry weight
e	Enrichment
ECP	Extracellular polysaccharides
E_f	Edwards foaminess (m^3)
FW	Fresh weight
k	Fluid consistency index ($Ns^n m^{-2}$)
K	Degrees Kelvin
k_L	Film transfer coefficient
k_La	Mass transfer coefficient
L	Length
MFRD	Mechanical rotating-disk foam-breaker
MW	Molecular weight
n	No of growth cycle replicates used to calculate the mean
n	Flow behaviour index (-)
no	Number
NAA	α-Naphthaleneacetic acid
P	Perimeter

PAGE	Polyacrylamide gel electrophoresis
PEG	Polyethylene glycol
PI	Isoelectric point
PPG	Polypropylene glycol
R	Gas constant (dyne cm K^{-1} mol^{-1})
S	Separation factor (-)
SDS	Sodium dodecyl sulphate
ST	Surface tension
T	Absolute temperature (K)
UCD	University College Dublin
V_f	Average foam volume (m^3)
V_b	Volumetric gas flowrate (m^3 s^{-1})
w	With antifoam
W	Width
w/o	Without antifoam
wt	Weight
xan	Xantham gum

Symbols

ΔC	Change in conductivity (mS cm^{-1})
ΔX	Change in cell concentration (g l^{-1})
Γ	Surfactant adsorbed (mol cm^{-2})
γ	Surface tension (dyne cm^{-1})
$\dot{\gamma}$	Shear rate (s^{-1})
μ	Fluid viscosity (N s m^{-2})
μ_a	Apparent viscosity
$\bar{\mu}$	Mean (section 4 1 4)
σ	Standard deviation
τ	Shear stress (N m^{-2})
$\sum$	Bikerman foaminess (s)

LIST OF FIGURES

LIST OF TABLES

Chapter 1

INTRODUCTION

Higher plant products and their derivatives are of great importance in the pharmaceutical, agricultural and food industries These products can be broadly separated into two categories, namely, primary and secondary metabolites Payne (1987) describes primary metabolites as those which are required for plant survival, and which generally are present in relatively large concentrations, but are frequently of a lesser commercial value, with uses for example, in the food industry Secondary metabolites are those which are produced to give the plant an advantage over the surrounding flora and are normally produced in comparatively low concentrations These typically find applications as insecticides, fragrances and drugs Twenty five percent of pharmaceutical prescription drugs are derived from plant sources (Stafford *et al* , 1986) Among those products are *Digitalis*, L-DOPA, morphine, codeine, digoxin and anticancer drugs such as vincristine, vinblastine and paclitaxel

Once a compound has been isolated from a plant and identified, it can frequently be produced by chemical synthesis techniques However, sometimes the structure of the biomolecule is complex or the chemical synthesis is too expensive and the product is extracted from whole plants, even though typically occurring at low concentrations Cultivation is a lengthy procedure which is, moreover, dependent on climatic factors Plant cell suspension culture systems present another alternative

Shikonin, a dye and anti-bacterial agent derived from *Lithospermum erythrorhizon*, is among the few plant cell metabolites currently produced on a commercial scale, via large scale plant cell fermentation processes (Curtin, 1983, Fujita, 1988) Shikonin is produced by Mitsui Petrochemicals in Japan DiCosmo and Misawa (1995) summarise the current extent of development in the production of pharmaceutical products by plant cell culture fermentation technology While Fett-Netto and DiCosmo (1996) deal specifically with the prospects for taxol However, large scale cultivation of plant cells for commercial purposes is very limited and has been hindered by a number of factors including the genetic instability of cell lines, low productivity and technical processing barriers associated with mixing, cell aggregation, foaming and adhesion of cells to the

reactor walls (Zhong *et al.*, 1992, Panda *et al.*, 1989). Moreover, large-scale fermentation is an inherently cost-intensive process, with operating costs exacerbated by the extended processing times associated with characteristically low growth rates of plant cells relative to bacterial or fungal systems.

Attempts to optimise plant cell suspension systems with regard to productivity have been directed towards both biological and processing issues (Tanaka *et al.*, 1983; Sahai and Knuth, 1985; Kim *et al.* (1991); Fukui and Tanaka, 1995). Foaming is among one of the process problems encountered in all aerated fermentation systems, *e.g.* bacterial, fungal, animal and plant cell systems. It is a common and generally undesirable phenomenon, leading to the potential process difficulties summarised in Table 1.1 (Vardar-Sukan, 1992), such as loss of medium, biomass fouling of exhaust systems and an increased risk of contamination. The development and stability of a foam is affected by physical and chemical parameters including cell line, medium composition, metabolite production, broth viscosity and surface tension as well as aeration and agitation conditions.

Table 1.1: Disadvantages of foaming in bioprocesses (Vardar-Sukan, 1992).

Physical problems	**Biological problems**
Increased effective reactor volume. Reduction in working volume. Enhanced gas holdup. Changes in air bubble size and composition. Reduction in apparent viscosity. Decreased power consumption. Decreased circulation rate. Changed pattern of dissolved gases due to heterogeneous dispersion. Lower heat and mass transfer rates. Invalid process data due to interference with electrodes. Incorrect monitoring and control.	Deposition of cells on upper part of bioreactor. Loss of culture fluid from exit lines causing product and bio-catalyst loss. Microbial lysis. Changes in microbial metabolism due to nutrient limitations. Froth floatation and foam separation causing preferential removal of surface active agents. Protein denaturation in the foam layer. Problems in sterile operation. Risk of environmental contamination.

In plant cell suspension cultures, foaming can be particularly severe, resulting in cellular depositions on internal vessel surfaces It can ultimately lead to the formation of crusts or "meringues" (Scragg, 1994) Although the specific oxygen requirements of plant cells are significantly lower than those of microbial systems, aeration and agitation rates can seldom be reduced accordingly, due to the characteristically high broth viscosity, which is primarily attributed to suspension morphology and extracellular polysaccharide secretion In bioreactors, the suppression of foam is normally achieved either via mechanical or chemical methods The former are generally considered to be unfavourable as, apart from the additional associated power requirements, these devices generate high shear rates, which could prove detrimental to shear sensitive plant cells Antifoam addition is more commonly employed However, antifoams are known to reduce gas-liquid mass transfer coefficients which, in turn, affect culture productivity

As one of the many process problems encountered in plant cell suspension systems, foaming has been chosen as the area of analysis for this work The literature survey reviews the factors influencing foaming and the mechanisms frequently employed for foam control in biological systems *Morinda citrifolia* is the cell line used for experimental analysis of foaming This cell line was selected because its properties are well characterised and reliably documented (Gallagher, 1987, Kieran *et al*, 1993, O'Donnell, 1992) and it has proven to be a reproducible, stable system over many years of batch cultivation In suspension cultures, which are maintained on a 21-day growth cycle, the cells form non-aggregating unbranched chains The secondary metabolite, anthraquinone, produced by *Morinda citrifolia*, has modest pharmaceutical potential (Suzuki and Matsumoto, 1988) However, using this stable cell line, foaming potential characterisation data can be generated, which may assist in the understanding of foaming in other plant cell systems of greater commercial value

The culture is characterised in terms of growth, pH, morphology, metabolite production (polysaccharide and protein), viscosity and surface tension Emphasis is focused on the impact of extracellular polysaccharide and protein on the foaming potential of cell-free broths These are the primary metabolites affecting broth viscosity and surface tension, which, in turn, greatly influence bubble film elasticity Model studies, using commercial protein (BSA) and a polysaccharide (xanthan gum) were performed to elucidate the influence of these individual constituents on the foaming behaviour of aqueous and medium-based solutions

Chapter 2

LITERATURE REVIEW

2 1 FOAM FORMATION AND STABILITY

Foam formation in biological systems is a complex process which is basically induced by the introduction of gases into the system In an aerated bioreactor the degree of foaming encountered when gas is introduced to the broth depends on both the biological characteristics of the system and the physical operating parameters Some of the important influential factors in foam formation are described and explained in this review

One of the most important influences on the characteristics of foaming in biological systems is the intensity of aeration and agitation conditions and the physical means by which both processes are achieved In stirred tank submerged fermentations, aeration and agitation are required since aeration control and three-phase dispersion are critical to support homogenous growth While bubble-free aeration (*e g* via surface aeration or oxygen diffusion through porous tubes) of stirred tank vessels, if correctly implemented, would minimise foaming in an agitated system, such approaches to aeration are suitable only for laboratory or pilot scale cultivation of organisms with low specific oxygen requirements In airlift bioreactors, although mechanical agitation is eliminated, aeration must be sufficient to support both growth and broth circulation throughout all parts of the system Therefore, in biological process, air introduction into the system frequently cannot be avoided and, depending on the broth characteristics, foam formation is a strong possibility Unless foam generation is understood and controlled, foaming can present significant problems for process control

A bubble consists of a gas surrounded by a liquid film A foam is formed in an aerated liquid when the rate of bubble formation at the liquid surface exceeds the rate of bubble break-up The problematic potential of a foam lies in its stability, which is largely dependent on medium components, which directly influence the physiological characteristics of the fluid, and by the physical process parameters such as methods of

aeration and agitation Some or all of the liquid film drains from between bubbles in a foam and if a thin film (called a lamella) remains, a stable foam is formed Otherwise the bubbles burst, causing foam collapse A continuous foaming solution will reach a stable, equilibrium foam height when the rate of bubble formation equals the rate of bubble collapse The phenomenon of fluid drainage from a foam and the mechanisms involved have been comprehensively examined by many authors, including Bikerman (1973) and Prins and van't Riet (1987)

However, the classification of foams, with respect to stability, is not well defined and individual researchers adopted different approaches to this topic, often basing their definitions on studies of particular fluid types Hall *et al* (1973) refer to an unstable foam as one which normally occurs in dilute solutions of short chain, aliphatic alcohol soluble solutions The thin film separating the bubbles drains rapidly Metastable foams, however, are typically formed in the presence of surfactants, such as soaps, detergents and proteins In this instance, a thin walled lamellae remains between the bubbles following liquid drainage Kitchener and Cooper (1959) classified foams according to lifetime A foam with a life span of less than twenty seconds was said to be unstable, all other foams were classified as metastable Despite different definitions of the degree of stability, it is clear that stability of a foam depends on its ability to resist the localised thinning of the lamellae Bubble size, surface tension and viscosity are three very important parameters in foam stability In fermentation systems, these factors are, in turn, dependent on aeration and agitation regimes, medium composition and extracellular secretions, solution pH, electrolyte composition and operating temperature (Viesteurs *et al* , 1982, Hall *et al* , 1973) Moreover, many of these parameters are inter-dependent and for instance, the medium composition significantly determines the electrolyte profile, while extracellular secretions, typically varying over the course of a batch cycle, may influence pH

2 1 1 Bubble Size

Small bubbles tend to pack very closely together, forming a close, well-established foam which is difficult to disrupt, while larger bubbles form a loose foam which bursts more effectively and is, thus, easier to control The type of sparger employed, its pore size and the rate of aeration can, therefore, greatly influence the type and extent of foam

formation However, Bikerman (1973) explains that, in general, pore/orifice size alone does not specify bubble size If pores are very close, as is the case with sintered spargers, bubbles can coalesce before release into the column fluid, fluid properties will also influence the bubble size prevailing at the liquid-foam interface Agitation methods and rates can contribute to bubble break-up, resulting in very small bubbles, which enhance the stability of the foam

2 1 2 Surface Tension, Viscosity and Film Elasticity

A knowledge of the influence of surface effects on foam formation and stability is necessary to understand the mechanisms by which foams are stabilised by some surfactants (*e g* proteins) and disrupted by others, such as antifoams A stable foam cannot be generated in a true solution, the bubbles emerging at the liquid surface will collapse immediately, as the surface effects are not sufficiently strong enough to maintain a liquid film between the bubbles Hall *et al* (1973) explain that the characteristics of this film are influenced by surface tension, bulk and surface viscosities and intermolecular forces In general, a reduction in surface tension below that of water (approximately 72mN m^{-1}, at 25°C) typically indicates the presence of surfactants which stabilise the lamellae Hall *et al* (1973) describe the relationship between surface tension, γ and surfactant concentration

$$\Gamma = \frac{d\gamma}{2RTd\ln C} \qquad (2\ 1)$$

where

Γ = surfactant adsorbed (mol cm^{-2})

R = gas constant (dyne cm K^{-1} mol^{-1})

T = absolute temperature (°K)

γ = surface tension (dyne cm^{-1})

C = concentration of solute (mol cm^{-3})

This relationship is illustrated in Figure 2 1

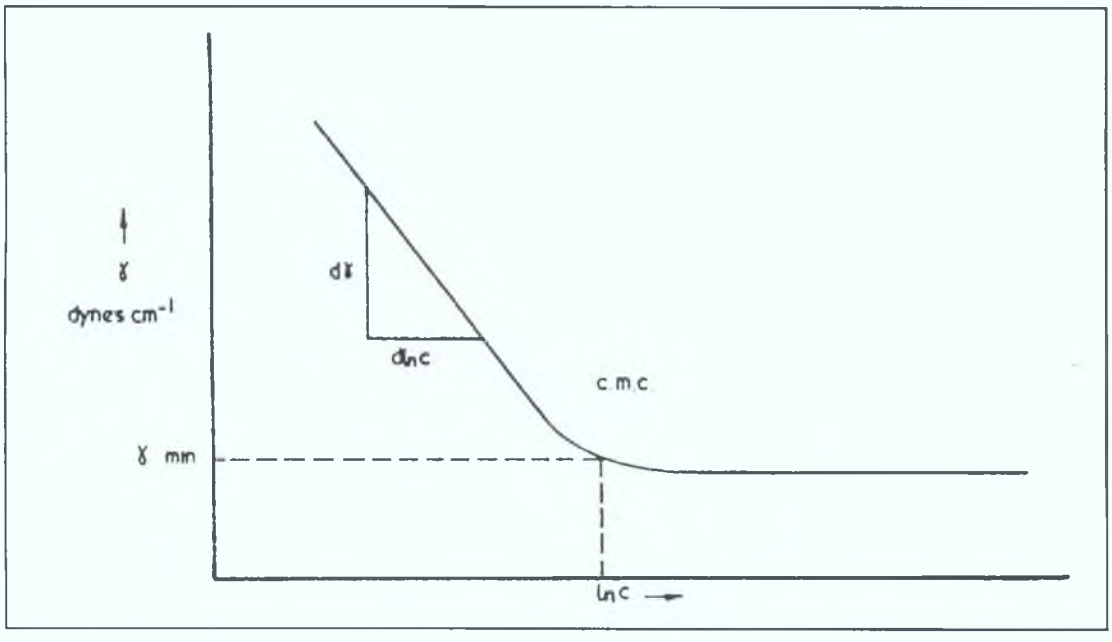

Figure 2.1: Relationship between surface tension and protein concentration (Hall *et al.*, 1973).

The levelling-off point of the plot corresponds to the saturation coverage of all interfaces with surfactant. Above this critical concentration (CMC point), the surfactant molecules form micelles and there is no further change in surface tension. This surface tension-surfactant concentration effect has been studied in model protein systems (Kalischewski *et al.*, 1979; Lalchev *et al.*, 1982;Varley *et al.*, 1996), confirming the proposal of Hall *et al.* (1973). The surface tension has been found to decrease rapidly as protein concentration increases; after a critical protein concentration is reached, there is no further significant change in surface tension, with increasing protein concentration. Typical fermentation broths have minimal surface tensions of 40 - 50 mN m^{-1}, due to the presence of natural surfactants such as proteins, peptides and fatty acids in the suspending fluid (Hall *et al.*, 1973).

Hall *et al.* (1973) explain that the difference between stable and unstable foams depends on the film elasticity of the foam. This is the term given to the ability of the film to resist any applied stress, which causes localised thinning of the lamellae and this characteristic is essential for maintenance of a stable structure. When a liquid film is stretched (due to an applied shear stress) the local concentration of surfactant molecules is decreased, as they space themselves out along the thinned region. This causes a local

increase in surface tension The imbalance of forces causes the surfactant molecules in the surrounding area to move towards this region to equalise surface tensions The resultant drag force causes an influx of liquid, hence counteracting the thinning action This is referred to as the 'self-heal' effect or Gibbs-Marangoni elasticity (Hall *et al*, 1973, Bikerman, 1973, Vardar-Sukan, 1992) The degree of elasticity is dependent on the type of surfactant present If the equilibrium surface tension is restored by the adsorption of more surfactant from the bulk solution, before the surface migration can occur, the 'self-heal' effect will not occur and film rupture is inevitable, (Hall *et al*, 1973, Vardar-Sukan, 1992)

Foam stability is also influenced by high bulk and surface viscosities Hall *et al* (1973) define surface viscosity as a two dimensional analogue of bulk viscosity A viscosity effect is attributable to interactions between adjacent molecules in a solution (*e g* hydrogen bonds) This viscosity influences foam formation and stability firstly, by decreasing the bubble coalescence rate m the bulk solution, causing bubbles to remain small and secondly, retarding the rate of fluid drainage from a foam, thereby maintaining the lamellae Vardar-Sukan (1992) explains that natural surfactants such as proteins have large surface viscosities, which display essentially 'plastic' rheological behaviour and therefore, have the ability to resist shear stress up to a certain yield value Bulk viscosity effects are extremely important in biological broths which are frequently of a relatively high viscosity due to the production of extracellular metabolites

Model studies, using substances to increase the bulk viscosity of a proteinaceous solution to determine the effect on foaming, have been performed by Mita *et al* (1977) and Bumbullis *et al* (1981) The latter found that the surface rheology of polymer and protein solutions can exhibit highly viscoelastic properties, while the bulk rheology was essentially Newtonian Mita *et al* (1977) used sucrose to increase the bulk viscosity of a gluten solution and found that as the viscosity was increased, the lifetime of the fluid in the foam also increased, resulting in enhanced foam stability

2 1 3 Medium Composition and Extracellular Secretions

The physiological characteristics of a fluid and hence, the foaming potential, are attributable to the presence of different substances in the fluid Therefore, in fermentation systems, substances present in the broth, either due to medium formulation or secretions by the cell line, may be of the utmost importance for foam formation and stability Particular organisms will produce different products which are released into the medium during cultivation, *e g* proteins, polysaccharides, alcohols and lipids The presence of these components can alter the surface tension and viscosity of the solution and cause changes in bubble coalescence, and liquid drainage properties, which further enhance the foaming potential of the fermentation broth For example, low alcohol concentrations, of approximately 1-2%, are known to promote foaming, (Vardar-Sukan, 1992) Proteins adsorb at the gas-liquid interface and enhance the stability of a foam while lipids are natural antifoams which tend to suppress foaming Mita *et al* (1977) illustrated this effect by adding fats to a gluten solution, which yielded a more labile foam Philips *et al* (1973) reported that the presence of a lipid monolayer inhibited the adsorption of the protein, casein, and the inhibitory effect of lipids on foams is explained further in Section 2 3 2

If, in a fermentation process, an extracellular protein is the desired product, then its concentration in the broth will ideally be high However, elevated protein levels will exacerbate foaming problems by enhancing stability It is also important to note that substantial amounts of protein may be present due to extracellular enzymes, cell lytic products and medium components According to Prins *et al* (1987), protein concentrations of 1 mg l^{-1} are sufficient to cause foam formation As this level of protein is found in almost all fermentation systems, it is evident that the majority of biological fermentations have the potential to foam

Proteins act to stabilise the foam, by extending their hydrophilic tails into the liquid layer while the hydrophobic entity forms a serious of foldings or a "train", at the interface The degree of stabilisation is not affected solely by the protein concentration but also by the mode of adsorption It is often difficult to desorb proteins once adsorbed as they are flexible and can alter their conformation when adsorbed and the stabilisation effect will depend on the type of protein present Many model studies have been performed to demonstrate the effect of protein concentration on foams (*e g*

Kalischewski *et al*, 1979, Wolfes and Schugerl, 1983) and foaming in real biological systems is frequently solely attributed to surfactant effects of protein constituents in the broth (*e g* Konig *et al*, 1979) However, Noble *et al* (1994) suggest that other biochemical factors could be linked to foaming since, in addition to proteins, carbohydrates, α-keto acids and other lipophilic biosurfactants (*e g* extracellular pigments) were also found to be concentrated in foam Szarka and Magyar (1969) investigated the effects of different plant extracts, as protein sources in fermentation media, in terms of surface tension, viscosity and foam stability Soya bean meal, corn steep liquor and peanut meal were used A surface tension value of 45 mN m^{-1} was observed for the soya bean supplemented medium Maximum foam stability occurred at a supplemented concentration of 4-5% and the addition of carbohydrates, such as glucose, exacerbated foam stability, as a result of increased viscosity It was suggested that foaming might be minimised by using combinations of supplements

As outlined in Section 2 1 2, viscosity has a significant role to play in foaming, and thus any substance contributing to this physiological parameter must also be considered In plant cell systems and activated sludge reactors, for example, extracellular polysaccharides (ECP) are known to pose particular problems for foam control since high levels of these macromolecules, which affect both viscosity and surface tension, can be secreted, (Kerley and Forster, 1995)

Apart from naturally occurring surfactants in fermentations, actual media constituents (*e g* salts) can also enhance foaming, by altering the physiological characteristics of the fluid The effect of ionic strength alterations (salt effects) on foaming and fluid properties has been well documented for model systems, as illustrated by the work of Mita *et al* (1977), Kalischewski *et al* (1979), Bumbullis and Schugerl (1981), Kotsaridu *et al* (1983), Wolfes and Schugerl (1983) and Ohkawa *et al* (1984c) Kalischewski *et al* (1979) showed that the minimum surface tension of a protein solution (BSA) in a citrate buffer was less than that of a water-based solution An interesting aspect of this study is that the addition of sodium chloride to the citrate buffer based solution caused a reduction in the surface tension, while the same addition to the water-based solution caused the surface tension to rise slightly This latter effect was attributed to the precipitation of protein from the solution, resulting in a lower dissolved BSA concentration However, for the BSA-water solution, foam formation

was greater when salt was added Mita and co-workers (1977) found that the addition of sodium chloride increased the stability of a gluten foam It was thought that the interfacial tension gradually reached the value prevailing at the isoelectric point, as the concentration of sodium chloride was increased Kotsaridu *et al* (1983) also found that foaminess increased with salt concentration and that the addition of sulphate ions (sodium sulphate) to the solution had a grater influence on foaming than chloride ions (sodium chloride), since the former has a greater ability to alter the ionic strength of a solution Studies by Wolfes and Schugerl (1983) also confirmed that salt addition alters the surface properties and foaming potential of protein solutions As salt concentration increased, the foaminess was observed to increase and surface tension decreased, as expected Only slight corresponding increases in surface viscosity values were observed

2 1 4 pH

The pH of a solution also has an important influence on foam stability (Cumper, 1953, Szarka and Magyar, 1969, Kotsaridu *et al* , 1983) Protein solutions display maximum foam stability at the isoelectric point (PI) It is at this point that proteins are least soluble and they loose their electric charge, forming a more compact conformation, simultaneously the rate of adsorption of surfactant molecules, at the liquid interface reaches a maximum (Mita *et al* , 1977) The isoelectric point of BSA is approximately 4 6 and this pH is exploited when foam formation with BSA is required (Varley *et al* , 1996) However, Kotsaridu *et al* (1983) illustrate that the effect of pH on foaming is quite a complex issue for BSA and severe structural conformation of the protein occurs with pH variation These workers found that the behaviour of BSA varied for buffered and non-buffered solutions, maintained at similar pH values In aqueous solutions, minimum and maximum foammess values were obained at pH values of 3 and 4, respectively, while in buffered solutions (citrate), maximum foaming potential was observed at a pH of 4 7 Szarka and Magyar (1969) found that foam stability was significantly elevated under acidic conditions for nutrient media containing protein supplements Mita *et al* (1977) also demonstrated the effect of pH on the lifetime of a foam At a pH of 7 5 (isoelectric point of gluten), the stability of the foam was at a maximum while the surface tension of the gluten solution had reached its minimum value The variation in surface tension of the gluten solution suggested the feasibility of using pH to manipulate the adsorption properties of a protein Proteins undergo

conformational changes with variations in pH and it is the conformational structure which determines how effectively the protein can adsorb at a liquid interface.

Obviously, the operating pH range for a particular fermentation will be largely specified by the cell type and thus if the fermentation pH falls in the proximity of the isoelectric point of the protein(s) present, foaming could be at its most problematic level.

2.1.5 Temperature

Foaming is generally reduced by an increase in bulk solution temperature. Boyd *et al.*, (1973) and Mac Ritchie *et al.*, (1973) suggest that the reduction in foam stability is attributable to temperature-related variations in both the surface and bulk viscosities of the fluid. The properties are generally assumed to decrease exponentially with increasing temperature, resulting in increased film drainage rates. Other temperature-related possibilities suggested include the evaporation of volatile components, which otherwise would contribute to foaming, or the deterioration of heat labile molecules, (Prins *et al.*, 1987). In biological systems, the range of applicable operating temperatures for a given fermentation is extremely limited and, under typical cultivation conditions, many of these effects can be neglected.

2.1.6 Sterilisation

The effect of sterilisation on the foaming potential of fermentation media has been studied by Szarka and Magyar (1969). High temperatures during sterilisation cause proteinaceous material to become hydrolysed and degraded (conformationally altered) and subsequently foam stability is found to increase, with increased exposure to high temperature conditions, *i.e.* sterilisation time. Although foam stability increased, the viscosity and surface tension of the media were unchanged during these studies, suggesting more complex and subtle effects. However, it is evident that sterilisation conditions are also critical in understanding foaming in fermentation systems. Susceptibility of a particular medium to these effects might warrant the introduction of alternative sterilisation regimes, involving shorter high-temperature exposure times or low temperature protocols (*e.g.* filtration) for solutions of the relevant components.

2 2 FOAM MEASUREMENT

In order to measure the foaming potential of a liquid, a method of analysis must be chosen Bikerman (1938 and 1973) and Cumper (1953) outline many different techniques employed Cumper (1953) summarises these techniques into four different categories, as follows

- Dynamic method this involves bubbling air into a solution and measuring some aspect of the foam generated, *e g* foam formation rate, stable foam height
- Static method measuring the rate at which liquid drains from a foam *e g* foam collapse time
- Single bubble method measuring the life-time of single bubbles introduced into a solution
- Size distribution method measurement of the change in surface area of the foam with respect to time

The dynamic and static methods are the most commonly used In this study, the dynamic method was employed, since it is of direct relevance to subsequent practical work and it is, indeed, favoured by the majority of workers

Throughout a large body of the work directed at characterisation of foaming under different operating conditions, a bubble column type apparatus is generally used Gas is introduced into a solution, through a sparging device, situated at the bottom of a long glass column The rate of foam formation has been used by some authors to characterise foaming potential For instance, Zhang *et al* (1992) defined foaminess in terms of the volume of foam collected in an overflow, per unit time More frequently, the stable height to which the foam rises is employed (*e g* Lee *et al* , 1993, Pandit, 1994)

A variety of methods have been developed to analyse foaming data One of the more frequently used is based on the concept of the fluid "foaminess", Σ, which has dimensions of time (s)

$$\text{Dimensionless foam volume} = \frac{\text{Volume of foam}(m^3)}{\text{Volume of liquid before foaming}(m^3)} \qquad (2.4)$$

This dimensionless foam volume proved to be suitable for relating the foaminess of plant cell fermentation broths to process parameters, including aeration rate, pH, cell biomass concentration and culture age. Using this method, the dimensionless foam volume should be independent of the sample volume used for foaming.

Noble *et al.* (1994) used a dimensionless index to quantify foaming in an aerated agitated vessel for fungal fermentations. The index values ranged between 0 and 5 and were based on the fractional vessel head-space occupied by the foam.

Using these foaminess factors, the effects of such parameters as gas flow rate, solute (surfactant) concentrations, temperature, pH can be observed. There is no single correct way to measure foaming in solutions and the choice of method is based on suitability for a particular application. However, this variety of methods makes it very difficult to directly compare data from different studies. The Bikerman foaminess factor, Σ, (equation 2.2) is most commonly used.

Comparison of experimental data for different studies is further complicated by very significant variations in the design of bubbling apparatus employed. Bikerman (1938 and 1973) suggests that foaminess, Σ, should be independent of sinter pore size and bubble column dimensions. Edwards *et al.*, (1982) reported sinter porosity is important for bubble column design purposes and subsequent bubble size formation. Therefore, comparison of data generated using different sparging devices must be undertaken with caution. Another influencing variant is the gas employed for foaming. For instance, in studies performed using aerobic systems, air or oxygen enriched air is used to support culture growth (*e.g.* Smart and Fowler, 1981; Blackall and Marshall, 1989). In wine production, foaming is typically associated with carbon dioxide evolution. However, for model foaming systems, either compressed air, carbon dioxide or nitrogen gas can be used. Carbon dioxide is seldom employed for model studies in order to avoid pH changes in the foaming solution. Nitrogen is often used since it increases foam stability by yielding smaller bubbles at the liquid-foam interface and thus foaminess is enhanced (*e.g.* Bumbullis and Schugerl, 1981; Molan *et al.*, 1982; Wolfes and Schugerl, 1983;

Kotsaridu *et al*, 1983, Ramani *et al*, 1993) The advantage of using air as a foaming gas is that it most closely mimics conditions encountered in typical aerobic fermentation environments

Thus quantitative comparison of data is only meaningful if all trials have been performed using a single apparatus design and foaming gas and if the same index of foaminess is employed for data analysis Qualitative comparison of profiles obtained from different studies can be undertaken albeit with caution

2 3 PROCESS CONSIDERATIONS AND FOAM CONTROL

Foam formation and stability are linked to a combination of process parameters and broth characteristics Thus, although the impact of a number of individual factors (*e g* viscosity, bubble size) have been largely elucidated, a solution to the problem of foaming is often a complex matter, which cannot be allowed to impinge on fundamental process requirements

2 3 1 Aeration, Agitation and Mass Transfer

In aerobic biological systems, oxygen must be supplied in sufficient quantities to satisfy cellular requirements throughout the fermentation In stirred tank reactors, air is typically introduced through a sparger at the vessel base and mechanical agitation is employed to disperse the gas phase In an airlift reactor, compressed air supplied at the base of the reactor riser fulfils both aeration and fluid circulation needs Ensuring a constant and sufficient supply of oxygen to all cells depends not only on the quantity of air introduced or the way in which it is provided, but on the availability of this gas to the cells Thus, availability is typically characterised in terms of a mass transfer coefficient, k_La, which is a measure of the rate of mass oxygen transfer from the gas to the liquid phase in a given system Use of k_La as a characteristic index of oxygen transfer efficiency implies that oxygen transfer from the gas phase to the liquid phase is the rate limiting step in the oxygen transfer process from the gas phase to the cell And, in general, this is the case However, where substances present in the medium are known to affect cell permeability to gaseous species, then k_La may not be representative of the system dynamics

Considering k_La in terms of k_L, the film transfer coefficient and a, the specific interfacial area available for mass transfer, it is obvious that higher values of a, corresponding to smaller bubbles enhance mass transfer Gas transfer rates are also dependent on the mobility of the bubble surface which affects the rate at which new liquid is brought into contact with the bubble and which also influences the k_L entity A change in either k_L or a will alter the rate of mass transfer The presence of surfactants in a solution can have conflicting effects on k_L and a For instance, proteins typically cause the gas/liquid interface to become more rigid, thus preventing bubble coalescence and maintaining small bubbles, while the resulting rigid interface would generally result in a reduction in k_L

There are numerous studies on the effects of surfactants on mass transfer in fermentation systems, some of which are discussed in section 2 4 For smaller bubbles (1-2 mm) the surfactant-associated reduction in k_L is significant However, in fermentations broths, bubbles are generally larger than 3 mm in diameter and it is thought that while part of the bottom of the bubble may be affected by the protein, most of the surface will remain relatively mobile Therefore, the overall effect of surfactants is to decrease bubble coalescence and hence, increase a (Prins and Van't Riet, 1987, Van't Riet and Van Sonsbeck, 1992) However, the net effect on mass transfer rates is determined by the relative magnitudes of the opposing trends

As concerns foaming, small bubbles, which favour mass transfer, also form more stable foams Thus, a compromise must be reached in an operation between acceptable foam height and mass transfer rates One way in which this can be achieved is by varying the surface properties of the liquid through the addition of antifoams

2 3 2 Antifoams

Antifoam is the general term given to a large variety of chemicals and natural substances known to reduce foaming in bioreactors Typically they are surface active compounds which enhance bubble coalescence They are composed of oils, fatty acids, esters, polyglycols and siloxanes (Prins and Van't Riet, 1987) and the choice of an antifoam depends on specific system requirements The desirable characteristics of an antifoaming agent are summarised in Table 2 1 (Vardar-Sukan, 1992)

Table 2 1 Desired characteristics of antifoams (adapted from Vardar-Sukan, 1992)

Fast foam breaking	Effectiveness at low concentration
Long lasting action	Stability during sterilisation
Nonexplosive	Insoluble in foaming media
Nonvolatile	No chemical reaction with finished product
Noncorrosive	No colour or odour imparted to the product
Low cost	Inability to reduce oxygen transfer rates
Negligible flammability	Ability to destroy surface elasticity and surface
Non-toxic to humans, microbes, animals *etc*	viscosity
Low BOD and COD values	Nonresistant to biooxidation or biodegradation
Resistant to metabolism by microbial species	High film incorporation and spreading
Inability to form corrosive products during	coefficients
sterilisation and fermentation	Low intra-molecular cohesive forces
Low surface tension	Presence of some hydrophobic character
Low interfacial tension	

Some ambiguity arises in the literature when the term 'antifoam' is also used to describe a defoaming agent A defoaming agent is a substance used to destroy a foam once formed, while technically, an antifoam is used to inhibit the initiation of foam formation The latter are more suitable for long term processes, while defoamers may be an attractive alternative for foam control in short fermentations For instance, di-ethyl ether is effective as a defoaming agent, but not as an antifoam, as it is volatile and is stripped from solution by aeration (Kitchner and Cooper, 1959)

The fact that surfactants such as proteins can enhance foaming and others such as antifoams have contrasting effects may appear a little confusing It is the nature of the interaction between an individual surface active agent and the gas-liquid interface which determines the outcome Various mechanisms for the action of different antifoams have been suggested Van't Riet *et al* (1984) and Prins and Van't Riet (1987) present a simple mechanism by which oil antifoams operate Figure 2 2 The oil droplets in the film migrate to the surface where a spreading effect is activated, leading to localised thinning of the lamellae and eventual film collapse The size of the oil droplet is important As it must be incorporated into a particular film, it must be small enough to enter the film but large enough to ensure sufficient surface movement to collapse the film Experiments performed by Van't Riet *et al* (1984) illustrate that a 1 μm droplet of

soy oil has the ability to collapse foam, while a 0 1 μm droplet had no effect Another mechanism proposed by Vardar-Sukan (1992) involved the displacement of adsorbed protein on the film surface by a low molecular weight surfactant, thus inactivating the stabilising effect of the protein on foaming Alternatively, the antifoam can spread along the surface of the film, causing liquid to be squeezed out and hence, thinning the film, which leads to collapse A more comprehensive review of available models is presented by Varder-Sukan (1992)

Lee *et al* (1993) performed studies on the effects and operating mechanisms of different antifoams, namely an aliphatic alcohol (n-octanol) polypropylene glycol (PPG) and a silicone emulsion It was suggested that n-octanol acted by "interfacial coalescence", whereby one bubble bursting triggers bursting in a neighbouring bubble at the top of the foam An alternate mechanism of "interbubble coalescence" was suggested for silicone-based antifoam In this case, the mean bubble size increased as the bubbles moved upwards through the foam Figure 2 3 illustrates the difference in foam structure produced by the two antifoams (Lee *et al* , 1993) The time required for foam control to occur can vary depending on the relevant mode of action Lee *et al* (1993) found that the silicone antifoam caused instantaneous "knockdown" of foam, depending on the droplet size, using PPG there was a lag time before foam rupture, while drainage occurred Vardar-Sukan (1991) used natural antifoams (oils) to determine the optimum concentrations for foam control and foam suppression It was concluded that the effective concentration required for optimum foam suppression, differed from that for foam control

It is important to consider the overall effects of an antifoam or defoamer on a particular process Foam collapse may be achieved at the expense of negative variations in growth characteristics, due to changes in gas transfer rates (Noble *et al* , 1994) The effects of antifoams on mass transfer have been well documented and the general consensus is that the addition of such compounds has a negative influence on mass transfer rates Kawase and Moo-Young (1990) give a concise description of some relevant experimental work on these effects in both stirred tank and bubble column reactors, using a Dow corning 1520 silicone antifoam Various mechanisms are suggested for the observed reduction in mass transfer coefficients Yagi and Yoshida (1974) completed broadly similar studies, relating oxygen transfer in tower fermenters to surfactant (Tween 85) and antifoam

addition (Dow corning antifoam emulsion), the negative influence of these additives on mass transfer was confirmed More recently, Liu *et al* (1994) showed that low concentrations of natural antifoams, such as lard, olive and castor oils, resulted in the expected reduction on k_La Surprisingly however, at concentrations of 0 25% (v/v) and above, a positive influence was observed

More specific applications of antifoams in biological processes are discussed in Section 2 4 However, from the technical data collected from model systems it is obvious that speculation of the type, concentration and mode of addition of antifoam chosen for a application is a complex procedure

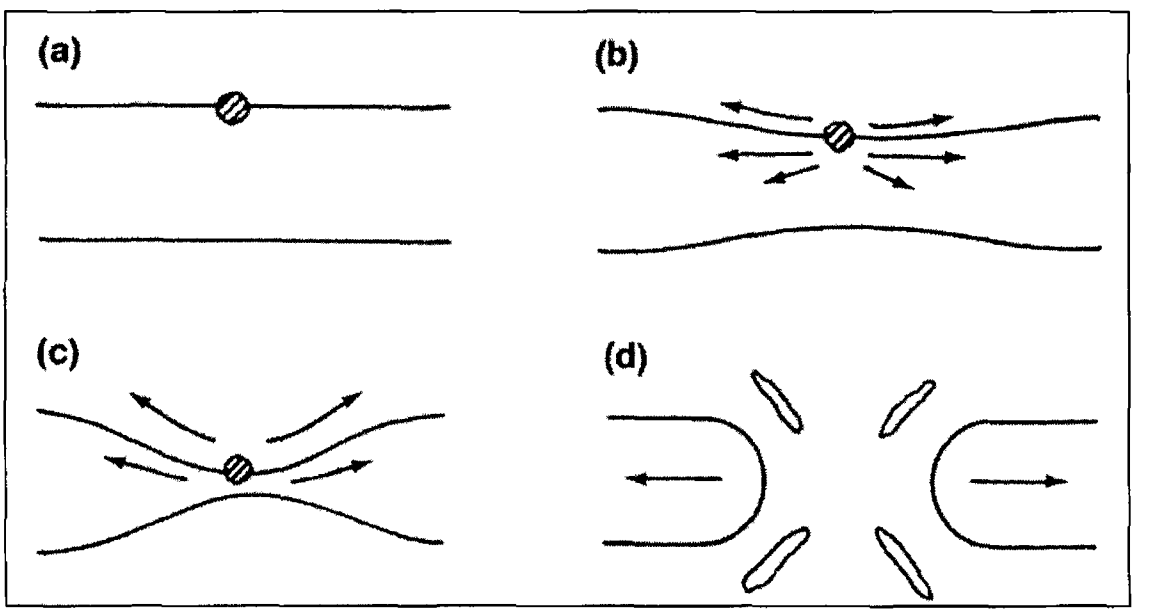

Figure 2 2 Sequence of events when a spreading particle causes local thinning in a foam film (Prins and van't Riet, 1987) (a) droplet contacts surface, (b) droplet spreads drawing liquid with it, (c) this process continues as the film thins, (d) film collapses

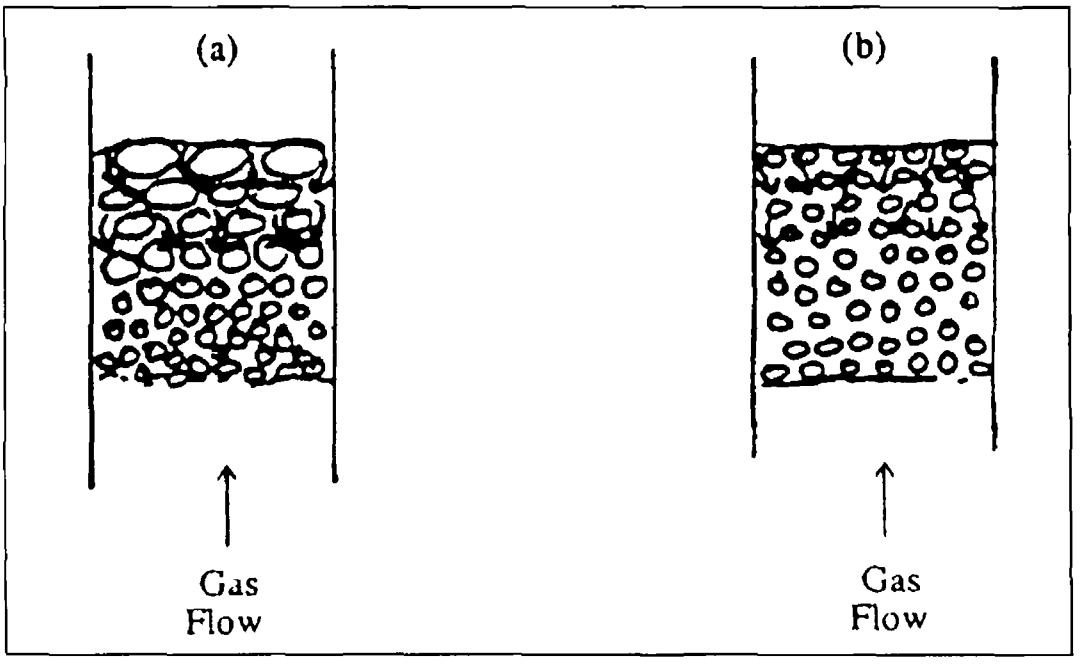

Figure 2 3 Models of gas-liquid separation (Lee *et al* , 1993)
(a) Interbubble mode, (b) Interfacial mode

2 3 3 Mechanical and Physical Foam Control

Mechanical foam breaking methods are generally considered uneconomical as the power requirements for such devices are high (Vardar-Sukan, 1992) However, some of the studies outlined in this section suggest that in certain circumstances the total power input is less in mechanically controlled systems than in systems employing antifoam for foam control However, the feasibility of mechanical control depends ultimately on the type of fermentation in question and the commercial value and importance of the product Vardar-Sukan (1992) explains that mechanical control methods may be desirable when antifoams constitute a toxicity hazard, cause unacceptable reduction in oxygen mass transfer, or are simply ineffective in controlling the foam On the negative side, if cells are entrapped in the foam, cell damage and lysis can occur as a result of the associated high shearing environment which, in turn, may reduce productivity and exacerbate downstream processing difficulties Mechanical and antifoam based methods can be employed simultaneously to achieve effective and efficient control In many applications, for example, a mechanical foam breaker may be supplemented by the addition of a chemical antifoam at a low concentration, (Hall *et al* ,1973)

Although there are many different types of mechanical foam breakers, the ideal requirements of any mechanical foam control device are as outlined by Hall *et al* (1973)

(i) minimum power consumption
(ii) simplicity of installation
(iii) robustness of construction
(iv) ease of cleaning and sterilisation
(v) minimum maintenance

Mechanical foam breakers are generally expensive to construct, due to their intrinsic design, scale-up/down may be difficult and furthermore, laboratory experimentation is expensive Charles and Wilson (1994) describe one typical mechanical foam breaker (Figure 2 4) which operates by drawing the foam into a high speed impeller by rotational centrifugal action and subjecting the foam to large mechanical forces, causing foam disruption

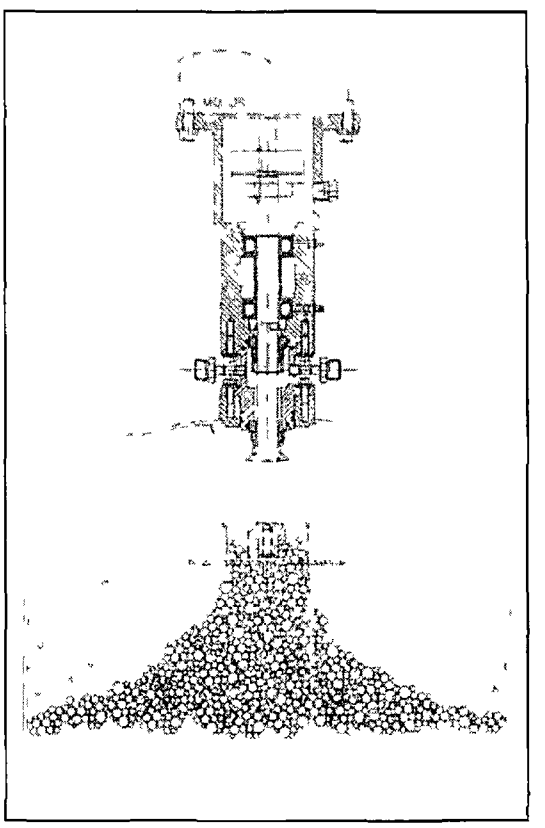

Figure 2 4 Mechanical foam breaker in which foam is destroyed by a high speed centrifugal impeller (Charles and Wilson, 1994)

Vardar-Sukan (1992) summarises mechanical control mechanisms into three categories

(i) When a sudden pressure drop is incurred by the foam, causing the bubbles to collapse, *e g* injectors, ejectors and orifices Cahoon (1997) describes the application of a pressure change technique for collapsing foams in a novel foam plug flow bioreactor, which is applicable to plant, animal and microbial culture systems

(ii) When the shear stress is increased by rapidly alternating pressure fields caused by high speed rotating disks, blades, and impellers Comprehensive studies have been performed on this type of mechanical foam breaking device in Japan For example, some of the literature available on the Mechanical Rotating-Disk Foam-breaker (MFRD), includes the work of Ohkawa *et al* (1984a,b), Takesono *et al* (1993a,b,c 1994, 1995), Yasukawa *et al* (1991a,b) and Andou *et al* (1996)

(iii) Centrifuges, cyclones where rotational forces cause the foam to burst, (Moller, 1988)

Ohkawa *et al* (1984a,c) and Takesano *et al* (1993a) showed that for model fluid systems (detergent solutions) a mechanical foam-breaker with a rotating disk installed in a stirred tank and tower fermenter, respectively, provided an effective means of foam control without the addition of antifoams Onodera *et al* (1995) similarly displayed the effectiveness of a MFRD for foam control in an aerated, agitated yeast fermentation Figure 2 5 (Ohkawa *et al* , 1984c), schematically illustrates a typical MFRD In these types of devices, liquid is fed to the centre of the disk and dispersed at high velocities created by the centrifugal forces generated by the rotating disk, onto the foam The critical disk speed for effective foam control is typically related to parameters such as liquid flow rate, air sparger rate and impeller dimensions

Ohkawa *et al* (1984b) compared the effectiveness of three different mechanical foam breaker designs in a bubble column, All devices operated on a similar basis of foam control, *i e* liquid dispersion over foam It was concluded that the foam breaking apparatus equipped with a rotating disk was most effective It was also concluded that the larger the rotating disk diameter, and the lower the gas flow rate, the more efficient the device with regard to power consumption However, in a bubble column, there is

obviously a limit below which gas flow rate cannot be reduced, without compromising system hydrodynamics

Andou *et al* (1996) examined the effects of three air sparger types in a bubble column (porous sintered glass bead filter, perforated plate and nozzle sparger) on the effectiveness and efficiency of a MFRD in regard to overall power consumption It was found that the porous sintered glass bead filter was the most favourable type of sparger for use in this bubble column with mechanical foam control

Yasukawa (1991a,b) analysed differences in power consumption profiles for an agitated, aerated vessel under antifoam control and mechanical foam control (MFRD) Takesono (1993b and 1995) performed a similar study on a bubble column In all cases, it was concluded that specific power consumption was lower for the mechanically controlled method than for the antifoam-controlled method This phenomenon was principally due to the larger mass transfer co-efficients and more favourable gas hold-up characteristics of the fluid in the absence of anti-foam These studies were conducted in an attempt to correlate data to aid in predicting the performance of MFRDs and their input requirements for further applications Viesturs *et al* (1982) provide a comprehensive summary of other types of mechanical foam breaking equipment and physical control mechanisms Physical methods of foam control include thermal, electrical and ultrasound However many microbes are very sensitive to such effects, thus eliminating these control mechanisms as practical options (Vardar-Sukan, 1992) However, there are some patented foam control devices, specifically designed for biological applications The Moscow-Chemical Equipment Institute (1988) describes an industrial foam breaker which achieves 100% foam suppression This unit consists of an arrangement of staggered electrodes mounted on a mixer shaft When the rings are rotated at 50 rpm, full suppression is achieved by applying an electric current (50V) to the electrodes This foam breaker is useful in microbiological, food and chemical industries A Portuguese patented electrical device (de Alencar Ximenes, 1994) consists of a sparking device installed above the liquid level, with electrodes strategically placed outwards and downwards towards the foam

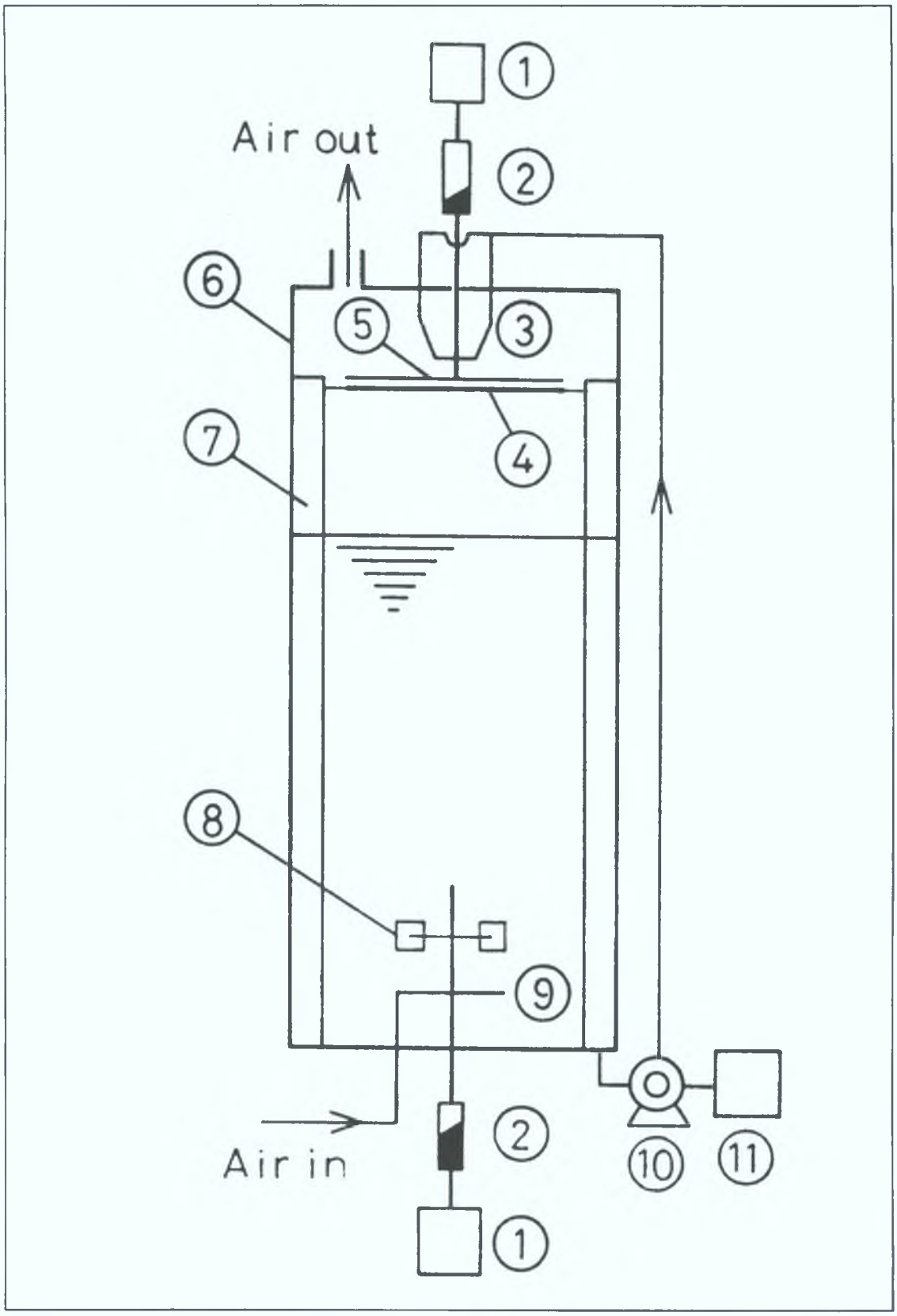

Figure 2.5: MFRD experimental apparatus (Ohkawa 1984c).1. Motor; 2. Torque meter; 3. Annular liquid feeder; 4. Foam impact plate; 5. Rotating disk; 6. Vessel; 7. Baffle plate; 8. Impeller; 9. Ring sparger; 10. Roller pump; 11. Flow control.

2 4 FOAMING STUDIES IN BIOLOGICAL SYSTEMS

2 4 1 Bacterial Systems

Koch *et al* (1995) examined the influence of different types of antifoaming agents on the performance of microbial cultures, specifically *Escherichia coli*, *Penicillium chrysogenum* and *Cephalosporium acremonium* In all cases, broth surface tension was found to initially decrease with increasing antifoam concentration, ultimately becoming concentration independent It was discovered that pure silicone oil was unsuitable for large scale fermentations due to low dispersion rates Pure PPG was ineffective for foam control PPG / silicone oil mixtures and a silicone oil emulsion proved to be the most effective agents It was also found that the effects of antifoaming agents on mass transfer were short-lived and that their presence did not influence either cell concentration or product formation significantly

Actinomycete cultures of *Nocardia amarae* were used by Blackall and Marshall (1989) to illustrate the cell-induced foam stabilisation effect associated with production of certain surfactants and the naturally hydrophobic cells, which are transported from the bulk phase to the foaming structure Cell-free broth showed a reduction in surface tension for seven day old cultures relative to that of whole broth, but the bubble structure was unstable and no stable foam was formed Washed cells (*i e* minus surfactant) showed no foaming potential either The implications from these studies was that both cells and surfactant were essential for creation of a stable foam It is believed that the cells within the bubble lamellae stabilise the bubbles by minimising the distance to be bridged by the liquid film A method was devised to counteract this stabilising effect Montmorillonite clay was added to the culture prior to foaming This method was effective for foam control and its inhibitory action was concentration dependent, with maximum efficiency at 100µg/ml The clay acts by enveloping the cells to camouflage their hydrophobic nature

In activated sludge systems, the production of stable foam in the aeration tank can lead to serious operational problems Filamentous bacteria are often associated with the formation of such foams and investigations have been undertaken (Fougias and Forester, 1994) to elucidate the relevant mechanisms involved Using known foam forming species, *Nocardia amarae, Nocardae pinensis, Rhodococcus spp* and *Microthrix*

paricella It is found that when n-hexadecane is present, *R rubra* exhibits enhanced growth and surface tension depression, promoting foam formation

Kerley and Forster (1995) investigated the effects of extracellular polymers secreted by the microorgasims *Microthrix parvicella* and *Nocardia amarae* on foam stability in activated sludge The type of ECP and its uronic acid content depends on the dominating microorganism As the amount of uronic acid in the ECP increases, the hydrophobicity of the solids increase, which is associated with foam formation The presence of polyvalent metal ions, *e g* aluminium, enhances the stability of such foams

From the available literature, it is evident that chemical antifoams are generally employed to combat foaming problems in fermentations Olivieri *et al* (1993) describe the use of antifoam for foam control in the production of a modified diphtheria toxin by *Corynebacterium diphtheriae* On the basis of this work, an alternative method of mechanical foam control was recommended to avoid the reduction in product yield, attributed to antifoam addition The experimental work was performed in a 35L bioreactor using a high speed centrifugal mechanical defoaming device (Fundafom R, Chemapak) In small-scale fermentations, producing high value products, it was concluded that mechanical foam breaking devices may provide an attractive alternative to antifoam control

2 4 2 Fungal and Yeast Systems

Because of the commercial significance of yeast and filamentous fungal fermentations and, in particular, due to the importance of foaming in fermented alcohol products, there is a body of literature on foaming in a limited number of the more important cell lines

Bahr *et al* (1991) and Bahr and Schugerl (1992) investigated the causes of foaming in continuous culture, in the absence of any antifoaming agent, using synthetic media which were variously carbon-, nitrogen- and phosphorus-limited Foaminess was found to be greatly influenced by dilution rate At low dilution rates, the cells produced extracellular lipids, causing large unstable foam lamellae and hence a low foaminess, at increased dilution rates, foaminess was greater, in the absence of lipids, which acted as natural antifoams

Saccharomyces cervisiae was studied by Molan *et al* (1982) in connection with foaming problems in wine-making The fermentation broth was fractionated with a view to determining the components responsible for foaminess The yeast cells themselves were found to contribute little to the observed foaminess, which was chiefly attributed to the protein content of the medium Maximum foaminess occurred at 5% ethanol concentration but higher alcohol concentrations had an antifoaming effect, which was consistent with observations that foaming in wine fermentations reaches a maximum during the early stages The stabilising effect of ethanol is related to its interaction with proteins The authors suggest that there is, perhaps, scope to control foaming in wine-making by changing the strain of yeast to produce lower levels of foaming proteins

Foaming in fungal cultures was studied by Noble *et al* (1994) and Konig *et al* (1979) Noble *et al* (1994) used cultures of *Penicillium herquei* and an Ingoldian fungus in a 20 L stirred tank fermentation, to determine the components responsible for foam formation It was confirmed that antifoam concentration and surface tension are inversely related for *P herquei* cultivations and as foaming commenced the surface tension increased It was suggested that not alone proteins and other surface active components were stripped from the broth due to foaming, but that the antifoam itself was also preferentially concentrated in the foam However, for the Ingoldian broth there was no obvious relationship between antifoam concentration and surface tension The formation of a stable foam was attributed to the presence of proteins, carbohydrates, L-keto acids and lipophilic biosurfactants and, in particular, extracellular pigments

In *Penicillium chrysogenum* fermentations (30 l internal loop reactor), Konig *et al* (1979) found that in the absence of antifoams, foaminess, Σ, was dependent on cultivation time, reaching a maximum at approximately 50 hours and subsequently declining The same trends did not apply for PEG Typ 300 antifoam-supplemented cultures, where the foaminess was observed to be independent of both time and gas flow rate When antifoam was added, the foaminess dropped instantaneously and remained constant thereafter In the absence of antifoam, foaming characteristics were strongly correlated to extracellular protein concentration

2 4 3 Plant Cell Systems

Although there is limited literature on large scale applications, foaming is prevalent in all aerated plant cell suspension cultures In severe cases, the cells entrapped in foam are deposited on the reactor wall headspace where a thick 'meringue' can form, which may extend across the entire diameter of the vessel (Scragg, 1994) Problems are exacerbated at industrial level, where high biomass yields are required to compensate for slow production rates (Doran, 1993) Although the specific oxygen requirements of plant cells (10^{1} mmol l^{-1} h^{-1}) are less than those of microbial systems (10^{2}-10^{3} mmol l^{-1} h^{-1}) (Kieran *et al* , 1997), high overall mass transfer rates are essential to support the high biomass concentrations and thus aeration and agitation techniques are important Excess of O_2 or the stripping of CO_2 at elevated aeration rates can lead to a reduction in growth rate and viability (Smart and Fowler, 1981) As a large proportion of cells are frequently incorporated into the foam, mechamcal foam breaking methods are generally not desirable as cell viability would be affected Moreover, because doubling times are high (20-100 hours), extended fermentation time is an important issue to consider in the choice of such an energy intensive control mechanism Overall, antifoams would appear more suitable for these cultures However, the associated reduction in oxygen mass transfer rates can be deleterious

Hawke *et al* (1962) showed that by using a silicone based antifoam with *Catharanthus roseus* plant cells, the growth pattern was altered, with an extended lag phase and reduced growth rate and biomass yield As previously discussed (Section 2 3 2), these effects are thought to be attributable to reduced oxygen transfer rates both from the gas to the liquid and from the liquid to the cell

Studies performed on *Atropa belladonna* suspensions in both stirred tank and bubble column reactors by Wongsamuth and Doran (1994), illustrated that foaming problems were not related to biomass concentration but were attributable to the characteristics of the cell-free broth and in particular, were correlated with protein content It was speculated that the protein moiety of the ECP secreted by the cells, (which was not measured but which has been estimated by other authors to be as high as 18%, *e g* Olson (1969), might also contribute to foaming However, this hypothesis was not independently tested by Wongsamuth and Doran Four different antifoams were examined Three of those tested, namely polypropylene glycol (PPG) 1025 and 2025

and antifoam C were effective in foam control Antifoam C and PPG 1023 had no adverse effects on cell growth at concentrations of up to 600 ppm in shake flasks However pluronic 6100 had detrimental effects at all levels When antifoam C was used in a stirred tank reactor, cell production was oxygen limited after two days It was also concluded that maximum biomass production declines with increasing reaction volume due to the necessity for increased antifoam addition, to control and prevent overflow Head space volumes and acceptable foam levels must be taken into consideration to optimise production as the maximum biomass concentration fell by 50%-70% following a 7-10% increase in working liquid volume, in the presence of the minimum levels of antifoam required to completely suppress foaming

Smart and Fowler (1981) used a silicone-based antifoam for experimental work performed in a 4 l glass reactor, equipped with a sparger of sinter porosity No 3, using suspension cultures of *Catharanthus roseus* They reported that while k_La values were reduced by approximately 75 %, growth rates remained essentially unchanged, although the overall biomass yield was reduced In contradiction to the generally negative reports on antifoam, Zhong *et al* (1992) indicated that antifoam can sometimes enhance production The addition of silicone A to suspension cultures of *Perilla frutescens* yielded very beneficial results with a seven-fold increase in anthocyanin pigment and a 3-fold increase in growth rate, due to the prevention of foaming and cell adhesion to reactor walls Li *et al* (1995) used mineral oil as an antifoaming agent in the cultivation of *Nicotiana tabacum* in a 5L stirred tank reactor It was found that a 5% (v/v) light mineral oil concentration was required for optimal foam control and the presence of this oil had a positive influence on biomass growth rates A comparative study using a silicon antifoam which suppressed foaming, revealed that this antifoam had a negative influence on growth

It should be noted that results obtained from antifoam studies in shake flasks are not necessarily representative of the behaviour which might be expected in stirred tank or air lift reactor configurations, containing 3 phase systems Extrapolation should be performed with caution Data should ideally be collected from systems which most closely mimic actual production conditions

2.4.4 Animal Cell Systems

Animal cell cultures are also prone to foaming, largely due to the presence of medium constituents such as serum. These cells are typically shear sensitive and they are easily damaged in foam (Cherry, 1992). Thus, use of a mechanical foam breaking method does not alter productivity, as cells entrained in the foam are already disrupted and of no benefit to the production process. For a $0.3m^3$ system Chisti (1993) explained that mechanical action resulted in debris deposition on the walls of the reactor but did not affect cell growth or viability in the broth. Large sparger holes ($\geq$ 1 mm) are recommended for aeration in medium containing serum as they form a more controllable foam structure. Smaller bubbles generate densely packed foam, which is less easily disrupted.

Looby and Griffths (1987) studied foaming in high density microcarrier perfusion cultures, where excessive foaming trapped the microcarriers. In this system, surface aeration was ineffective and direct sparging unacceptable; thus a compromise between foaming and aeration requirements was met by employing a spin filter sparging system. The bubbles generated do not come in direct contact with cells and thus high system aeration rates can be tolerated by the cells.

Handa-Corrigan *et al.* (1989) explain that in antifoam-supplemented media, cell damage occurs due to the rapid bursting of bubbles. Without antifoams, cell damage occurs due to the actual loss of cells into the foam and by the physical shearing effect during liquid drainage from lamellae. Pluronic F-68 can be used to stabilise foam and cells do not penetrate into this stable structure. In a monoclonal antibody production process using a mouse-mouse hybridoma cell line in both stirred and sparged bioreactors (2 l and 1.8 l, respectively), Zhang *et al.* (1992) found that foam formation and subsequent cell damage created problems for cell growth in serum-supplemented and serum-free media. Pluronic F-68 was again used to protect the cells. However, in serum-free medium devoid of cells, medium components were degraded (*e.g.* essential growth factors and proteins) by continuous air sparging and this effect was not inhibited in the presence of Pluronic F-68. Pluronic F-68 does not eliminate foam and Zhang *et al.* (1992) found that 10% of the culture medium was lost in foaming; however, in actual broths no cell debris was found, suggesting that no cell death occurred in the foam. Further experimentation revealed that by adding antifoam C and pluronic F-68 to cultures, no losses in cell

growth occurred up to antifoam concentrations of 200 ppm and foaming was completely eliminated However higher concentrations of the monoclonal antibody were observed in cultures containing 200 ppm of antifoam due to increased specific antibody production rates at low cell concentrations The results suggest that in stirred, sparged bioreactors, the optimal medium for this animal cell culture contained 0 2% w/v pluronic F-68 and 10-50 ppm of antifoam C agent

A newly developed defoaming method, using a hydrophobic net, was outlined by Ishida *et al* (1990) The foam-eliminating net, which was tested in cultivation of rat ascites hepatoma cell JTC-1 and mouse-mouse hybridoma cell STK-1, was composed of polysiloyane The foam was effectively disrupted when it made contact with the net Without the net, the medium almost instantly overflowed when air was sparged into the system whereas, with the net intact, the foam was completely eliminated in the presence of continuous air sparging This method shows potential for further applications, not only for animal cell cultures but perhaps for other biological systems

2 5 BENEFICIAL EFFECTS OF FOAMIMG

As outlined in the preceding sections, foaming is generally perceived as a negative or undesirable phenomenon in biological systems However, there is a substantial body of literature devoted to the beneficial exploitation of the foaming nature of biological systems, whereby cells, proteins, enzymes and DNA can be differentially separated from fermentation broth, minimising the costs of subsequent separation techniques Schweitzer (1979) and Thomas and Wilkner (1977) present comprehensive descriptions of foam fractionation and floatation Thomas and Wilkner (1977) summarise various applications of this technology in experimental studies In brief, the liquid surrounding bubbles becomes enriched with surface active species (*e g* proteins) which are subsequently carried into the foam with the bubbles The concentration of the species in the collapsed foam (foamate) is high in comparison to the bulk solution In cell flotation processes, if the component of interest is not surface active it can be attached to surface active 'collectors' and thus transported into the foam Grieves and Wang (1996) show how a cationic surfactant was used as both a foam stabiliser and as a 'collector' for *Escherichia coli* cells

2 5 1 Cell Flotation

Gehle *et al* (1984) describe a process in which yeast cells of *Hansenula polymorpha* are recovered by continuous foam floatation, thus eliminating the need for energy-intensive centrifugal separators The efficiency of such a system can be described in terms of a separation factor, S, defined as,

$$S = \frac{\text{cell concentration in foam}}{\text{cell concentration in residue}} \qquad (2\ 5)$$

On the basis of bench and pilot scale bubble column operations, a separation factor of 812 was achieved in these trials, with scope for further improvements if the foaminess could be reduced while increasing the mean residence time of the foam in the column, *i e* by reducing the liquid hold-up in the foam The same yeast was used by Bahr *et al* (1991 and 1992), for a similar operation and it was found that recovery by floatation was promoted by high dilution rates in continuous cultivation and that the efficiency of the separation operation was influenced by the foaminess of the culture broth, with total cell recovery (100%) possible under optimal operating conditions These studies also highlighted the influence of extracellular protein and lipid excretions on the foaminess of the broth and subsequent cell separation factors

Parthasarathy *et al* (1988) and Ramani *et al* (1993) used the yeast *Saccharomyces carlsbergensis* for modelling cell separation from fermentation broths in terms of foamate cell concentration (collapsed foam) and bulk liquid cell concentration in a series of foaming experiments Ramani *et al* (1993) related the drainage rate of fluid from a static foam to the separation factor As the foam drains and liquid hold-up decreases, the separation factor increases Parthasarathy *et al* (1988) found that the effects of bubble size and aeration rate on separation efficiency were very significant As expected, smaller bubble sizes yielded a higher cell removal rate from solution into the foam, since, even at the same air flow rate, smaller bubbles provide larger specific interfacial areas However, larger bubbles yield overall higher separation factors, as the liquid hold-up in the foam is also reduced for large bubbles Thus, it was concluded by both Parthasarathy *et al* (1988) and Ramani *et al* (1993) that the overall cell separation factor for a fermentation system is greater at larger bubble sizes

Many studies have been performed to determine the influence of parameters such as bubble diameter, gas-flow rate and foam height on the separation factor However, the reports issued have, to a certain extent, been contradictory While Parthasarathy *et al* (1988) found that larger bubbles favour separation, Viehweg and Schugerl (1983) suggest that smaller bubbles, larger bubble column diameters, low medium feed rates, high aeration rates and increased height of the foaming apparatus improve the cell separation factor Viehweg and Schugerl (1983) reported enhanced separation at higher gas flow rates while Parthasarathy *et al* (1988) found to the contrary

In a foam floatation study with plant cells (*Atropa belladonna*) in a bubble column system, Wongsamuth and Doran (1994) reported that 55% of cells were recovered in the foam after 30 minutes and 75% after 90 minutes Floatation was not significantly affected by culture age, or over a wide range of pH values (pH 3 5 to 8 5) Cell viability was high (90-100%) for all culture ages and foaming times tested

It is difficult to compare different experimental results due to the variations in experimental apparatus, fermentation conditions and cell systems which inevitably affect the data Despite the inevitable inconsistencies however, the general consensus is that cell separation by flotation is a very effective process

2 5 2 Biomolecule Fractionation

The potential to exploit foaming separation processes is not limited to cells and separation of proteins and DNA has also been documented Protein fractionation has been studied by Mohan and Lyddiatt (1994), Brown *et al* (1990), Varley *et al* (1996), Nobel (1994) and Uraizee and Narsimhan (1990b, 1996) DNA and protein partitioning has been achieved by Lalchev *et al* (1982) Uraizee and Narsimhan (1990a) present a literature review on foam fractionation of proteins and enzymes, whereby proteins and enzymes are preferentially concentrated in the foam due to the selective adsorption of surface proteins at the hquid-gas interface This process has proven successful in many applications, such as the removal of non-biodegradable detergents from waste water and enzyme separation from a mixture of enzymes or proteins (*e g* fermentation broths, animal tissue, organ homogenates and plant extracts)

Mohan and Lyddiatt (1994) investigated the differential drainage of proteins from foam, using a commercial beer The protein was concentrated in the initial foam and differentially drained over a period of 30 minutes This method shows potential as a primary step in downstream processing of proteins and could prove to be an inexpensive technique for recovering proteins from dilute solutions on a large scale Brown *et al* (1990) used BSA in a model system to demonstrate the effectiveness of protein recovery from dilute waste effluent Protein fractionation was optimal at low concentrations (<1% wt), contrary to other separation techniques such as ultrafiltration, where only highly concentrated solutions are economically feasible The efficiency of the system, in this work, is expressed in terms of enrichment, e, where,

$$e = \frac{\text{concentration in product(foaming fraction)}}{\text{concentration in feed}} \qquad (2\,6)$$

Highest enrichment was obtained at low feed concentrations, low superficial gas velocities and larger bubble sizes

Uraizee and Narsimhan (1996) modelled protein enrichment in foams, using BSA solutions in a continuous foam fractionation column As observed by Parthasarathy *et al* (1988) for cell separation, protein separation was found to be enhanced at larger bubble sizes and lower aeration rates It was also concluded that low feed rates and larger foam heights were most effective and that beyond a critical liquid volume, foam enrichment increased with increasing liquid volume

The preferential foam fractionation of proteins was also illustrated by Varley *et al* (1996) in a model system containing a mixture of proteins, namely, BSA, lysozyme and conalbumin In a mixture of proteins, the protein with the lowest surface tension should be preferentially stripped into the foam Experiments were effected at the isoelectric point of the required protein and a solution containing two proteins was used in any one trial For BSA and lysozyme, the ratio of BSA to lysozyme in the foamate was much greater than in the residual liquid or in the initial solution Therefore, partitioning was achieved, although, there were significant protein losses (up to 31%) due to protein aggregation and/or degradation As with all foam separation methods, the smaller the relevant quantity of fluid contained in the foamate, the more effective the separation process Therefore, operating parameters must be optimised for any particular system to maximum fluid drainage, reduce protein loss and thus enhance enrichment

Lalchev *et al* (1982) used BSA-DNA and Lysozyme-DNA model systems to optimise DNA/protein separation via foam fractionation It was concluded that a 'dry' foam (after film drainage) enhanced separation These model systems assisting in practical DNA - protein separation from chromatin, a complex structure of naturally occurring DNA and proteins

Gehle and Schugerl (1984) investigated the removal of penicillin G from aqueous solutions via foam floatation The presence of low concentrations of this antibiotic in waste water hindered effective biological treatment of effluent Since penicillin was not itself enriched in the foam, collector was used This complex was enriched in the foam and 95% penicillin separation was achieved, using long chain aliphatic collector molecules

A foam fractionation step was also used by Phae and Shoda (1991) to facilitate the recovery of the anti-fungal antibiotic, iturin Lower aeration rates (0 1 vvm) yielded more effective antibiotic separation, since at higher aeration rates foam was generated more rapidly and incorporated more medium, yielding a lower iturin concentration This application has potential for large scale fermentations, and offers scale up advantages over other small scale separation processes such as membrane filtration and chromatography

CONCLUSION

The tendency of biological fluids to foam is very common and unfortunately solutions to associated problems are not always either evident or simple Individual cell lines create specific foam forming substances and fermentation operating conditions can frequently enhance their effects on foaming potential Recently, foaming potential has been beneficially exploited in novel separation processes but in general, it is an undesirable phenomenon The two principal methods employed for foam control in fermentation systems are antifoam addition and mechanical foam breaking Antifoams are more frequently used in bioprocesses as mechanical control can prove to be uneconomical Many types of antifoams exist and the choice is generally system specific However, frequently the use of antifoams is not feasible due to the negative

effects on mass transfer and toxicity effects Moreover, antifoams are often prohibited in the manufacture of food and pharmaceutical grade products

Evaluation of foaming potential of biological fluids is typically performed in purpose-built bubbling devices, rather than under actual process conditions This literature review has described and evaluated the systems and measurement indices most commonly used in such work and identified specific associated limitations

Chapter 3

EXPERIMENTAL METHODS[1]

3 1 PLANT CELL SUSPENSION CULTURE MAINTENANCE

Plant cell suspension cultures of *Morinda citrifolia* (Rubiaceae) were obtained from Dr Graham Wilson, from the Department of Botany at University College Dublin This cell line originated from callus cultures originally donated by Professor M H Zenk, at the University of Munich, Germany

Suspensions were maintained, in this laboratory, in 250 ml Erlenmeyer flasks containing 100 ml of suspension culture In the latter stages of the culture cycle, suspensions were typically a vibrant orange colour, as depicted in Figure 3 1 Flasks were agitated on an orbital shaker (Gallenkamp SGM 300) at a rotational speed of approximately 100 rpm The cultivation temperature was 25°C ±1°C A lighting cycle of 16 hours illumination of warm white light followed by 8 hours of darkness was in operation

Suspensions were sub-cultured every 21 days, using a 10% (by volume) inoculum A modified Gamborg B5 medium (Gamborg, 1968) was used, the components of which are outlined in Tables 3 1 and 3 2 The concentration of some constituents (specifically FeNa(EDTA), $CoCl_2\ 6H_2O$, $CuSO_4\ 5H_2O$, $ZnSO_4\ 7H_2O$, $MnSO_4\ 4H_2O$ and $NaH_2PO_4\ 2H_2O$) differed from those employed in the original medium NAA was employed in place of Indole-3-acetic acid and N-Z amine was also added This modified medium has been used by Dr Wilson and other workers (*e g* Kieran 1993), to maintain this cell line Deionised water was obtained from a Millipore (Milli-U10, UK) water purification system Prior to autoclaving, medium pH was adjusted to a value of 5 5 using 0 1 M HCl An autoclavable syringe (Socorex, Switzerland) fitted with a 3 mm bore cannula was employed for inoculation, to minimise damage to cells and to ensure that accurate volumes were transferred Attempts to use wide bore 10 ml sterile plastic pipettes for inoculation transfers were unsuccessful, as the viscous suspensions tended to adhere to the walls, preventing accurate volume measurement The assembled syringe

[1] Raw data is presented in Appendix B

containing approximately 3 ml of deionised water and the culture flasks containing fresh medium were autoclaved at 121°C for 20 minutes (Tomy SS-325, Japan), where polystyrene foam bungs (Cortex Foams Ltd., Cork) were used as an alternative to cotton wool. All sterile work was performed in a Microflow laminar air flow cabinet.

Figure 3.1: *Morinda citrifolia* suspension cultures, in a 1000 ml Erlenmeyer flask.

Table 3.1: Medium composition

Component	per 1 litre
X20 Concentrate	50.0 ml
Sucrose	20.0 g
N-Z Amine	2.0 g
NAA **	1.86 ml
$NaH_2PO_4.2H_2O$	0.1695 g

* Casein enzymatic hydrolysate from bovine milk.

** 1 g l^{-1} solution of α-Naphthaleneacetic acid (NAA) in absolute ethanol (stored at 4°C).

Table 3 2 X20 Medium concentrate composition *

Nutrient	g l^{-1}	Nutrient	g l^{-1}
Macroelements		**Microelements**	
$CaCl_2$ $6H_2O$	4 40	KI	0 0150
$(NH_4)_2SO_4$	2 68	$MnSO_4$ $4H_2O$ **	0 2620
$MgSO_4$ $7H_2O$	5 00	$ZnSO_4$ $7H_2O$	0 0600
KNO_3	50 0	H_3BO_4	0 0600
FeNa(EDTA)	0 56	$NaMoO_4$ $2H_2O$	0 0050
Vitamins		$CuSO_4$ $5H_2O$	0 0088
Nicotinic acid	0 02	$CoCl_2$ $6H_2O$	0 0050
Thiamine HCl	0 20		
Mesoinositol	2 00		
Pyridoxin HCl	0 02		

* This concentrate is stored at -20°C and thawed in a 70°C waterbath as required

** $MgSO_4$ $7H_2O$ is dissolved separately in boiling deionised water

3 2 SUSPENSION CULTURE GROWTH CHARACTERISTICS

3 2 1 Biomass Assays

Suspension growth profiles were established in terms of fresh weight, dry weight and cell number Fresh weight (FW) measurements were obtained by vacuum filtering a suspension sample (5-20 ml) through filter paper (Whatmans no 1) and recording the weight of the filtered cake The fresh weight was calculated as follows

$$FW\ (g\ l^{-1}) = \left(\frac{\text{Wt of filtered cake and paper (g)} - \text{Wt of vacuum filtered moist paper (g)}}{\text{Volume of suspension filtered (l)}} \right) \qquad (3\ 1)$$

Suspension dry weight was determined by allowing the filtered cake to dry in an oven, at 80°C for 24 hours, and then measuring the weight of the dried cake Dry weight was calculated according to the equation

$$DW\ (g\ l^{-1}) = \left(\frac{\text{Wt of dried filtered cake and paper (g)} - \text{Wt of dried paper (g)}}{\text{Volume of suspension filtered (l)}} \right) \qquad (3\ 2)$$

Cell number was determined using a Sedgewick Rafter counting chamber (S50, Graticules Ltd , England) A 1 ml aliquot of an appropriate suspension dilution was transferred to the chamber The chamber was mounted on the stage of a transmisson

light microscope (Biomed, Leitz Wetzlar, Germany) and viewed under the 10X objective and the numbers of cells in 20 graticule squares were counted Dilution factors of between 100 and 1000 were employed, depending on culture age, to yield between 5 and 15 cells per square A 4 g l^{-1} solution of KNO_3 in deionised water was used for dilution purposes, to maintain the osmotic balance between the cells and the suspending fluid (Gallagher, 1987) The counting chamber consists of 1000 squares and, as the chamber contains a total volume of 1 ml, the capacity of each square is 0 001 ml Thus, cell number was calculated according to the following equation,

$$\text{Cell density (cells ml}^{-1}) = \frac{\text{Average number of cells per square x Dilution factor}}{\text{Sample volume per field of view (i e 0 001 ml)}} \qquad (3\ 3)$$

Cell viability, performed in tandem with cell number counts, was determined using the Evans blue dye exclusion technique (Gaff, 1971) The membrane of non-viable cells is permeable to the dye molecules and, when viewed under the microscope, these cells are seen to be stained blue A volume of 0 33 ml of a 0 25 g l^{-1} solution of Evans blue, in deionised water, was added to 10 ml of suspension cells The suspension was thoroughly mixed and allowed to stand for a 5 minute period Percentage viability was determined using the equation,

$$\%\ \text{Viability} = \left(\frac{\text{Total number of cells - Number of stained cells}}{\text{Total number of cells}}\right) \text{x } 100 \qquad (3\ 4)$$

3 2 2 pH

Culture pH was monitored each day during the growth cycle, using a WTW pH 539 meter (WTW, Germany) The pH and temperature probes were immersed in a thoroughly mixed cell suspension and the pH reading was allowed to stabilise The pH probe was routinely calibrated using pH 7 and pH 4 buffers

3 2 3 Conductivity

Conductivity was measured over the course of the growth cycle, to examine the possibility of using this technique as a means of assessing culture growth The use of

conductivity for monitoring growth in plant cell systems has been investigated by Taya *et al* (1989) and Ryu *et al* (1990)

Measurements were performed using a WTW LF-537 conductivity meter (WTW, Germany) Suspensions were mixed thoroughly by gentle vortexing The probe was immersed in the suspension, ensuring that all bubbles were excluded from the electrode region of the probe In the event that suspensions were clumpy, it was found that conductivity readings did not stabilise Reliable readings were obtained only from homogeneous suspensions

3 3 IMAGE ANALYSIS MORPHOLOGICAL STUDIES

3 3 1 Background

Image analysis is a computer aided method for analysing objects It is a non-biased procedure, which is capable of converting a digital image into comprehensive data An image is transmitted from a microscope or macroviewer, via a camera, to an image analyser, where it is visually displayed on a colour monitor Specific image analysis software packages allow the user to design a program, to extract specific data for the component under observation

Vecht-Lifshitz and Ison (1992) present an extensive literature review of the many different biotechnological applications of image analysis in the fields of microbiology, biomedical research, biochemistry and biochemical engineering Image analysis is a rapid, accurate means of assessing the morphological aspects of microbiological systems While previously, the compilation of size distribution data or other morphological parameters was labour intensive and tedious, it can now be transformed into a relatively rapid procedure using image analysis

There is a limited amount of published material on the use of image analysis in plant cell studies However, it has been applied to various areas of plant cell research including growth measurement (Olofsdotter *et al* 1993), somatic embryogenesis and genetic tranformations (Schopke *et al*, 1997) Smith *et al* (1995) investigated pigment accumulation by the anthocyanin-producing plant cell line, *Ajuga pyramidalis* The quantification of biomass and anthocyanin levels in callus cultures can be non-

destructively measured without compromising the aseptic cultivation environment Productive pigment-producing callus cells can be selected for seeding suspension cultures and in theory the colour image analysis showed potential for use in fermentation systems by imaging the suspension via a viewing port This would eliminate the necessity for sampling and hence, reduce the risk of contamination, which is extremely advantageous in plant cell systems, due to their extreme vulnerability because of their lengthy cultivation periods required and their susceptibility to microbial contamination Schopke *et al* (1997) used a simple grey threshold detection method for assessing the effectiveness of different techniques for genetic transformation of embryogenic plant cell suspension cultures of Cassava, an important crop in tropical regions The method was based on the detection of coloured spots which resulted from a histological assay for an encoded enzyme

In regard to suspension cultures of *Morinda citrifolia*, most of the work to date on morphological characterisation has been carried out at University College Dublin (Curtin, 1991, Kieran *et al* 1993, Murtagh, 1994) Curtin (1991) collected data using a microscope and an eyepiece micrometre Kieran *et al* (1993) investigated the potential of image analysis for assessing the morphological characteristics of this suspension culture, using a semi-automatic program and a Quantimet Q520 imaging system Using a purpose built system, Murray and O' Malley (1993) researched the separation of over-lapping chains and identified specific difficulties associated with this process In the current study, the use of adequate dilution factors minimised the proportion of over-lapping chains in a sample, any over-lapping elements present were not analysed This greatly reduced the complexity of the program required

In this laboratory, a Leica Q500 MC image analysis system (Cambridge, UK) was employed, which was connected to a TV camera (CCD type) mounted on an Olympus BX40 (Japan) microscope The measurement procedure was implemented via a Quips operating routine, specifically designed for this particular application The Quips software package has many versatile operating features, some of which are described briefly later in this section Depending on the complexity of the designed program, a time consuming procedure can be transformed into a totally automatic or a semi-automatic operation In this particular instance, a semi-automatic program was designed to facilitate measurement of *Morinda citrifolia* suspension culture morphological

characteristics, with regard to chain length, chain width, cell length and the number of cells per chain, throughout the cell cycle This program was designed to perform a preliminary investigation of the potential of image analysis in the assessment of plant cell suspension cultures, with a view to facilitating the eventual design of a more efficient and effective program for reliable plant cell morphological characteristic determination

This image analysis system has many functions and comprehensive treatment of the entire operation range is beyond the scope of this report However, a brief overview of the different stages required for processing an image is presented below and a preliminary description of the particular functions used in the program (Appendix A) designed for this study is provided

3 3 2 Method

Morinda citrifolia suspension samples were diluted, using a 4 g l^{-1} solution of KNO_3 (1/200-1/1000), to yield approximately 2-4 chains per field of view To reduce the possibility of overlapping or clumps of chains, the cell suspension was vortexed gently and thoroughly between each dilution step and again prior to taking a sample The program was not designed to process crossed-over chains, therefore, if such chains appear in a field of view, they are ignored

One drop of a diluted sample was placed on a slide and covered by a clean cover slip, which was sealed around the edges by petroleum jelly to eliminate the evaporative effect due to heat generated by the microscope lighting Each field of view was selected randomly and every effort was made to ensure a non-biased selection of cells

Kieran *et al* (1993) devised a method to measure the morphological parameters of *Morinda citrifolia* using a semi-automatic image analysis routine Validation studies revealed that a sample of 100 chains corresponding to a minimum of 250 cells was sufficient to ensure reproducible and reliable data for a population of cells Therefore, approximately 100 chains were analysed for each sample, in this work

An image analysis program can be separated into different sections Operation parameters must be defined in a 'setup' routine and sample images acquired, chains or

cells detected, processed and measured; the data must be acquired in a suitable format for manipulation, to elucidate the morphological information in a comprehensible logical manner. In this study, chain length and width, the number of cells per chain and the length of individual cells were evaluated using the designed Quips program, as presented in Appendix A. Unfortunately, in this preliminary study, it was not possible to fully automate the procedure, although significant improvements on comparable earlier routines were achieved.

A schematic flowchart of this program is presented in Figure 3.2. Each step of the program was designed by estimating which procedures/operations were useful, based on the theoretical information available in the user manual, followed by a trial and error effectiveness evaluation. The steps involved in each stage are further explained below.

1) Program Initiation (Setup):

All binary images are cleared to erase any previously stored images. The grey level threshold is set, as further explained under 'image acquisition'. An output display results window is set up. The number of fields of view required and the minimum number of chains required are specified. For normal procedures, the chain number is set at 100 and the number of fields of view at 50.

2) Image Acquisition

A suitable lens must be selected for capturing the images under the microscope In this instance, the 4X lens was selected for the operation. This must be specified in the program. At this magnification, one pixel is equivalent to 2.09 μm.

One field of view 384,000 equally spaced pixels or detection points, arranged in a rectangular 750 x 512 grid. A pixel is the smallest resolvable area in the field of view. The system operates on a grey level detection basis. A grey level values defines colour between black and white. Black is assigned a value of 0 and white a value of 255. Any value between 0 and 255 corresponds to a specific grey level, *i.e.* the level 5 is very dark and the level 250 is almost pure white. An image is recorded as a range of grey levels, each pixel having a certain intensity.

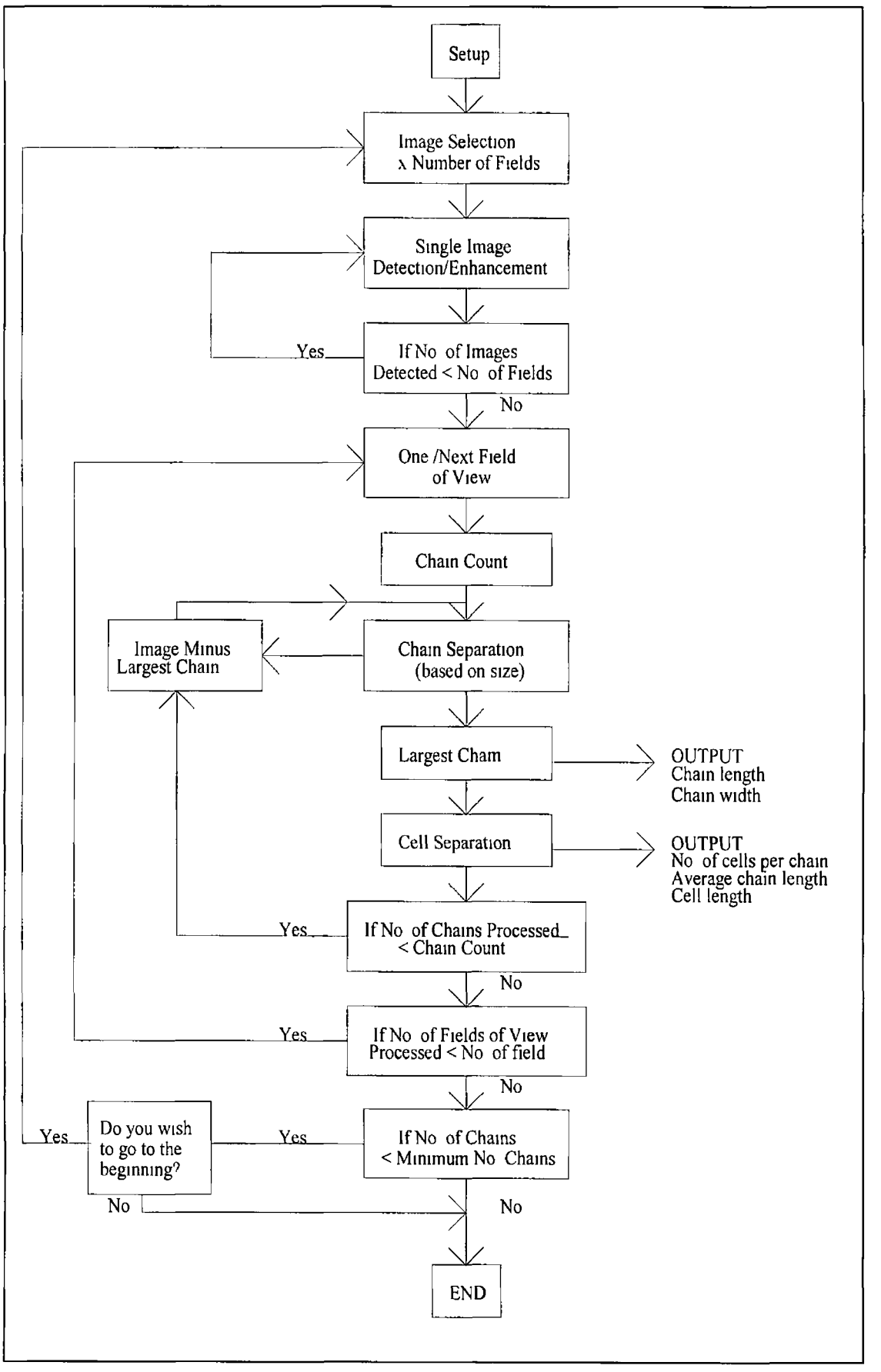

Figure 3 2 Flowchart of image analysis operating program

When the image is in focus, the 'image acquire' function is chosen and this 'freezes' the image and acquires it. This image can be saved to a file prior to further processing or it can be manipulated immediately. In this program, all required fields of view are selected and stored as grey image files, before the program proceeds to the next step.

3) Grey Image Enhancement, Image Detection and Binary Enhancement

The program was designed to initiate a control loop to process each field of view separately. Therefore, each grey image file is retrieved separately. Grey image enhancement involves the altering of this image to increase its potential for further processing of included features. There are certain planes available for storing grey images. For instance, the image can be altered and saved to a different grey image plane. Therefore, both initial and altered images are individually accessible. There are various grey image processing facilities (*e.g.* Bsharpen, WSharpen, Square, Log *etc.*), however, only a 'Bsharpen' transform is used in this study, by which black detail is emphasised. It is a useful method for enhancing the contrast between an object and its surroundings.

Image detection entails the separation of a feature or an image from the rest of the surroundings based on a grey level intensity difference. It is a vital step in the imaging process. There are different ways of discerning what is chosen or detected. In this application, a threshold grey level is selected manually for each field of view. Whether a pixel is included or detected, depends on the grey level detection of this pixel, relative to the threshold. Selected objects, *i.e.* objects with a grey level equal to or greater than this specified threshold are automatically highlighted on the screen image as the threshold is altered. A minimum level is manually selected which allows full detection of the entire cell wall. This is crucial in further separation techniques. Little variation in this threshold level is required during the detection of each field of view, since the light intensity does not change significantly.

Sometimes, in addition to chains, cellular debris and other unwanted objects, such as dust particles, are detected. A manual step is included to select only the chains of interest. This eliminates the need for particle size filters and allows the exclusion of unsuitable crossed chains that cannot be processed. If required, this manual step also allows 'tidy-up' editing and binary image processing, to prepare the detected image for accurate measurement and eliminate any unwanted detected objects. The manual operations occasionally used were the 'erase' and 'draw' functions. If there was a small

undetected gap in the cell wall, it could be rectified and drawn into the detected image Alternatively, if there was an unwanted object adjoining a chain, it could be erased manually Generally, manual alteration steps were avoided, if possible However, at certain stages in the cycle it was a useful facility

Each field of view is stored as a binary file, containing the detected and selected images (chains) only When the program has finished detecting one field of view, it loops to process the next field of view When all fields of view have been completed, the manual section of the program is completed and the remainder of the program is totally automated

4) Binary Image Manipulation and Measurement

Multiple trial and error attempts are necessary to facilitate the development of a user friendly, effective and efficient program for the measurement of chain and cell parameters A loop is initiated to process each frame/field of view When more than one chain is present in a frame, the program is sub-looped to process the largest chain first, followed by the next largest, until no chains remain and the program then continues to the next field of view

Automatic alterations Skeletonisation, pruning, image filling and logical image plane combination steps were the only features used (Figure 3 3) However, many more processing feature such as dilation (expanding an image) and erosion (thinning/ shrinking an image) exist

'Skeletonisation' involves the thinning of a detected image to a single-pixel line (Figure 3 3A) It is different to a simple erosion step since it does not segment an object Pruning involves the shortening of branches of a skeletonised image If any short branches extend from the outline, they are removed Image 'filling' (3 3B) involves the total detection of an enclosed, outlined object Logical combination steps allow the user to add, subtract or select common part of two images In this study only the subtraction of one image plane from another is exploited (Figure 3 3C), in order to reject the area common to two images This was the chief step used for separating the individual cells in a chain, the skeletonised cell walls were subtracted from the filled image to produce separated cells The associated reduction in size is negligible When the cells are separated, the program counts the number of cells per chain

Figure 3 3 Schematic representation of binary image processing steps

(A) Skeletonisation

(i) (ii)

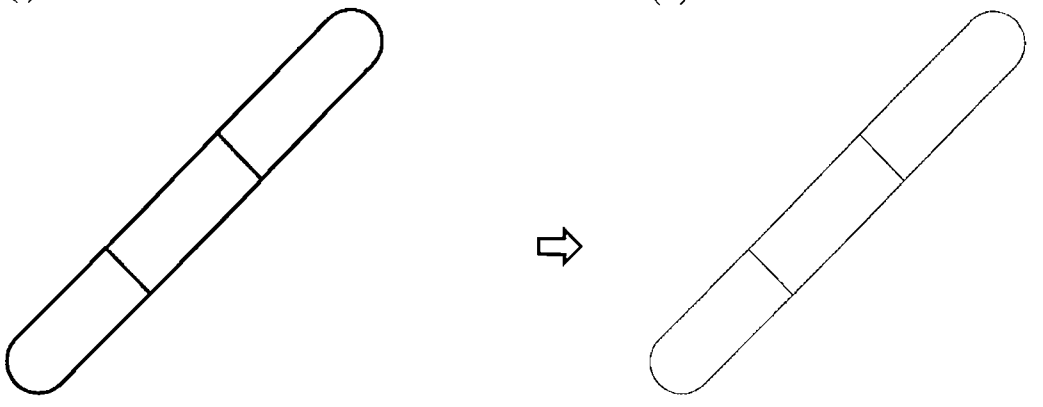

(B) Filling

(i) (ii)

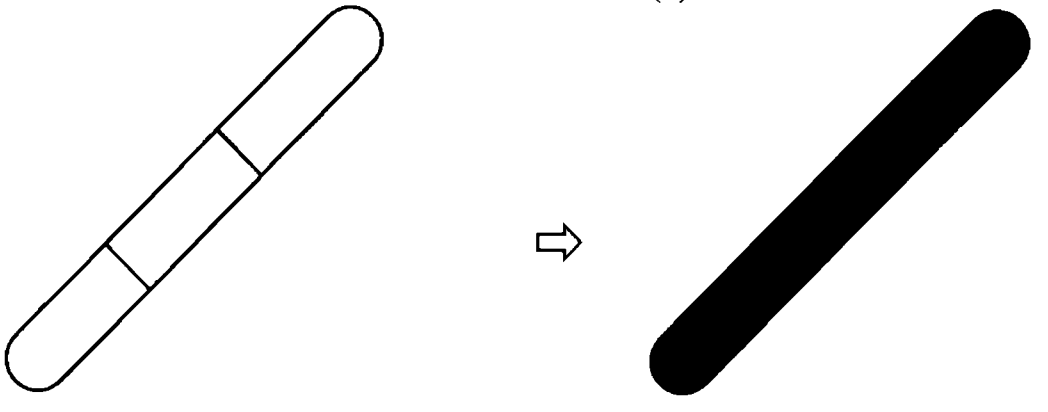

(C) Logical Operation (Subtraction B(ii) - A(ii))

(i) (ii)

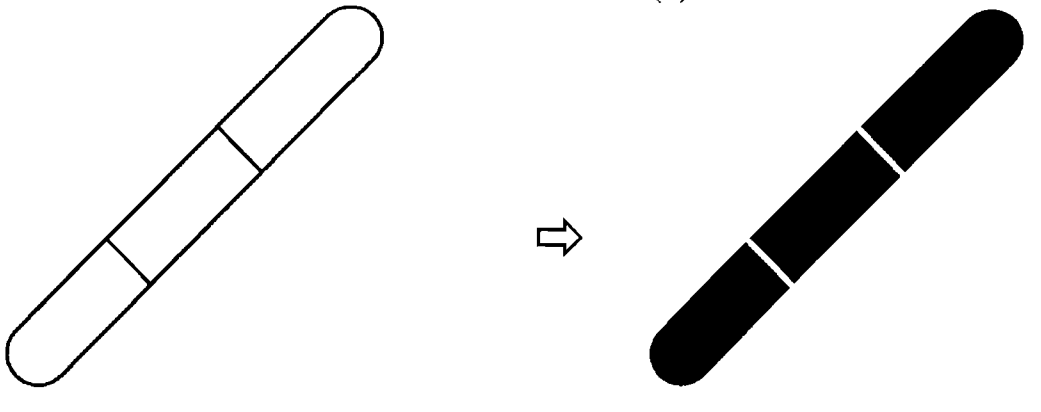

Although the image analysis systems supports a wide range of measurement features, the only parameters relevant to this study are area, perimeter, length and width Each parameter is measured in terms of pixel units, which are subsequently converted into metric values using the pixel calibration factor There are two methods of measuring length used in this study, the applications of which are further explained as follows,

Feret method Feret length is the distance between two parallel lines which are tangential to the object Many feret measurements of a chain or cell can be taken, the longest of which is defined as the length and the shortest of which is the width This method is accurate for the measurement of cell length, since the curvature over the length of the cell is minimal However, for the measurement of chain length, the extent of curvature is appreciable and thus an alternate method is used

Quadratic interpolation method The calculation of the length and width is based on the principle that a chain is considered as a cylindrical object, and hence, the two dimensional image projected on a screen is rectangular Whether a given chain is straight or curved, the area and perimeter remain unchanged Therefore, this eliminates the error factor associated with curvature using the feret method The area and perimeter of the 'filled' chain are measured automatically The filled image must be used, since the perimeter includes all detected boundaries If the image is not filled, each cell wall dividing the chain would be considered in the recorded perimeter The calculation of the relative length and width is based on the geometrical principles of a rectangular object, according to the following series of equations

$$A = LW$$

$$\Rightarrow \quad W = A/L \qquad (3\ 5)$$

$$P = 2L + 2W$$

$$\Rightarrow \quad P = 2L + 2\,(A/L)$$

$$\Rightarrow \quad PL = 2L^2 + 2A$$

$$\Rightarrow \quad 2L^2 - PL + 2A = 0$$

Solving this quadratic equation for L,

$$L = \frac{P + (P^2 - 16A)^{1/2}}{4} \tag{3.6}$$

and

$$W = \frac{P - (P^2 - 16A)^{1/2}}{4} \tag{3.7}$$

Assuming that L > W, Equation 3.6 represents the length of the chain and equation 3.7 the width.

Due to the characteristically rounded ends of a chain, there is inevitably a slight error encountered in the assumption of a simple rectangular shape. However, according to Kieran *et al.* (1993), there is only approximately a 4% underestimation error in chain length, for an average chain of 500 μm.

Therefore, for chains, the length and width are calculated using equations 3.6 and 3.7 and for cells, the ferret method is used. As data are generated the results are outputted to a display window. Upon completion of each chain processing, the program loops back to the next chain or the next field of view, as appropriate.

5) Program Termination

The program continues until all fields of view have been processed. If the required number of chains have been analysed, the program terminates. Alternatively, if an inadequate number has been recorded, options are available to the user to select more fields of view, or to terminate the program.

6) Data Manipulation

The data generated during measurement must be compiled for subsequent analysis. The program sends the relevant information for measured parameters to a specific site in the display window. These data can then be visually inspected and saved as an array of data, for further manipulation. In this instance, the output window was manually saved as a Sigma Plot file (Jandel Scientific, Germany). The data were arranged to facilitate the generation of log-normal size distribution profiles, using Sigma Plot transforms. A log-normal curve is fitted to the data using the Sigma Plot software 'curve fit' facility.

3 3 3 Program Validation

The reliability of the program in regard to the accuracy of individual chain and cell length measurements is validated by comparing the data generated using the program with manual measurements collected for the same chains and cells, using the image analysis system Initially, the semi-automatic program was run as described in Section 3 3 2, images were acquired, analysed and the data recorded A manual program was designed to recall the original grey images acquired using the semi-automatic program and chain length and width were measured manually, using the computer mouse as a digitising tablet The relevant data were recorded manually and later correlated with the automatic measurement data Thus, manually and automatically derived data for the same population of chains were available to assess the validity and accuracy of the designed program Figures 3 4 and 3 5 illustrate the errors encountered for cell and chain length, respectively The % error was calculated according to the equation

$$\% \text{ Error} = \frac{\text{Manual measurement - Automatic measurement}}{\text{Manual measurement}} \times 100 \qquad (3\ 8)$$

From a practical point of view, the manual procedure was both difficult and time consuming to implement, since it required considerable manual dexterity in the use of the mouse However, manual validation using a minimum of 25 chains confirmed that the semi-automatic program was analysing chain and cell parameters relatively accurately, thus verifying the calculation algorithms Percentage errors of $\pm$6% and $\pm$4% were observed for cell and chain length measurements, respectively The error encountered for cell length measurement is seen to be slightly higher than for chain measurement and this result is quite understandable, since the individual cells are smaller and the manual error is thus increased, as it is at the beginning and end of the measurement process using the mouse, that most difficulty is encountered However, this validation was only completed for a day 11 culture and for further comprehensive studies, validation should ideally be effected for every day of the culture cycle using a minimum of 100 chains The time taken to completely analyse 100 chains using the semi-automated routine was approximately 60 minutes, the corresponding time for the manual process would be approximately 4 hours

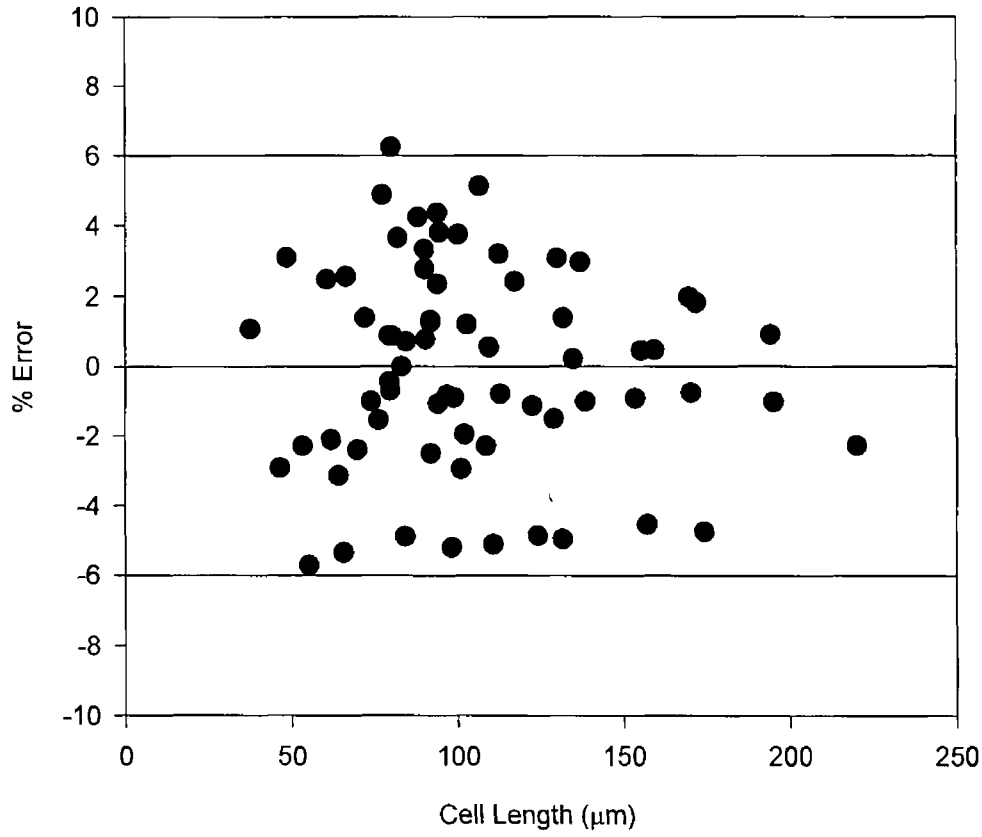

Figure 3 4 Automatic versus manual cell length measurement error margin

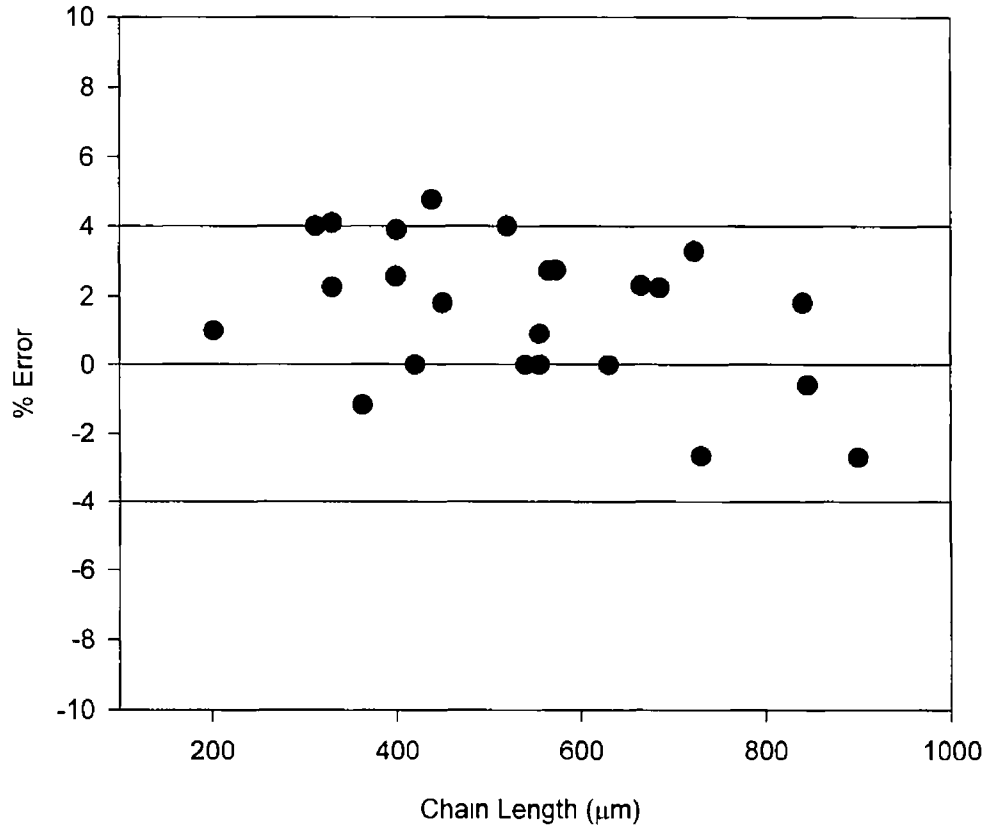

Figure 3 5 Automatic versus manual chain length measurement error margin

As mentioned previously, the chain linear dimensions (*i e* length and width) were calculated on the basis of area and perimeter measurements, however, the cell lengths were measured using the ferret method, since the curvature was considered to be minimal A validation experiment was performed, by comparing the average cell length calculated from the chain length data, (*i e* the average chain length on a particular culture day, was divided by the average number of cells per chain to obtain the average length of a cells), with the average measured cell length (ferret method) The % accuracy was calculated by the following equation

$$\% \text{ Accuracy} = \frac{\text{Measured average cell length}}{\text{Calculated average cell length}} \times 100 \qquad (3\ 9)$$

Figure 3 6 illustrates that there was there was a minimum accuracy of 93% on day 5, when the cells were at their longest during a batch growth cycle

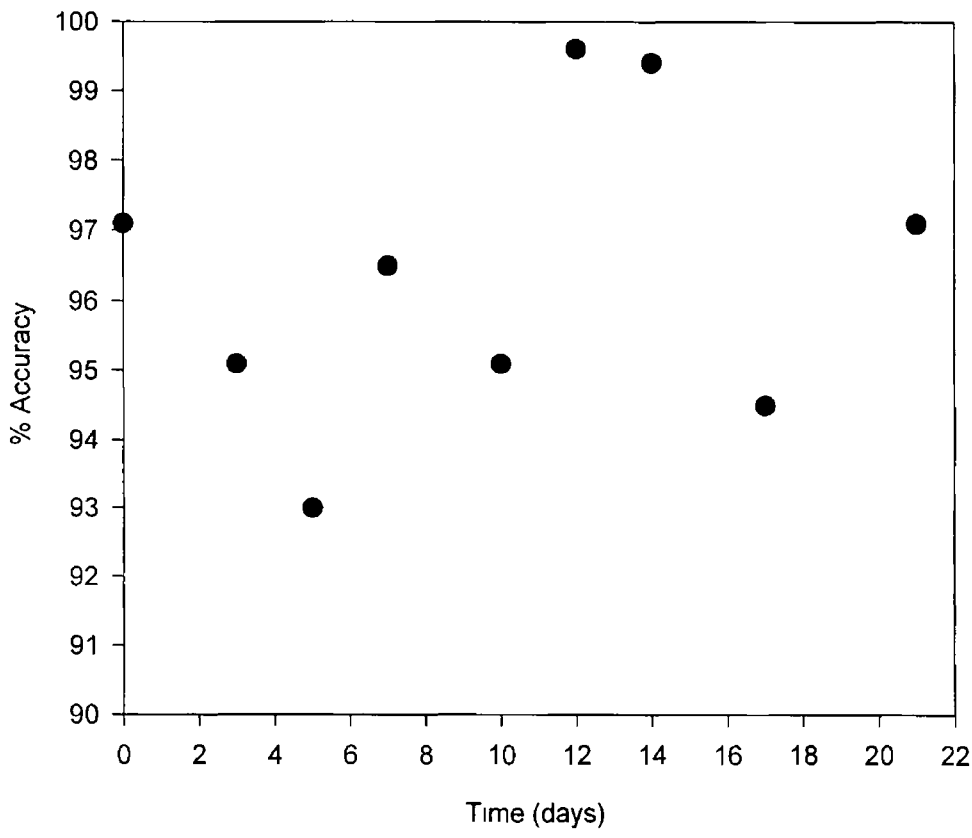

Figure 3 6 Cell length measurement accuracy

3 4 CELL-FREE BROTH ANALYSES

Cell-free broth was obtained by vacuum filtering whole suspension broth through Whatmans no 1 filter paper The collected filtrate was then centrifuged at 3000g, for 20 minutes (Sorval RC-5B, Du Pont), to remove any remaining cellular debris

3 4 1 Rheological Studies

Rheological data were collected for cell-free broth throughout the 21 day growth cycle ECP standard solutions, as well as solutions of xanthan and Bovine Serum Albumin (BSA) were analysed using the same method

Rheological data were collected using a Brookfield cone and plate viscometer (DV-I+) and a Brookfield rotating cylinder viscometer (DV-II+) with a UL adapter (Brookfield, USA) Shear rates of between 40 and 750 s^{-1} were investigated As both viscometers were found to yield identical results, the cone and plate model was used for the majority of samples This device requires a sample volume of 0 5 ml, as opposed to a 16 ml sample for the DVII+ model All samples were incubated at 25°C prior to analysis For each rotational speed an apparent viscosity (μ_a) and a percentage torque reading were recorded Readings outside the acceptable torque limits of 10-90% were disregarded The shear rate (s^{-1}) was calculated by multiplying the rotational speed (rpm) by a factor of 7 5 for the cone and plate DV-I+ model and a factor of 1 22 for the DV-II+ model

In a Newtonian fluid, the generated shear stress is directly proportional to the imposed shear rate The constant of proportionality is known as the fluid viscosity, *i e*

$$\tau = \mu \gamma \qquad (3\ 10)$$

where

τ = shear stress ($N\ m^{-2}$)

γ = shear rate (s^{-1})

μ = fluid viscosity ($N\ s\ m^{-2}$)

Thus, for a Newtonian fluid, a plot of shear stress as a function of shear rate yields a straight line, through the origin, with a slope equal to the viscosity (Figure 3 7) If the fluid is non-Newtonian, a different profile is observed Figure 3 7 also illustrates the

general shape of flow curves for pseudoplastic, dilatant and plastic fluids For all non-Newtonian fluids, it is only possible to specify an apparent viscosity Apparent viscosity (μ_a) is dependent on the prevailing shear rate and is defined by the following equation,

$$\mu_a = \frac{\tau}{\gamma} \qquad (3\ 11)$$

Pseudoplastic behaviour, which is common in biological fluids (Atkinson and Mavituna, 1991) is often described by a power-law model of the form,

$$\tau = k\gamma^n \qquad (3\ 12)$$

where

k = fluid consistency index ($N\ s^n\ m^{-2}$)

n = flow behaviour index (-)

The flow behaviour index has a value of less than 1 for pseudoplastic fluids Values greater than 1 describe dilatant behaviour The k and n values for particular fluids can be determined from apparent viscosity data collected over a range of shear rates, by manipulation of equations 3 11 and 3 12, to yield,

$$\ln \mu_a = \ln k + (n-1) \ln \gamma \qquad (3\ 13)$$

Hence, a plot of the natural log of apparent viscosity as a function of the natural log of shear rate yields a straight line, of slope (n-1), intercepting the y-axis at ln k In the analysis of all fluids investigated in this work, flow curves (rheograms) were generated in order to facilitate preliminary characterisation of the fluid If the rheogram was linear, the fluid was considered to be Newtonian, otherwise further analysis was required as described above

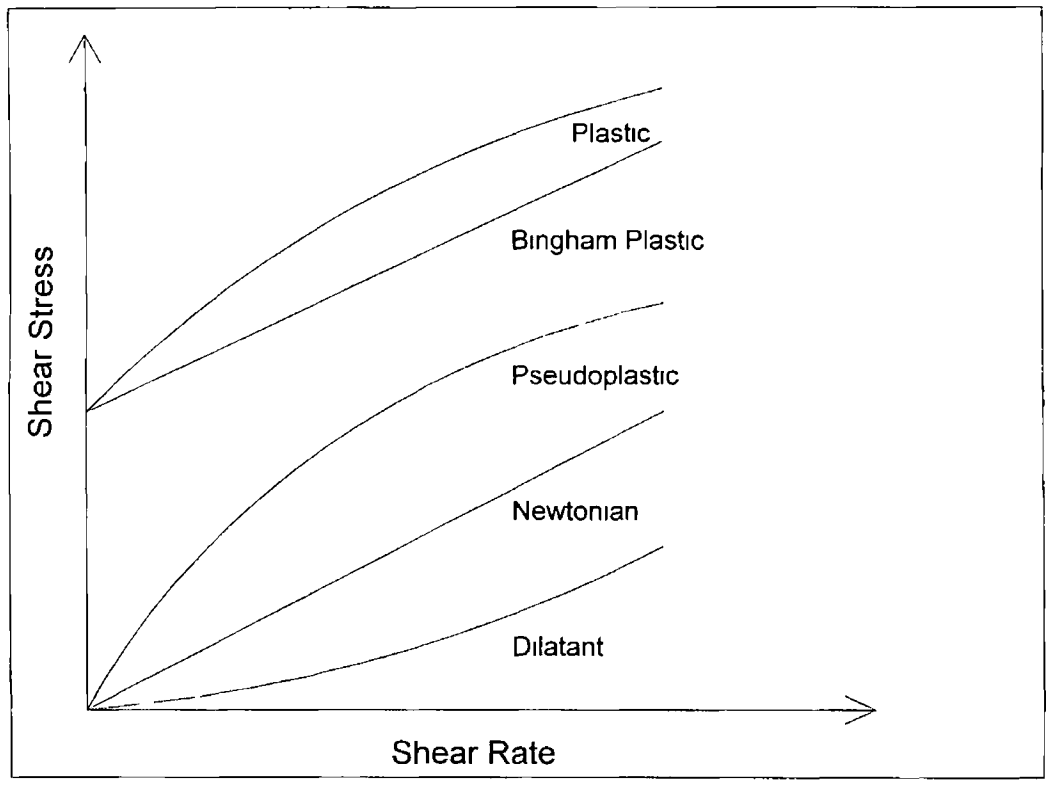

Figure 3 7 Characteristic flow curves (rheograms) for Newtonian and non-Newtonian fluids

3 4 2 Surface Tension

Surface tension data were collected for cell-free broth samples throughout the culture cycle A torsion balance (White Elec Inst Co Ltd , England) with a platinum ring attachment was used for surface tension measurements Solutions were allowed to equilibrate at room temperature (typically 20°C) before a sample, of approximately 10 ml, was transferred to the concave sample plate For some solutions the surface tension was observed to change with time Therefore, an initial reading was taken immediately after the sample was transferred to the glass plate (instantaneous reading) and subsequent readings were recorded at 5 minute intervals until the surface tension was observed to have stabilised (equilibrium reading)

3 4 3 Extracellular Polysaccharide Isolation and Quantification

Smith and Pace (1982) review the many extraction methods that can be used for isolating polysaccharides Lower alcohols (methanol, ethanol and propanol) and acetone are widely used in both laboratory and commercial applications The separation protocol employed for the isolation of ECPs from suspension cultures of *Morinda citrifolia* was adapted from a technique developed by Wilson (1995) for the same cell line This

protocol was similar to purification methods used by Uchiyama *et al* (1993) and Otsuji *et al* (1994) for other plant cell lines

A known volume of cell-free broth, typically 50 ml, was adjusted to an 80% v/v ethanol concentration, by the addition of absolute ethanol (*e g* 200 ml ethanol was added to 50 ml of cell-free broth) This solution was mixed thoroughly by repeated inversion and was allowed to precipitate overnight at 0-4°C The ECP precipitate was recovered by centrifugation at 3500g for 15 minutes, at a temperature of 4°C and was then resuspended in a minimal quantity of deionised water These precipitation and recovery steps were repeated again for each sample The resulting solution was dialysed against deionised water for a minimum of 24 hours at 0-4°C, under agitation and placed in a dried and preweighed container The sample was lyophilised (Super Modulyo, Edwards) for 3 days and the container and sample were immediately reweighed The ECP concentration in the sample assayed was calculated as follows,

$$\text{ECP conc } (g\,l^{-1}) = \frac{(\text{Wt of lyophilised container + sample})\,(g) - \text{Wt of container } (g)}{\text{Volume of sample } (l)} \qquad (3\ 14)$$

Using a Bradford assay (Section 3 4 4) some protein was detected in the partially purified ECP solutions The maximum error in the determined ECP concentration, attributable to protein contamination, was calculated as follows,

$$\%\ \text{Protein content} = \frac{\text{Protein Content}}{\text{Total ECP and Protein Content}} \times 100 \qquad (3\ 15)$$

3 4 4 Protein Quantification

The micro-bradford assay (Bradford, 1976) was used for the quantification of protein in cell-free broth It is a rapid and reproducible method for protein determination However, like most standard methods (*e g* Lowry method), it only detects free protein, The same method was used by Wongsamuth and Doran (1994) for protein quantification in a different plant cell line The basic principle of this assay is the binding of the dye, Coomassie Brilliant Blue G250, to the protein This results in a colour change in the dye from red to blue, which is detected spectrophotometrically (Unicam 8625), as the maximum absorbance of the dye shifts from 465 nm to 595 nm Bradford reagent was prepared by dissolving 100 mg Coomassie Brilliant Blue G250 in 50 ml of 95% ethanol

This solution was mixed with 100 ml of phosphoric acid (85%) and brought to a final volume of 1 l with deionised water It was then filtered through Whatmans no 1 filter paper, to remove any undissolved solute It was stored in an amber bottle at ambient temperature for a maximum period of one month

Standard solutions (0 0 - 0 1 mg ml $^{-1}$) were prepared by dissolving an appropriate quantity of BSA in deionised water For the micro assay, a 0 1 ml sample of either cell-free broth or standard was added to 1 ml of reagent The solution was gently vortexed and the absorbance, at 595 nm, was recorded after a period of 5 minutes Samples were prepared in triplicate but only duplicate samples were assayed spectrophotometrically, unless significant differences were observed in the optical density of the first two samples A standard curve was constructed (Figure 3 8), correlating absorbance to protein concentration A second order regression curve fitted the data, yielding coefficients of greater than 0 99 Hence, the protein concentration of unknown samples could be determined on the basis of absorbance, using the standard curve In all cases, the reagent was filtered prior to use, to remove any precipitate formed during storage A fresh standard curve was prepared for each batch of samples analysed

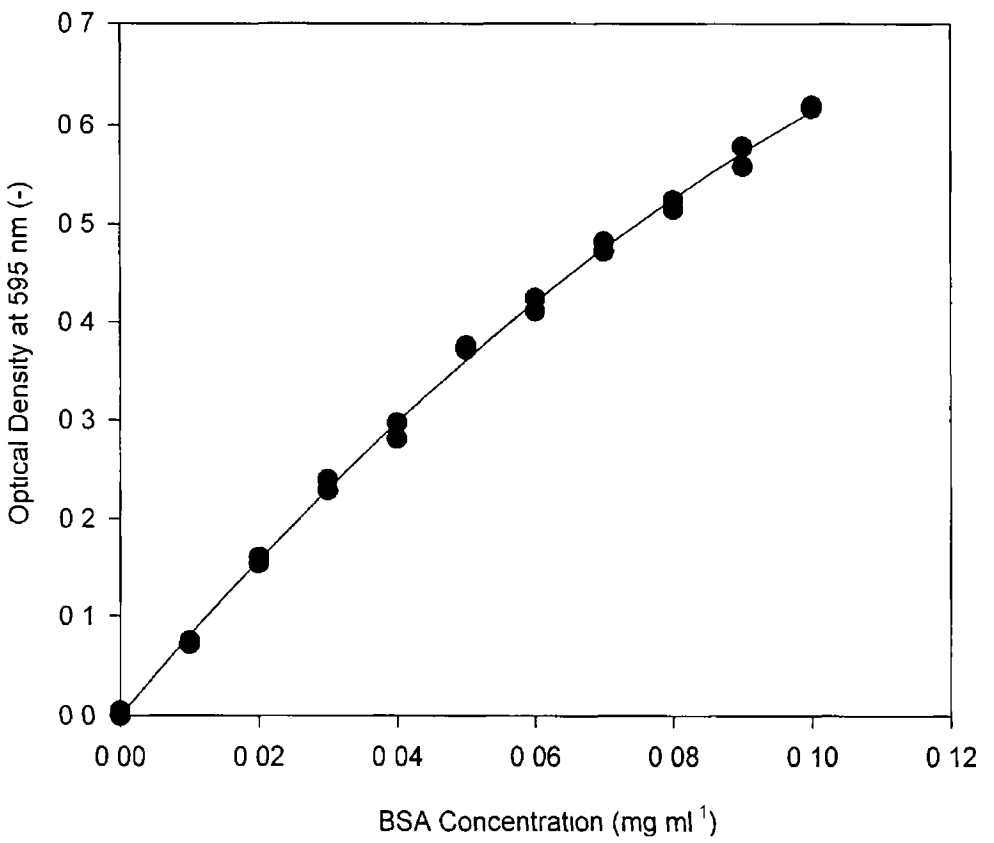

Figure 3 8 Typical BSA standard curve for protein determination, using the micro-Bradford assay

3 5 POLYSACCHARIDE AND PROTEIN STUDIES

In order to identify the influence of ECP and protein on both the surface tension and viscosity of cell-free broth, these components should ideally be separated from one another before analysis However, ECPs precipitated from the broth were known to contain a protein component Efforts to achieve isolation of ECPs and proteins are described below Model systems, namely xanthan gum and BSA solutions, were employed to mimic the influence of pure polysaccharide and protein, respectively, on the fluid properties investigated

3 5 1 ECP Standard Solutions

Method No 1 An appropriate quantity of lyophilised ECP was dissolved in the relevant solution, namely water or medium, to formulate the highest standard concentration (*e g* 0 2 g of dried ECP in 100 ml of solvent for a 2 0 g l^{-1} ECP standard) This solution was further diluted to make standards of lower concentrations The ECP solutions were agitated, at room temperature, until all particles dissolved It was observed that solutions prepared in deionised water had a pH of approximately 4 and were found to be unstable since the ECP appeared to precipitate out of solution Therefore, these solutions could not be used for subsequent analysis However, medium (pH 5 5) proved to be a more compatible solution and was used for the formulation of all ECP standard solutions The rheological and surface tension characteristics of these solutions were analysed, as described in Section 3 4 1 and 3 4 2

Method No 2 An alternative technique for making solutions of known ECP concentration was devised because an ECP solution in water was required for foaming experiments (Section 3 7 2) ECP was partially purified as previously described (Section 3 4 3) but prior to the final precipitation step the sample was dialysed for 24 hours at 4°C Following the final precipitation step, the ECP was not redissolved in water The ECP was semi-dried at 25°C for 5-8 hours The ECP was then redissolved in the appropriate fluid (water or medium) A sample of this solution was lyophilised to ascertain the exact ECP concentration and the solution was further diluted if required

3 5 2 Protein Isolation and Characterisation

Attempts were made to isolate protein from cell-free broth, via an ammonium sulphate precipitation step (Harris and Angal, 1989) This is a technique which is frequently used for bulk protein recovery It is known to reduce the risk of irreversible denaturation, which is common to other organic salt precipitation methods

Ammonium Sulphate Extracellular Protein Precipitation

Ammomium sulphate was ground into a fine powder using a pestle and mortar before it was slowly added, under agitation on ice, to the broth An 80% salt saturation solution (561 g l^{1}) was used for complete protein precipitation It was evident from an early stage, before all the salt was added, that the ECP precipitated out of solution with the protein Therefore, this method was considered to be unsuitable for this work and further recovery steps were not completed It proved impossible to separate out protein and ECP by basic separation techniques A more complex separation procedure, such as gel filtration or chromatography would be necessary to achieve effective separation In any case, a more thorough study is required to achieve separation of broth ECP and protein, however, such experimentation was beyond the scope of this project

Techniques involving combined ethanol and tri-chloroacetic acid treatments were employed by Wagner *et al* (1988) and Proksch and Wagner (1987), to separate polysaccharides and proteins secreted by plant cell cultures of *Echinacea purpurea* Ion-exchange chromatography and gel filtration were used to characterise the polysaccharides This approach has potential for future work with *Morinda citrifolia* broths However, an investigation into the effect of tri-chloroacetic acid on the integrity of the proteins and polysaccharides would be necessary If denatured or structurally altered in any way, the foaming potential could be significantly affected

Intracellular Protein Isolation

Attempts were also made to obtain protein extracts from harvested biomass Tornkvist (1996) suggests that if the total intracellular protein composition is reflected in the cell-free broth protein composition, then its presence is attributable to cell leakage or cell lysis It was necessary to investigate if proteins present in the cell-free broth were similar to intracellular proteins recovered from disrupted *Morinda citrifolia* plant cells It was envisaged that if the two fractions were similar, it might be possible to obtain a

protein solution without an ECP constituent, for further investigation Disrupted cells released their cellular contents into the suspending fluid (deionised water) and the protein composition was then analysed using polyacrylamide gel electrophoresis (PAGE) under denatured conditions, to assess the protein content of the two fractions

The intracellular proteins were extracted according to the schematic protocol presented in Figure 3 9 Cells (170 g l^{-1} fresh weight) were removed from suspension by vacuum filtration, washed in deionised water and refiltered The cells were repeatedly frozen (3 times) with liquid nitrogen and thawed, while crushing with a mortar and pestle Chilled deiomsed water (300 ml) was used to resuspend the partially disrupted cells and the suspension was vortexed with glass beads for 5 minutes The mixture was then vacuum filtered and the filtrate was centrifuged for 15 minutes at 3000g to remove any remaining cellular debris This solution contained intracellular components, including anthraquinone (bright yellow m colour) On the basis of this sample, the average extracted protein concentration observed, via the Bradford method, for an 18 day old culture, was 0 025 mg ml^{-1} This corresponds to a protein recovery yield of 0 043 mg protein per g fresh weight An ultrafiltration step was then performed to concentrate the extract to a volume of approximately 20 ml, using an Amicon stirred cell 500 ml model system, with a 76 mm Ym 30 diaflo ultrafiltration membrane The concentrate was diluted with deionised water to a volume of approximately 200 ml and the ultrafiltration step was repeated, to dilute out contaminating substances, this step was repeated again It was evident, from the colour of the solution that anthraquinone levels were reduced but that not all anthraquinone was removed, by this step The final solution was diluted to an appropriate volume with deionised water

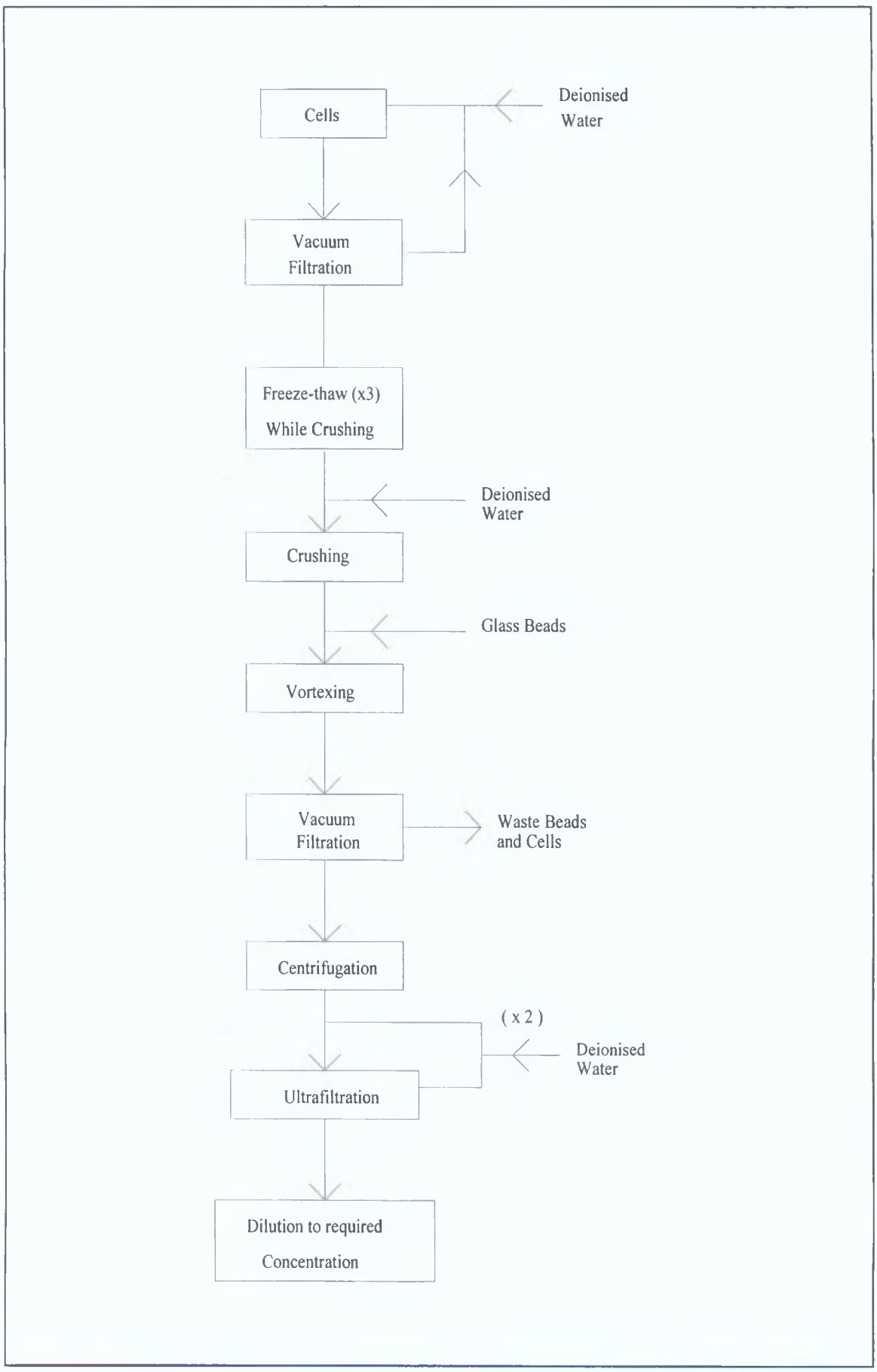

Figure 3.9: Protocol for extraction of intracellular proteins from suspension cells.

Protein Electrophoresis

Electrophoresis is used to separate and resolve a number of proteins on the basis of their different mobilities in an electric field This mobility is, in turn, a function of size, charge and the shape of the molecule Sodium dodecylsulphate (SDS) is an ionic detergent used to denature proteins It acts by wrapping around the polypeptide backbone, conferring a negative charge to all proteins in proportion to the length of the protein, thus resulting in a uniform charge density for all proteins Therefore, resolution is based exclusively on molecular weight and is independent of charge Polyacrylamide, the solid support matrix, is composed of acrylamide monomers, covalently crosslinked by N-N-methylene bisacrylamide, which hold the structure together The pores constituted by this bridging effect are responsible for the molecular sieving action of the gel

A protocol adapted from Maniatis (1989) was used with a mini-gel electrophoresis system (Atto) A 12% resolving gel and a 5% stacking gel were chosen to give an effective range of separation Table 3 3 details the composition of these gels As the samples to be analysed were not adequately concentrated, a 5X SDS gel-loading buffer was made up (Table 3 4) and samples were diluted to a 1X SDS loading buffer concentration (*i e* 4 parts sample 1 part 5X SDS loading buffer) The running buffer (pH 8 3) contained 25 mM Tris base, 250 mM glycine and 0 1% SDS The generator, (Consort E443), was set at 25 mA per gel A molecular weight marker (Murk 12^{TN}, Novex) was used alongside the samples The composition of this marker is outlined in Table 3 5 The refractive index (R_f) was calculated by dividing the displacement of a band by the total displacement of the dye front A semi-log plot of the MW as a function of refractive index should yield a straight line, which acts as a standard curve, against which the size of unknown proteins can be subsequently calculated, on the basis of refractive index values Figure 3 10 represent the log MW- refractive index relationship for the markers used in this system The linear regression coefficient was 0 955 A macro-gel system would be more beneficial, for accuracy of refractive index value calculation, since better resolution would be achieved

A quick stain Coomassie Brilliant Blue colloidal dye reagent (Boehringer Mannheim, UK) was used to stain the dye The positions of the protein bands were identified and the results compared

Table 3 3 Tris-glycine PAGE-SDS gels

Component	12% Resolving gel (25ml)	5% Stacking gel (5ml)
Deionised water	8 20 ml	3 40 ml
30% Acrylamide mix	10 00 ml	0 83 ml
1 0 M Tris (pH 6 8)	—	0 63 ml
1 5 M Tris (pH 8 8)	6 30 ml	—
10% SDS	0 25 ml	0 05 ml
10% Ammonium persulphate	0 25 ml	0 05 ml
TEMED	0 01 ml	0 005 ml

Table 3 4 5X SDS Loading buffer

Composition
250 mM Tris Cl (pH 6 8)
500 mM Dithiothreitol
10 % SDS
0 5 % Bromophenol blue
50% Glycerol

Table 3 5 Molecular weight marker

Composition	Molecular weight
Myosin	200,000 D
Galactosidase	116,300 D
Phosphorylase b	97,400 D
BSA	66,300 D
Lactate dehydrogenase	36,500 D
Carbonic anhydrase	31,000 D
Trypsin inhibitor	21,500 D
Lysozyme	14,400 D
Aprotinin	6,000 D

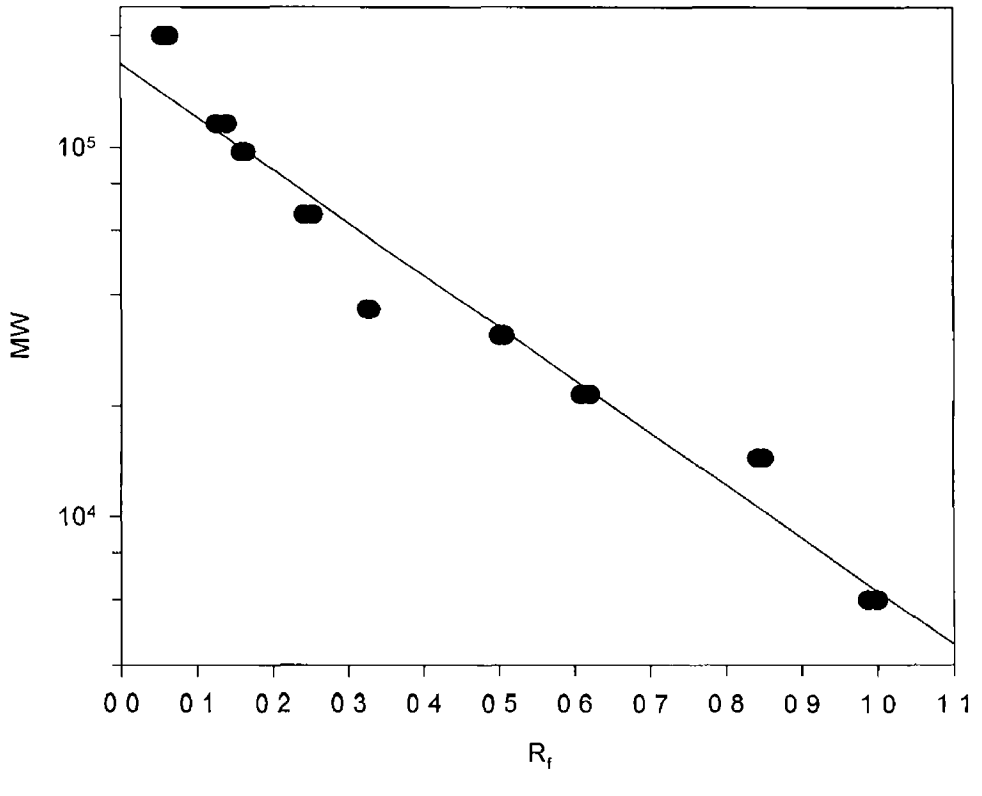

Figure 3 10 Sample standard curve for molecular weight determination

3 5 3 Protein Degradation

A protein digestion step was required for foaming analysis studies (Section 3 7) As neither the nature nor the composition of proteins present in the broth were known, a non-specific protease was required The enzyme Pronase (Sigma Chemicals, UK) was chosen In addition to illustrating its success in protein digestion techniques, Tornkvist (1996) established that Pronase has no effect on foaming This was confirmed in foaming trials on medium-based Pronase solutions, using column B4a in the current work

Pronase, at a concentration of 2 mg ml^{-1}, was used in the digestion of both cell-free broth (day 18) and 0 05 mg ml^{-1} solutions of BSA Solution pH was adjusted to the optimum value for enzymatic activity, *i e* pH 7 5, using 0 1 M HCl Solutions were incubated under gentle agitation at 37°C (optimum temperature) for 4 hours The pH of the control solutions (BSA and cell-free broth without Pronase addition) was also adjusted to a pH value of 7 5 and the solutions were incubated under the same conditions Following the incubation period, all solutions were returned to their original pH, prior to further analysis

Table 3 6 summarises the pH of solutions before and after the incubation period The protein composition of all samples and the degree of protein degradation by Pronase was qualitatively determined using electrophoresis The solutions were then used for further foaming studies, (Section 3 7) The ECP precipitated out of solution in the cell-free broth (solution 1) upon protein degradation, and it was not possible to reverse the action via agitation or pH adjustment, therefore, this solution was vacuum filtered, through Whatmans no 1 filter paper, to remove the undesirable gel-like particles for foaming experimentation

Table 3 6 pH of digestion solution

Solution No / Description		pH			Pronase
		Before Adjustment	Beginning of Incubation	End of Incubation	
1	Cell-free broth	5 36	7 5	4 8	✓
2	Control cell-free broth	5 36	7 5	7 45	×
3	BSA	7 0	7 5	7 4	✓
4	Control BSA	7 0	7 5	7 5	×

3 5 4 Model System Studies

Xanthan gum solutions were prepared by dissolving dried xanthan (Sigma Chemicals) in water or medium, *e g* a 0 02% xanthan solution (w/v) is made by dissolving 0 2 g xanthan in 1 l of fluid Upon addition of xanthan, it was necessary to agitate the solution at high speed, at room temperature, for a lengthy period of time, typically 2 to 4 hours, to ensure complete dissolution BSA solutions were formulated in water, medium or xanthan solution, by dissolving the appropriate quantity of BSA (Sigma Chemicals) in the appropriate fluid Upon addition of BSA, the solution was agitated gently, to avoid foaming, at room temperature, for approximately 10 to 20 minutes The pH, surface tension and viscosity of these solutions were examined by the same methods described under Sections 3 2 2, 3 4 1 and 3 4 2, respectively, for cell-free broths

3 6 BUBBLE COLUMN DESIGN AND VALIDATION

The main objective in the design of a bubble column was to create an apparatus which produces reproducible, stable foams Four of the most important parameters to consider are gas dispersion, column dimensions, ease of maintenance and cost of manufacture Many bubbling columns have been designed by other researchers to suit their experimental requirements, including Wongsamuth and Doran (1994), Kawase *et al* (1990), Edwards *et al* (1982), Lalchev *et al* (1982), Bumbullis and Schugerl (1981), Mita *et al* (1976) and Cumper (1953) For example, Cumper used a glass sintered membrane (40-50μm pore size), which extended across the entire cross-section of the bubble column, of diameter 3 6 cm, while Mita employed a sintered glass sparger (porosity no 3) with a diameter of 3 cm in a bubble column with a 4 0 cm internal diameter Sie and Schugerl (1983) used a column 5 5 cm in diameter with a porous glass aerator of 1cm in diameter (G4 fritt) Bikerman (1973) described different types of gas diffusion devices typically used for such applications, including pipe spargers and sintered diffuser devices As outlined in Section 2 1 1, small bubbles contribute to foam stability Bubble size distribution is further influenced by aeration rates and the prevailing fluid properties For the dynamic method of foam measurement chosen, two criteria must be met It must be possible to produce a stable measurable foam, *i e* steady state must be reached and secondly, the foams generated must be reproducible and consistent

3 6 1 Bubble Column Design and Operation

Taking the parameters important in column design into consideration, two different designs, illustrated in Figures 3 11 (Type A) and 3 12 (Type B), were employed for these foaming studies Sintered dispersion devices of different porosity numbers were used and the corresponding pore sizes are summarised in Table 3 7 Flat sintered glass discs were used for Type A bubble columns, while cylindrical sintered glass diffuser bulbs were employed for Type B bubble columns Table 3 8 outlines the combination of column type and sinter porosities investigated for each model designed

Table 3 7 Sintered device pore size

Porosity Number	Pore size (μm)
0	160 - 250
1	100 - 160
2	40 -100
3	16 - 40
4	10 - 16

Table 3 8 Bubble columns investigated

Column Type/No	Sparging device	Porosity No	No Produced
A1	Flat disc	0	2 (a, b)
A2	Flat disc	1	1
B1	Porous Stone	unknown	1
B2	Bulb	0	1
B3	Bulb	1	1
B4	Bulb	3	2 (a, b)
B5*	Bulb	3	1

* A Perspex column was used

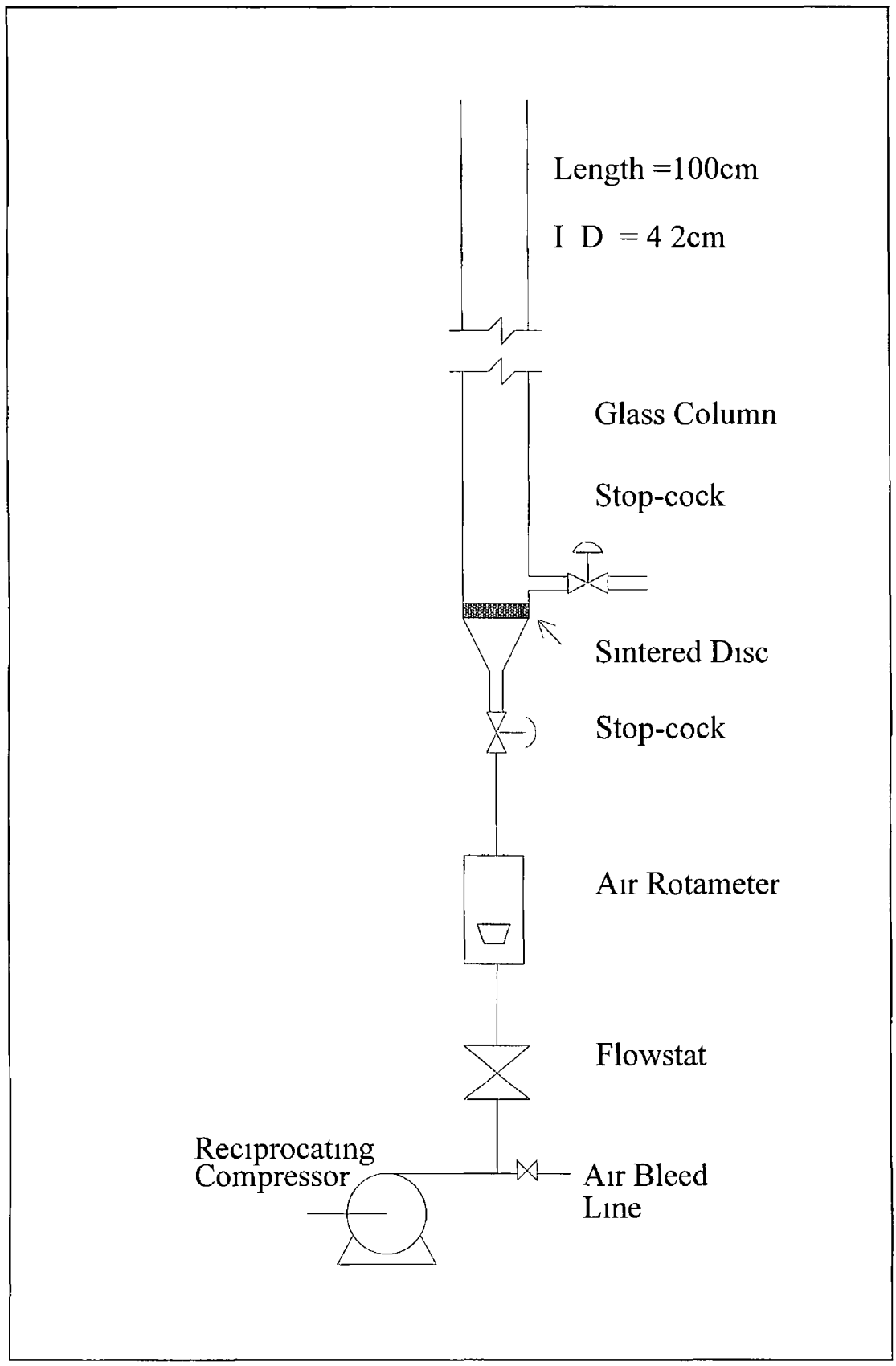

Figure 3 11 Schematic diagram of the experimental apparatus employing Column Type A

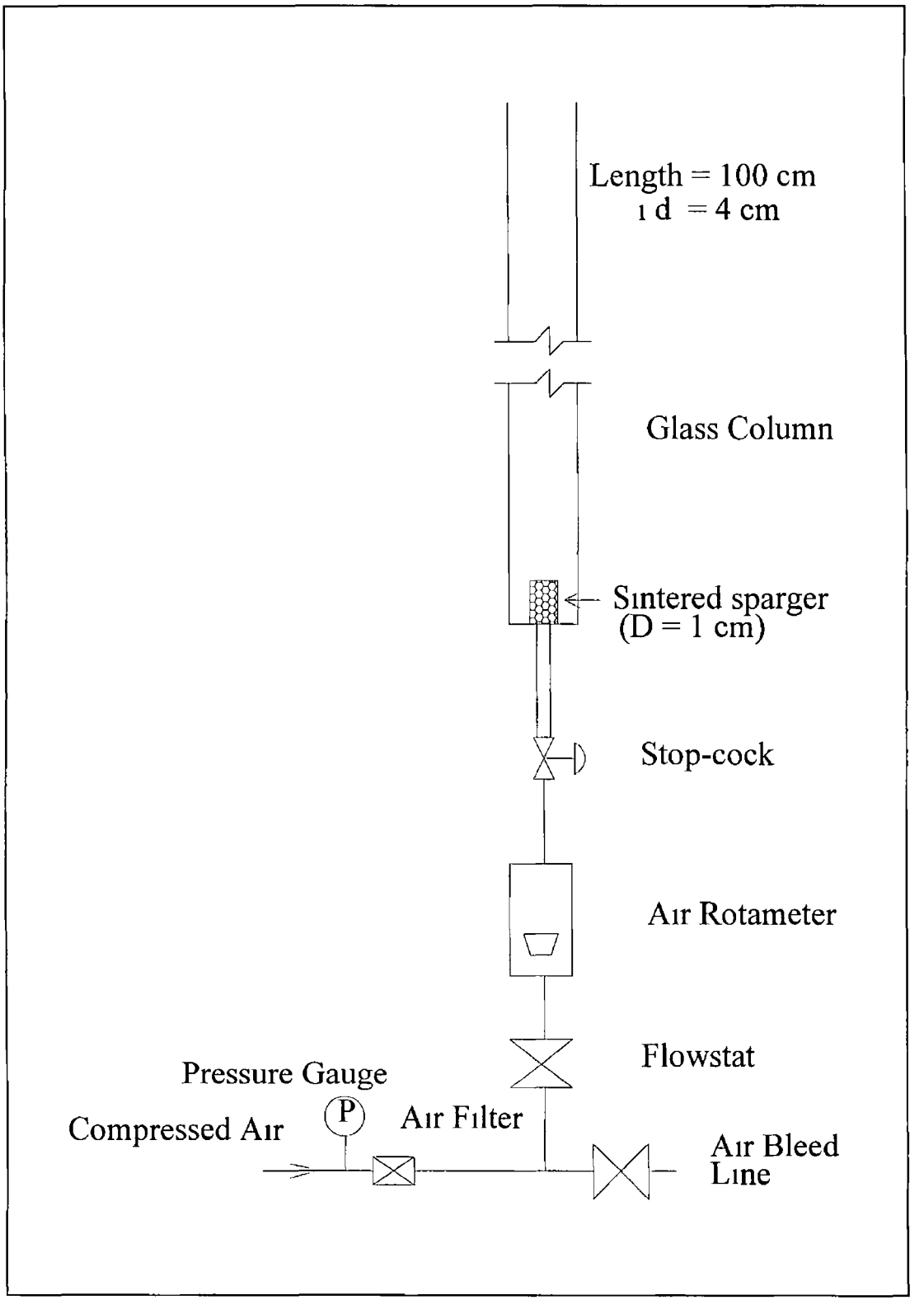

Figure 3 12 Schematic diagram of the experimental apparatus employing Column Type B

Bubble Column Type A

Figure 3 11 shows a schematic diagram of the column and the entire ancillary experimental apparatus A flat glass sintered disc (Bibby Pyrex) of diameter 4 0 cm was inserted (glass blown) into a 1 m length glass column, of internal diameter 4 2 cm (AGB Glassworks, Ireland) A conical section beneath the disc promoted good air dispersion The column was connected to an air supply by a short length of silicone tubing attached to the base of the column A reciprocating compressor (B100 Dep , Charles Austen Pumps Ltd , UK) was used for aeration purposes The compressor outlet was connected to a diaphragm flowstat controller (Platon, UK), to immediately dampen air surges A rotameter (Platon, UK) installed downstream from the flowstat was used for air flow rate regulation and measurement Two rotameters were employed, depending on the flow rate required The smaller rotameter was capable of measuring and controlling air flow rates in the range 0 33 to 12 5 ml s^{-1}, while the larger had an operation range of between 5 and 20 ml s^{-1} A bleed line installed between the pump and the flowstat was used to manually regulate pressure in the system Liquid samples were introduced to the column through a side arm near the base of the column, above the sintered disc, using a peristaltic pump An adhesive measuring tape, with 1 mm graduations, was attached to the outside of the column, to facilitate measurement of foam heights

Bubble Column Type B

Figure 3 12 shows how this column design deviates from Type A A cylindrical gas dispersion unit, approximately 1 0 cm in diameter and 1 5 cm high, was inserted into a Perspex disc Modified gas dispersion bulbs (Bibby Pyrex) were used for bubble columns B2-B5 The original gas dispersion bulb, when purchased, consisted of the porous bulb connected to a 30 cm hollow glass tube, this tube was cut to approximately 5 cm, incorporation into the apparatus The cylindrical gas dispersion unit used for bubble column B1 was a standard porous aeration stone, of the type used in domestic fish tanks Unfortunately, the porosity of this device is unknown This type of cylindrical gas dispersion unit was chosen as an alternative to the flat sintered discs employed in Type A, which proved unreliable (Section 3 6 3) The bulb was glued, with an epoxy resin, in position This Perspex disc containing the porous element was secured to the base of the glass column using Parafilm™, reinforced with masking tape to ensure no leakage occurred This bottom segment could thus be conveniently removed for cleaning and maintenance purposes A conical segment at the base of the

column, as in Type A, was not required. The inlet air line was connected directly to the bulb unit. A Perspex column (B5) was investigated as an alternative to glass, in a trial study on the suitability of Perspex for these studies.

It was observed, in the Type A design, that the inlet port at the side of the column disturbed bubble flow pattern, therefore, no side port was incorporated into the Type B design. Samples were pumped into the column via a silicone tube, lowered down from above. After charging, the tube was carefully removed, to avoid wetting the interior of the column walls above the liquid level. The ancilliary equipment employed was similar to that described for Type A, except the filtered air was supplied via a pneumatic compressor unit (Schrader Bellows, UK) at a gauge pressure of 0.6 bar. This overall design is simpler, cheaper to manufacture and easier to maintain than Type A.

Operation and Maintenance

All columns were installed on a purpose built metal support stand, (Figure 3.13). Orientation was routinely checked, using a spirit level, before each foaming experiment The basic procedure for all foaming experiments was essentially the same. Samples (either 80 ml or 50 ml samples as appropriate) were incubated at 20°C and introduced into the column. The initial fluid height was recorded. The airflow rate was adjusted to the appropriate setting, and the height of the foam and level of the residual unfoamed fluid were recorded at 30 second intervals, until an equilibrium position was reached. For spargers with a porosity number less than 3, it was necessary to take special precautions to avoid backflow of liquid through the sintered element. This was achieved by maintaining a slight positive pressure on the underside of the disc/bulb while introducing the fluid sample. Calibration of rotameters employed was routinely checked using liquid displacement.

Following each foaming trial, the column was washed thoroughly with a hot dilute solution of Teepol, rinsed repeatedly in hot and cold water and finally in deionised water. The column was then dried in a warm oven. Columns were washed occasionally in dilute HCl and warm dilute NaOH. The sintered gas dispersion devices were cleaned at least weekly in hot NaOH (at a temperature of approximately 60°C) and in 5M H_2SO_4. This rigorous cleaning procedure was essential, as microbial growth was found to occur in the sintered devices if they were not maintained correctly.

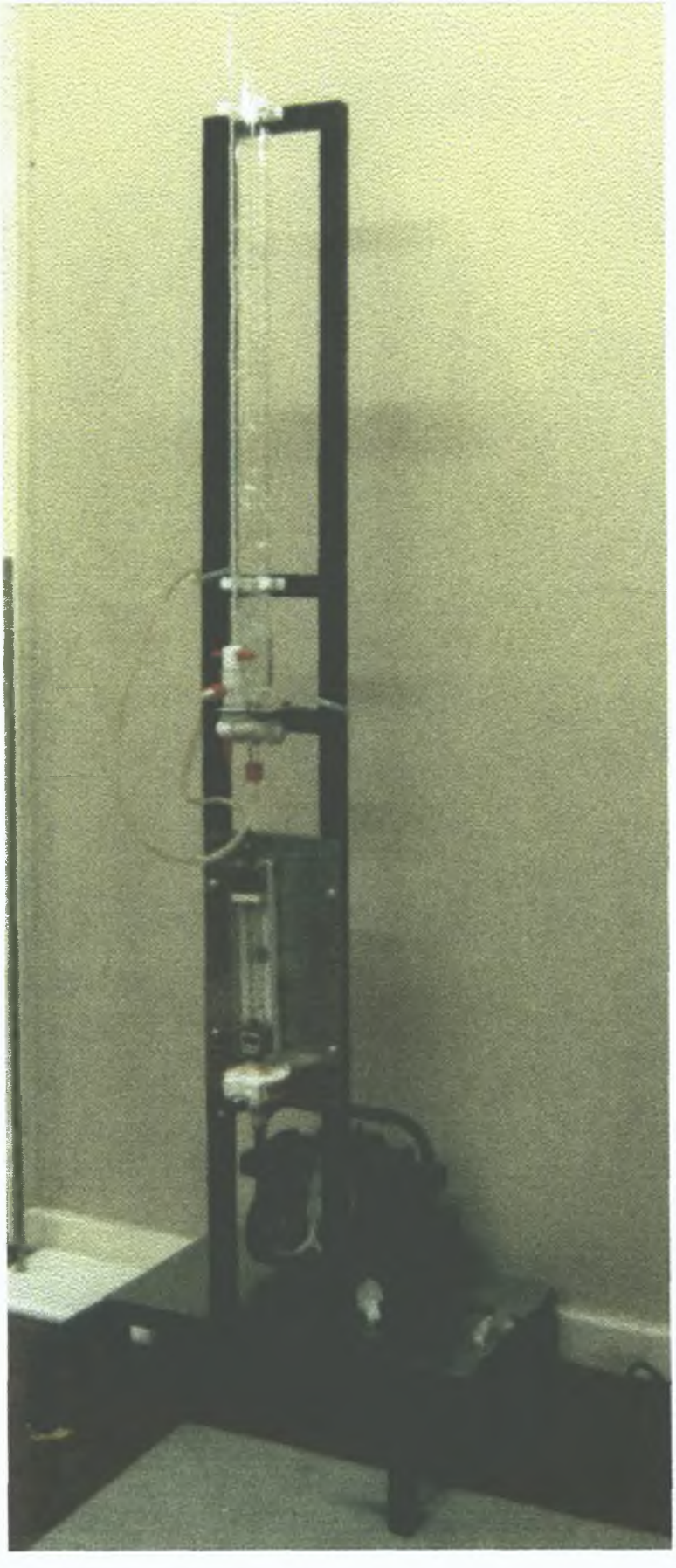

Figure: 3.13: Bubble column foaming apparatus - Type A (Individual components as labelled in Figures 3.11).

3 6 2 Validation Studies

Pandit (1994) worked with Teepol in a study on foaming using a column of approximately twice the size of the apparatus employed in this study (i e 2 4 m in height and 8 8 cm in diameter) A distributor plate incorporating sixty two 1 mm holes was used for air sparging Thus, the bubbles formed were of a considerable size Validation trials performed in thus study with the two most dilute Teepol solutions, used by Pandit, (*i e* 0 5 and 1 0 g l^{-1}), in Column A1a (sinter pore size 160 -250 μm) were unsuccessful The foam generated at a Teepol concentration of 1 g l^{-1} did not stabilise, but continued to rise beyond the vertical limit of the designed apparatus and at a concentration of 0 5 g l^{-1}, the foam was unstable Therefore, Teepol solutions were considered inappropriate for further validation purposes

BSA has been employed in many foaming studies to date and BSA solutions in deionised water (0 0-1 0 mg ml^{-1}) were found to be more suitable in the current work All bubble columns, outlined in Table 3 8, were subjected to rigorous validation trials, to ensure that the design was appropriate for experimental use (*i e* bubble distribution patterns were suitable for producing reproducible stable foam heights) However, only two columns were found to be suitable for further foaming analysis, namely the first Column A1 design, and the first Column B4 design, referred to as Column A1a and Column B4a in subsequent work Since, these are the only columns of importance, only validation experimental parameters for these columns will be presented For all columns, the BSA concentrations and aeration rates for validation were selected by experimental trial and error, on the basis that they ensured uniform bubble distribution, generating a stable homogeneous foam which was retained inside the bubble column

Column A1a was validated using 0 5 and 1 0 mg ml^{-1} solutions of BSA in deionised water, at air flow rates of between 3 33 and 16 67 ml s^{-1} (corresponding to a range 2 5 to 12 5 vvm) Lower BSA concentrations (*i e* 0 2 mg ml^{-1}) did not produce significant foam heights The range of flow rates selected ensured good bubble distribution, and produced foams of suitable measurable heights for the particular solution Unfortunately, the range of flow rates that could be used was small, due to size restraints of the column and thus only limited data could be collected The range of BSA solution concentrations and aeration rates validated in Column A1a are summarised in Table 3 9

Table 3 9 Column A1a validation experiments

BSA Concentration (mg ml^{-1})	Aeration Rate (ml s^{-1})
0 5	3 33, 8 33, 16 67
1 0	3 33, 8 33

Column B4a was validated using BSA solution concentrations of between 0 1 and 1 0 mg ml^{-1}, at air flow rates of between 1 0 and 4 ml s^{-1} (corresponding to 0 75 to 3 0 vvm) As expected, not all aeration rates could be used for all BSA concentrations, due to the same limiting factor (*i e* column height), as applied for Column A1a Table 3 10 summarises the combination of BSA concentrations and aeration rates employed for validation of 80 ml samples in Column B4a The validation of a 50ml sample volumes, as opposed to 80ml, was performed using a 0 5 mg ml^{-1} solution of BSA, at a range of aeration rates between 1 0 and 3 6 ml s^{-1} The results where compared to that of the 80 ml aliquot to determine if 50 ml was an adequate sample volume The smaller sample volume was employed due to experimental difficulties encountered with an 80 ml sample volume in subsequent foaming work (Section 3 7)

Table 3 10 Column B4a validation experiments

BSA Concentration (mg ml^{-1})	Aeration Rate (ml s^{-1})
0 1	1 2, 1 9, 3 0
0 2	1 0, 1 25, 1 9, 2 25, 2 4, 2 8
0 5	1 0, 1 7, 2 0, 2 4, 2 7, 3 6
1 0	1 25, 2 0, 2 5

For all columns employed for further foaming analyses, validation checks were repeated at regular intervals to confirm the reproducibility of column performance

3 6 3 Column Design Development

After a 6 month working period, a deterioration in the performance of Column A1 was observed and was thought to be attributable to erosion and/or clogging of pores in the sintered disc Although stringent cleaning protocols were implemented, it was not possible to reverse the effect A similar design, nominally identical to the first was constructed (Column A1b) However, bubble distribution was uneven and the reproducibility of the foaming behaviour in this model was poor, it was not used for foaming studies Column A2 was then constructed This model was similar to Column A1 except that a sintered disc of smaller pore size (porosity 1) was used, in an attempt to

promote better bubble distribution However, no stable foams were formed in Column A2, under any of the conditions investigated (0 2 - 1 0 mg ml^{-1} BSA, 3 33 - 16 67 ml s^{-1} air) and therefore, it was not used for further work As previously mentioned, Column A1a is the only example of a Type A design which was successfully validated Foaming data for cell-free broth solutions were collected during the first five months of its operation, (*i e* while reliable consistent performance was assured)

Type B columns were developed in a bid to overcome some of the difficulties described above It has been reported by Mita *et al* (1977), Bumbullis and Schugerl (1981) and Sie and Schugerl (1983) that a smaller air dispersion device, which concentrates the bubbling towards the centre of the column creates a more evenly distributed foam and hence, porous bulbs and stones were investigated as alternate sparging devices

Column B1 produced uniform bubble distribution patterns, yielding stable foams at BSA concentrations in the range 0 1-0 5 mg ml^{-1} for aeration rates between 1 5 and 3 33 ml s^{-1} However, the porous stone was not sufficiently robust for extended use It was observed to disintegrate gradually, thereby, disturbing stable foam generation Reproducibility of performance could only be assured, for each stone, for approximately 1 week of routine operation and each stone produced slightly different foaminess data for identical solutions Therefore, this design was not employed for subsequent foaming studies

A more robust air dispersion device was obviously required and gas dispersion bulb units were installed in Columns B2 and B3 As previously stated, the glass tubes connecting to the sintered bulbs, were cut to a length of 5 cm However, these units produced unevenly distributed streams of relatively large bubbles, in comparison to the porous stone used in Column B1 Consequently, stable foams were not achieved

Column B4a, having a bulb of smaller sinter pore size (porosity 3), produced the most reliable foams As previously stated, this column was successfully validated and a reproducible set of validation data was compiled This column was observed to perform reliably over a 5 month period, after which time deterioration was observed and the column was withdrawn from service Another, nominally identical, column was constructed (Column B4b), which again produced stable foams, although slightly

different heights were recorded, under the same operating conditions for identical solution concentrations. Data collected from this column could not be directly compared with earlier data collected for the same column design (Column B4a), therefore, no further trials were performed.

A glass column by its very nature is a very fragile piece of equipment and Perspex was investigated as an alternative material for column design. However, on the basis of experience with Column B5, Perspex was found to be unsuitable for foaming experiments. Although foam was successfully generated, after a period of time the core of the foam was observed to disintegrate, leaving a stable shell at the walls of the column. The build up of static on the Perspex may possibly have caused the bubbles to cling to the column while the core of the foam drained. No foaming data were collected using this column.

3.7 FOAMING STUDIES

3.7.1 Cell-Free Broth Foaminess through the Growth cycle

Foaming potential studies were conducted using Columns A1a and B4a. Experiments were performed on cell-free broth samples, which were prepared as outlined in Section 3.4 on days 0, 3, 6, 8, 11, 14, 17 and 21 of the batch growth cycle.

Using Column A1a (porosity 0), 80 ml aliquots of untreated cell-free broth, at the cultures ages outlined above, were tested at air flow rates of 3.33, 8.33 and 16.67 ml s^{-1}, according to the operational procedure described in Section 3.6.1, for this Column Type.

Following numerous trial and error attempts to identify a suitable range of air flow rates, for foaminess studies of cell-free broths, throughout the growth cycle, using Column B4a (porosity 3), only a single air flow rate of 1.0 ml s^{-1} could be used for these solutions. It also proved necessary to reduce the sample volume to 50 ml from the standard 80 ml sample, as even at minimal air flow rates of 1.0 ml s^{-1}, the larger volume produced foams which exceeded the capacity of the column. At higher air flow rates, the quantity of liquid incorporated into the foam, particularly at the later stages of the growth cycle, was too great to ensure sufficient liquid coverage above the air dispersion device. At lower aeration rates, flow rate stabilisation was difficult and bubble

distribution did not appear homogeneous Therefore, for all further applications using this bubble column, 50 ml samples were only employed at an aeration rate of 1 ml s^{-1}

Cell-free broth was recovered, after foaming, for a day 11 sample, at which stage culture foaminess was maximal, after foaming, by removing the plate at the base of the column and collecting the fluid in a container The viscosity and protein content of this solution were determined and compared to the corresponding values before foaming commenced

3 7 2 pH Effects on Foaminess

Cell Free Broth

The effect of pH on the foaming potential of cell-free broths was assessed, within the pH range 4 to 6, using Column B4a This range was chosen as these are the limits of pH variation throughout the normal growth cycle The pH was adjusted using low molarity HCl or NaOH, as appropriate, prior to foaming experiments Different molarity HCl and NaOH were used, to minimise the extent of sample dilution

Suspension Isolates

Using standard Column B4a operating conditions (*i e* 50ml samples, 1 ml s^{-1} air flow rate), experiments were performed on both aqueous and medium-based partially purified ECP solutions at pH values of between 4 and 7 ECP solutions were formulated as described in method no 2 (section 3 5 1) and pH was controlled by the addition of low molarity HCl

3 7 3 Foaminess Evaluation of Protease Digested Samples

The foaming potential of protease digested samples of cell-free broth and 0 5 mg ml^{-1} BSA solutions was determined However, prior to foaming, the cell-free broth digested sample was observed to contain precipitated ECP and therefore, attempts were made to foam the solution with the suspended particles and again after their removal by filtration The foaminess of the control solutions, without enzyme, was investigated to observe the effects of incubation at 37°C and pH adjustments on the cell-free broth and BSA solutions Section 3 5 3 describes the protocol employed for the preparation of these samples

3 7 4 Model System Foaminess Studies

All experimentation was performed using Column B4a, at an air flow rate of approximately 1 ml s^{-1}, using a 50 ml sample volume, as described in Section 3 6 1 Solutions of varying concentrations of xanthan gum and BSA were foamed, to elucidate the effect of each component on foaminess Table 3 11 summarises the range of experimental conditions examined Solutions were prepared, as described in section 3 5 4

Table 3 11 Composition of model foaming solutions

Trial No	BSA (mg ml^{-1})	Xanthan (%)	Base Fluid
1	0 - 1 0	—	water
2	0 - 0 2	—	medium
3	0 - 0 2	0 02	water
4	0 - 0 1	0 02	medium
5	0 2	0 - 0 04	water
6	0 1	0 - 0 03	medium
7	—	0 - 0 04	water
8	—	0 - 0 04	medium

3 8 ANTIFOAM STUDIES

3 8 1 Effect on Suspension Growth and Foaming Characteristics

The effect of a silicone antifoamng agent (BDH, England) on the growth, productivity and foaming potential of *Morinda citrifolia* suspension cultures was determined A single antifoam concentration of 100 ppm was investigated As the antifoam was very viscous, accurate pipetting proved difficult Therefore, a quantity of weighed antifoam was washed from a weighing boat into the medium The resulting solution was agitated for 30 minutes to ensure complete dispersion of the antifoam The antifoam-enriched medium was dispensed into Erlenmeyer flasks Autoclaving and subculturing were then performed as described in Section 3 1 The fresh and dry weights, pH, protein and ECP content, surface tension, viscosity and Bikerman foaminess of all antifoam-enriched broths were investigated, using the methods previously described for culture broths The results were directly compared to those for cell suspensions cultivated without antifoam

3 8 2 Investigation of Antifoam Degradation during Cultivation

A comparison was made between the effect on foaming of antifoam added as described above, before subculturing and antifoam added directly to extracted cell-free broth immediately prior to foaming In the latter instance, the antifoam was not present during autoclaving or culture growth The antifoam was added to the cell-free broth in a similar manner to that described above This study was performed to examine the loss of antifoam activity during cultivation

A preliminary analysis of the foaming potential of a day 11 cell-free broth was performed using direct addition of silicone antifoam at a concentration of 100 ppm and 50 ppm On day 11, in a normal cell cycle, foaming is maximal for this plant cell suspension system

Chapter 4

RESULTS[2]

4 1 *MORINDA CITRIFOLIA* SUSPENSION GROWTH CHARACTERISTICS

4 1 1 Suspension Biomass Growth Profiles

The growth characteristics of *Morinda citrifolia* suspensions, grown in 250 ml shake flasks, are broadly similar to those of typical microbiological systems Distinctive lag, exponential and stationary phases are identified On inoculation, the culture enters a lag phase of 3-4 days, after which an exponential phase is observed for the following 8-10 days (on the basis of cell number and fresh weight) For the remaining 7 days, the cultures are in the stationary phase, during which the biomass concentration declines slowly Figure 4 1 shows the variation in fresh and dry weight biomass concentrations throughout the twenty-one day growth cycle Errors bars indicate the standard error calculated for six independent growth cycles Where fresh weight is used as a growth profile reference in subsequent graphs, the error bars are omitted for clarity The suspension fresh weight increases approximately 10 fold from 30 g l^{-1}, while the dry weight varies between about 1 g l^{-1} and 14 g l^{-1} Figure 4 2 shows that the cell number typically increases from 0 5 × 10^6 cells ml^{-1} at inoculation, to 5 0 × 10^6 cells ml^{-1} at the end of the cycle Doubling times of approximately 60 and 65 hours are calculated for this system under the prevailing growth conditions on the basis of dry weight and cell number, respectively Observed variations in the growth profiles were thought to be attributable to unavoidable variations in incubation conditions (*i e* temperature, 25° ± 1°C and orbital shaker speed ± 10 rpm)

4 1 2 Suspension pH Profile

The variation in suspension pH over the course of the growth cycle is indicated in Figure 4 3 The error bars represent the standard error for six growth cycles At inoculation, the suspension pH is 5 5 During the first 6 days the pH falls to approximately 4 0, after which it increases to a maximum of approximately 5 8 and eventually levels off during the stationary phase The fresh weight profile is presented

[2] Raw data is presented in Appendix C

with the pH curve, to indicate the various stages throughout the growth cycle during which the pH changes

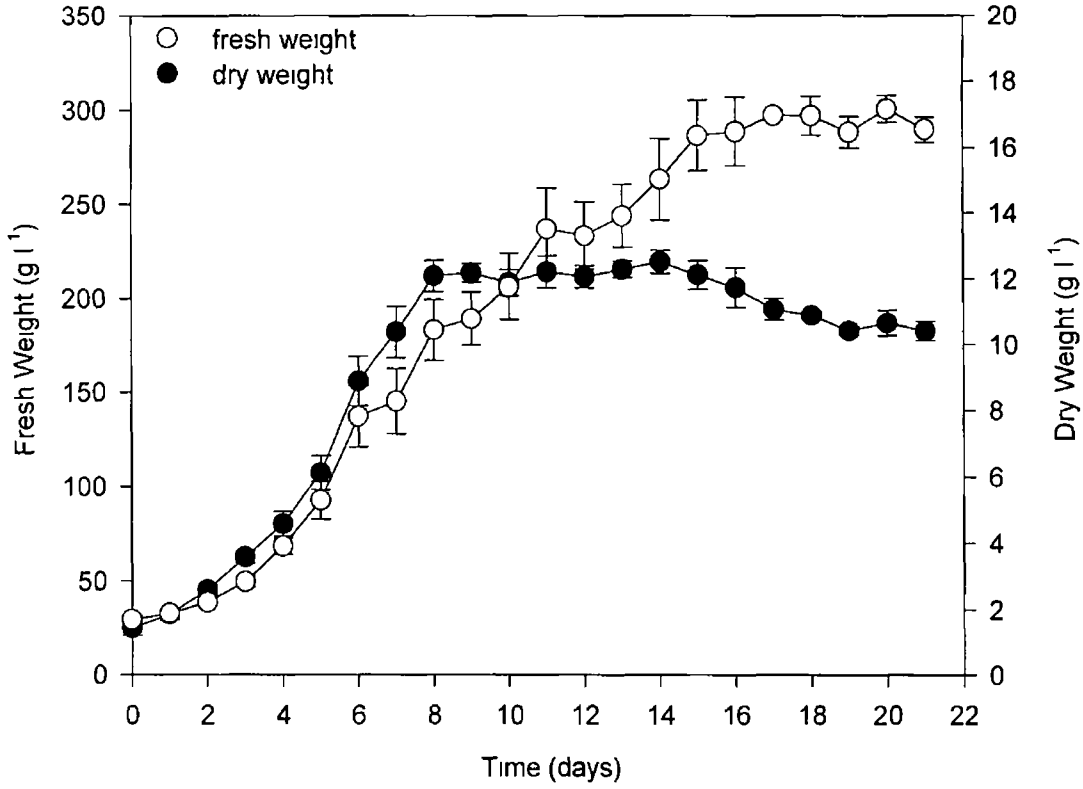

Figure 4 1 Fresh and dry weight growth profiles for *Morinda citrifolia* suspension cultures, grown in 250 ml shake flasks (No of replicates (n) = 6)

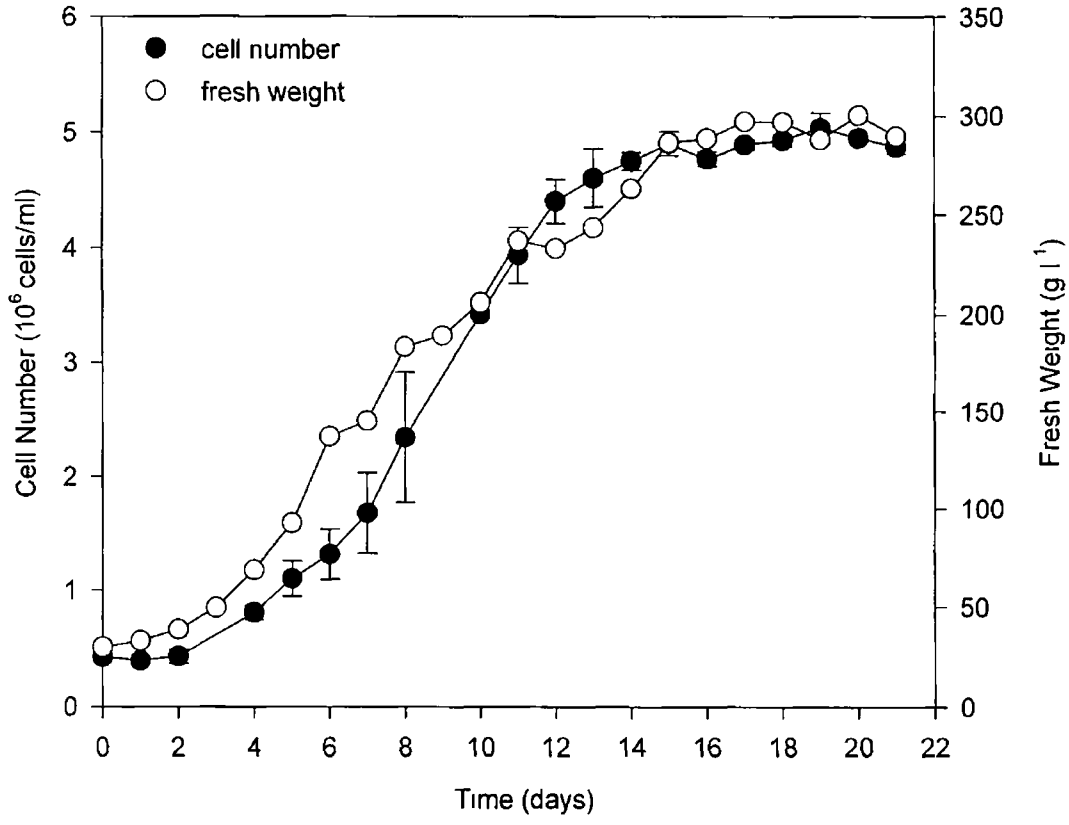

Figure 4 2· Fresh weight and cell number growth profiles for *Morinda citrifolia* suspension cultures, grown in 250 ml shake flasks (n= 3)

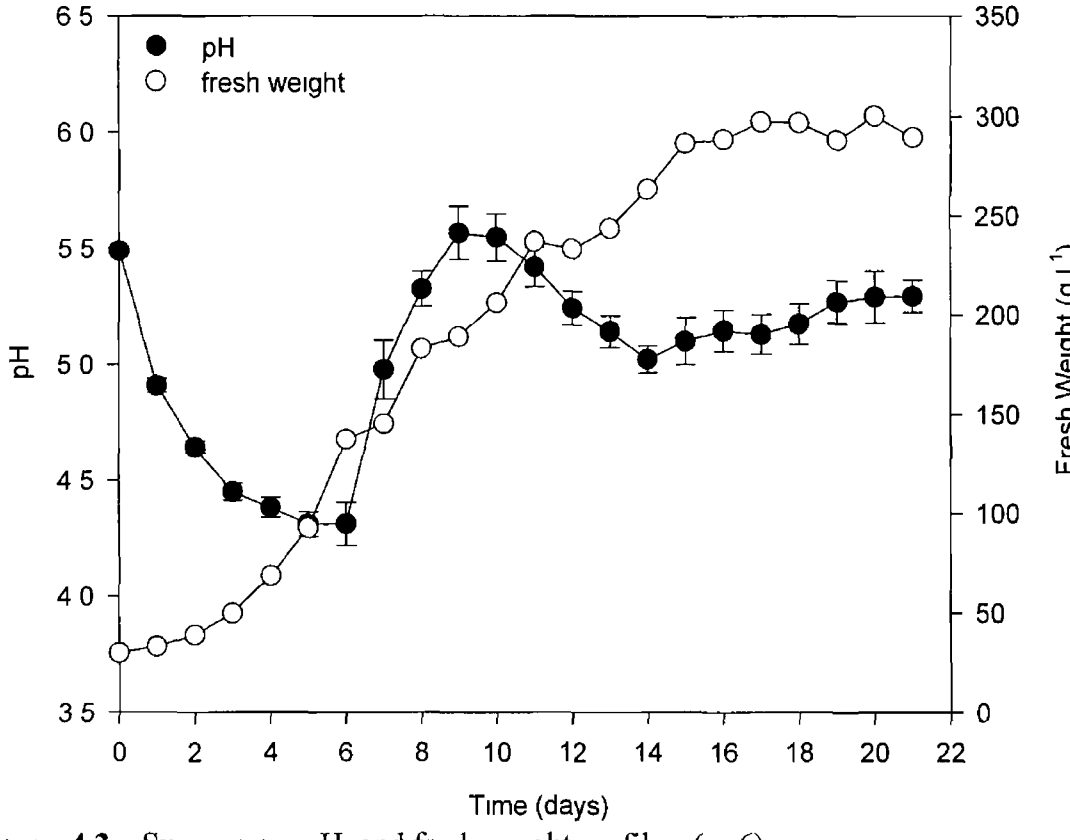

Figure 4 3 Suspension pH and fresh weight profiles (n=6)

4 1 3 Suspension Conductivity

The suspension conductivity, as measured throughout the growth cycle, is shown in Figure 4 4 Conductivity decreases gradually during the lag phase and proceeds to decrease more rapidly, as the culture requirements increase during the exponential growth phase Towards the end of the cycle, as existing cells are maintained but cell replication is minimal, conductivity is seen to decrease more slowly The relationships between biomass concentrations and conductivity are illustrated in Figures 4 5 and 4 6 These data indicate the potential for using conductivity as a rapid means of monitoring growth for this plant cell suspension culture The correlation of conductivity with fresh weight (Figure 4 5) and cell number (Figure 4 6) is evident, with linear regression coefficients of 0 993 and 0 991, respectively The dry weight relationship is also linear for the first nine days of the cycle, displaying a linear regression coefficient of 0 992 (Figure 4 5) However, no direct correlation applies for the remainder of the growth cycle It can be seen from the dry weight profile (Figure 4 1) that during this time, the dry weight falls gradually The slopes of the indicated lines, for the growth cycle illustrated, are 0 0068 (mS cm^{-1}) / (gl^{-1}) with respect to fresh weight, 0 0958 (mS cm^{-1}) / (gl^{-1}) with respect to dry weight (for the first nine days) and 0 3907 (mS cm^{-1}) / (10^6 cells ml^{-1}), for cell number

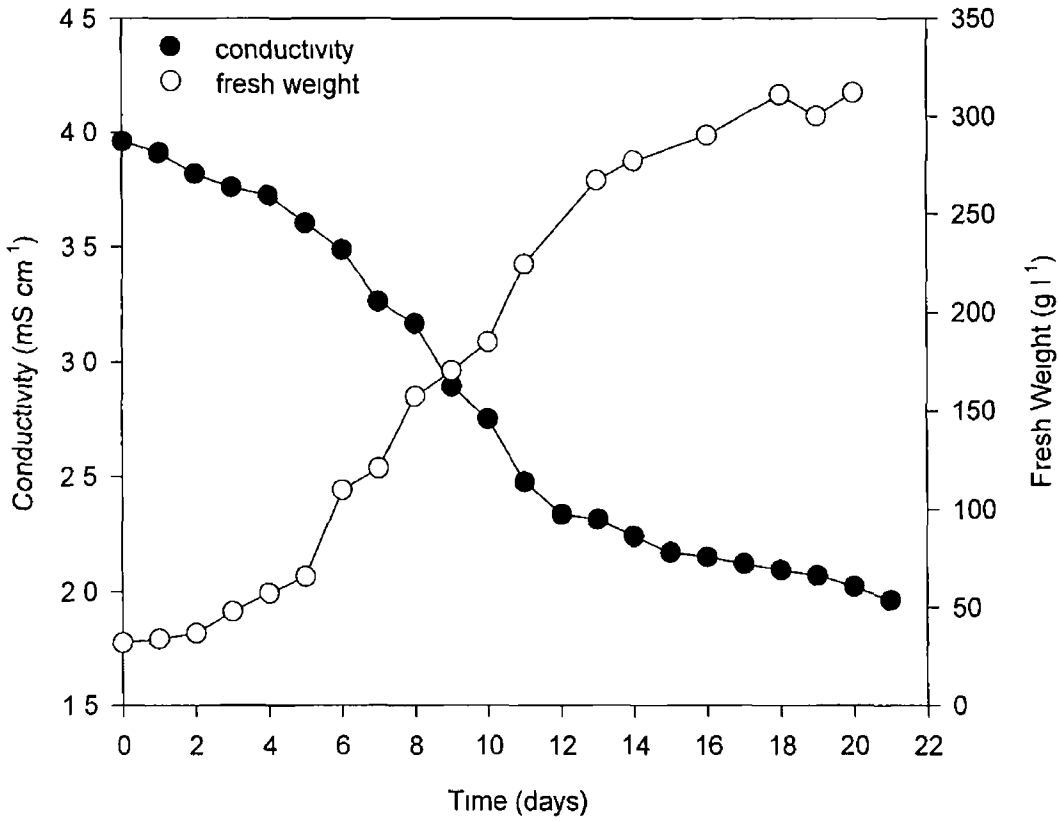

Figure 4 4 Suspension conductivity and fresh weight profiles

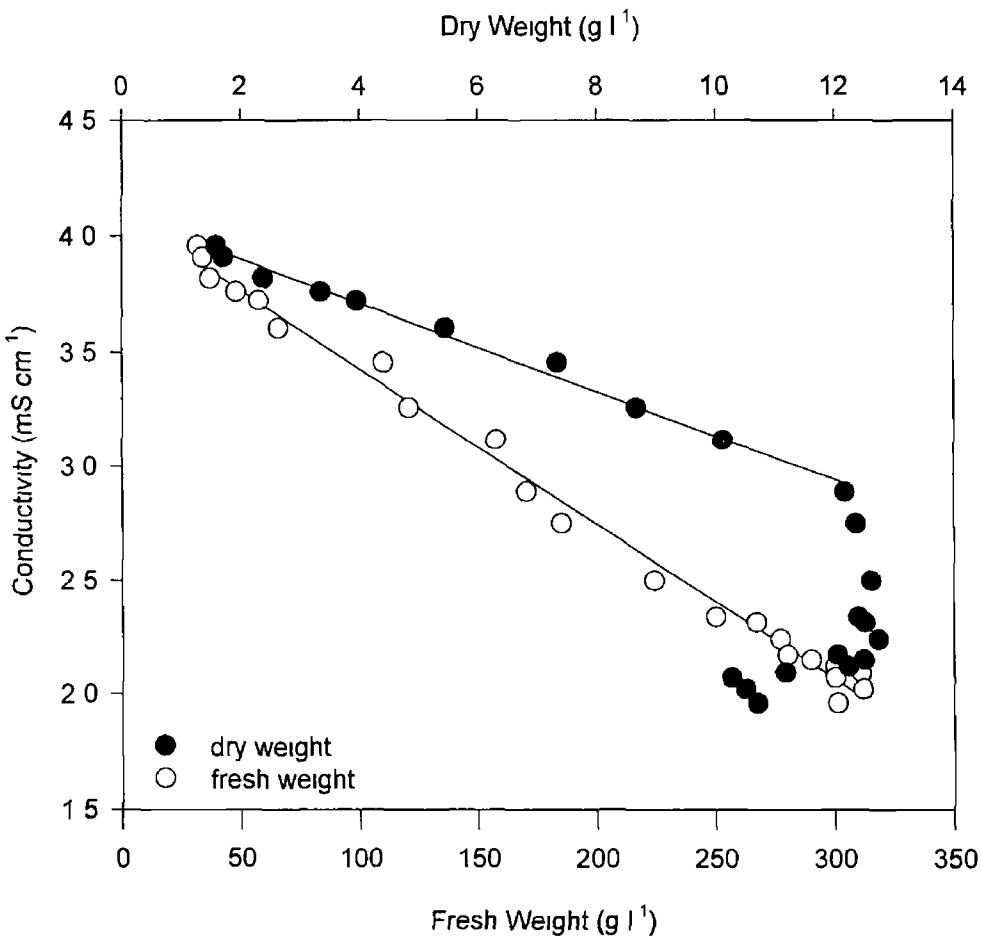

Figure 4 5 Variation of broth conductivity with fresh and dry weight

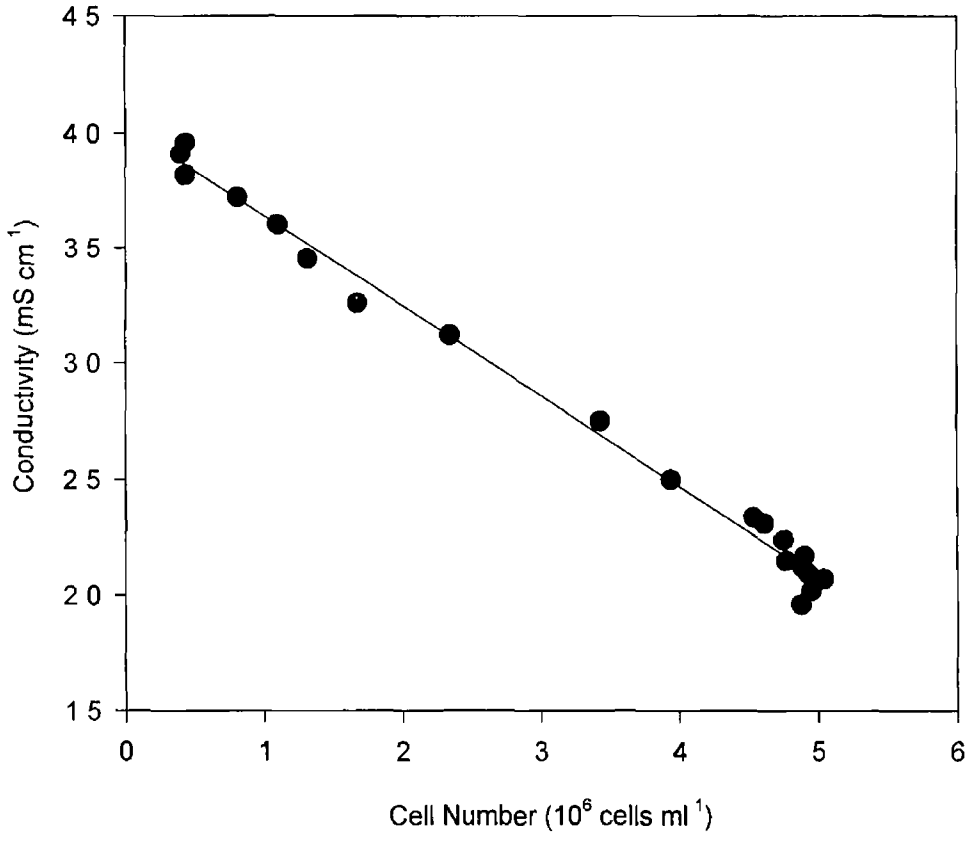

Figure 4 6 Variation of broth conductivity with cell number

4 1 4 Suspension Morphology

When grown in shake flasks, *Morinda citrifolia* cultures have been characterised as homogeneous suspensions of cylindrical, unbranched cell chains, (Kieran, 1993) Figure 4 7 captures a typical suspension sample viewed through a microscope Chains are unbranched and can consist of between one and fifteen cells, although, are more frequently comprised of 2 to 5 cells

Figure 4 8 illustrates the variation in average chain length and number of cells per chain over the course of the culture cycle While single cells are found, the average number of cells per chain was approximately 4, reaching a maximum (4 8 cells/chain) in the latter stages of the growth cycle (days 14 -21) when cell replication is minimal and the culture is in the stationary phase The minimum number of cells per chain was observed on day 5 (2 7 cells/chain), as elongated chains containing fewer cells per chain prepared for cell replication Average chain lengths varied between approximately 350 μm and 430 μm through out the growth cycle, although chains as long as 1000 μm were observed, particularly in the early exponential phase The maximum chain lengths were observed on day 3, as cells elongated in preparation for cell division and hence the chain length

was subsequently greater. The variation in average chain length over the course of the growth cycle was quite erratic and this will be discussed further in Section 5.1.3.

Figure 4.9 shows the average cell length and chain or cell width, as the culture matures. Average cell length varied between approximately 83 μm and 120 μm during the growth cycle and cells reached lengths of approximately 250 μm, with the most significant increases occurring in the early exponential phase. Maximum cell length was observed on day 5, as expected, at the initial stages of cell replication. Towards the end of the late exponential phase and into the stationary phase, cell length began to stabilise, as cell replication and cell growth ceased. The chain and cell width (both identical) remains relatively constant at approximately 37 μm throughout the culture cycle. While Figure 4.8 and 4.9 represent mean values of the relevant morphological characteristics, the proportion of different-sized chains and cells varied during the culture cycle, as illustrated in the log-normal distribution profiles for chain length and cell length, Figures 4.10 and 4.11, respectively. Both profiles reflect similar patterns as the culture matures. For example, the distribution widths are greatest between days 3 and 7, signifying a more heterogeneous population. Cell length varied between 40 and 200 μm. Conversely, in the early and later parts of the cycle, there is greater proportion of medium sized cells and fewer larger cells. Cell length varied between 40 and 150 μm.

Figure 4.7: Micrograph of *M. citrifolia* suspension cultures (Evans Blue stained).

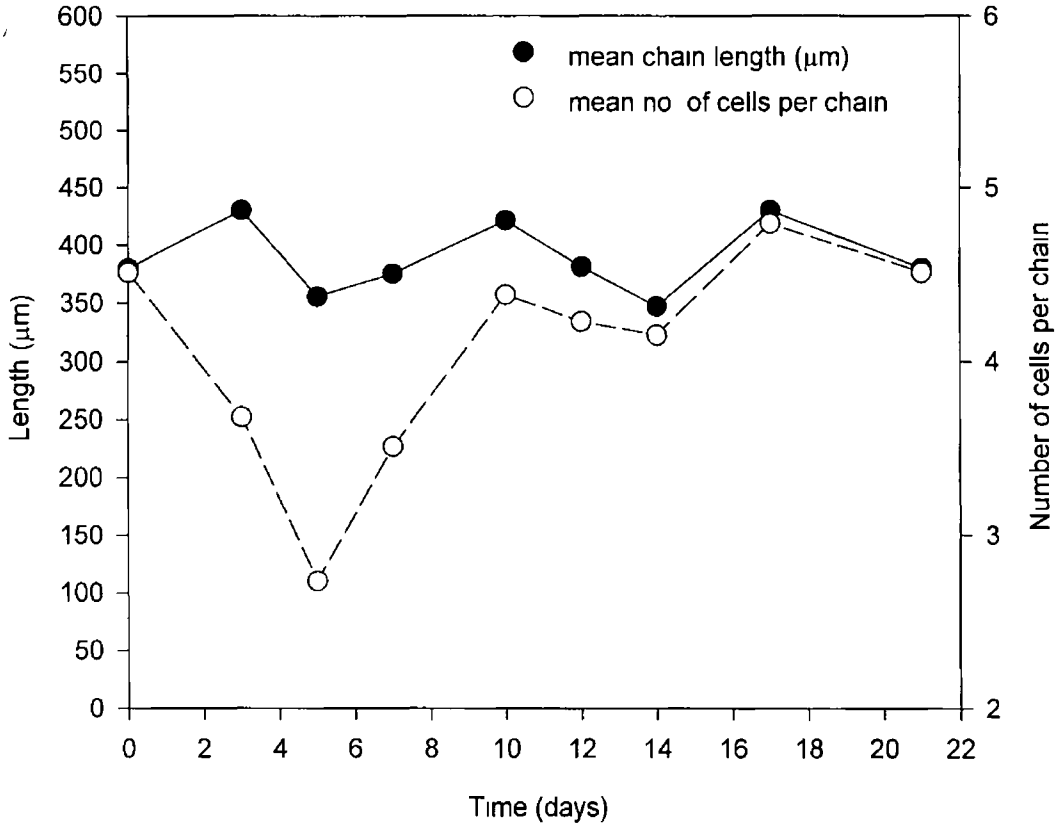

Figure 4 8 Average chain length and number of cells per chain morphological profiles

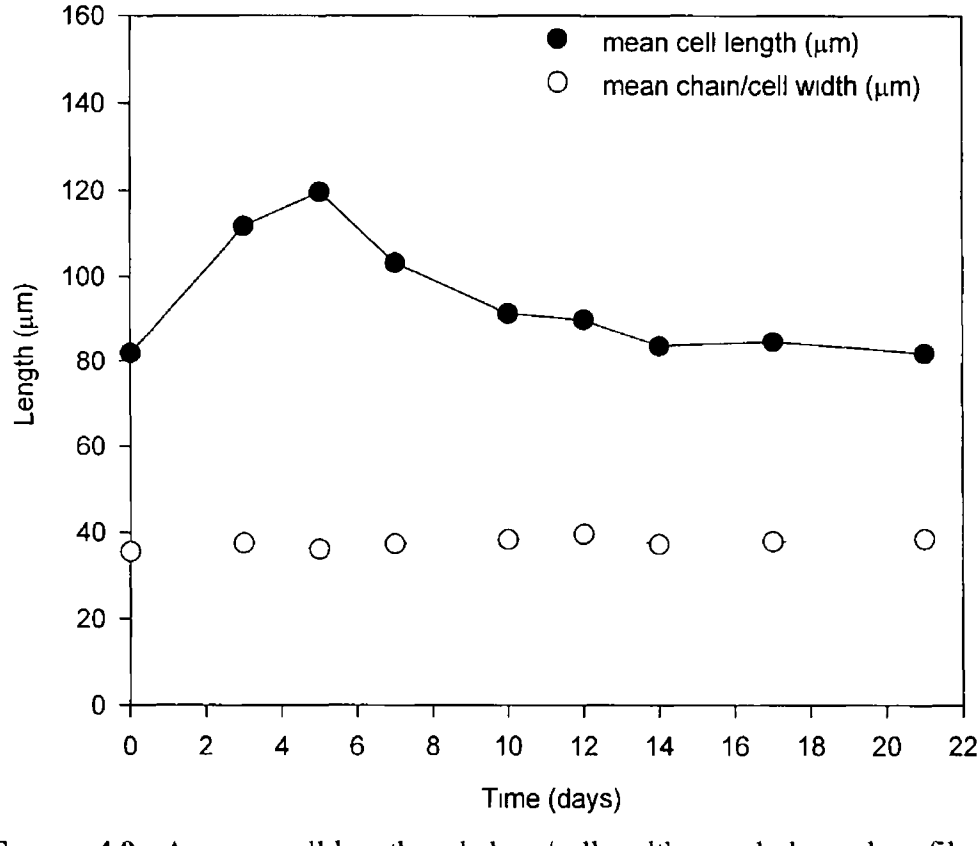

Figure 4 9 Average cell length and chain/cell width morphological profiles

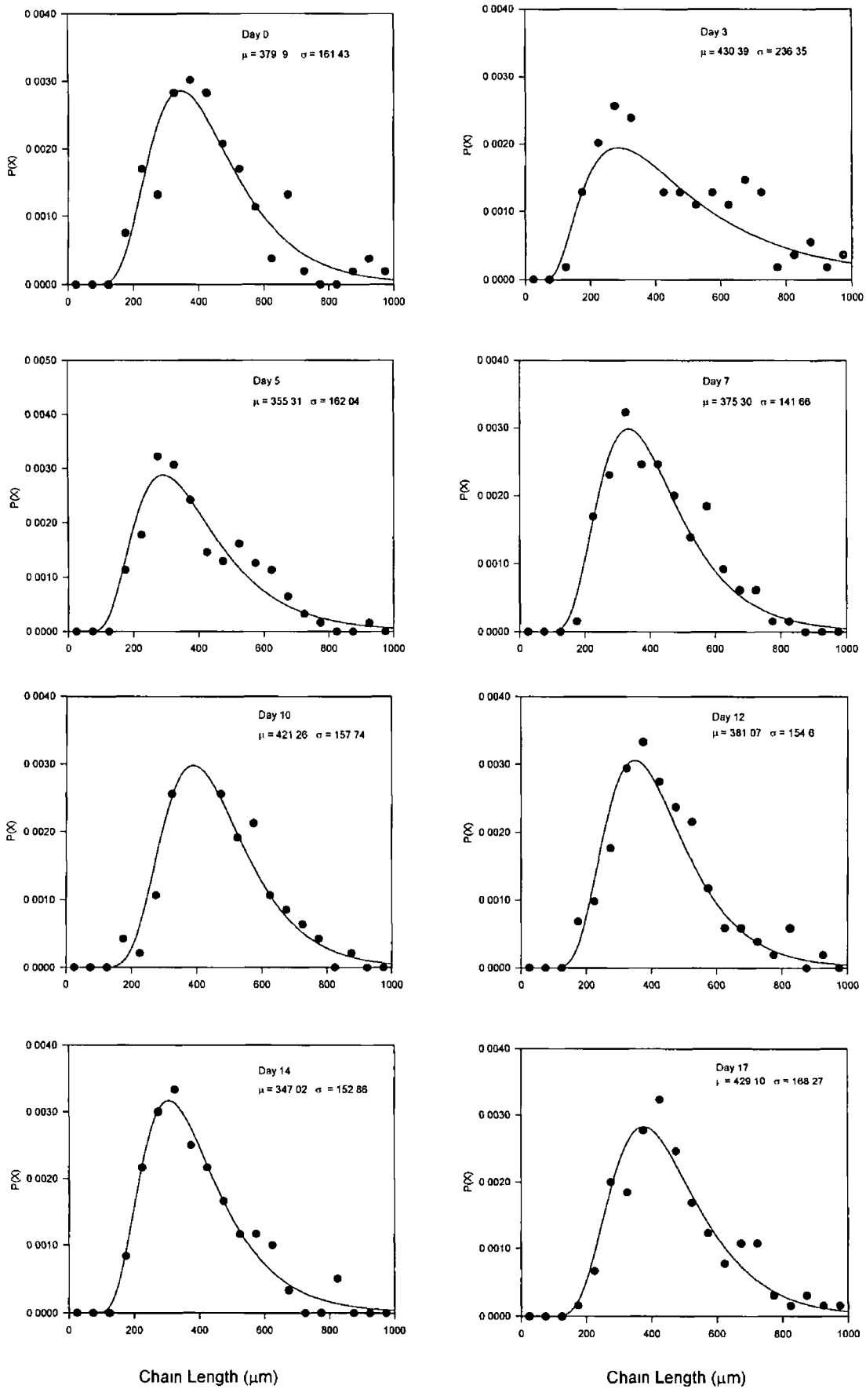

Figure 4 10 Log-normal chain length size distribution profiles for *Morinda citrifolia* suspensions, grown in 250 ml shake flasks (mean and standard deviation values quoted in μm)

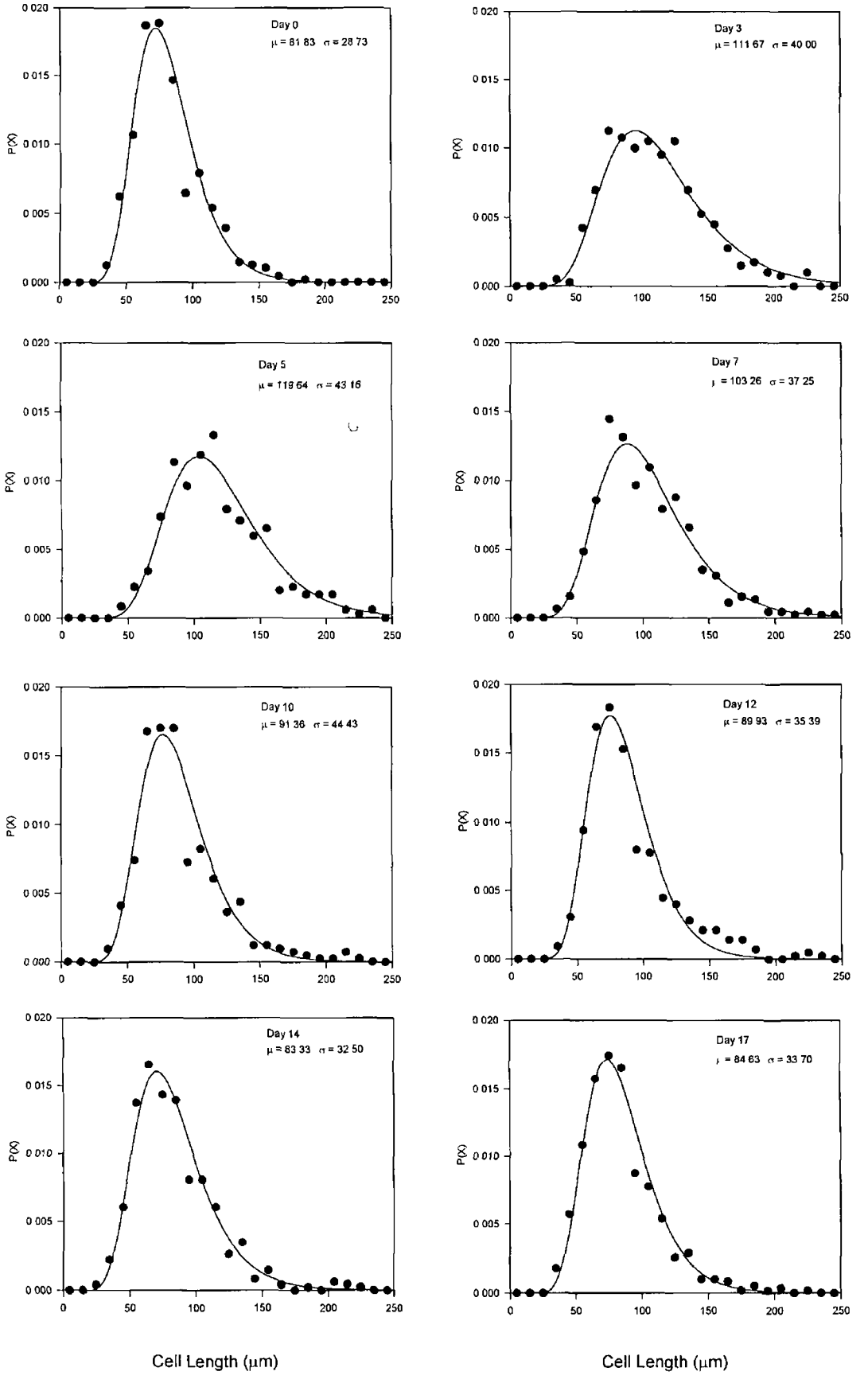

Figure 4 11 Log-normal cell length size distribution profiles for *Morinda citrifolia* suspensions, grown in 250 ml shake flasks (mean and standard deviation values quoted in μm)

4 2 1 Metabolite Profiles

The concentration profiles for protein and ECP in cell-free broths are illustrated in Figures 4 12 and 4 13, respectively Error bars represent the standard errors over five growth cycles It is apparent that production of both metabolites closely follows biomass production A slightly more extended lag phase is evident before exponential patterns are observed and maximum concentrations are maintained throughout the stationary phase Over the course of the growth cycle, the protein concentration increases from 0 01 mg ml^{-1} to 0 1 mg ml^{-1}, with a maximum production rate of 0 014 mg ml^{-1} day^{-1} during the exponential phase (days 5 to 9) The ECP concentration varies from 0 15 g l^{-1} to 1 9 g l^{-1} of cell-free broth, with maximum production rates of 0 282 g l^{-1} day^{-1} between days 5 and 9

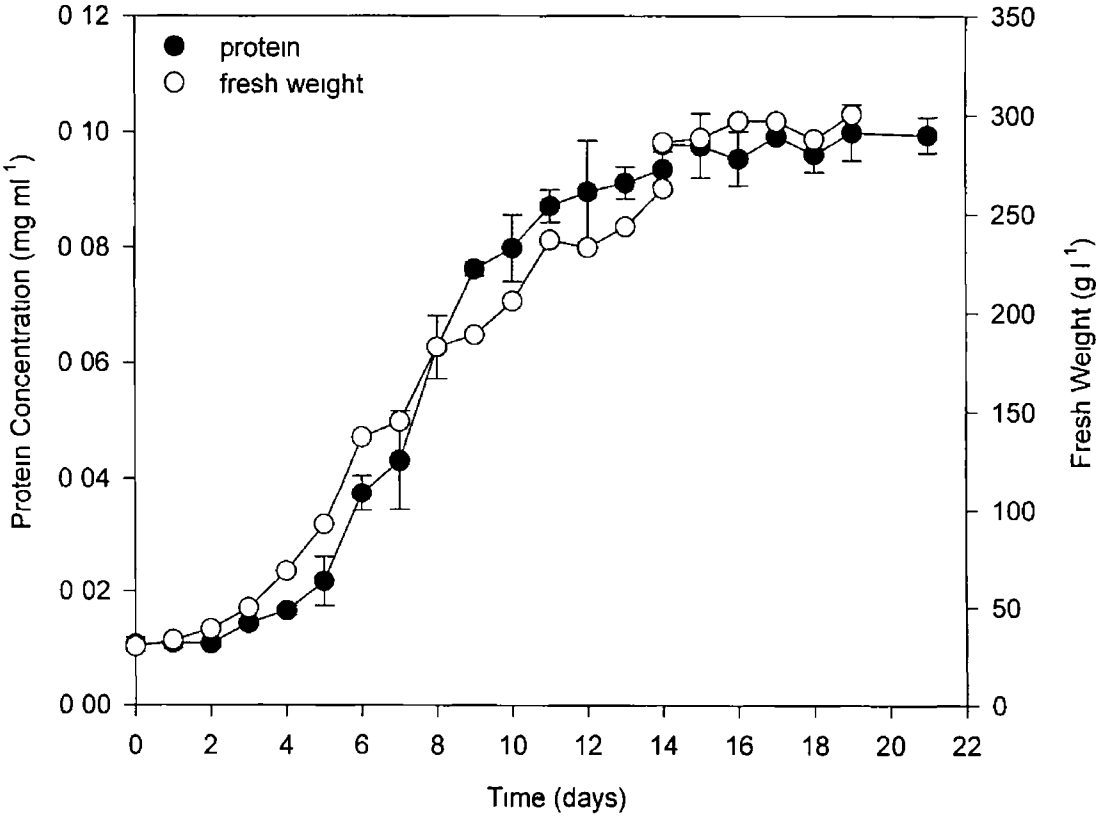

Figure 4 12· Protein content of the cell-free broth with reference growth profile (n = 5)

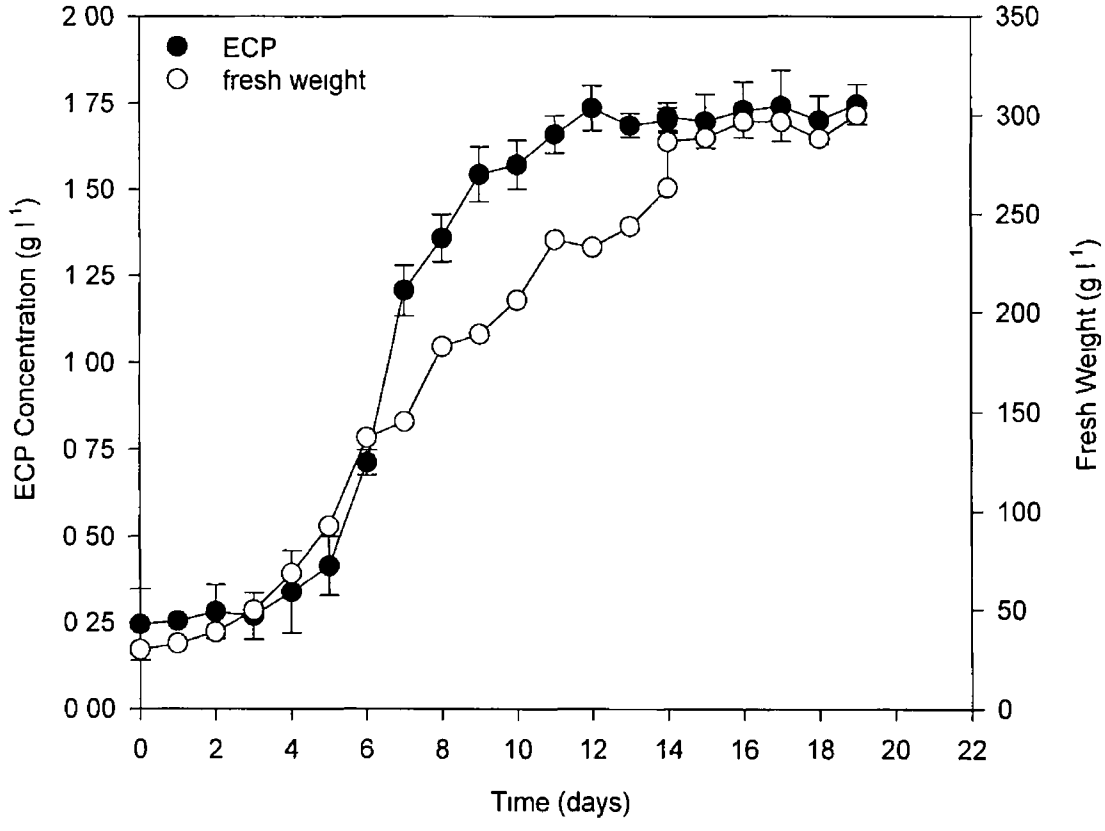

Figure 4 13 Polysaccharide content of the cell-free broth with reference growth profile (n = 5)

4 2 2 Rheological Analysis

The viscosity of the cell free broth changes throughout the growth cycle due to the secretion of metabolites such as polysaccharides However, at all stages the cell-free broth was found to exhibit essentially Newtonian characteristics Rheograms for selected days of the cycle are illustrated in Figure 4 14, where the straight lines fitted to the data indicate Newtonian behaviour Alternatively, applying a power law model to the data, it was found that the flow behaviour index (n) varied between 0 910 and 1 085 throughout the culture cycle Values of approximately 0 95 were most prevalent However, these values are within the range of experimental error for viscosity measurement and given the available data, it is reasonable to characterise these broths as essentially Newtonian fluids Variations in broth viscosity, as the culture matures, are shown in Figure 4 15 Error bars indicate the standard error for 5 growth cycles Viscosity ranges from approximately 1 1 mN s m^2 to 5 5 mN s m^2

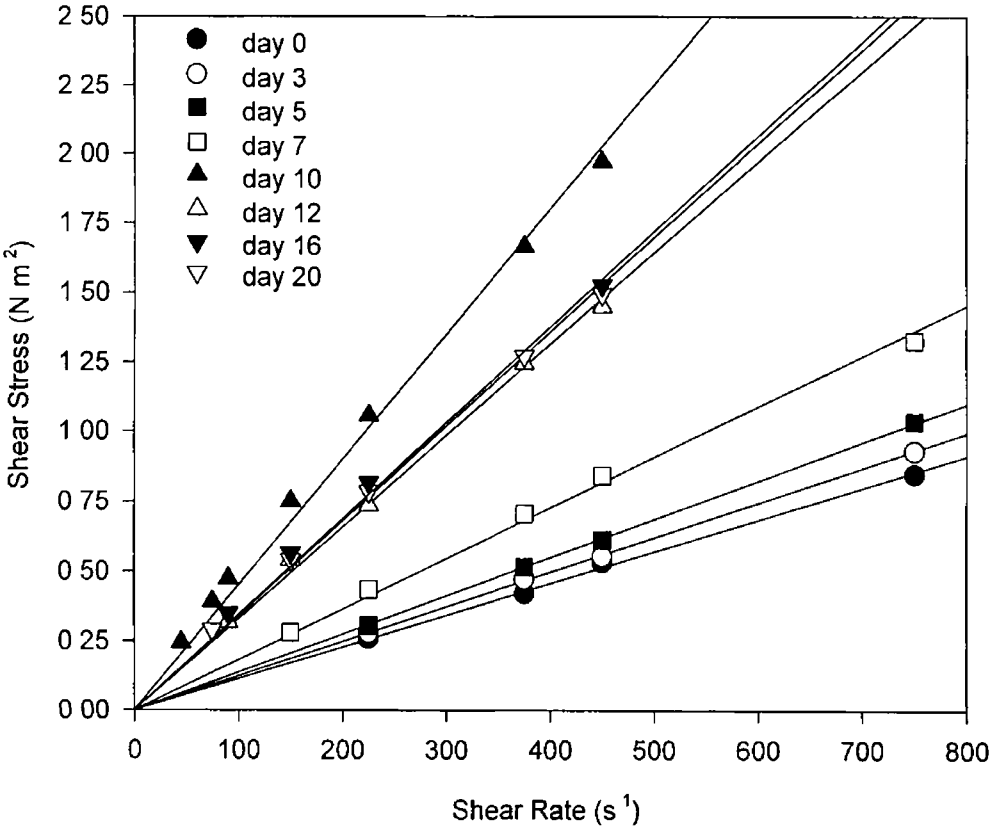

Figure 4 14 Rheograms for cell-free broth of different culture ages

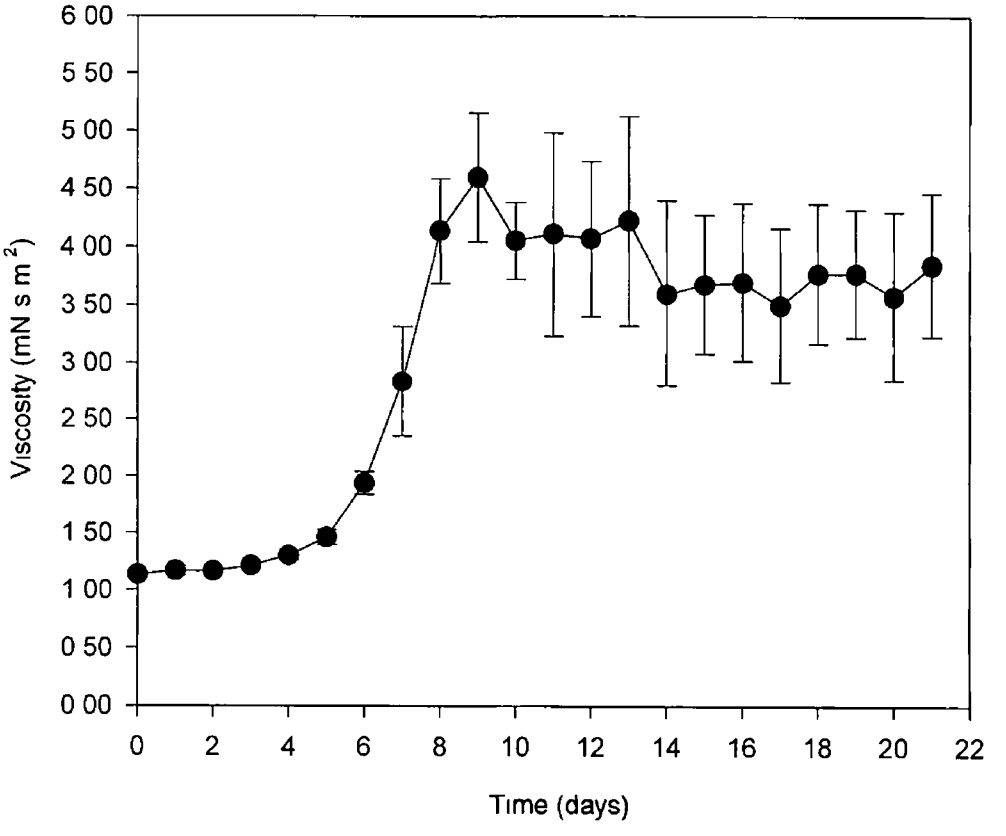

Figure 4 15 Viscosity profile for cell-free broth throughout the growth cycle (n = 5)

4 2 3 Surface Tension Profiles

During the development of measurement protocols, it has been found that surface tension of a cell-free broth sample decreases if the solution is allowed to stand for a period of time The initial reading is referred to as the "instantaneous" surface tension and the "equilibrium" measurement is the final reading, evaluated when the surface tension has ceased to change with time The surface tension profile for cell-free broth throughout the growth cycle is shown in Figure 4 16 The instantaneous values range from 0 071 N m^{-1}, on day 0, to a minimum of approximately 0 056 N m^{-1} at day 14, while the equilibrium values decrease from 0 067 N m^{-1}, on day 0, to 0 050 Nm^{-1} at day 12 Trends are similar for both and in both cases, there is a rapid reduction in surface tension between day 0 and day 6 Relative to the level achieved by the end of the growth cycle, the extracellular protein and polysaccharide concentrations do not begin to increase greatly until day 5 However, if just the interval between day 0 and day 5 is considered, the protein level rises from 0 01 to 0 02 g l^{-1}, which represents a two-fold increase in concentration This corresponds to a reduction in equilibrium surface tension values from approximately 0 0665 to 0 0550 N m^{-1} Only equilibrium surface tension values are considered for further analysis in this work

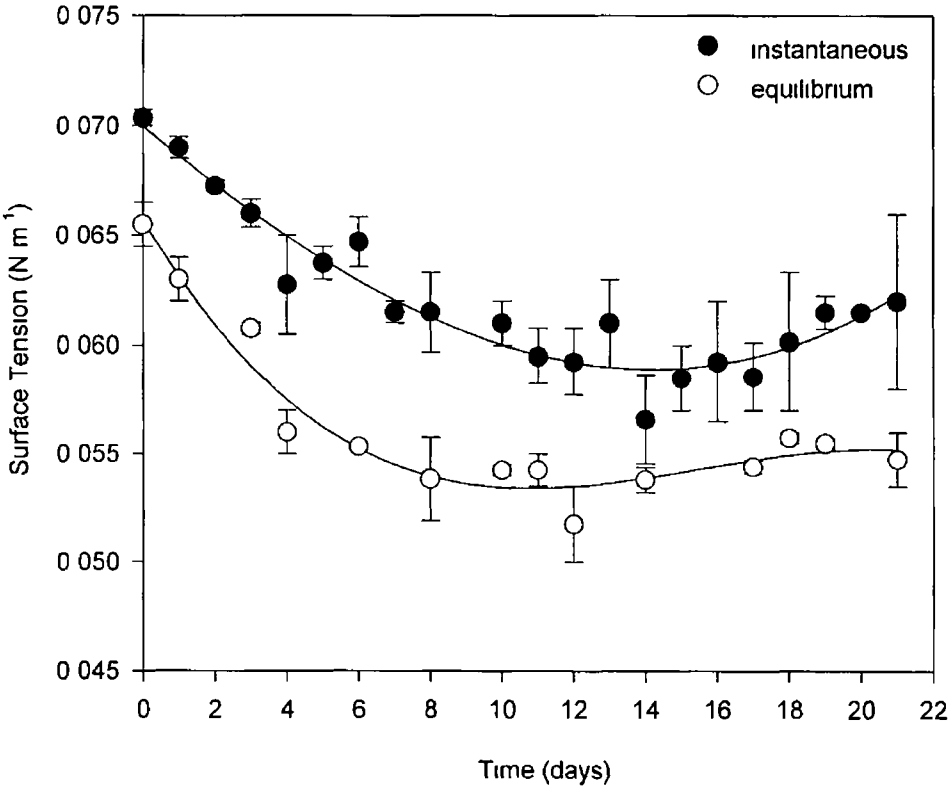

Figure 4 16 Variation in "instantaneous" (n=6) and "equilibrium" (n=4) surface tension of the cell-free broth over the course of the growth cycle (A third order polynomial curve has been fitted to the data for presentation purposes)

In order to investigate the effect of pH on surface tension, a series of cell-free broths from different stages of the growth cycle were subjected to pH shifts and the surface tension of the resulting fluids was determined A pH range of 4 to 6 was investigated The equilibrium surface tension of these solutions were measured and the results are displayed in Table 4 1 The basic method for altering the pH, *i e* addition of NaOH and HCl, resulted in very slight broth dilution Although this dilution does not alter metabolite concentrations significantly, it may have an effect on the surface tension, due to a salt effect

Table 4 1 Surface tension of natural and pH altered cell-free broths

Day	ST of Original Broth (N m ^{1})	ST of Broth pH 4 (N m ^{1})	ST of Broth pH 6 (N m^{-1})
0	0 0660 (pH 5 48)	0 0650	0 0665
3	0 0605 (pH 4 48)	0 0620	0 0635
6	0 0555 (pH 4 02)	0 0570	0 0575
8	0 0560 (pH 4 91)	0 0560	0 0550
11	0 0535 (pH 5 11)	0 0535	0 0540
14	0 0530 (pH 5 32)	0 0540	0 0550
17	0 0540 (pH 5 35)	0 0540	0 0560

Because of the natural variations in the pH of the original broths employed, it is difficult to identify an underlying trend in the effect of pH shifts on surface tension The observed variations with pH, in the range 4 to 6 are small, no greater than $\pm$ 5 % in any case and it is arguable that these changes may be within the limits of experimental error for the surface tension meter employed

4 3 BROTH ECP AND PROTEIN SEPARATION

4 3 1 ECP and Protein Precipitation

The alcohol precipitation-purification method for ECPs was not entirely successful in isolating pure ECPs as, in addition to the precipitation of ECPs, some proteins were simultaneously precipitated Protein content was detected in the resuspended samples, using the Bradford assay and visualised on a PAGE-SDS electrophoresis gel (Figure 4 17) The band indicated that the total protein fraction of the cell-free broth (lanes 4 and 5) was represented in the ECP isolate (lanes 2 and 3) Although one protein (16 kd) was present in the ECP solutions at a lower concentrations, overall the protein characteristics of both were nominally identical The maximum protein content of the cell-free broth occurred during the later stages of the growth cycle, when the corresponding protein and ECP levels were approximately 0 1 mg ml^{-1} and 1 8 g l^{-1}, respectively Therefore, assuming all the protein was precipitated, the maximum error in the quantification of ECPs, due to protein contamination, is 5 6%

Attempts to remove the protein via ammonium sulphate precipitation were also unsuccessful, as the ECP also precipitated out of solution with the protein

4 3 2 Enzymatic Protein Digestion

An attempt to enzymatically remove the protein from cell-free broth (containing both polysaccharide and protein) was unsuccessful as, although the protein was digested, ECP also precipitated out of solution Plant cell suspensions are known to produce ECPs with relatively high protein content (Moore, 1973, Uchiyama *et al*, 1993) The Bradford method assays for free protein, therefore, protein attached to a polysaccharide would not be detected It is probable that in addition to the digestion of free protein, the protein moiety of the ECP was also digested Therefore, the integrity of the ECP may have been altered, causing it to precipitate out of solution

BSA was used as a control substrate for the enzymatic protein digestion procedure The electrophoretic profiles of proteins present in the cell free broth and in the BSA solution prior to enzyme degradation (lanes 8 and 7, respectively) and following the proteolytic step (lanes 4 and 5, respectively) are presented in Figure 4 18 It is seen that the enzyme

totally degrades the BSA and after degradation only protein bands of the enzyme are clearly identified There is a faint additional band (a) which could represent a degradation peptide at a molecular weight of approximately 31 kd for BSA The presence of degradation peptides is more evident in the digested cell-free broth sample There is distinctive band (b) at approximately 21 kd, which is found in neither the enzyme nor the broth fraction There is also a distinct smear effect at the bottom of the gel in lane 4, which could correspond to unresolved small peptides, present in the solution, following the proteolytic step It is evident however, that the enzyme is very effective in degrading the main proteins found both in the cell-free broth and in BSA solutions at a concentration of 0 5 mg ml^{-1}

4 3 3 Intracellular Protein Extraction

The electrophoretic protein profiles of extracellular ECPs found in the cell-free broth and intracellular protein, extracted from the cells, are also illustrated in Figure 4 17 There is a significant difference between the qualitative protein content of the extracellular proteins in the cell-free broth (lanes 4 and 5) and the intracellular protein isolate (lane 1) The main proteins in the intracellular fraction were found to have molecular weights of approximately 23 kd, 1 kd and 14 kd while there was little trace of protein bands which represented the extracellular proteins There are some faint bands present, which possibly represent the residual broth, which was not successfully removed from the cells, prior to crushing This approach, to obtain a similar protein fraction (without ECP) to the proteins present in the cell-free broth, was not pursued since the intracellular protein isolate was not representative of the extracellular proteins present in the cell-free broth It is possible that the proteins present in the intracellular fractions are those which disengaged from the cell membrane and wall, during the physical isolation procedure

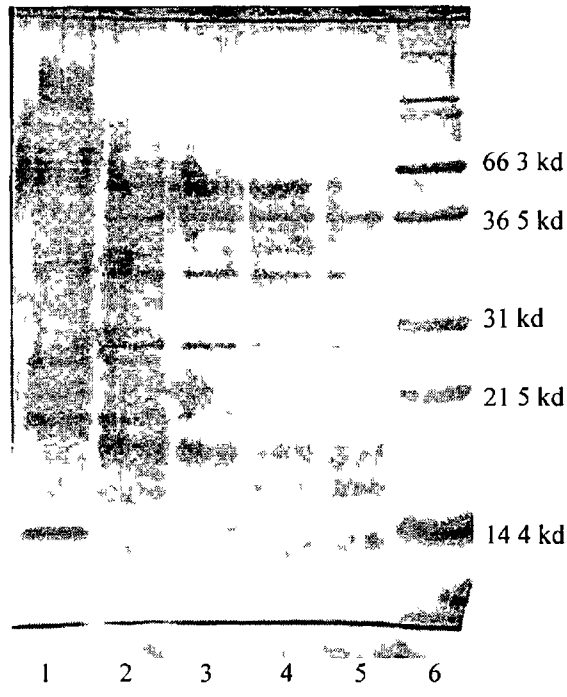

Figure 4 17 Intracellular protein, cell-free broth and ECP standard solution protein profiles (Lanes 1=Intracellular protein extract, 2,3=ECP/protein isolate, 4,5=broth, 6=marker)

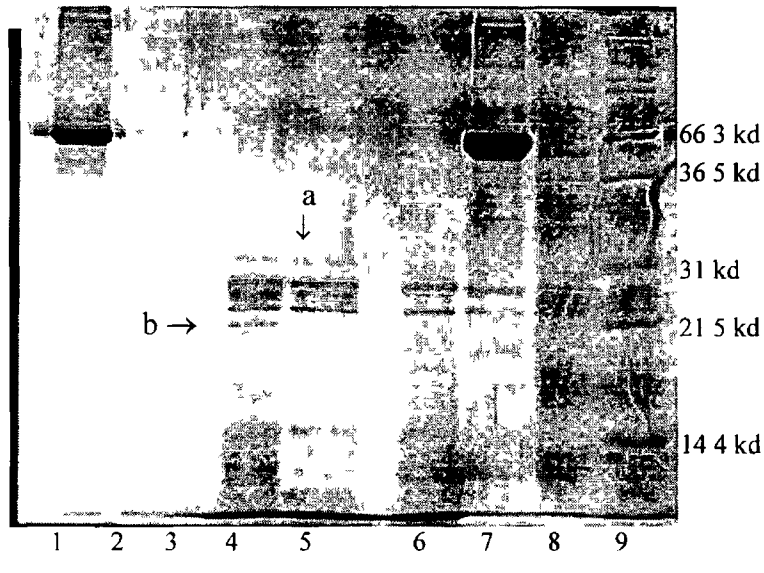

Figure 4 18 Enzymatic protein digestion of cell-free broth and BSA Band (a) and (b) represent possible degradation peptides following the protease digestion of BSA and cell-free broth, respectively (Lanes 1=BSA, 2=blank, 3=medium, 4=broth & enzyme, 5=BSA & enzyme 6=enzyme solution 7=BSA, 8=broth, 9= marker)

4.4 Polysaccharide and Protein Effects on Viscosity and Surface Tension

4.4.1 Effect of Cell-Free Broth Metabolites on Viscosity and Surface Tension

Viscosity: The partially purified ECPs were isolated from the cell-broth and freeze dried. They were subsequently resuspended in medium to formulate standard ECP solutions of known concentrations. The rheological characteristics of these standard solutions were then assessed.

Figure 4.19 shows rheograms for standard ECP solutions. As a first effort at characterisation, straight lines (corresponding to Newtonian behaviour) have been fitted to the data. However, it appears that the fluids exhibit progressively non-Newtonian behaviour with increasing ECP concentration. Applying a power law model to the data, the calculated consistency index (k) and flow behaviour index (n) are illustrated in Figure 4.20. The flow consistency index increases from 1.07 mN s^n m^{-2} for pure medium to 24.9 mN s^n m^{-2} for a 2.0 g l^{-1} ECP solution. The flow behaviour index decreases from 0.99 for pure medium to 0.75, as the ECP standard concentration increases. The cell-free broth is considered to be Newtonian at all stages of the growth cycle (Section 4.2.2). To illustrate the similarity of the effect of ECPs on viscosity in both the standard solutions and the broth, the apparent viscosity of each solution at 225 s^{-1} was calculated and the data are illustrated in Figure 4.21. The similarity is evident except for deviations at the higher concentrations corresponding to the reduction in broth viscosity observed towards the end of the growth cycle (Figure 4.15), although the ECP content remained relatively constant (Figure 4.13). These data suggest that some structural degradation of the ECP, not reflected in the overall concentration values, may be occurring during the later stages of the growth cycle.

Since extracellular proteins could not be separated from the broth effectively, the influence of cell-free protein alone on the rheology of the fluid could not be investigated. However, the effect of intracellular protein on viscosity was investigated. It was determined that aqueous or medium-based solutions of these proteins, at a concentration of 0.033 mg ml^{-1}, had a viscosity similar to that of pure water, *i.e.* 1.0 mN s m^{-2}. Higher concentrations of these proteins were not available for analysis. However, at the protein concentration observed, it is unlikely that the protein content of ECP standards solution or of the cell-free broth contributed to the viscosity of the solutions.

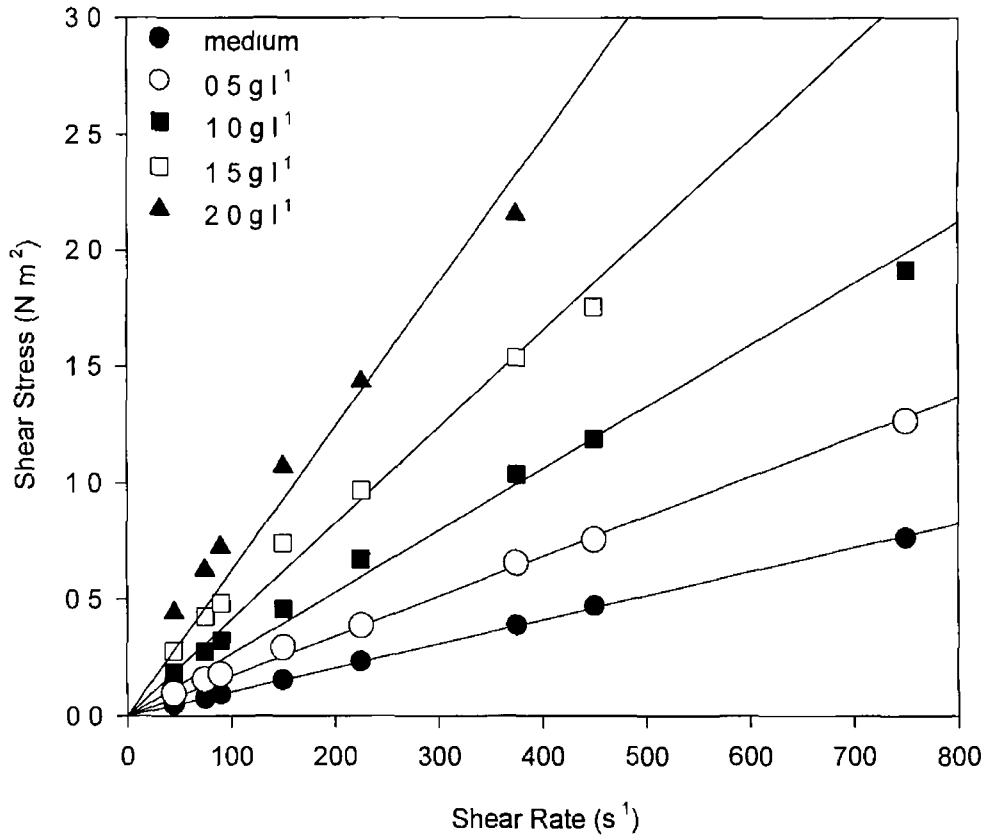

Figure 4 19 Rheograms for standard ECP solutions in medium (The fitted lines represent Newtonian behaviour)

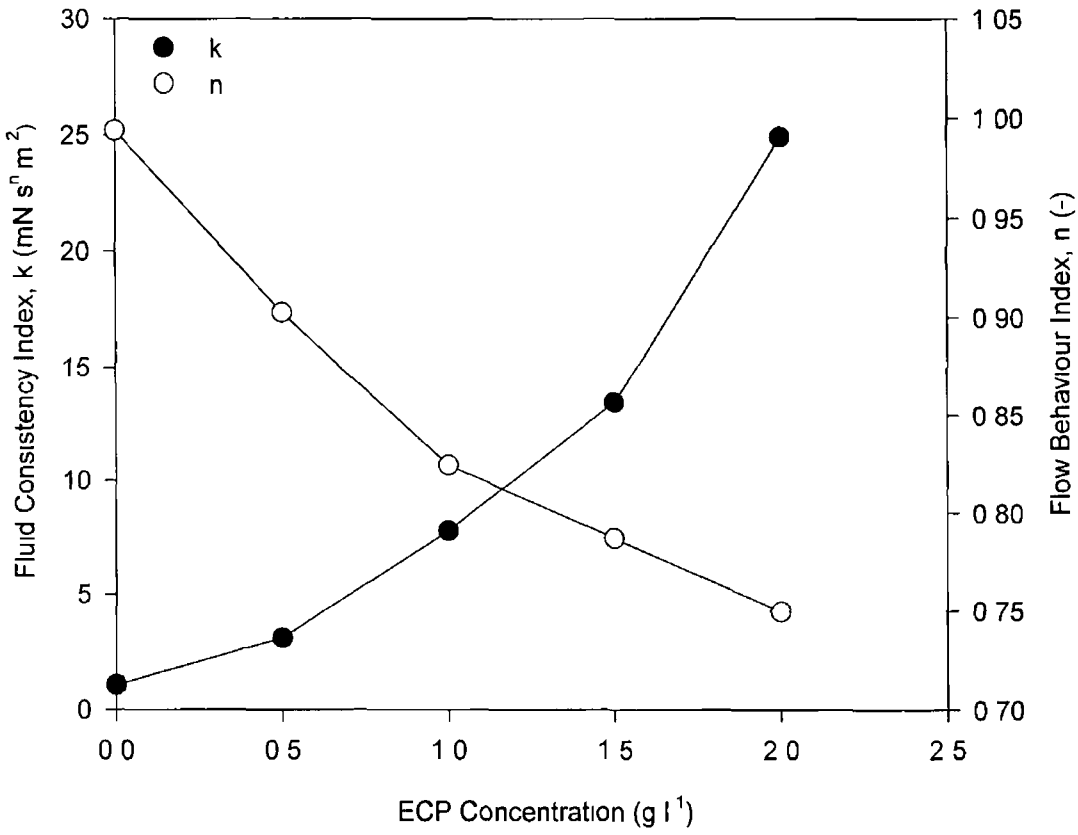

Figure 4 20 Variation of power law parameters with ECP concentration in standard solutions

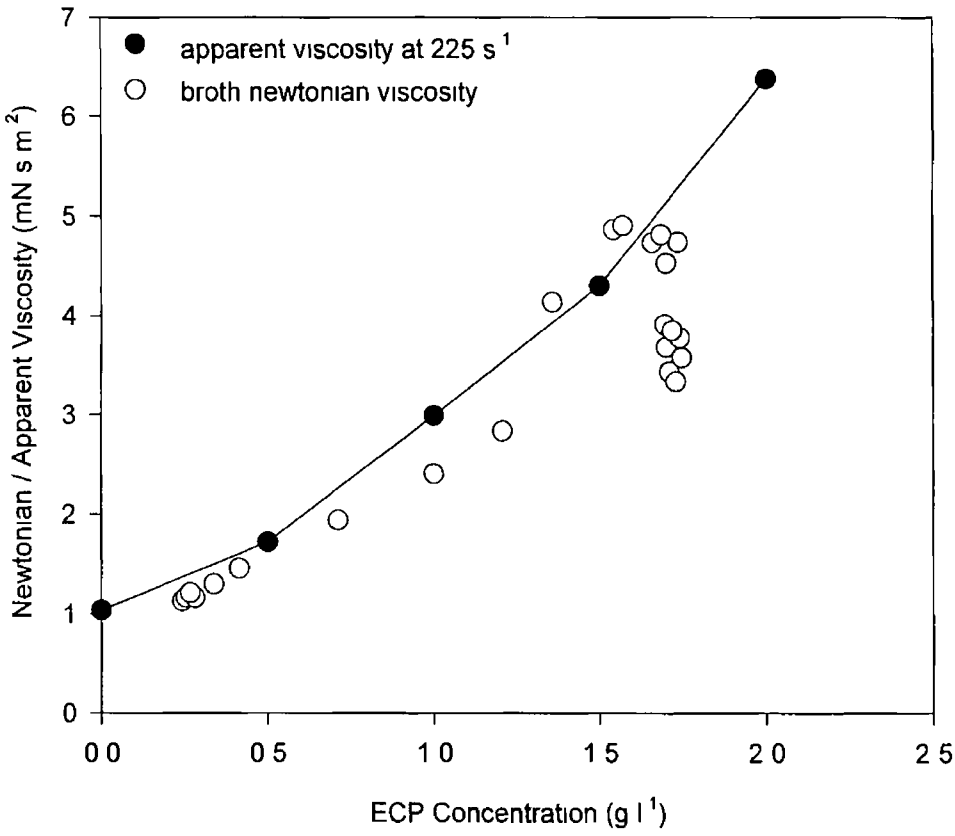

Figure 4 21 Effect of ECP concentration on the viscosity of standard ECP solutions (evaluated at 225 s^{-1}) and untreated cell-free broths

Surface Tension Surface tension effects are frequently attributed to proteins and from Figure 4 22, it can be seen that the surface tension of the cell-free broth decreases very rapidly as the protein concentration increases from 0 1 mg ml^{-1} to 0 2 mg ml^{-1}, corresponding to days 0 to 5 of the growth cycle This shows the strong influence of very low concentrations of protein on surface tension, with a saturation-type effect prevailing thereafter This profile mimics the typical trend observed during the culture cycle and hence, indicates protein as a major influencing factor in surface tension

For the ECP standard solutions, surface tension decreases linearly with increasing ECP concentration from a maximum value of 0 070 N m^{-1} for medium, to a value of 0 0615 N m^{-1} for a 2 0 g l^{-1} ECP solution (Figure 4 23) A totally different relationship is apparent when ECP concentration and surface tension variation of the cell-free broth are compared However, the differences between the effects of protein and ECP (containing the inseparable protein moiety) on surface tension are apparent

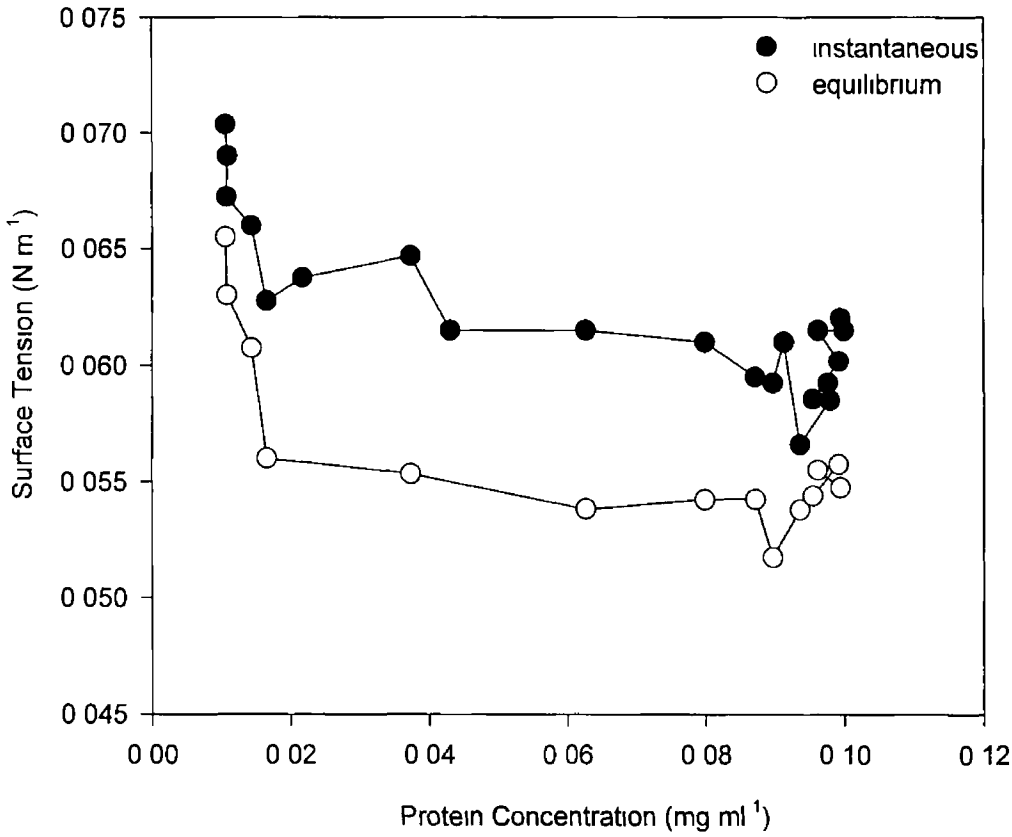

Figure 4 22 Variation in surface tension with respect to the protein content of the cell-free broth

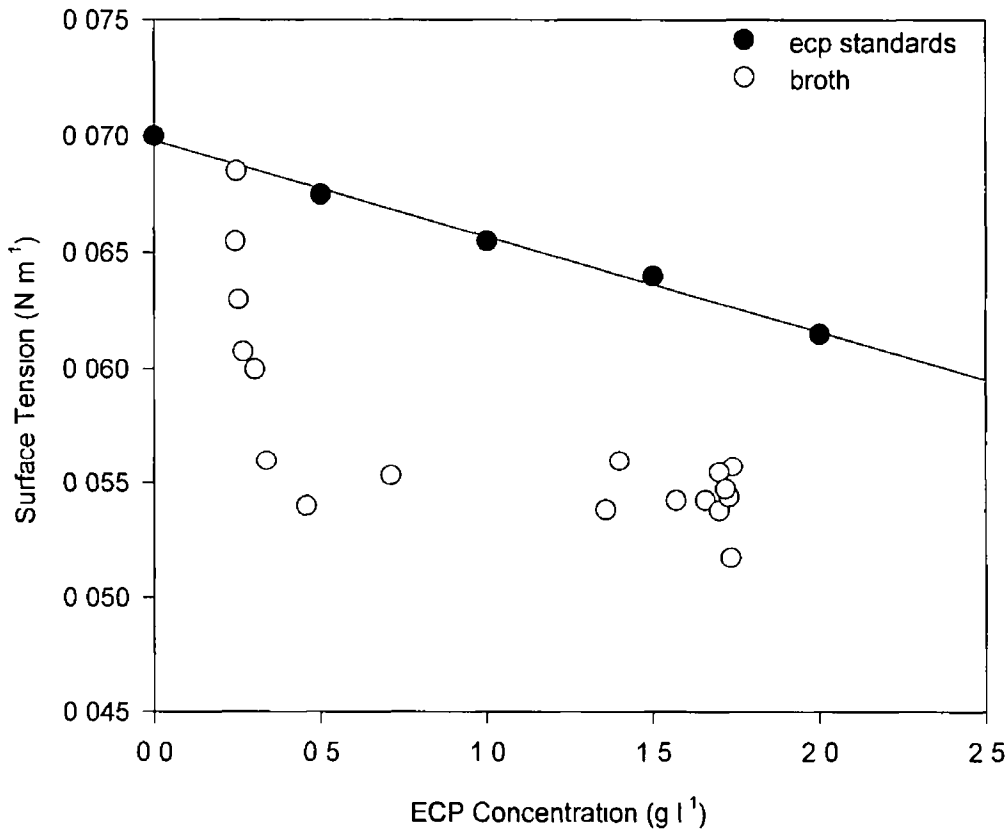

Figure 4 23 Influence of ECP concentration on surface tension for standard ECP solutions and cell-free broth samples

4 4 2 Model System Studies - Viscosity and Surface Tension

Viscosity Modeling of the influence of protein concentration on viscosity was observed using BSA, in both deionised water and medium solutions The viscosity was found to be unchanged over the concentration range 0 0-2 0 mg ml ^{1}, with all solutions displaying Newtonian characteristics The measured viscosities of water and medium based solutions were 1 02 mN s m ^{2} and 1 07 mN s m ^{2}, respectively The range of protein concentration investigated greatly exceeds that found in *Morinda citrifolia* cell-free broths It was also established that at a concentration of 0 2 mg ml ^{1}, BSA had no effect on the viscosity of xanthan gum solutions

To illustrate the influence of a pure polysaccharide on viscosity, experiments were performed, using xanthan gum solutions as a model system Figure 4 24 shows that at a shear rate of 225 s ^{1}, the apparent viscosity increases from 1 0 mN s m ^{2} for deionised water, to 4 08 mN s m ^{2} for a 0 04% solution of xanthan gum in water Corresponding solutions of xanthan gum in medium have slightly lower apparent viscosities, however the difference is small and could be attributed to experimental error, in both viscosity measurement and solution formulation

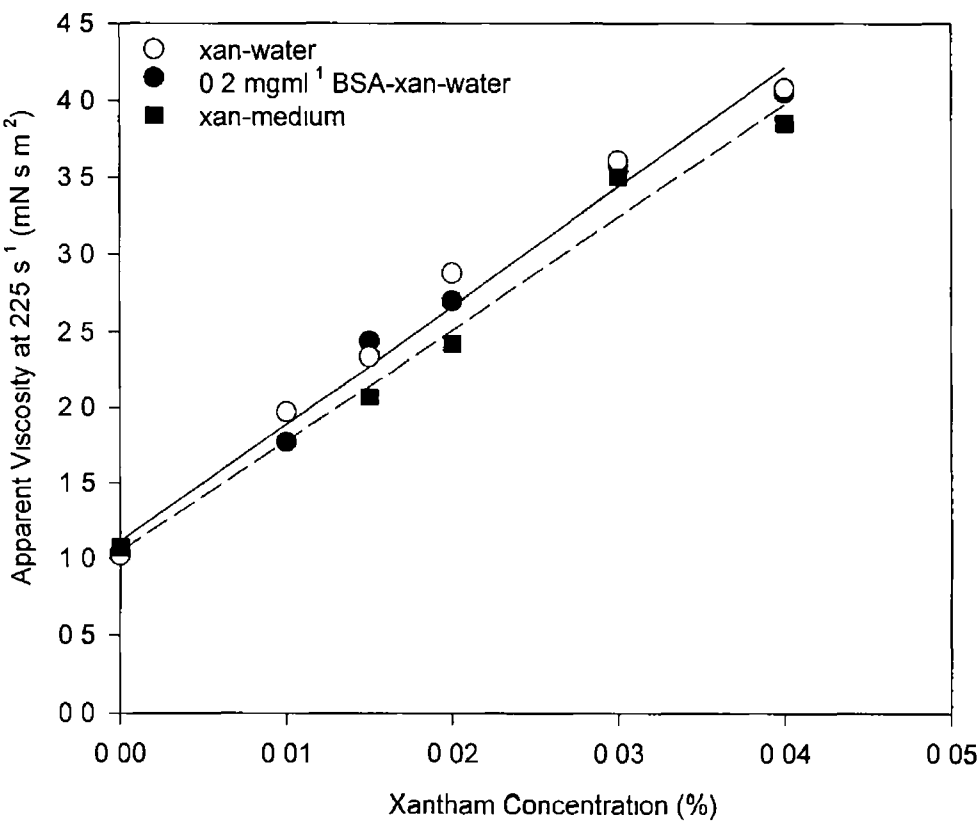

Figure 4 24 The effect of xanthan gum concentration on apparent viscosity (evaluated at 225 s ^{1}) for xanthan-water ( ), xanthan-medium (----) and 0 2 mg ml ^{1} BSA - xanthan-water (—) solutions

Surface Tension Using xanthan gum solutions (both water and medium based) as model systems, it was observed that at concentrations of between 0 005% and 0 04 %, xanthan gum had no significant effect on surface tension The observed surface tension values for all xanthan-water solutions were between 0 0720 and 0 0725 N m^{-1}, xanthan-medium solutions exhibited slightly lower surface tension values of between 0 0685 and 0 0710 N m^{-1} The surface tension of BSA solutions in water (0 0 - 0 1 mg ml^{-1}) decreased until a BSA saturation concentration was reached, at approximately 0 01 mg ml^{-1}, as illustrated in Figure 4 25

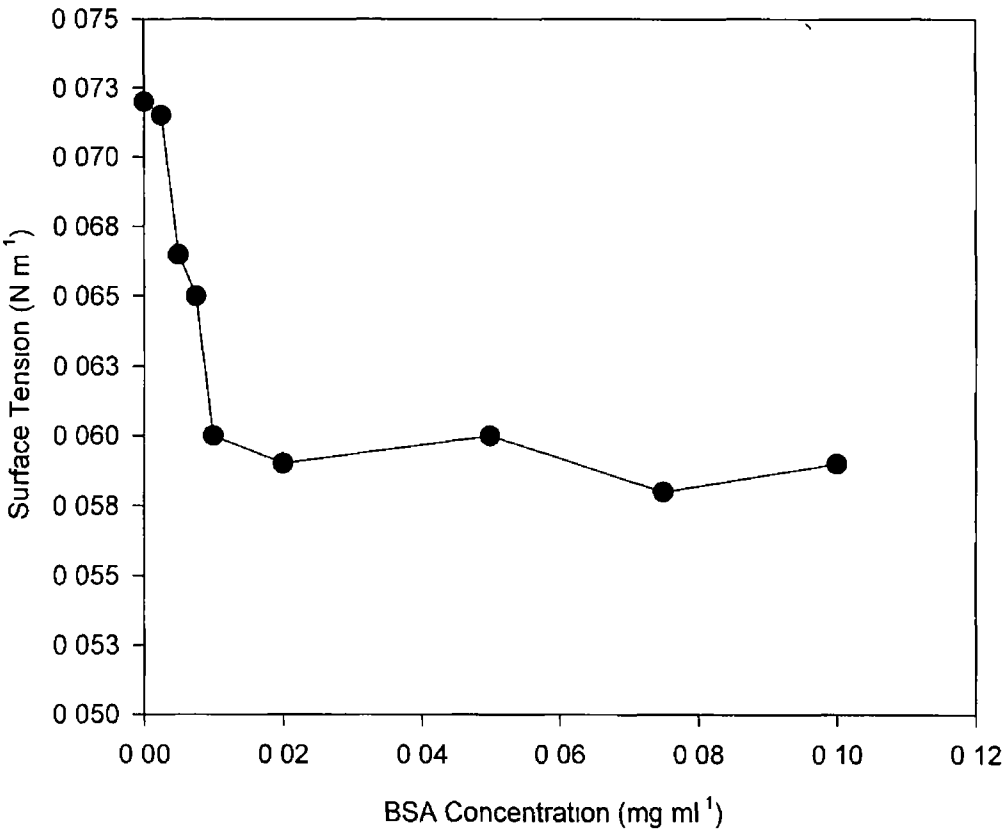

Figure 4 25 Relationship between BSA concentration and surface tension

4 5 BUBBLE COLUMN VALIDATION

The validation of each column is critical to ensure that reproducible and consistent results can be obtained for all solutions analysed Validation trials with each of the columns investigated are described in Section 3 6 The two most successful designs (Column A1a and Column B4a) were used in all subsequent foaming studies

4 5 1 Validation of Column A1a

This column was validated using 80 ml aliquots of 0 5 and 1 0 mg ml^{-1} solutions of BSA in deionised water, at three different aeration rates (3 33, 8 33 and 16 67 ml s^{-1}) Figure 4 26 depicts the rate of foam generation for a 0 5 mg ml^{-1} BSA solution At flow rates of 3 33, 8 33 and 16 67 ml s^{-1}, the stable foam heights recorded were approximately 18, 48 and 85 cm, respectively Similar patterns were obtained for 1 0 mg ml^{-1} solutions of BSA At all aeration rates investigated the foam grew very rapidly prior to stabilising Typical methods for analysing the foaminess of a solution are discussed in Section 2 2 For the work reported here, the validation results were typically analysed using three different methods Bikerman foaminess (bik, equation 2 2), dimensionless volume (dim, equation 2 4) and Edwards index (equation 2 3) Bikerman and dimensionless volume foaminess values for all validation trials in this column (Table 3 9) are illustrated in Figure 4 27 At both BSA concentrations, the dimensionless foaminess increases with increasing aeration rate, as expected As anticipated, the Bikerman value remains practically constant over the range of aeration rates investigated, at approximately 75 s and 139 s for 0 5 and 1 0 mg ml^{-1} BSA solutions, respectively Both foaminess indices clearly show that the 1 0 mg ml^{-1} solution has greater foaming potential than the 0 5 mg ml^{-1} solution The Edwards method proved unsuccessful for this particular column design No trend was observed in the data and hence, this method was not used in subsequent analyses in this work Although the Bikerman or dimensionless indices are equally acceptable for the measurement of foaminess for BSA solutions, the Bikerman method is employed in further analyses as it allows comparison of results obtained from foaming runs performed at slightly different aeration rates to be accurately compared

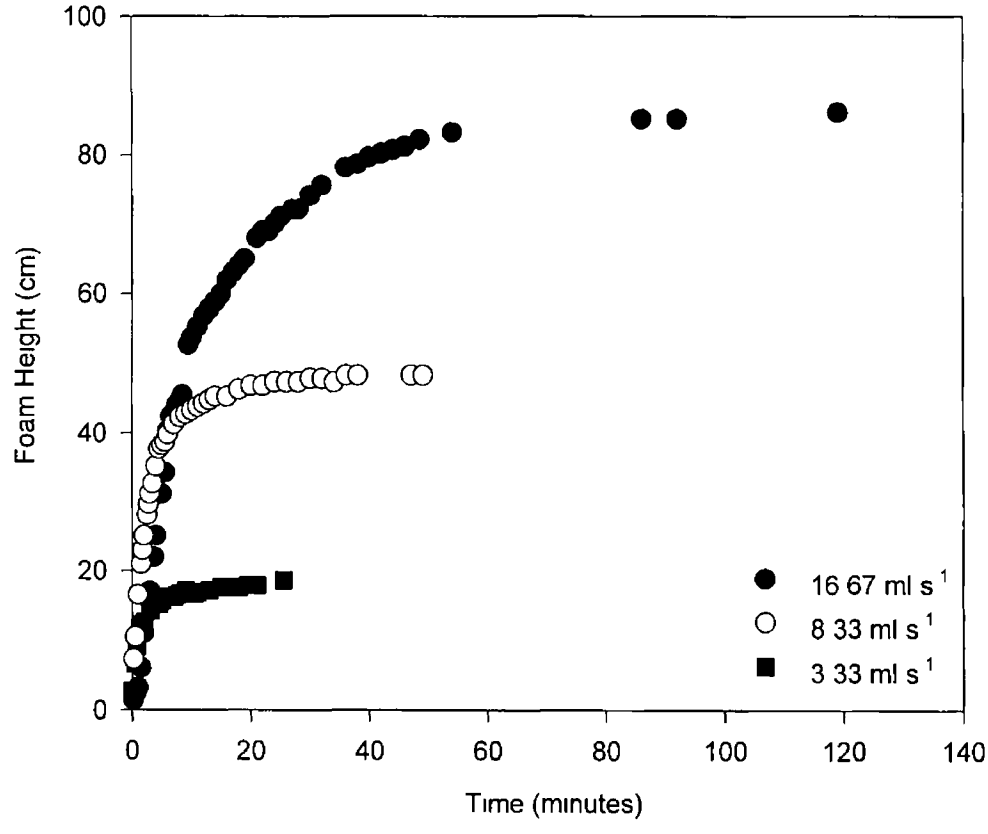

Figure 4 26 Generation of foam in a 0 5 mg ml ^{1} solution of BSA, at different flow rates, in column A1a

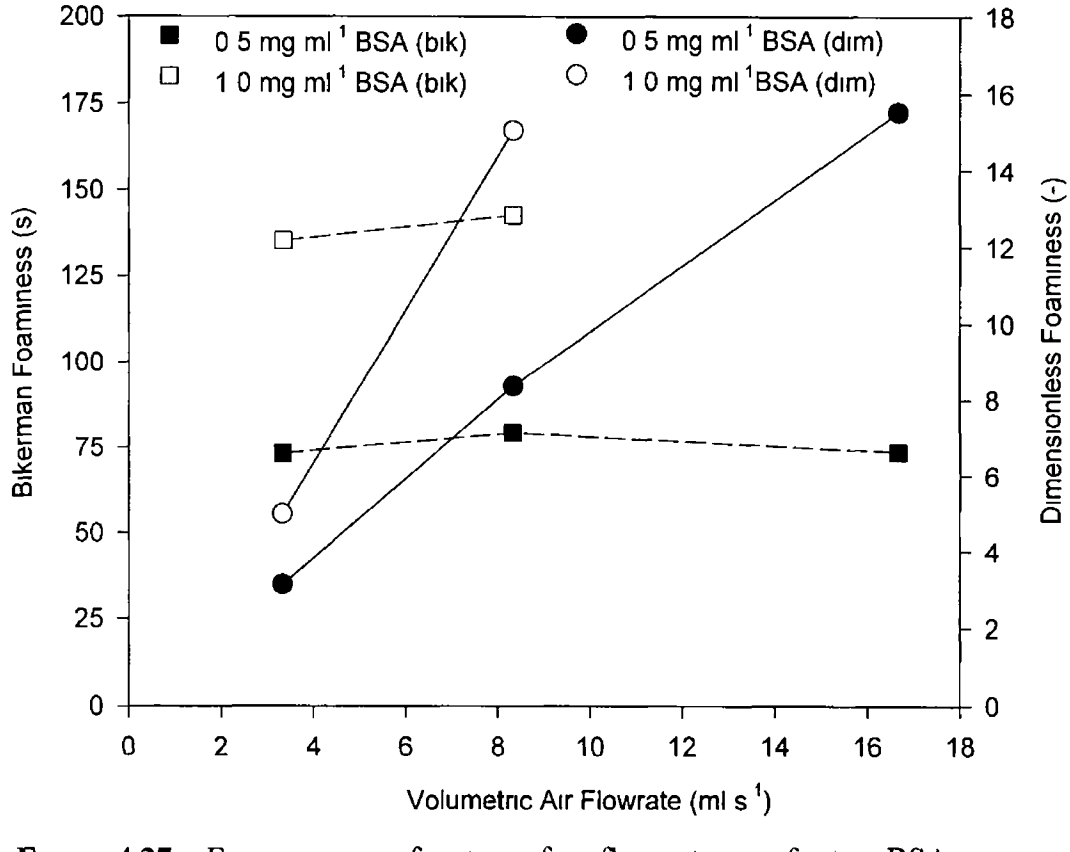

Figure 4 27 Foaminess as a function of air flow rate rate, for two BSA concentrations, in column A1a

4 5 2 Validation of Column B4a

The smaller pore size of the sparging element in this apparatus allowed the use of lower aeration rates (1 0 - 4 0 ml s^{-1}) and a wider range of BSA concentrations (0 1 - 1 0 mg ml^{-1} in deionised water) The conditions for all validation experiments performed in this column are summarised in Table 3 10 More corroborating validation information than could be generated using Column A1a was collected Figure 4 28 shows the increase in foam height, with respect to time, for a 0 5 mg ml^{-1} BSA solution, at 3 different aeration rates Again, both Bikerman and dimensionless indices were used Figure 4 29 shows that the dimensionless index ranges from a value of approximately 2, for a 0 1 mg ml^{-1} solution of BSA at 1 0 ml s^{-1}, to a value of 12 for a BSA concentration of 1 0 mg ml^{-1}, at a flow rate of 2 5 ml s^{-1} The relationship between dimensionless foaminess and volumetric air flow rate is linear, with regression coefficients of 0 975 or greater for each of the fitted lines indicated The Bikerman results are illustrated in Figure 4 30 The values, for each concentration, vary only slightly over the range of aeration rates investigated, the solid lines represent mean values The Bikerman foaminess ranges from approximately 160 seconds for a 0 1 mg ml^{-1} solution of BSA to 410 seconds at a BSA concentration of 1 0 mg ml^{-1} The relationship between foaminess and BSA concentration is shown in Figure 4 31 The Bikerman value was calculated on the basis of the average air flow rate over the duration of the run The linear regression coefficients for all plotted lines are greater than 0 99

For the validation data described above, sample volumes of 80 ml were employed The comparative data for a 50 ml sample volume are presented in Figure 4 32 By definition, the dimensionless foaminess is the volume of foam per volume of foaming solution, hence foaminess, as quantified by this method, should be identical for any sample volume, at a constant aeration rate Since the dimensionless foam volumes for the two different working liquid volumes are essentially identical, the feasibility of using a 50 ml sample is confirmed The Bikerman foaminess is approximately 275s for an 80 ml sample and 180s for a 50 ml sample, *i e* the 50 ml Bikerman foaminess is approximately 65% of the 80 ml value, as would be expected Therefore, this bubble column (Column B4a) can reasonably be used with a sample volume of between 50 and 80 ml

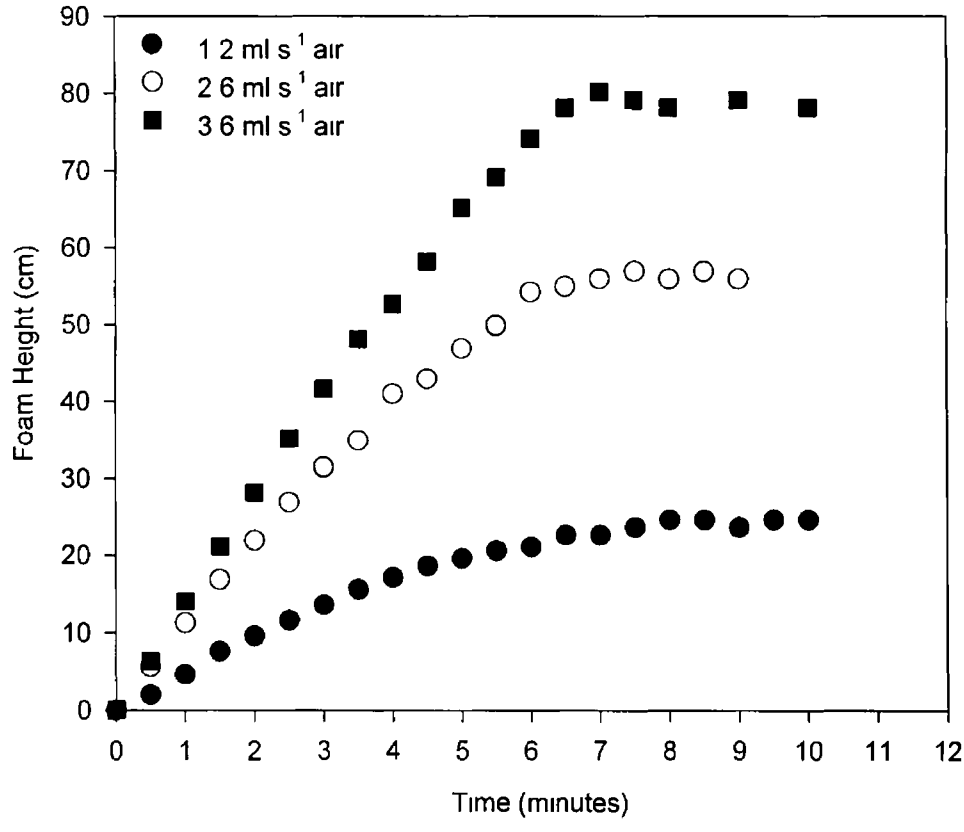

Figure 4 28 Effect of aeration rate on foam generation profile for a 0 5 mg ml ^{1} BSA solution, in column B4a

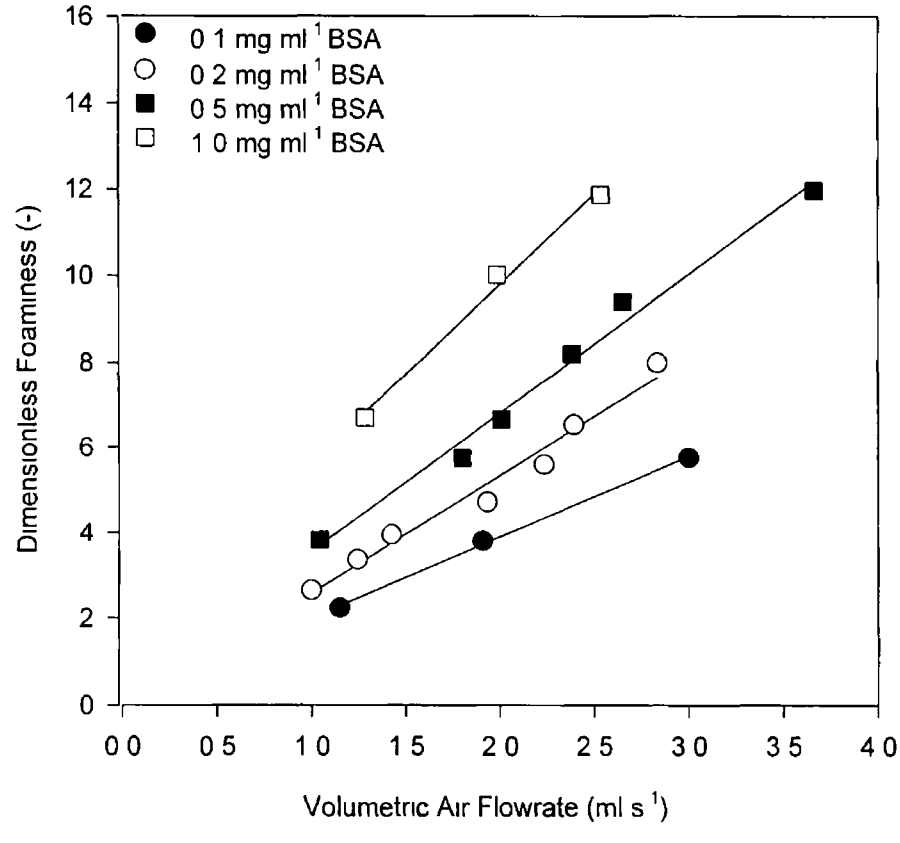

Figure 4 29 Dimensionless foaminess as a function of air flow rate for various concentrations of BSA, in column B4a

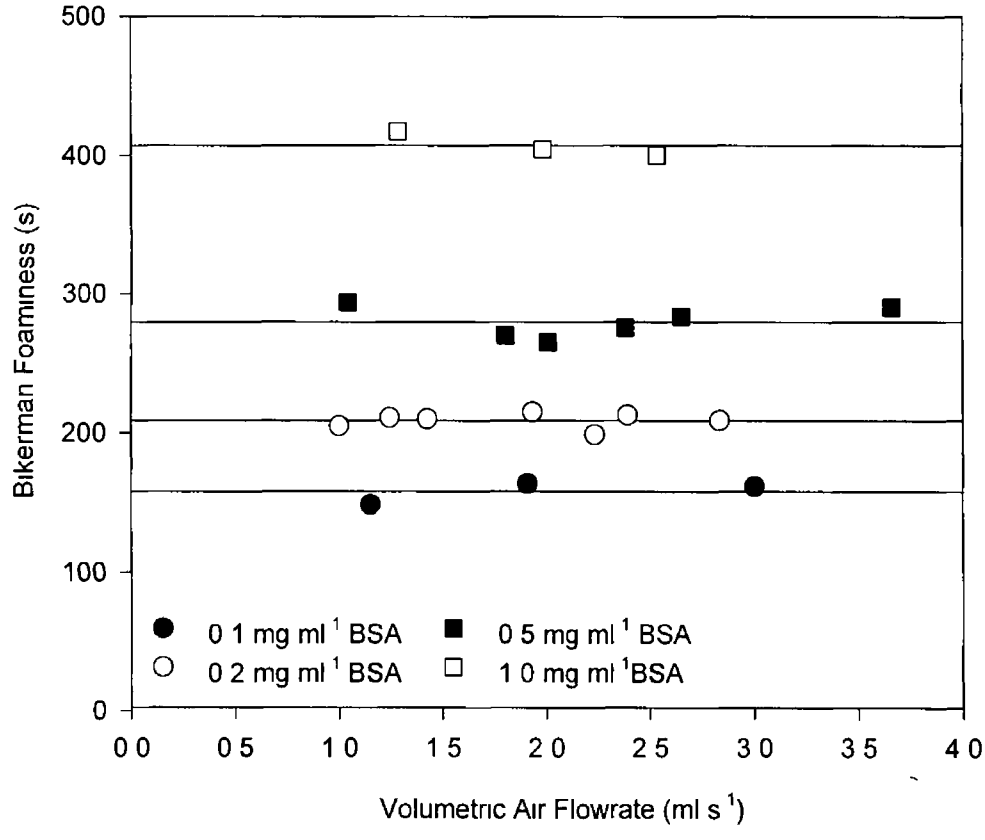

Figure 4 30 Bikerman foaminess as a function of air flow rate for various concentrations of BSA, in column B4a

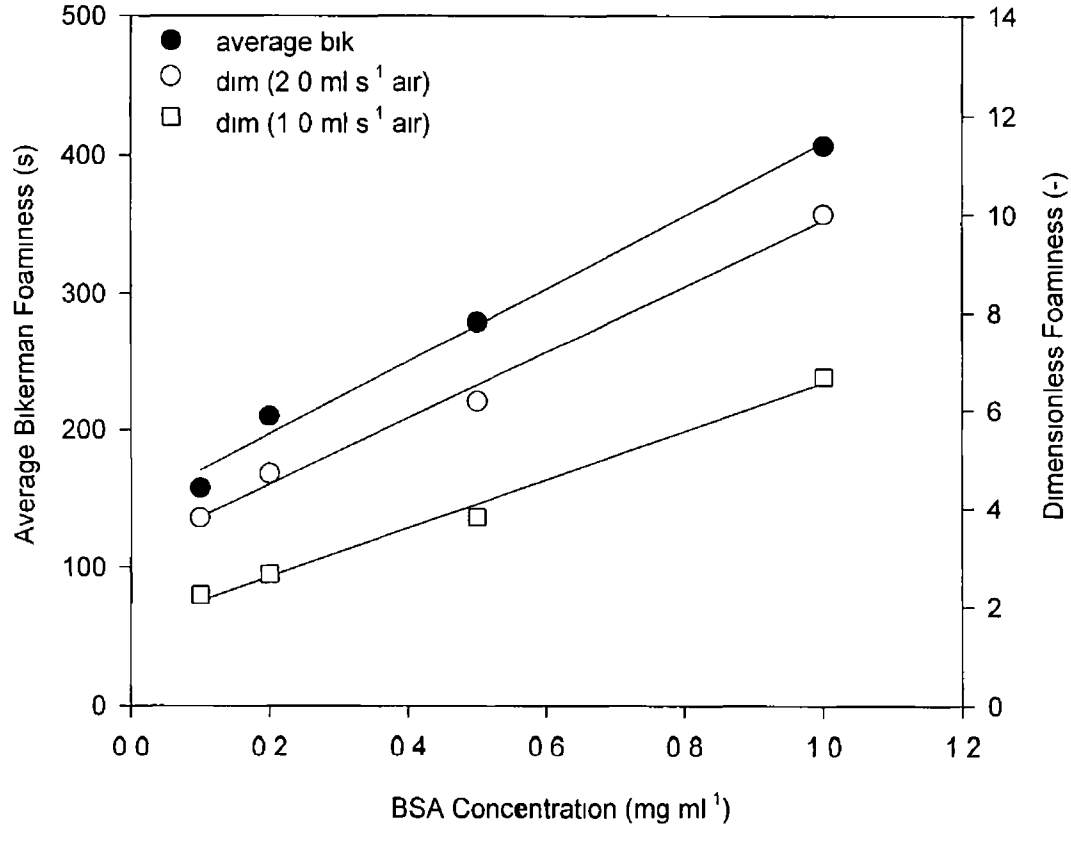

Figure 4 31 Foaminess as a function of BSA concentration, in column B4a

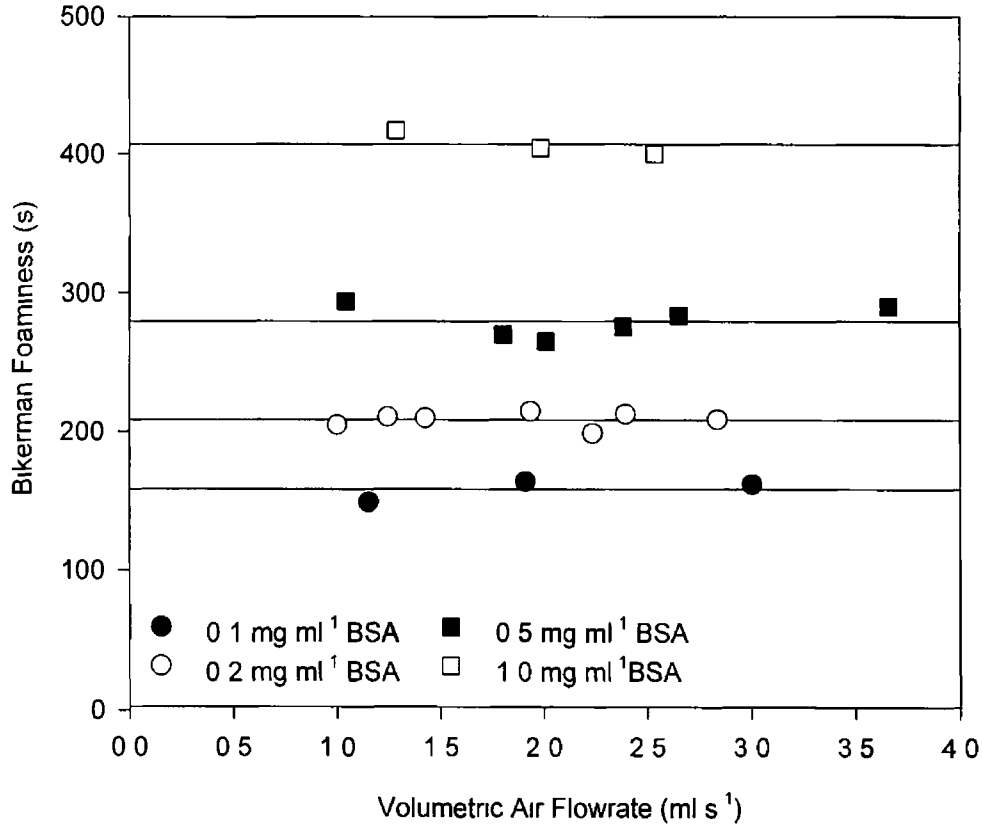

Figure 4 30 Bikerman foaminess as a function of air flow rate for various concentrations of BSA, in column B4a

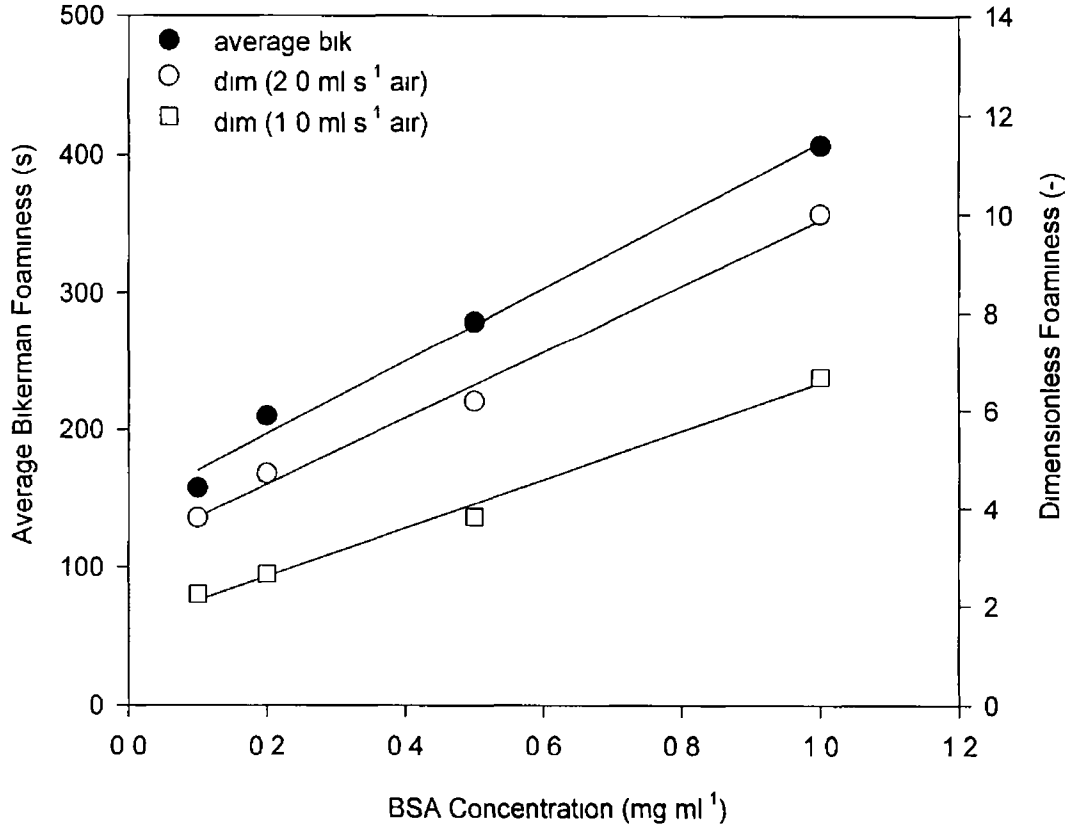

Figure 4 31 Foaminess as a function of BSA concentration, in column B4a

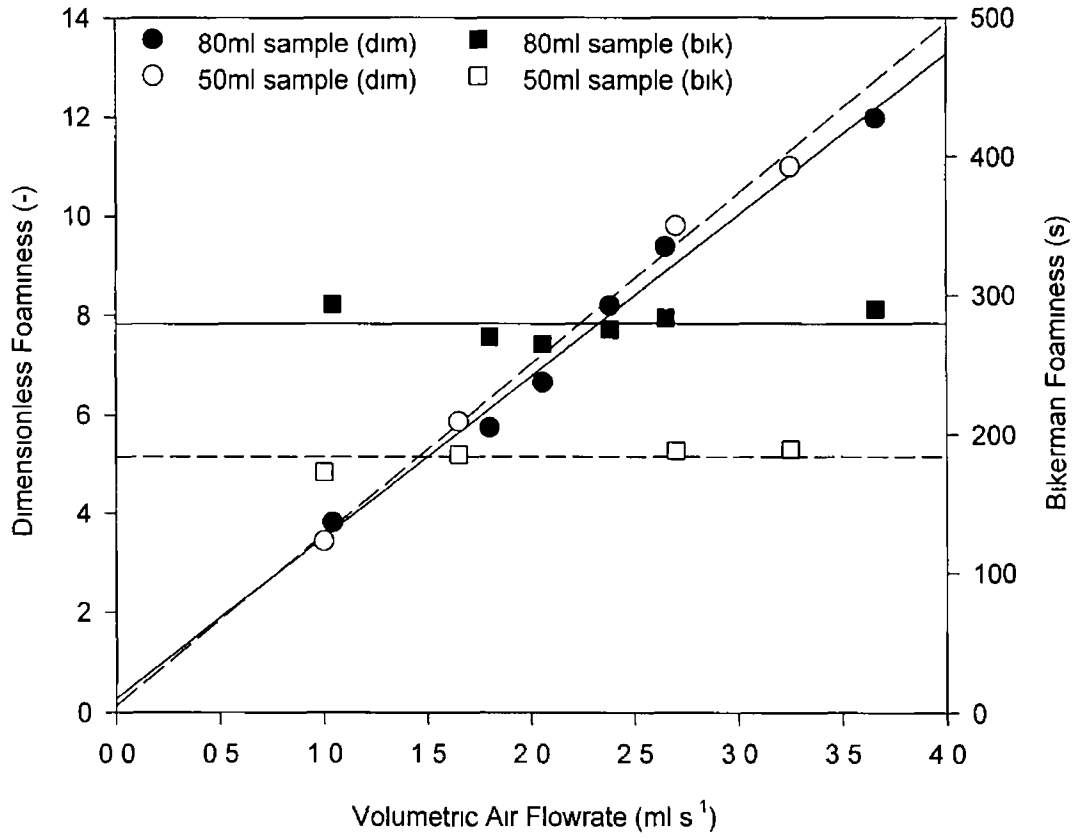

Figure 4 32 Foaminess at varying air flow rates for 80ml (——) and 50ml (----) samples of 0 5 mg ml ^{1} BSA, in column B4a

4 6 FOAMING ANALYSIS OF CELL-FREE BROTHS

4 6 1 Column A1a

The foams produced by cell-free broth samples were generally small and/or very unstable For the first 6 days of the cycle, the foam generated, at all 3 aeration rates investigated (3 33, 8 33 and 16 67 ml s ^{1}), reached a maximum height of no more than 5 cm At a flow rate of 16 67 ml s ^{1}, this corresponds to a Bikerman foaminess of approximately 4 s As the culture matured, the instability of the generated foams increased and for these broths it was not possible to identify stable foam heights By day 8, a flow rate of 3 33 ml s ^{1} yielded a foam which reached a maximum height of 20 cm (Bikerman foaminess equivalent of 83 2 s) and then disintegrated to a height of 2 cm, leaving residues on the column wall Residual material inevitably interfered with subsequent foaming behaviour The foam continued to increase and break in this manner Occasionally, transient ring structures rose up the column and disintegrated No

pattern or cyclic nature was identified At higher air flow rates, the instability was exacerbated Similar patterns were observed for the remainder of the cycle, with unstable foam pieces reaching maximum heights of 55 cm Since, no definable stable foam height could be identified, it is evident that this column design was not capable of producing measurable quantifiable foam for assessing foaming potential in cell-free broths of *Morinda citrifolia*

4 6 2 Column B4a

The pattern of foam generation and stability for the cell-free broth samples analysed can be characterised as follows, the foam rose at a constant rate until it reached a critical height, (recorded for analysis), at which point the middle of the foam degenerated until the foam eventually broke, after this time the foam continued to break and form small films and foam units, which rose, independently, up the column However, the top foam section continued to rise and the cumulative volume of all coherent segments approximated the total volume of foam generated prior to the onset of foam breakage Therefore, the height reached by the foam immediately prior to degeneration was used for calculating the foaming potential of these cell-free broth samples Attempts were made to employ either the height at which the foam broke completely or the height after a 5 minute foaming interval as a characteristic index of foaming behaviour, but the results were unintelligible

Figure 4 33 shows Bikerman and dimensionless foaminess profiles throughout a single culture cycle, which range from 60 to 600s and from 50 to 12 5, respectively As anticipated, the contours of both profiles are similar and thus both are appropriate for measuring foaminess in this system However, the Bikerman method is employed for all further analysis, for reasons previously outlined The mean foaminess over 2 culture cycles and the calculated standard errors are presented in Figure 4 34 The foaming potential is minimal up to day 3, after which time it increases steadily until days 11 to 14, when it reaches a maximum of approximately 600 s A gradual reduction to approximately 500 s is observed over the remaining ten days of the growth cycle (*i e* during the stationary phase)

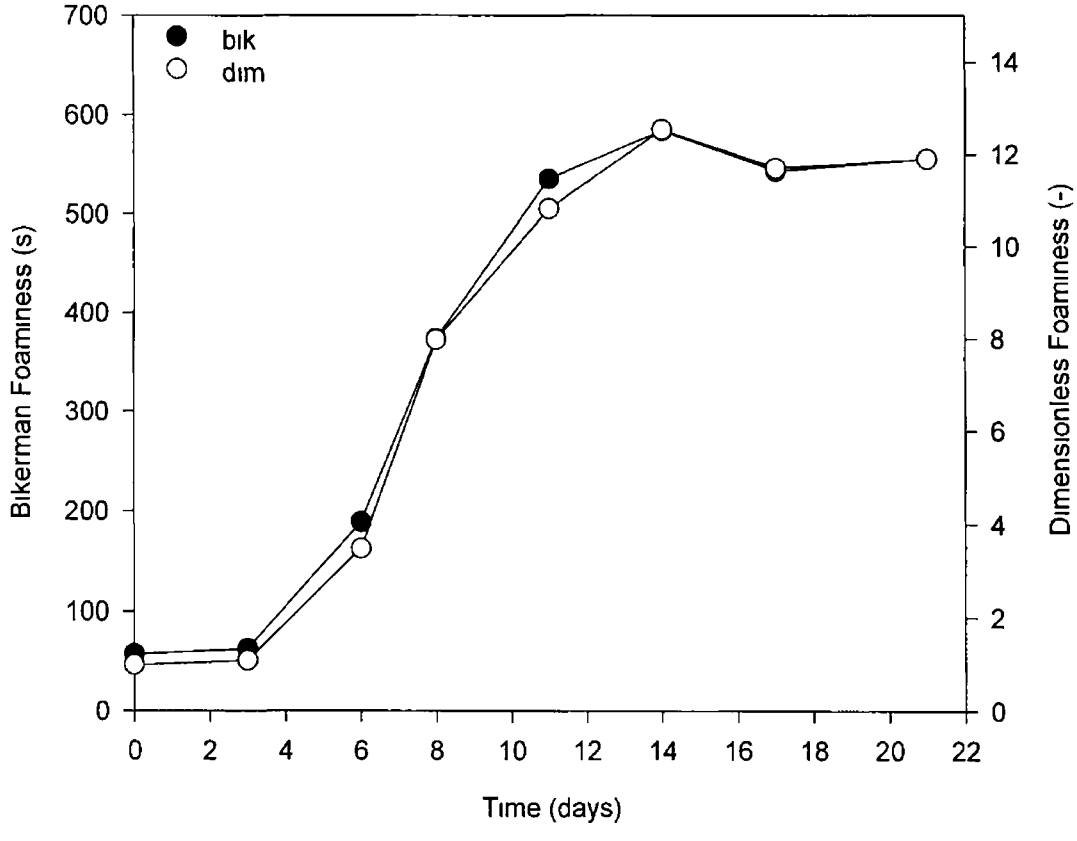

Figure 4 33 Cell-free broth foaminess profile throughout the growth cycle, in column B4a (n=2)

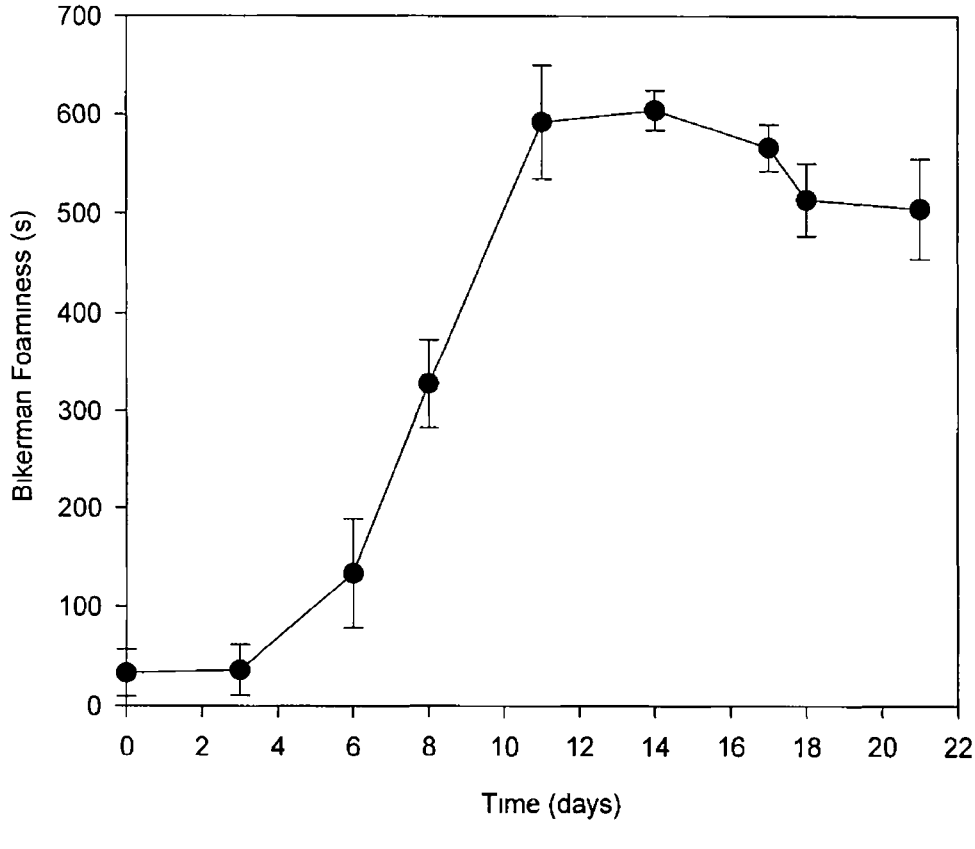

Figure 4 34 Bikerman foaminess throughout the growth cycle, in column B4a (n = 2)

Effect of pH on Foaminess of Cell-free Broth

The effect of pH on the foaminess of cell-free broths was established for one growth cycle and the results are illustrated in Figure 4 35 During the initial days (days 0 to 6) of the growth cycle, the variation in foaminess is small across the entire pH range investigated (pH 4 - 6) However as the culture matures, there is some evidence of pH dependencies Foaminess appears to reduce slightly as the pH increases from a pH value of 4 to 5 On day 14, a slight decrease in foaminess was observed as the pH increased from a value of 4 to 5 35 and a more pronounced foaminess decline was seen as the pH continued to increase to pH 6 On day 17, a substantial decrease in foaminess accompanied the reduction in pH from a value of 5 1 to 4 Unfortunately however, there was no sample available for further pH effect analysis As Figure 4 35 indicates, the relative change in foaminess with respect to pH is not constant over the entire cycle, with variations in the relationship from day to day

The respective surface tension values of cell-free broths at the various pH values investigated are summarised in Table 4 1 As reported in Section 4 2 3, the surface tension did not vary significantly with these pH alterations, therefore, it is difficult to attribute the slight differences in foaminess directly to surface tension

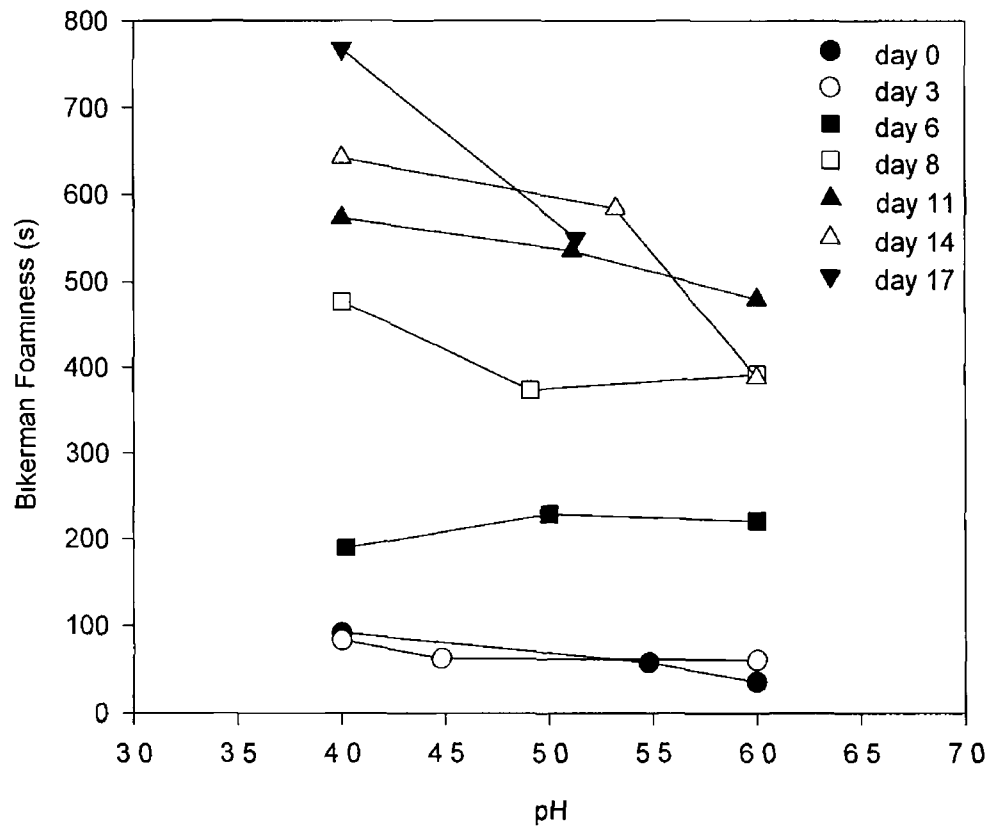

Figure 4 35 The effect of pH on foaminess of cell-free broth, in column B4a

Foamed cell-free broth sample analysis

When the residual liquid was recovered following a foaming experiment, for a day 11 cell-free broth sample, it was found that the protein content was reduced from 0 091 mg ml^{-1} to 0 056 mg ml^{-1}, as a result of foaming The viscosity of this sample, which is representative of the ECP content, was only reduced from 4 01 to 3 74 mN s m^{-2}, thus indicating that proteins were stripped from solution by foaming, while the bulk of ECPs remained in the cell-free broth solution

The surface tension of this solution was found to have increased from 0 0540 to 0 0710 M m^{-1}, due to foaming Figure 4 22 shows that for untreated cell-free broths at protein concentrations in excess of approximately 0 2 mg ml^{-1}, the surface tension does not vary considerably Therefore, the high surface tension value at a protein concentration of 0 056 mg ml^{-1} in the residual broth following foaming suggests that some proteins were differentially removed by foaming and these proteins were the principal cause of surface activity in the cell-free broth It is well established (Section 2 5 2) that some proteins have a greater effect on surface tension and are preferentially removed by foaming

4 7 POLYSACCHARIDE AND PROTEIN EFFECTS ON FOAMINESS

4 7 1 Influence of Cell Suspension Metabolites on Foaming

The change in foaming potential is caused by variation in broth composition The relationships between cell-free broth foaminess and protein and ECP concentrations are shown in Figures 4 36 and 4 37, respectively Both profiles indicate linear relationships, with regression coefficients of 0 988 for protein and 0 993 for ECP However, it must be remembered that both metabolites are produced simultaneously during the growth cycle (Figures 4 12 and 4 13) Figures 4 38 and 4 39 illustrate the relationship between foaming potential and cell-free broth surface tension and viscosity, respectively It is seen that there is no substantial foaming at a surface tension value greater than approximately 0 057 N m^{-1}, corresponding to the first 3 days of the growth cycle (Figure 4 16) A linear relationship between foaminess and viscosity is also apparent, as anticipated, since apparent viscosity is strongly correlated with ECP concentration for conditions investigated (Figure 4 24)

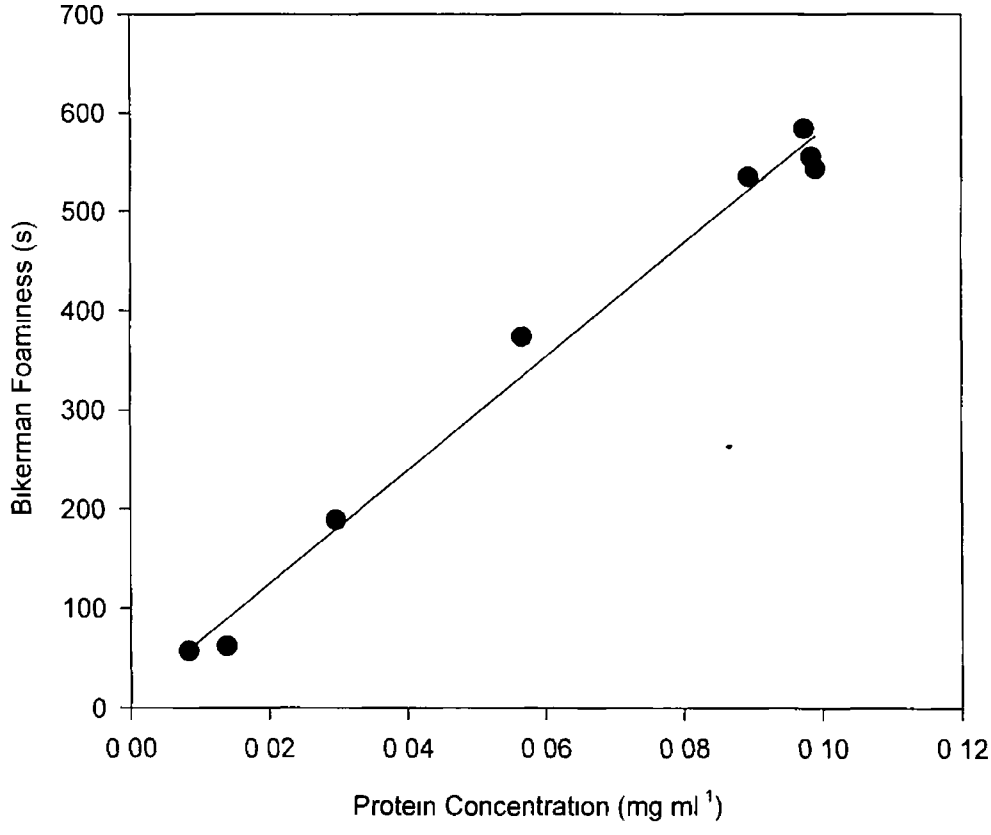

Figure 4 36 Foaminess as a function of cell-free broth protein concentration

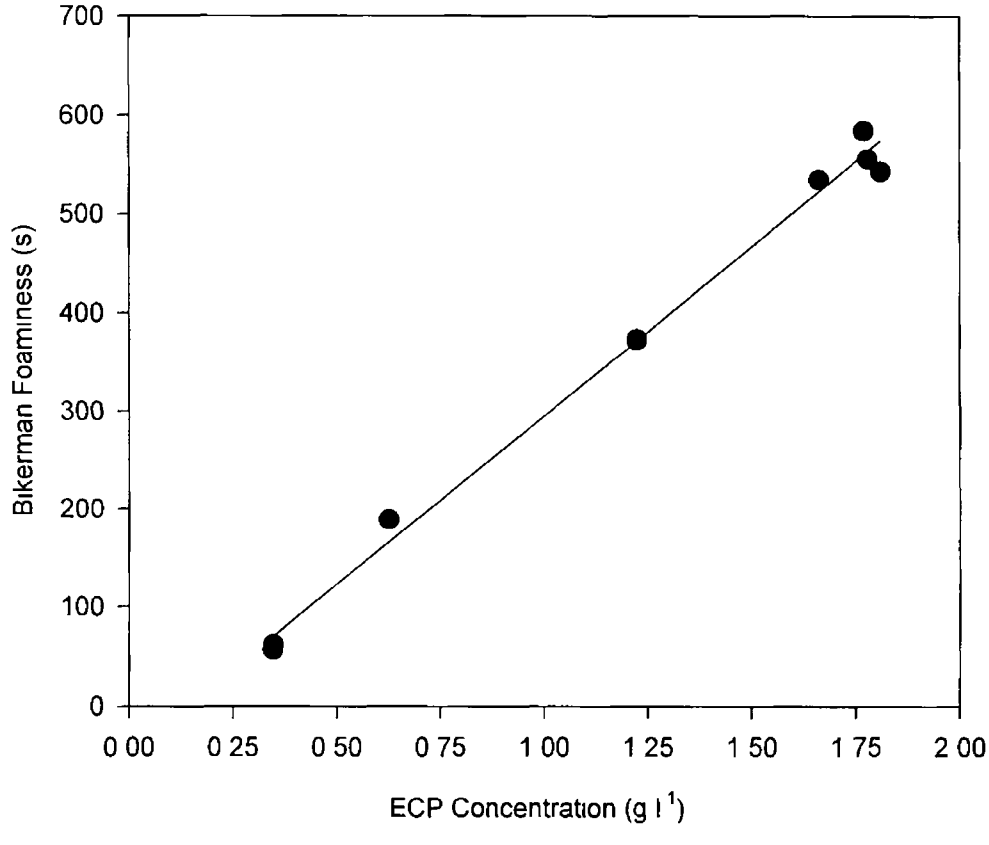

Figure 4 37 Foaminess as a function of cell-free broth ECP concentration

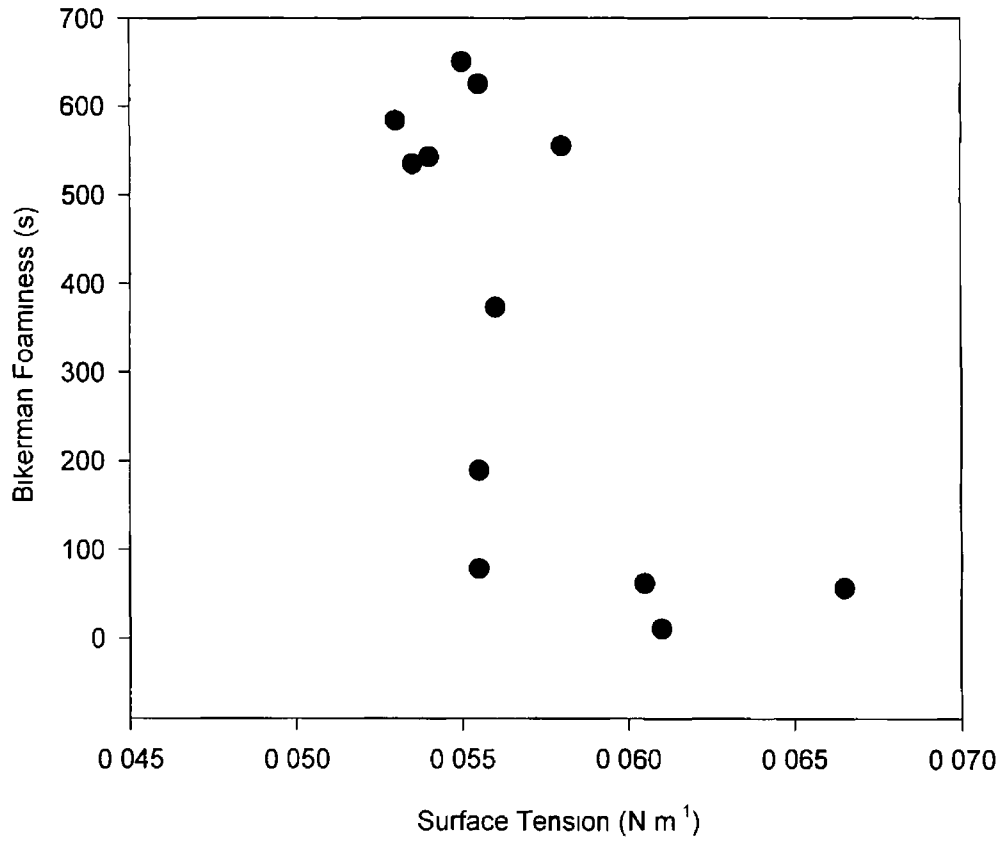

Figure 4 38 Foaminess variation with surface tension for cell-free broth

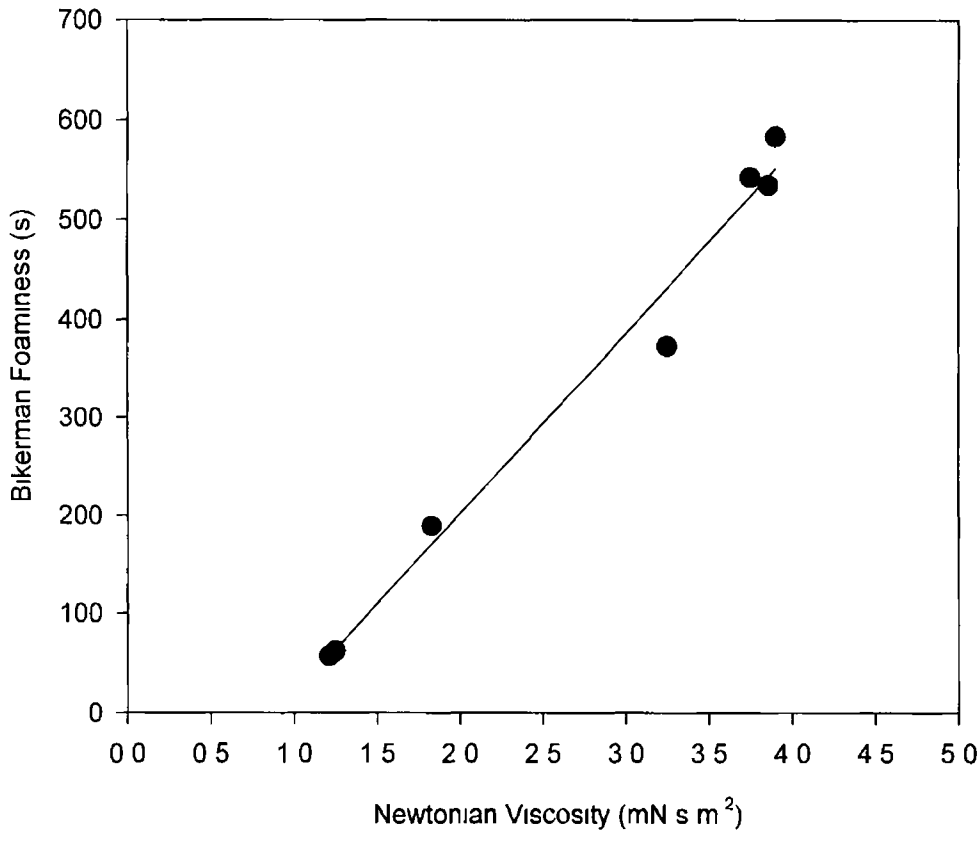

Figure 4 39 Dependency of foaminess on cell-free broth viscosity

As separation procedures to separate the ECP and protein constituents of the cell-free broth were unsuccessful (Section 4 3), foaming experiments were conducted on isolated ECP / protein solutions, in water and medium The properties of these solutions and the observed foaminess values are summarized in Table 4 2 The ECP and protein concentrations in both aqueous and medium based solutions were nominally 200 g l^{-1} and 0 09 mg ml^{-1}, respectively The unadjusted pH of the aqueous solution was 4 41 and that of the medium based solution was 5 47 For the aqueous solutions, the maximum Bikerman foaminess values recorded during experiments performed at pH values of between 4 0 and 7 0 were essentially similar, with a value of 65 s This corresponds to a foam height of only 5 4 cm and hence, the foaming capacity of these solutions was negligible However, when medium was used as the base solvent, the foam generated overflowed the bubble column corresponding to a minimum Bikerman foaminess of 1200 s In this context it is very interesting to note that medium alone has a foaminess value of 40s, equivalent to approximately 3 3 cm of foam, at an air flow rate of 1 ml s^{-1} Increasing the air flow rate does not increase the foaming potential of medium These results suggest that it is the interaction between medium components and the plant cell metabolites secreted during growth (*i e* proteins and/or ECPs) that is responsible for the excessive foaminess of cell-free broths

In attempting to differentiate between the effects of ECPs and protein on foaminess, a crude intracellular protein isolate was formed in deionised water Although the results of a PAGE-SDS gel electrophoresis (Section 4 3 3) indicated that the main proteins present in the intracellular protein isolate were different to the extracellular proteins found in the cell-free broth, foaming studies were performed on the extract, to examine the foaming potential in an aqueous solution Table 4 2 also contains information on this solution The Bikerman foaminess of this isolated protein solution (0 033 mg ml^{-1}, ST = 0 0565) was approximately 35 s, hence the foaming was minimal The instantaneous and equilibrium surface tension values were identical This effect could perhaps be related to the viscosity of this solution, since viscous forces retard liquid flow (Bikerman, 1973), therefore increased viscosity may hinder the migration of surfactant molecules to the liquid surface thus causing extended time periods for the surface tension of viscous solutions to equilibrate Therefore, in non-viscous solutions (protein isolate), the equilibrium surface tension can be reached relatively instantaneously

Table 4 2 Foaming solution properties

Solution	ECP ($g l^{-1}$)	Protein ($mg ml^{-1}$)	Surface Tension ($N m^{-1}$)	Newtonian Viscosity ($mN s m^{-2}$)	pH	Bikerman Foaminess (s)
ECP/protein in water	198	0 093	inst =0 071 equil =0 064	4 2	4 - 7	65 (maximum)
ECP/protein in medium	201	0 088	inst =0 066 equil =0 062	4 0	5 5	1200 (minimum)
Protein isolate in water	N/A	0 033	inst =0 0565 equil =0 0565	1 04	5 01	35

4 7 2 Model System Studies - Foaminess

Xanthan gum (xan) and BSA were used to model the effects of protein and polysaccharides on foaminess As shown in Section 4 4 2, xanthan gum alters the viscosity (Figure 4 24), while BSA significantly effects the surface tension (Figure 4 25) Since these components alter the physical aspects of a fluid, known to affect foaming potential (Section 2 1), their influence on foaminess was assessed, in an effort to model foaming m biological systems

Aqueous and medium based solutions were investigated, to evaluate the effect of medium on foaming Figure 4 40 shows the relationship between Bikerman foaminess and BSA protein concentration, for Trial No 1 and Trial 2 solutions (Table 3 11) The 0 2 mg ml^{-1} solution of BSA in water (Trial No 1) had a foaminess of approximately 200 s, while the 0 2 mg ml^{-1} solution of BSA in medium (Trial No 2) displayed a foaminess of approximately 950 s, thereby reinforcing the significance of the interaction between medium components and protein on foaming potential

The effect of BSA concentration on a more viscous solution (0 02% xanthan) is illustrated in Figure 4 41, for water (Trial No 3) and medium (Trial No 4) based solutions As expected, the medium based solution has a greater foaming potential with an 8-fold difference observed at a BSA concentration of 0 1 mg ml^{-1} The data presented in Figures 4 40 and 4 41 for the aqueous solutions (Trials No 1 and 3) are presented together in Figure 4 42, for comparison purposes The influence of viscosity on the foaming potential of a protein solution is thus evident The apparent viscosities of the solutions are approximately 1 0 (BSA-water) and 2 5 (BSA-0 02% xan) mN s m^{2} The foaminess of both water and xanthan-water based protein solutions are similar up to a protein concentration of 0 1 mg ml^{-1}, after which significant differences arise The more

viscous solution has a foaminess of approximately 430 s, as opposed to approximately 210 s, for the purely aqueous solution, at a BSA concentration of 0 2 mg ml ^{1}

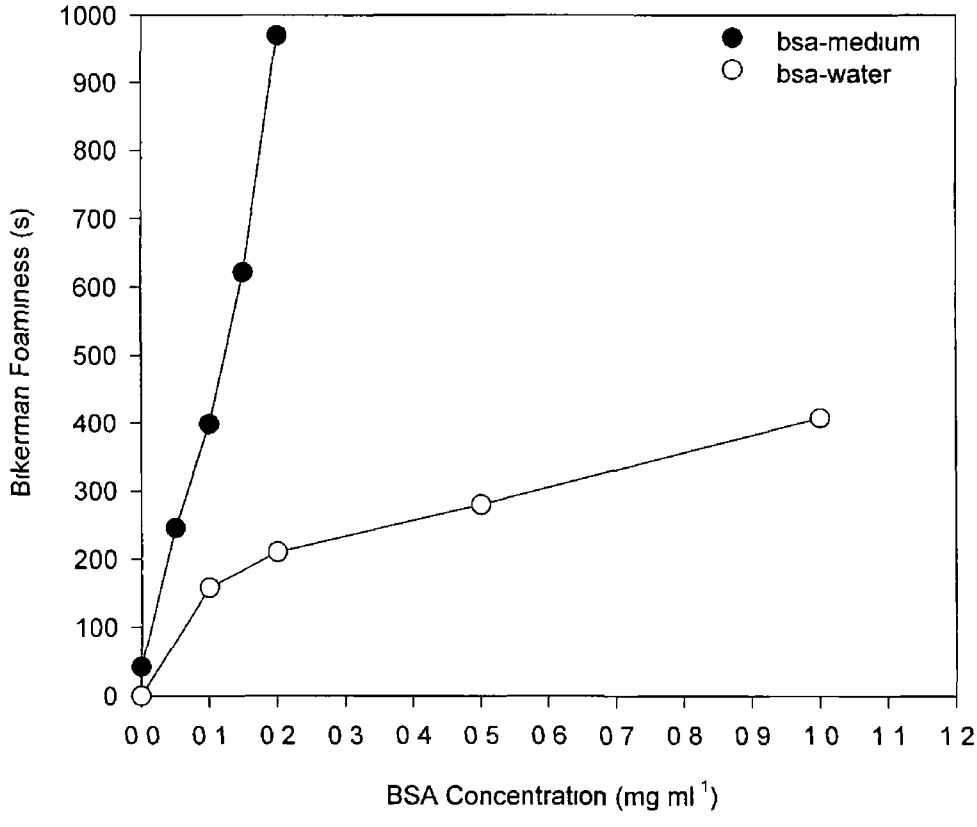

Figure 4 40 Comparison between the foaming potential of BSA solutions in water and medium

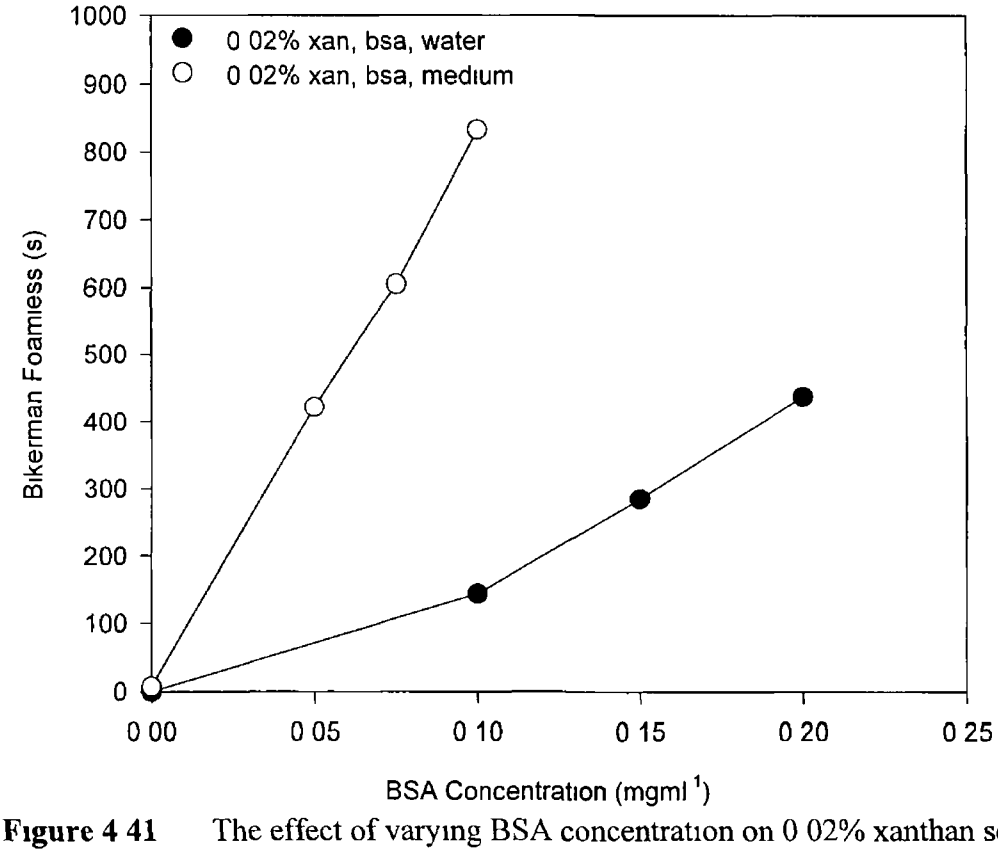

Figure 4 41 The effect of varying BSA concentration on 0 02% xanthan solutions in medium and water

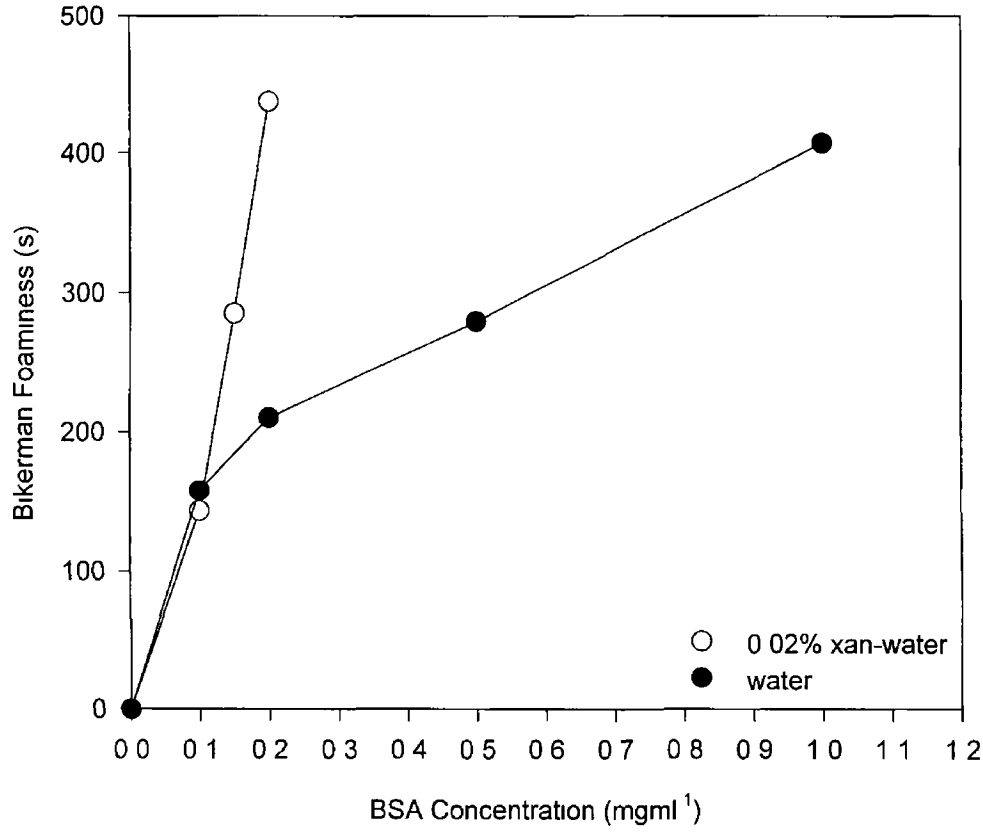

Figure 4 42 Comparison of the effects of BSA concentration on aqueous and 0 02% xanthan gum-water solutions

Figure 4 43 shows, in more detail, the effect of increasing viscosity (via increasing xanthan gum concentration) on the foaming characteristics of a protein solution BSA concentrations of 0 2 mg ml ^{1} in water (Trial no 5) and 0 1 mg ml ^{1} in medium (Trial No 6) were chosen for analysis, at an air flow rate of 1 0 ml s ^{1}, as used for all foaming experiments involving model systems Under these conditions, a range of xanthan concentrations could be investigated, all producing measurable foam heights Bikerman foaminess values ranged from 400 s to 1000 s for xanthan concentrations of 0 0% to 0 02% in the medium-based solution (0 1 mg ml ^{1} BSA), while the foaming potential of the aqueous solution (0 2 mg ml ^{1} BSA) increased from 200 s to 1000 s as xanthan concentration increases from 0 0% to 0 04% Pure xanthan in either deionised water (Trial No 7) or medium (Trial no 8) displayed no foaming potential for the range of xanthan concentrations (0 0% to 0 04%) investigated Thus, it has been established that xanthan contributes to the stabilisation of foams generated in protein solutions, although xanthan solutions alone do not foam

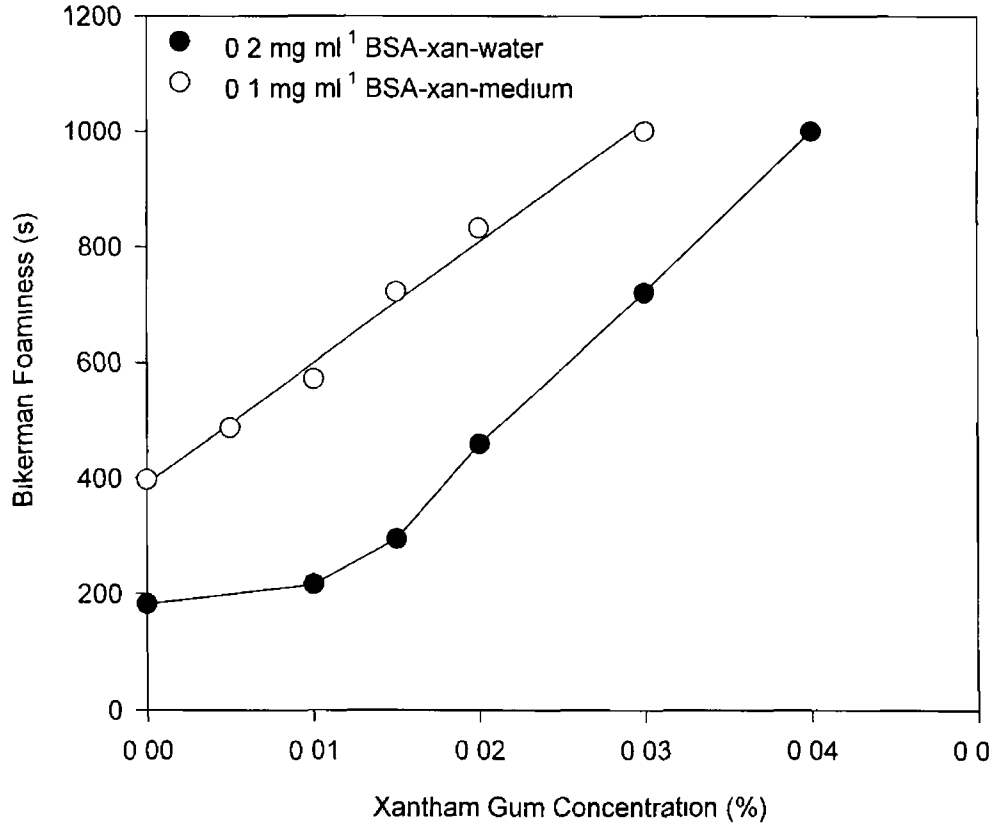

Figure 4 43 The effect of xanthan gum on BSA solutions in water and medium

4 8 ANTIFOAM STUDY

4 8 1 Effects of a Silicone Antifoam on Culture Growth Characteristics

A preliminary investigation of the effects of a silicone-based antifoam on the growth of *Morinda citrifolia* suspension cultures and on the foaming potential of cell-free broth throughout the growth cycle was performed The presence of the silicone antifoam (100 ppm) in the culture medium did affect the dry weight growth patterns of the culture, as can be seen from Figure 4 44 However, fresh weight profiles were observed to deviate slightly after day 12 Similar pH profiles were recorded for cell-free broths with and without antifoam, (Table 4 3) It can be seen from Figures 4 45 and 4 46, that culture productivity, in terms of both proteins and ECPs, was also unaffected

From Table 4 3, can be seen that no significant variation in either viscosity or surface tension was attributable to the presence of antifoam However, the direct addition of antifoam (50 or 100 ppm) to the extracted cell-free broth, caused the equilibrium surface tension to substantially decrease from 0 056 to 0 044 N m^{1} This suggests that the

antifoam may bind to the biomass during cultivation or during filtration to recover cell-free broth,, in which case these measurements may not accurately represent conditions prevailing in the cultivation vessel.

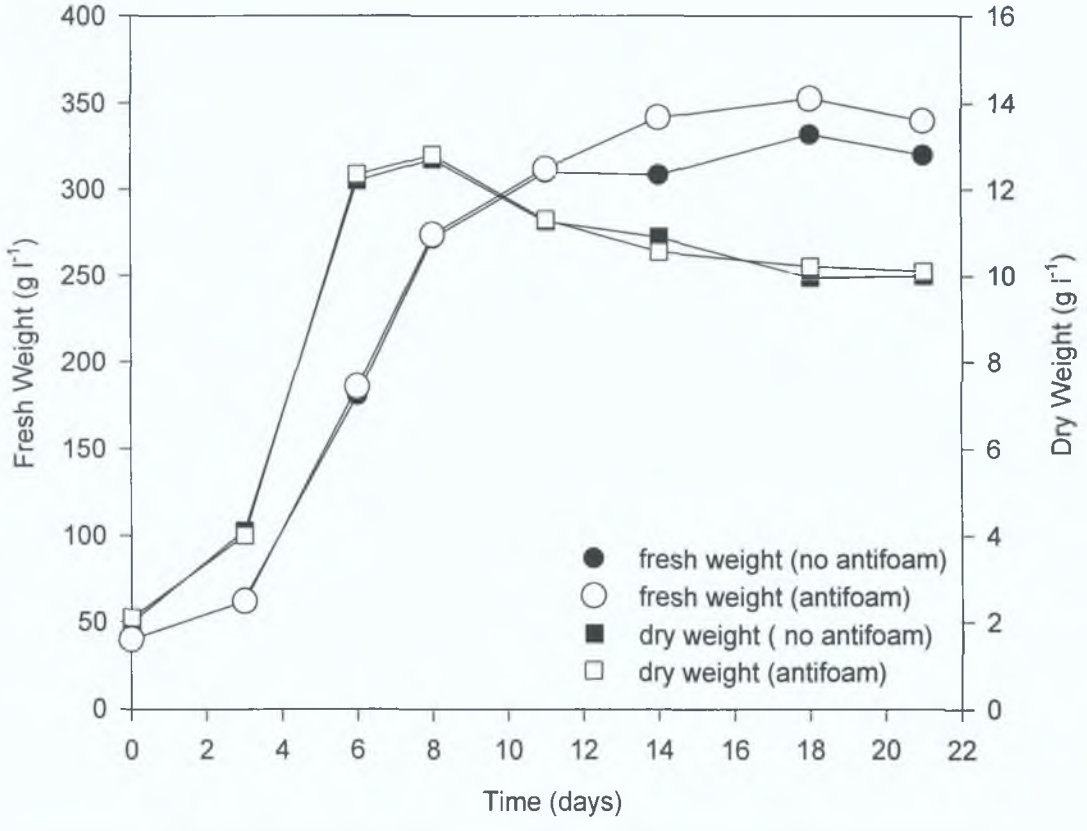

Figure 4.44: The effects of a silicone antifoam (100 ppm) on biomass growth.

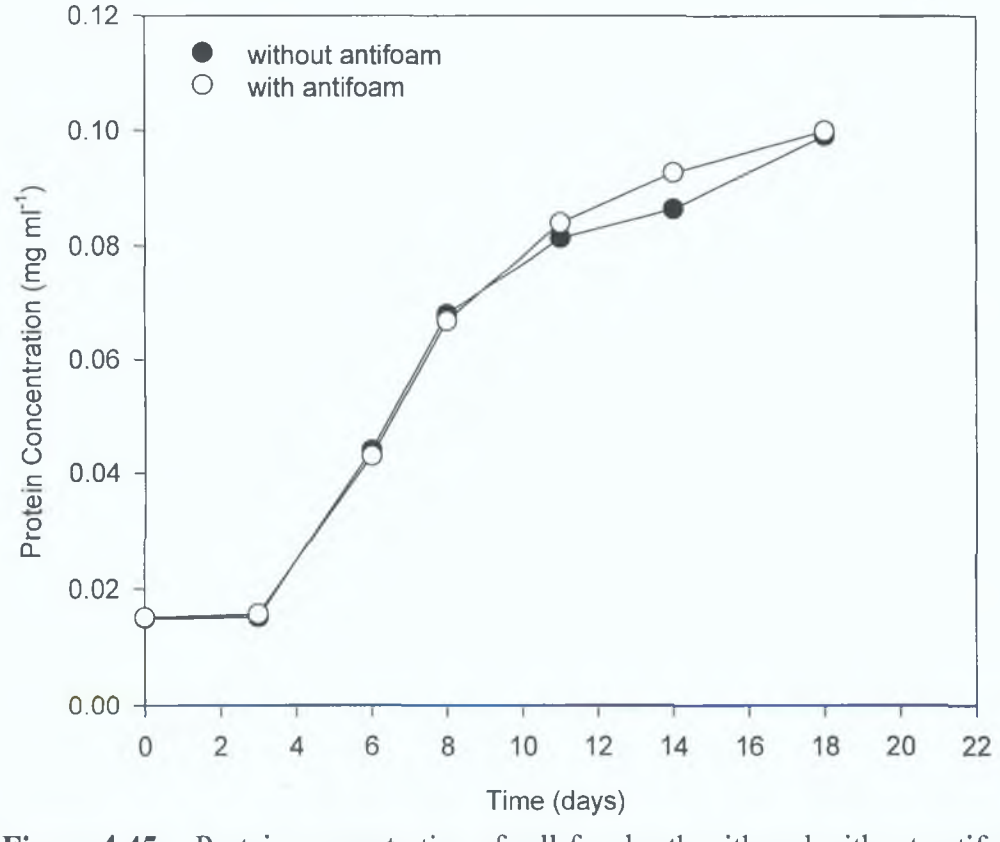

Figure 4.45: Protein concentration of cell-free broth with and without antifoam.

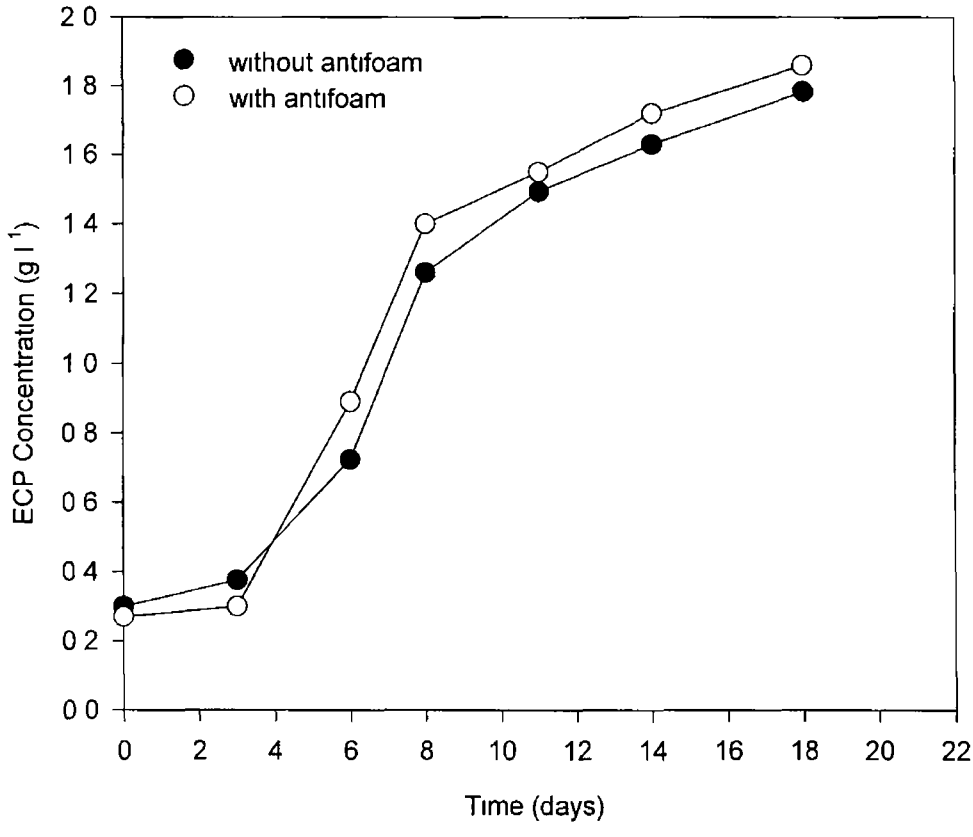

Figure 4 46 ECP concentration of cell-free broth, with and without antifoam

Table 4 3 Comparison between the characteristics of cell-free broths, with and without antifoam (100 ppm)

Cell-Free Broth Day	**Cell-free Broth pH**		**Surface Tension N m^{-1}**		**Viscosity mN s m^{-2}**	
	w/o	w	w/o	w	w/o	w
0	5 48	5 47	0 0650	0 0640	1 10	1 08
3	4 34	4 36	0 0610	0 0590	1 32	1 30
6	4 83	4 95	0 0555	0 0565	2 20	2 24
8	5 53	5 69	0 0500	0 0545	4 29	3 88
11	5 80	5 85	0 0550	0 0550	4 54	4 00
14	5 30	5 60	0 0555	0 0560	3 98	3 82
18	5 43	5 58	0 0560	0 0565	3 80	3 61

Note Without antifoam (w/o), With antifoam (w)

4 8 2 Effects of a Silicone Antifoam on Foaminess

Figure 4 47 shows the variation in the Bikerman foaminess over the course of one growth cycle for a set of suspensions to which 100 ppm of antifoam was added prior to inoculation, a corresponding control is illustrated for comparison purposes It can be seen that the Bikerman foaminess, throughout the growth cycle, is greatly reduced by the presence of antifoam By day 11, the foaminess of the control cell-free broth has reached a value of 640 s, while that of cell-free broth containing antifoam is less than 100 s Direct addition of antifoam (100 ppm) to cell-free broth, prior to foaming, resulted in a complete retardation of foam generation An identical result was observed for the direct addition of antifoam, at a concentration of 50 ppm, to cell-free broth prior to foaming

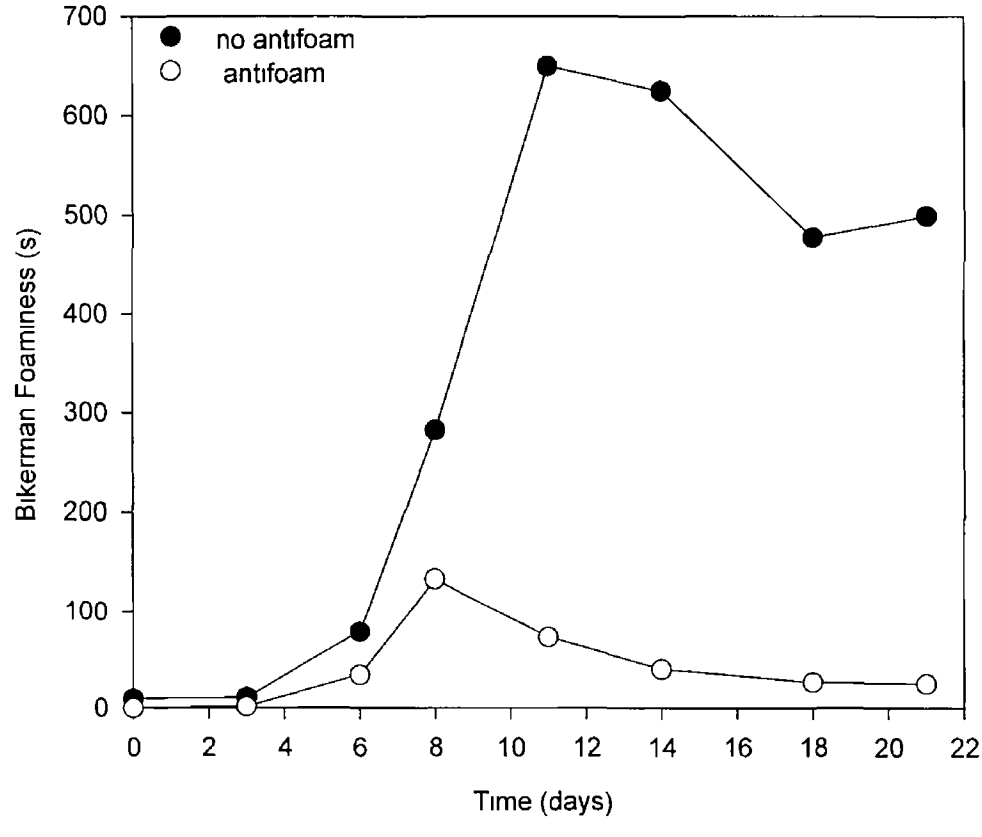

Figure 4 47 The effect of a silicone antifoam on the foaming potential of cell-free broth

Chapter 5

DISCUSSION

5 1 GROWTH CHARACTERISTICS OF *MORINDA CITRIFOLIA* SUSPENSION CULTURES

5 1 1 Analysis of Growth Profiles using Conventional Indicators

During batch cultivation of *Morinda citrifolia* suspension cultures, growth characteristics typical of many plant cell suspension systems were observed The duration of the growth cycle depends on the cell line being cultivated However, the growth profiles normally exhibit distinctive lag, exponential and stationary phases The duration of each phase again depends on the cell line being cultivated and on the growth conditions Sub-culturing is normally performed before the cultures enter a death phase Such growth patterns are observed for, among others, the cell lines *Pyrus communis* L (Ryu *et al*, 1990), *Nicotiana tabacum* (Hooker *et al*, 1990) and *Catharanthus roseus* (Snape *et al*, 1989) For example, Hooker *et al* (1990) reported that suspension cultures of *Nicotiana tabacum*, sub-cultured on the basis of a 7 days growth cycle, were seen to display a lag phase of 1 day, followed by an exponential phase of 6 days

The growth characteristics of *Morinda citrifolia* have been well documented by other authors, (*e g* Zenk, 1975, Curtin, 1991, Dornenburg and Knorr, 1992, Kieran, 1993) However, given the variety of methods employed for monitoring the suspension culture in this work, some further comments on observed trends are appropriate During the course of a typical 21 day growth cycle, it is seen that there is a slight rise in both fresh and dry weights during the lag phase, which is due to the accumulation of nutrients by the cells and the growth of individual cells, in preparation for cell division Hence, the cell number is constant but the biomass weights increase slightly At this point in the cycle, black particles can be seen in the cells, when viewed under a microscope These are carbohydrates which are accumulated and stored intracellularly From Figures 4 1 and 4 2, it is evident that the dry weight stabilises on day 8, while the fresh weight and cell number continue to increase At this point in the cycle, it is obvious that cell division is continuing, as cell number increases and fresh weight increases accordingly The fact that the dry weight does not increase correspondingly is possibly due to the

depletion of intracellular starch reserves and reduction in average cell size (Figure 4 9) At all stages throughout the 21 day growth cycle the cell viability for these batch cultures, (as determined using the Evans blue dye exclusion technique), is greater than 95% Even during the final days of the cycle there is no visual evidence of significant loss of viability or of cell lysis Therefore, the slight decrease in dry weight is not representative of the onset of a decline phase and it can be concluded that the culture is still in the late stationary phase when subcultured on day 21

Dornenburg and Knorr (1992) cultured *Morinda citrifolia* cell under different inoculation and incubation conditions (23 5 °C and 24 day cycle) to those employed in this work Although, a broadly similar fresh weight profile is reported, the maximum biomass concentration observed was 260 g l^{1}, as opposed to 300 gl^{1} under the working conditions in this laboratory A slightly longer lag phase is also evident and is thought to be largely attributable to lower incubation temperature The biomass growth profiles observed by Kieran *et al* (1993), for suspension cultures of *Morinda citrifolia*, were very similar to the results obtained in this study

The pH of the culture (Figure 4 3) decreases rapidly until day 5-6, when it reaches a pH value of approximately 4 2, after which it increases rapidly until day 9 and eventually stabilises between at a pH value of between 5 0 and 5 5 Similar behaviour was also observed by Zenk (1975) for suspension cultures of *Morinda citrifolia* The fluctuation of pH is common in plant cell systems, Wongsamuth and Doran (1994) found that the pH varied from 5 2 on day 2 to a value of 6 0 on day 14 for suspension cultures of *Atropa belladonna*

5 1 2 Broth Conductivity Profile

Many methods have been used to monitor growth in plant cell suspension cultures Among the most common techniques are those used in this study, *i e* fresh weight, dry weight and cell number Although these conventional methods are reliable, they are time consuming and labour intensive There is an obvious need for alternative methods, ideally suitable for on-line application during large scale cultivation in bioreactors, and a number of such methods have been proposed and investigated For example, Tanaka *et al* (1992) reported that off-line turbidimetric measurement of cell concentration was

possible in homogeneous, disperse plant cell suspension cultures of *Catharanthus roseus* and *Oryza sativa* Although there is potential for online application, specialised cuvettes are required for this spectrophotmetric analysis technique in its current off-line configuration

The use of electrical conductivity as a means for estimating biomass concentration in plant cell systems has been investigated by a number of authors, including Hahlbrock (1975), Ryu and Roamani (1989), Taya *et al* (1989) and Kwok *et al* (1992) This method was investigated in this work to assess the feasibility of using conductivity measurements as a basis for monitoring suspension cultures of *Morinda citrifolia*

The results, illustrated in Figures 4 5 and 4 6, reveal a strong linear correlation between conductivity and fresh weight, and conductivity and cell number, over the entire growth cycle However, linearity between dry weight and conductivity is confined to the first 9 days of the growth cycle, before the dry weight profile enters the stationary phase From this point on, as the cell number and fresh weight continue to increase, the broth conductivity continues to decrease as the broth becomes nutrient depleted However, the dry cell weight decreases slightly, as previously explained (Section 5 1 1) and a linear correlation is not appropriate for the remainder of the cycle

Hahlbrock (1975) examined this technique using five different plant cell lines, namely *Petroselinum hortense*, *Glycine max*, *Haplopappus gracilis*, *Cicer arietinum* and *Acer pseudoplatanus* The mechanism by which conductivity relates to certain stages of the growth cycle and its limitations are outlined It was found that the conductivity of many plant cell cultures is directly related to nitrate (nitrogen) uptake by the cells and that 'mirror' images of conductivity and biomass concentration profiles are commonly observed until the end of the linear growth phase, when nitrate levels are depleted It is hypothesised, based on work by other authors (*e g* Nash and Davis, 1972), that subsequent changes in conductivity are related to the uptake of other ions (*e g* phosphorus) during the latter stages of the growth cycle However, variations for different cell lines and medium compositions would be expected A mirror image-type relationship is evident for *Morinda citrifolia* culturing in this laboratory (Figure 4 4)

Kwok *et al* (1992) question the simplicity of the direct relationship ($\Delta x/\Delta c$) between cell concentration (x) and broth conductivity (c) and suggest that inoculum size effects must also be considered These workers found that although a good linear relationship is generally obtained between cell mass and conductivity, when examined in more detail, $\Delta x/\Delta c$ is found to vary during the growth cycle It is reported that if the biomass concentration is calculated in the later stages of the growth cycle, on the basis of $\Delta x/\Delta c$ calculated at the beginning of the cycle, errors of up to 35% and 26% can result for suspension cultures of *Atropa belladonna* and *Solanum aviculare*, respectively On the basis of a study of 14 different methods of assessing growth in the cell line *Pyrus communis*, Ryu *et al* (1989) concluded that conductivity was the most effective biosensing method for monitoring the growth of this system However, applicability for an individual cell line must be thoroughly investigated before utilisation, as there is evidence that results may depend on the cell line, medium composition and inoculum conditions

In the preliminary trial carried out as a part of this study, the data collected indicate the suitability of this method of growth measurement Although this technique was not used for further growth analyses, its potential for on-line monitoring applications in plant cell suspension cultures is evident However, a more comprehensive study is required, to identify possible alterations in the relationship between conductivity and biomass concentration, due to deviations in inoculum concentrations or growth variations

5 1 3 Image Analysis and Suspension Morphology

In the semi-automatic program designed for this work, detected images were manually 'tidied up', all separations and measurements of chains and cells were automatically performed Kieran *et al* (1993) and Murtagh (1994) also used a semi-automatic image analysis routine, but each chain was manually edited for segmentation into cells In their work, the time required to process 100 chains was 2 5 hours, whereas, m this work, the time required was approximately 1 hour Therefore, this program represented a significant improvement in terms of both processing time and ease of cell separation This processing time could be further, and significantly, reduced by eliminating the grey processing step, which takes up a considerable amount of time for each field of view It is hypothesized that this grey imaging step could be eliminated without a significant

loss in detection accuracy The use of phase contrast would be an interesting route to examine, for initial image acquisition Also, it is possible that the manual selection of chains, following detection, could be eliminated if additional binary filtration steps were further investigated

The average chain and cell lengths for *Morinda citrifolia* were observed to vary from approximately 350 μm to 430 μm and 81 μm to 120 μm, respectively, chain width was approximately 37 μm Suspensions of the same cell line, studied by Kieran *et al* (1993) displayed typical chain and cell lengths, throughout the growth cycle, in the ranges 450 μm to 680 μm and 101 μm to 164 μm, respectively These values are approximately 30% larger than those observed in this laboratory However, the average chain width was 30 μm, which is slightly smaller than that observed in this study The number of cells per chain observed by Kieran *et al* varied between an average of 3 2 on day 7 to 5 4 on day 1 In this work, the minimum average of 2 7 was observed on day 5 and the maximum of 4 79 on day 17 Therefore, the average number of cells per chain was also different, although minimal values in both studies occurred at the early stages of cell replication

The trend in cell length, as the culture matures, is similar, with elongation occurring during the lag and early exponential phases and the cell length declines in the later stages to a relatively invariant size by the stationary phase In this study, the maximum error observed in validation studies for measuring cell length indicated that there was up to a 7% error encountered between measuring cells via the 'quadratic' method (based on area and perimeter) and the Feret method used in the programme (Figure 3 5) Perhaps for long chains, the Feret method is inappropriate, since the curvature of the chain cannot be neglected This could account for slight losses in cell length, although not to the extent evident between the two studies Qualitatively, it was visually observed that chains from cultures grown in UCD were longer and thinner, although no comparative analysis was performed Since there was no difference in sub-culturing procedures or in the medium employed, it is possible that the observed variations were attributable to the agitation pitch of the shaker table or some other unverified physical cultivation conditions, such as light intensity (although it should not influence the non-photosynthesising cell cultures), which affected culture growth Cultures grown in UCD were also visually observed to have a more vibrant orange colour than those in grown

for this work, which ultimately verifies some slight difference in cultivation This difference in morphology is indeed an interesting phenomena and highlights the vulnerability and susceptibility of plant cells, like other biological systems, to slight environmental changes

As discussed, the cell length is observed to change as expected throughout the cycle, however, the variation in chain length (Figure 4 8) deviated from previously reported trends (Kieran *et al*, 1993) Perhaps a sample size of 100 chains does not yield a statistically representative distribution Alternatively, it may be, in part, attributable to flask-flask variations This hypothesis should ideally be investigated using a stirred tank system, of a scale at which cultivation conditions are unaffected by repeated sampling over the course of the growth cycle

Log-normal size distribution models appear to adequately describe the chain and cell length data obtained for *Morinda citrifolia*, over the course of the growth cycle (Figures 4 10 and 4 11) Similar distribution patterns were observed by Kieran *et al* (1993) The appropriateness of log-normal modelling of plant cell cultures has also been suggested by other researchers, for instance, Tanaka (1987) for plant cell suspensions of *Agrostema githago* and *Nicotiana tabacum* and Scragg *et al* (1987) for the cell line *Catharanthus roseus* The proportions of larger chains and cells increase in the early exponential phase and fall again by the stationary phase, to yield greater proportions of smaller chains/cells A smoother fit is obtained for the cell length data, again suggesting that a sample size of greater than 100 chains might be appropriate A more intensive validation procedure for this particular programme would eliminate the possibility of an inadequate sample size

This preliminary investigative study established a more rapid image analysis procedure for the morphological characterisation of *Morinda citrifolia* However, there is still considerable potential for optimising this algorithm and obtaining more comprehensive morphological data for this plant cell line It must be reiterated that the data presented in this work are representative of a single culture cycle and therefore, a more thorough investigation is necessary for conclusive and reliable morphological characterisation

5 2 CELL-FREE BROTH CHARACTERISTICS

5 2 1 Metabolite Content

Secondary metabolite production has been comprehensively studied in a range of plant cell lines, due to the commercial potential of many of these compounds For instance, Sahai and Shuler (1983) and Hooker *et al* (1990) studied the cell line *Nicotiana tabacum* Kim *et al* (1991) researched the production of berberine, an isoquinoline alkaloid, by *Thalictrum rugosum* Stafford *et al* (1986) describe the different relationships between biomass production and general metabolite production in all biological systems There is also a substantial body of information available in the literature concerning the optimisation of production and extraction of the intracellular metabolite, anthraquinone, in suspension cultures of *Morinda citrifolia* (Wagner and Vogelmann, 1974, Zenk *et al*, 1975, Dornenburg and Knorr, 1992, 1994, Gagendoorn *et al*, 1994, Bassetti and Tramper, 1994, 1995, Bassetti *et al* 1996) Studies have shown (*e g* Kieran, 1993) that the production of anthraquinone in *Morinda citrifolia* suspension cultures is growth associated, but lags slightly behind biomass production This behaviour is not unusual for plant cell systems and Kim *et al* (1991) and Payne *et al* (1988) observed similar growth-associated kinetics for alkaloid production in suspension cultures of *Thalictrum rugosum* and *Catharanthus roseus,* respectively Since, alkaloid substances are not generally known to effect the foaminess of biological systems and moreover, since anthraqumone is retained intracellularly, this metabolite was not the focus of this study However, many studies have been performed to quantify and model antraquinone production in these suspension cultures Kieran (1993) used similar growth conditions for batch cultivation of suspension cultures of *Morinda citrifolia* and it was reported that antraquinone constituted less than 3% DW (approximately 0 3 g l^{-1}) during a typical growth cycle Due to their comparative commercial insignificance there is relatively little information available on production levels of extracellular ECPs and proteins in plant cell systems From the results presented in this work, it can be seen that the production of both these metabolites in *Morinda citrifolia* cultures is also growth associated, although lagging behind biomass production by approximately one day (Figures 4 8 and 4 9)

Maximum protein concentrations of 0 1 mg ml^{-1} were determined in *Morinda citrifolia* cell-free broth samples This is approximately twice the maximum protein concentration

observed by Wongsamuth and Doran (1994) in cultures of *Atropa belladonna* However, Olson *et al* (1969) reported that in *Nicotiana tabacum*, the maximum protein concentration of the cell-free broth was approximately 0 144 mg ml^{-1}, corresponding to 12% of the recovered macromolecules Thorup *et al* (1994) reported that proteins which displayed anti-viral (HIV-1) and anti-tumour activities were produced by *Trichosanthes kirilowii*, although protein concentrations were not specified

Extracellular polysaccharides are known to be produced by fungal (Stasmopoulos and Seviour, 1992), bacterial (Jeanes *et al*, 1961, Lebrun *et al*, 1994, Takeda *et al*, 1994, Moreno *et al*, 1998), and plant (Uchiyama *et al*, 1993, Otsuji *et al*, 1994) systems Example of polysaccharides include xanthan, alginate, pullulan, dextran and glucans ECPs consists of many different components, including galacturonic acid, arabinose, xylose, rhamanose, mannose and glucose Mathematical modelling of intracellular and extracellular polysaccharide production for the plant cell line, *Symphytum officinale* was performed by Glicklis *et al* (1998) It was, reasonably, assumed that polysaccharide production is growth associated and the model was useful for simulating the growth and polysaccharide production in this plant cell system

Under normal growth conditions, in this study, the maximum ECP concentration observed in *Morinda citrifolia* cell-free broth was 1 9 g l^{-1} This is typical of the ECP levels reported for other plant cell lines, cultivated in shake flasks For example, Otsuji *et al* (1994) investigated ECP production by the plant cell line *Polianthes tuberosa* It was found that in White, Gamborg and Linsmeier and Skoog media, ECP concentrations of 1 1, 1 1 and 1 4 g l^{-1} were observed, respectively By optimising the constituents of Linsmeier and Skoog media, concentrations of 4 1 g l^{-1} were obtained in shake flask cultures Subsequent studies in a 30 l Jar fermentor, operated over a 1 month period, yielded ECP levels of 4 6 g l^{-1} The increase was attributable to both media constituents and improved oxygen mass transfer in the agitated bioreactors These ECPs are commercially produced for use in the cosmetics industry (Otsuji *et al*, 1994) Uchiyama *et al* (1993) reported a maximum ECP level of 1 72 g l^{-1} in cultures of *Mentha* cells The relative composition of these *Mentha* ECPs, with regard to polysaccharide sub-units, varied over the course of the growth cycle and the protein content was reported to be approximately 10% In suspension cultures of *Nicotiana tabacum*, Olson *et al* (1969) reported that polysaccharide levels of approximately 1 06

g l^{-1} were recovered; this value constituted 88% of the total macromolecules recovered. Therefore, the levels of ECPs recovered from *Morinda citrifolia* cell-free broths are typical of those in other plant cell suspension cultures.

The composition of ECPs recovered from suspension cultures of *Morinda citrifolia* was not characterised and therefore, it is not known if the composition varied from that produced by other cell lines and/or if it is subject to time related variations. However, both are likely possibilities. It was observed that when the broth was subjected to non-specific protease degradation, the ECP precipitated irreversibly out of solution. This indicates that the solubility of the ECP is altered, by protein degradation, which in turn suggests that there is a protein moiety in the ECP. Therefore, when this is degraded, the entire structure of the ECP is disrupted and becomes unstable. The presence of a proteinaceous moiety in plant cell ECPs is not unusual and Uchiyama *et al.* (1993) reported that ECPs produced by *Mentha* cells were found have an approximately protein content of 10%. The implications of this are further discussed in Section 5.4.

5.2.2 Rheological Characterisation.

Throughout the entire growth cycle, the viscosity of *Morinda citrifolia* cell-free broth, was found to exhibit essentially Newtonian characteristics. This is not unusual for cell-free broth of plant cell cultures; Kato *et al.* (1978) reported similar results for cell-free broths of *Nicotiana tabacum* cultures, for which viscosity varied between 0.9 and 2.2 mN s m^{-2}. However, the whole broth suspension displayed non-Newtonian characteristics and the apparent viscosity increased by a factor of 27.5, over the course of the growth cycle. Although not investigated in this work, whole broth suspensions of *Morinda citrifolia* have also been reported to display non-Newtonian behaviour (Kieran *et al.* 1993, 1995 and Vogelmann *et al.*, 1978). Rheological characterisation studies of *Morinda citrifolia* suspensions, cultivated under conditions similar to those reported in this study, are described by Kieran *et al.* (1993, 1995). A helical ribbon impeller was used in conjunction with a conventional viscometer head to overcome processing difficulties typically encountered with biological suspensions in narrow gap viscometers. It was reported that suspensions with a biomass concentration of up to 50 g l^{-1}, based on fresh weight, behaved as Newtonian fluids and thereafter, non-Newtonian behaviour prevailed. Vogelmann reported that thixotropic behaviour was observed for

Morinda citrifolia suspensions with a fresh weight of 500 g l^{-1} In a study of 10 plant cell lines, Curtis and Emery (1993) suggest that the non-Newtonian behaviour of some plant cell suspension cultures is related to the elongation of cells at very high cell densities However, on the basis of the information available in the literature, it appears that whole broth suspensions of plant cells typically display non-Newtonian characteristics, while cell-free broths generally exhibit Newtonian characteristics

In this study, viscosities of between 1 and 5 5 mN s m^{-2} were recorded for cell-free broths of *Morinda citrifolia*, although, on occasions, viscosities as high as 10 mN s m^{-2} were observed These unusually elevated viscosity levels were thought to be attributable to temperature fluctuations in the growth room, however, they were not, surprisingly, directly correlated with elevated ECP concentrations It is, therefore, postulated that perhaps different types of ECPs are produced Indeed, this is an area where the production of ECPs by suspension cultures of *Morinda citrifolia* requires further investigation and understanding

The increase in cell-free broth viscosity, over the course of the growth cycle, is attributable to the secretion of metabolites Figure 4 15 illustrates the rapid increase in the viscosity of the cell-free broth between days 5 and 9, corresponding to the increase in ECP concentration It is evident that protein concentration also follows the same production profile However, at the protein concentration found in the broth, its effect on viscosity is negligible, as is evident from the results for isolated intracellular protein fractions (Table 4 1) and later in model BSA solutions (Section 4 4 2)

The influence of macromolecules on the viscosity of broths is a well known and was demonstrated by Olson *et al* (1969) with the cell line *Nicotiana tabacum* Using polygalacturonase to degrade the polysaccharide constituent of resuspended macromolecules, a rapid reduction in viscosity occurred, on addition of the enzyme, thus, confirming the dependency of viscosity on the polysaccharide In the current work, the viscosity effect can be largely attributed to ECP concentration The relationship between viscosity and ECP concentration is illustrated in Figure 4 21, where it is clear that the apparent viscosity of the ECP standards and the viscosity of the cell-free broths, at equivalent ECP concentrations are generally similar However, from concentrations of approximately 1 75 g l^{-1} there is a substantial discrepancy between the

fluids, suggesting that at these elevated ECP levels, the relationship is more complex. It is evident from Figures 4.13 and 4.15 that although the ECP concentration remains essentially constant during the stationary phase of the growth cycle, the viscosity tends to decrease slightly. This effect can possibly be attributed to structural changes in the ECP, while the overall concentration remains constant.

Variations were observed between the rheological behaviour of cell-free broths of *Morinda citrifolia* and resuspended ECP solutions. While the cell-free broth displayed Newtonian characteristics (Figure 4.14), the resuspended ECPs could be classified as non-Newtonian fluid (Figures 4.19, 4.20). Rheograms for solutions of resuspended ECPs reveal a slightly pseudoplastic behaviour, with flow behaviour and consistency indices (Figure 4.20) which vary with ECP concentration. It appears reasonable to suggest that these discrepancies may be attributable to alterations in the conformation and integrity of the ECP during the isolation and drying procedures. As reported in Section 3.5.1, the freeze-dried ECPs tended to come out of solution easily, when redissolved in water, although they appeared to be more stable in medium.

The influence of polysaccharides on viscosity is well known and is extensively exploited in the food and pharmaceutical industries. For the purpose of this work, model studies on xanthan gum were performed, to simulate viscosity variations in cell-free broth. A linear relationship was observed (Figure 4.24) between apparent viscosity and xanthan concentration in the range 0 to 0.04%. These concentrations were chosen to produce apparent viscosities of up to 4.0 mN s^n m^{-2}, at a shear rate of 225 s^{-1}, which are representative of the viscosities encountered in cell-free broths. A linear relationship was also reported by Charles and Wilson (1978) for a wider range of xanthan concentrations. Although xanthan is used as a model polysaccharide, it cannot be considered to resemble the ECP produced in the broth. as no data are available. However, use of xanthan as a model system clearly indicates the effectiveness of a polysaccharide in elevating the viscosity of a solution. The addition of BSA, up to a concentration of 0.2 mg ml^{-1}, to any of the investigated xanthan solutions, confirmed the inability of this protein to alter the viscosity of the solution. Although BSA is not representative of the actual plant proteins present in the broth, it is very unlikely that any viscosity effects can be attributed to protein content.

5 2 3 Surface Tension Characterisation

The instantaneous' and equilibrium' surface tensions profiles (Figure 4 16) of cell free broth follow a similar pattern, although the latter values are typically lower than the former, by approximately 0 005 N m^{-1} The concept of a stabilisation period for surface tension measurement in biological broths has been reported by other workers, (*e g* Konig *et al*, 1979) and the equilibrium value is typically quoted in the majority of reports For the cell-free broths investigated here, minimum 'instantaneous' surface tensions of 0 055 N m^{-1}, have been occasionally observed, although this profile typically stabilises at a value of approximately 0 06 N m^{-1} For the equilibrium' surface tension profile, a minimum value of 0 05 N m^{-1} was observed, occurring at days 8 to 12, although more frequently values stabilised at approximately 0 055 N m^{-1} To avoid confusion when referring to other work, only the 'equilibrium' surface tension is considered here However, the deviations between the instantaneous and equilibrium values highlight the need for careful experimental procedure when collecting surface tension data

There is a substantial body of data available on surface tension in microbiological and model systems and the surface tension of *Morinda citrifolia* cell-free broths is slightly higher than those typically reported for other biological cultures For example, Wolfe and Schugerl (1983) found that the surface tension of microbial cultures of *Escherichia coli* and *Hansenula polymorpha* were approximately 0 045 and 0 048 N m^{-1}, respectively Neither broth displayed significant variations in surface tension throughout the cultivation period Hall *et al* (1973) reported that in general, the presence of natural surfactants in biological fermentation systems results in minimum surface tension values of between 0 04 and 0 05 N m^{-1} There is very limited information available on surface tension in plant cell systems For cell suspension cultures of *Atropa belladonna*, the cell-free broth surface tension varied little throughout the entire growth cycle, with average values of 0 046 N m^{-1} (Wongsamuth and Doran, 1994), protein concentration in these suspensions varied between 0 02 mg ml^{-1} and 0 053 mg ml^{-1} In this study, the effect of metabolites, other than ECPs and proteins on surface tension values was not investigated and as suggested by Noble (1994), other macromolecules may be secreted which might also affect the surface tension of the broth However, it is evident from Figure 4 38 that after day 5, the surface tension had reached its saturation coverage limit (Section 2 1 2) and thereafter, any increase in protein concentration effect Figure 4 22

provides the basis for this conclusion, where it can be seen that the surface tension decreased rapidly until a protein concentration of approximately 0 02 mg ml^{-1} (day 5) was reached Further increases in protein concentration had no apparent effect on the surface tension

The influence of ECPs on surface tension can be considered negligible For ECP standard solutions, the overall effect of increasing ECP concentration was a slight reduction in broth surface tension, however, in cell-free broths, collected throughout the culture growth cycle, broths with corresponding ECP concentrations displayed much lower surface tension values (Figure 4 23) The differences between the surface tension data for standard ECP solutions and cell-free broths, at equivalent ECP concentrations, confirm that this component is not the primary influencing factor on surface tension in cell-free broth

The influence of BSA on surface tension has been extensively studied (*e g* Kalischewski *et al*, 1979, Lalchev *et al*, 1982, Sie and Schugerl, 1983, Wolfe and Schugerl, 1983) For example, Wolfe and Schugerl (1983) reported that the surface tension of BSA solutions in nutrient medium decreased from 0 051 N m^{-1}, for a BSA concentration of 0 005 mg ml^{-1}, to a value of 0 047 N m^{-1}, for a 0 2 mg ml^{-1} solution Studies performed in this work, using BSA as a model system, to demonstrate the influence of proteins on surface tension, also verified this relationship

Although the total protein composition of the intracellular protein extract has been shown to be different to that of the cell-free broth (Section 4 3 3), the surface tension of this extract was evaluated, to again demonstrate the effect of protein on surface tension The surface tension of a 0 033 mg ml^{-1} intracellular protein extract (in water) was 0 056 N m^{-1}, which corresponded to that observed in the cell-free broth It is possible that the additional proteins, present in the intracellular isolate, are membrane bound proteins, which were liberated during the intensive crushing stage in the extraction protocol This is a suggestion that requires further development and investigation, before a definite conclusion can be reached

Although BSA, intracellular protein and proteins found in the cell-free broth cannot be quantitatively compared, it is reasonable to attribute the decrease in surface tension to the protein content of the broth

5 3 BUBBLE COLUMN DESIGN AND VALIDATION

The various bubble column designs employed and the rationale for modifications implemented are described in Section 3 6 The most challenging aspect of the design is the development of a gas dispersion device which evenly distributes bubbles of a relatively tight size distribution If such conditions cannot be assured then sections of the foam generated are not homogeneous and are of varying stability, sections of the foam may disintegrate prematurely Columns A1a and B4a were the only designs which meet the validation criteria However, the ability of Column A1a to produce a stable foam and the inability of a nominally identical design (Column A1b) and a similar design with a smaller sparger pore size (Column A2), to produce stable foams cannot be easily explained It can only be assumed that there is variability in the sintered disks, which are nominally identical and that it was fortuitous that the sintered disc used in Column A1a was suitable for achieving uniform bubble distribution and hence, stable foams in BSA solutions

Using similar sparger pore sizes (Porosity 0 and 1), in the bubble column Type B design (Columns B2, B3), the bubble distribution was also unreliable and validation was not successful Operational difficulties have been reported by other authors, (*e g* Edwards *et al* , 1982 and informally communicated by other workers) and the general consensus is that sintered discs with large pore sizes (*i e* small porosity numbers) are not recommended for foaming studies in relatively small columns However, the significant pressure drops associated with use of higher porosity numbers (*i e* smaller average pore size) also present operational difficulties

In general, smaller pore sizes result in taller foams for a specific sample volume and therefore, this limits the practical range of experimental conditions which can be investigated in a given column While a longer bubble column might be advantageous, in that it would increase the capacity for foam retention and thus, increase the range of accessible operating conditions, ease of maintenance and handling would be severely reduced Efforts to validate a more robust Perspex column were unsuccessful as Perspex proved to be unsuitable for use in foaming work There is no evidence in the literature of bubble columns constructed of any material, other than glass

The susceptibility of sintered discs and bulbs to microbial contamination was evident and although rigorous cleaning procedures were adopted, the performance of all sintered devices was observed to diminish with time The resulting foaming variability, in nominally identical systems, was a severe impediment to this work and renders comparison between data collected from different columns, or from the same column over extended time periods, difficult For long term studies, an alternative material, such as sintered steel, might produce a more reliable gas dispersion device, possessing a greater resistance to abrasion associated with essential cleaning procedures or other degenerating influences (Wongsamuth and Doran, 1994) For the purpose of this study, comparisons of results are, accordingly, limited to data collected from individual columns during a time period in which the column performance can be reliably validated using standard solutions, as described in Section 3 6

While there is a substantial body of material in the literature on foaming in model systems using BSA, there are a number of factors which make comparison between different studies difficult (Section 2 2) Therefore, it is difficult to quantitatively compare foaming data, reported in the literature, to this work Additionally, many of the bubble columns described in the literature are designed for the purposes of protein separation studies (*e g* Lalchev, 1982, Bahr, 1991, Ramani *et al*, 1993, Mohan and Lyddiatt, 1994) In such cases, solution foaminess is not the subject of investigation, since foaming is operated continuously The objective of these studies is to optimise foam fractionation techniques There is very limited literature on actual foaminess quantification in these systems

Bikerman (1938) reports that Bikerman foaminess values for a particular solution are independent of the bubble column dimensions, and of the sintered disc porosity employed (Table 3 7) with porosity data However, the results obtained in the present work do not conform with these findings The foam stabilisation effect of smaller bubbles is evident from the different data obtained for a 0 5 mg ml^{-1} solution of BSA in water, in the two working column designs Column A1a (porosity 0) generated a stable foam of approximately 18 cm, at a flow rate of 3 33 ml s^{-1}, while in Column B4a (porosity 3) a foam height of approximately 80 cm was obtained, at a very similar aeration rate of 3 36 ml s^{-1} These data correspond to Bikerman foaminess values of approximately 75 s and 280 s, respectively Because of the differences in design

between Columns A1a and B4a, it is not possible to conclusively identify any single factor responsible for the observed variations in foaming behaviour, but it is likely that the most significant effects are attributable to differences in bubble size Kalischewski *et al* (1979) and Wolfe and Schugerl (1983), using a G4-frit sintered glass disc, reported Bikerman values of approximately 1000 s for a of 1 mg ml^{-1} BSA solution (in bidistilled water), whereas in this work, a Bikerman value of approximately 420 s was observed, using a glass sinter (porosity 3) It should be noted that it is unclear whether Kalischewski *et al* (1979) used nitrogen or air to induce foaming Kotsaridu *et al* (1983) also performed studies on BSA in bi-distilled water, using a G4-frit porous membrane and nitrogen gas as opposed to air However, considering that these solutions contained salts, it was not possible to make a comparison The general implication is that the Bikerman foaminess index does not appear to be independent of sinter porosity Unfortunately, the range of sinter porosities investigated by Bikerman (1938) was not quoted

The Edwards index (equation 2 3) was unsuitable as a method of analysis for the data generated in validation trials for both column designs employed in this work, as a longer, thinner column would be required for accurate application of this index Edwards *et al* (1982) used a bubble column of internal diameter 1 2 cm and length 55 cm, with a glass sintered disc (10 μm pore size), requiring a liquid sample of 10 ml For this apparatus, it was reported that a linear relation was evident between foaminess and BSA concentration, at a specific aeration rate and that foaminess increased linearly with increasing aeration rates, for a given BSA concentration These patterns are analogous to those obtained in this work

As outlined in Section 4 5 1, both the dimensionless foam volume and the Bikerman foaminess methods of analysis proved successful, although, only the relative foaming patterns, rather than values for the foaminess indices can be compared Edwards *et al* (1982) suggest that the non-linear relationships between foaminess (bik) and surfactant concentration, reported by both Cumper (1953) and Kalischewski *et al* (1979), were associated with back pressure problems, due to varying foam heights produced by the stronger foaming solutions A similar non-linear effect was observed by Edwards and co-workers prior to correcting this fault in column design On this basis, the linear relationships obtained in the current validation trials, for foaminess and BSA

concentration, in the range to 0 1 to 1 0 mg ml^{-1} (Figure 4 31) and foaminess and aeration rate (Figure 4 29 and 4 30) suggest the validity of the column designs and operation protocol Thus, it can be assumed that the foaming patterns obtained in the validation studies are representative of BSA foaming characteristics in general

Validation of Column B4a using 50 ml sample volumes was successful, thus demonstrating the reliability of this smaller sample volume for foaming experimentation At a given BSA concentration, the dimensionless indices for both sample volumes were practically identical, as expected (Figure 4 32), while, the Bikerman indices were different This indicates that, under these conditions, the Bikerman foaminess is not independent of sample volume The minimum sample volume for the given column design and foaming solution has not been reached and below this minimum level the influence of volume size cannot be neglected However, the Bikerman method of analysis was chosen to present the results as it can accommodate the slight variations in aeration rates, which were unavoidable during different foaming runs The sample volume employed, in any given column, for a given set of runs was constant and therefore, the dimensionless method of analysis held no advantage

5 4 CELL -FREE BROTH FOAMINESS

5 4 1 Foaminess Characterisation

The unstable foam generated using Column A1a was caused by a combination of the relatively large pore size of the sintered disc sparger, which produced large bubbles from the onset of foaming and the nature of the broth being foamed It was not possible to estimate a stable height of the foam and therefore, neither Bikerman nor dimensionless foaminess values for the cell-free broth were calculated Although stable foams were produced using BSA in validation studies, this bubble column is evidently unsuitable for analysing the foaming potential of cell-free broths of *Morinda citrifolia* BSA is a purely proteinaceous substance and obviously has a stronger foaming potential than broth samples

Column B4a was successful in characterising the foaming potential of cell-free broths As described in Section 4 6 2, it was observed that stable foams were formed, of a height which depended on culture age, but in each case after the maximum height was reached the foams destabilised and separated into sections, which then rose up the column This is analogous to the foams produced in Column A1a, except that a substantial measurable stable foam was initially generated using column B4a and the sections of foam rising up the column were more compact and stable It is likely that stable foams were initially generated for the cell-free broths when bubbles were relatively small, but as foaming time progressed, the extent of film drainage and bubble coalescence increased within the foam and hence, the bubbles reached a larger size causing destabilisation of the foam However, as it was visually evident that the foam destabilised from the bottom upwards, another aspect to consider is the depletion of surface active molecules m the remaining broth This effect has been observed by other workers and Konig *et al* (1979) increased the sample size employed with a view to minimising the reduction in surface active components, due to foam enrichment Although this concept was not examined in detail m this work, it was ascertained that on day 11, the protein content of the residual cell-free broth, recovered after foaming, was reduced substantially from 0 091 mg ml^{-1} to 0 056 mg ml^{-1}, as a consequence of foaming Therefore, although the protein content is not fully depleted, it is greatly reduced and thus, it is likely to be a significant factor in the reduction of foam stability with regard to time Further analysis to evaluate the composition of the broth before and after foaming was not performed, but studies could, perhaps, determine if the selective absorption of specific proteins occurred, after which the stability of the foam generated at the liquid-foam interface was weaker This hypothesis is supported by the surface tension data of the residual broth, as discussed in Section 4 6 2

Pandit (1994) used model systems to demonstrate the effect of smaller bubble sizes on the ability of a substance to produce foam, using a bubble column and an agitated vessel The agitator broke the bubbles into smaller sizes which consequently created a more stable foam structure In the work presented here, there is an immense difference between the stability and extent of foam generated for cell-free broths, using sintered spargers of different porosity numbers (No 3 and No 1) This trend is observed not alone for the cell-free broths but also for the model BSA systems investigated

The foaming characteristics of cell-free broths, throughout the duration of the *Morinda citrifolia* growth cycle, are discussed with respect to the data collected using Column B4a only and it was seen that foaminess ranged from approximately 40 s, on day 0, to a value of over 600 s, between days 11 and 14 (Figure 4 33) The sample volume used in this work was 50 ml, since at various stages during the culture cycle the foam overflowed the column, at minimal aeration rates, , when an 80 ml sample volume was employed The column was 1 m in height and the height of an 80 ml sample of broth was approximately 6 cm This gives an indication of the extent of foaming that occurred for this broth Thus, one can envisage the potential foaming capabilities of an agitated fermentation system, without foam control

There is a limited body of literature available on foaming potential quantification in other plant cell systems The foaming potential profile of cell-free broths of *Morinda citrifolia* cultures observed is similar to that reported for the plant cell line, *Atropa belladonna* (Wongsamuth and Doran, 1994), with foaminess represented in terms of dimensionless foam volume However, variations in foaming potential between the two cultures cannot be conclusively determined by a direct comparison of results, due to differences between the two bubble column designs Wongsamuth and Doran (1994) employed a sintered metal sparger, but the porosity of the device was not indicated The bubble column employed for foaming stability studies had a diameter of 4 9 cm and a height of 63 cm and was, therefore, similar in both volume and aspect ratio to columns designed for the current work The maximum dimensionless volume for cell-free broths of *Atropa belladonna* was approximately 9, while the corresponding value for *Morinda citrifolia* in this study reaches a maximum of approximately 13 It must also be noted that the protein concentration of the latter cultures is approximately twice that reported for *Atropa belladonna*

From the information available on foaming in other biological systems (Section 2 4) it is apparent that increases in foaminess with culture age, observed in *Morinda citrifolia* cell-free broth, are typical for biological systems

As presented in Section 2 1 4, the influencing effect of pH on foaming is well documented and in this work, the general trend observed was a slight reduction in foaminess, with increasing pH The results presented are those of a single set of trials,

and were carried out within the pH range encountered throughout the growth (*i e* pH 4 to pH 6) Although minimal quantities of acid or base were added to the cell-free broths, to alter the pH, these additions constitute a possible source of error, in terms of dilution of the broths or slight salt effects, which may affect foaminess of the broths A more comprehensive study, perhaps using a wider pH range and multiple samples, is necessary to confirm any definite relationships between pH and foaminess and eliminate the uncertainties outlined above

5 4 2 The Effect of Culture Proteins/Surface Tension on Foaminess

The significance of proteins for foaming potential has been firmly established in fermentation systems, (*e g* Konig *et al*, 1979) As referenced in Section 2 1 3, Noble (1994) reported the effects of other surface active components on foaminess and suggested that in addition to the influence of proteins on foams, lipophilic biosurfactants, carbohydrates and α-keto acids contribute significantly to foaming It was suggested that interactions between proteins and carbohydrates may enhance foaming in fungal fermentation systems and that the problem of foaming is more complex than suggested simply by the presence or absence of extracellular protein This is, indeed, likely for cell-free broths of *Morinda citrifolia* analysed in this work Attempts to relate the foaminess of *Morinda citrifolia* cell-free broth to extracellular protein and ECPs concentration are illustrated in Figures 4 36 and 4 37 Although linear relationships between foaminess and protein concentration and foaminess and ECP concentration were observed in the broths, it was not possible to attribute the variation in foaming potential solely to either one of the constituents, as both are produced simultaneously (Figures 4 12 and 4 13) Moreover, these are but two of the metabolites produced by the cells and other substances produced could also influence broth foaminess Since complete component isolation was not achieved, it was not possible to identify if one component alone was responsible for foaming

Attempts to relate the foaminess of the broth to equilibrium surface tension (Figure 4 38) showed that at surface tension values greater than approximately 0 056 N m^{-1}, the foaming potential of the broth was negligible This represented the initial stage of the growth cycle (Figure 4 16), when metabolite secretion was only commencing As foaminess continued to increase, it is seen from Figure 4 38 that the surface tension does

not vary significantly This is explained by Figure 4 22, which displays the relationship between protein concentration and surface tension and it is evident that an increase in protein concentration, after a certain minimum level (critical value) is reached, has little effect on surface tension Therefore, although protein concentration and hence foaminess increase rapidly, surface tension remains relatively unchanged

5 4 3 The Effects of ECPs on Foaminess

A linear relationship was observed between viscosity and foaminess (Figure 4 39) This would be expected, as the ECP concentration and viscosity (Figure 4 15) are closely related Mita *et al* (1977) also demonstrated that the stability of a foam increased with an increase in viscosity for model protein and sugar solutions As outlined in Section 2 1 2, it is known that viscosity influences foaming, by retarding film drainage, thereby stabilising the foam On day 11, the ECP content of the bulk liquid sample before and after foaming showed a negligible reduction in ECP concentration, due to foaming Therefore, unlike proteins, they were not preferentially partitioned into the foam This supports the concept that ECPs influence foaminess due to their viscosity effect alone, rather than via any associated surface-active properties It is known that plant cell ECPs contain protein (*e g* Uchiyama *et al* , 1993), but it is unlikely that this moiety influences surface tension substantially, considering that ECPs were not partitioned into the foam (Section 4 6 2) and due to evidence that there was only a slight reduction in the surface tension of standard solutions at high ECP concentrations (5 2 3) It is thus believed that it is not the surface activity of the ECP, that significantly affects surface tension

5 4 4 ECP/Protein Isolate Foaminess Studies

Since ECP and proteins could not be separated, experiments were performed on redissolved ECP solutions (containing protein) in deionised water and in medium The results presented in Section 4 7 1 prove that a medium interaction effect is of the utmost importance in the foaming potential of the redissolved isolate Since both aqueous and medium-based solutions contained nominally identical levels of ECPs and proteins and neither medium alone nor extracted ECP in deionised water displayed any significant foaminess, the importance of the interaction between medium components and ECP/protein isolate is obvious The medium contains many salts and nutrients (Section

3.1), any one or combination of which could be responsible for the elevated foaminess in this ECP/protein isolate solution. Accordingly, this ultimately suggests it is the medium which exacerbates foaming problems in *Morinda citrifolia* cell-free broths.

Although, it is has been shown that the ECP/protein constituent of the cell-free broth contributes to foaming, it was not possible, in this work, to definitely confirm if this effect was solely due to the ECP or protein content of the isolate. It is more likely that a combination effect of both is responsible, with the protein constituting the primary influence on foaming and the ECP having a secondary effect due to film drainage retardation. Noble (1994) in studies using other biological broths, also concluded that carbohydrates, among other compounds, can act as foam stabilisation agents, and contribute to foaminess in fungal fermentations. However, in this instance, a full characterisation of the isolate is required, prior to eliminating the effects of any other possible components, before any firm conclusions can be drawn. Additionally, studies in which the concentration of individual medium components is varied might be used to identify the key constituents in medium-protein and/or medium-ECP interactions.

5.5 MODEL SYSTEM STUDIES - FOAMINESS ANALYSIS.

There is a substantial body of information in the literature confirming the significance of proteins on foaming in microbial and model systems, including studies performed by Molan *et al.* (1982), Wolfe and Schugerl (1983) and Tornkvist *et al.* (1996). However, there is limited material available on the influence of viscosity on foaming. The effect of viscosity on foams has been discussed by Mita *et al.* (1977) for gluten solutions, but there is an absence of specific studies in fermentation systems. Therefore, model studies were executed using BSA as a protein source and xanthan gum as a polysaccharide source, to induce variations in solution surface tension and viscosity, respectively

The stabilisation effect of medium on the foaminess of BSA and xanthan solutions revealed that the protein (BSA) solution was enormously affected by medium interactions, as depicted in Figure 4.40. A 0.2 mg ml^{-1} BSA medium based solution displays a 5-fold higher foaminess than that of an equivalent aqueous solution. Considering that no interactive effect was observed for xanthan solutions, this suggests

that the interactive effect between medium and cell-free broth metabolites is likely to depend on the proteins present, rather than on ECPs.

The contribution of a viscosity effect (xanthan gum concentration) to foaming, for water based protein solutions is highlighted in Figure 4.42. It is also evident from Figure 4.43 that a relatively linear relationship exists between the concentration of xanthan and foaminess, for a 0.1 mg ml^{-1} BSA in medium. However, the relationship between foaminess and xanthan concentration, for a 0.2 mg ml^{-1} BSA-water solution, is not linear until a xanthan concentration of 0.01 % is reached. Therefore, although the influence of viscosity on a protein foam is verified, the overall foaming potential and foaminess-polysaccharide characteristic relationship are influenced by the base solvent, *i.e.* water or medium.

5.6 PRELIMINARY ANTIFOAM STUDY

It is evident that the addition of a silicone antifoam prior to subculturing does not significantly affect the growth characteristics of the suspension, in terms of biomass dry weight, metabolite yields (ECP and protein), pH, viscosity or surface tension. However, the slight but consistent reduction in biomass (fresh weight) after day 12, suggest that antifoam may affect the cell characteristics in suspension. Since the dry weight was unaltered, it is possible that the cells in suspensions containing antifoam retained more liquid than those without antifoam. It would be necessary to perform corresponding cell number counts and assess the morphology, via image analysis, for cultures with and without antifoam, in order to conclusively determine if growth is significantly affected. It was visually observed that culture suspensions with antifoam were paler than suspensions without antifoam. This suggests metabolic changes in anthraquinone production.

With regard to foaming potential, a very substantial influence is observed, in antifoam supplemented broth samples, with foaming capacity greatly reduced, over the entire growth cycle. The maximum Bikerman foaminess of the cell-free broth throughout the growth cycle was reduced from a maximum of 650 s (day 11), in the absence of antifoam, to a value of 120 s (day 8) in the presence of a silicone antifoam (100 ppm).

However, in general the foaminess values were maintained under 50 s It is not clear why foaminess was at a local maximum on day 8 for the culture containing antifoam, as this feature does not correspond to a maximum in viscosity or a significantly different surface tension (Table 4 3) However, it is reasonable to suggest that this antifoam shows good potential for effective and efficient foam control in suspension cultures of *Morinda citrifolia*, since the growth characteristics were relatively unaffected and foam control was achieved

There was a very significant difference observed between the effect of antifoam when added directly to the cell-free broth prior to foaming and when added to the medium prior to subculturing A 50 ppm concentration of antifoam was sufficient to completely suppress any foam formation of cell free broth on day 11, the culture age where maximal foaminess is observed It is possible that antifoam might be partially degraded upon autoclaving, alternatively it could be absorbed into or onto the cells, meaning that only a fraction of it would be extracted in the cell-free broth

The surface tensions of the cell-free broths containing 50 ppm and 100 ppm of antifoam, added directly to the broth prior to foaming, were identical This shows that a minimal surface tension level was reached by 50 ppm However, lower concentrations were not investigated and therefore, the critical coverage level for this antifoam was not determined It is likely that lower antifoam concentrations, might be sufficient to completely suppress foaming The effect of heat sterilisation (autoclaving) on the antifoam is another aspect that requires further work before this antifoam could be added directly to fermentation systems Perhaps, the reduced performance of the antifoam, when added to the cultures prior to subculturing, is related to the sterilisation of the antifoam Other method of sterilisation, such as filtration, are available if this antifoam is proven to be partially heat labile

Chapter 6

Conclusions and Recommendations

Morinda citrifolia suspension cultures, grown in 250 ml Erlenmeyer shake flasks, over a 21 day growth cycle, were characterised in terms of biomass production, conductivity, suspension morphology, pH, supernatant extracellular protein and polysaccharide concentrations, viscosity, surface tension and foaming potential

Biomass profiles were typical of other plant cell suspension cultures, displaying distinctive lag, exponential and stationary growth phases Preliminary conductivity studies revealed a linear relationship between biomass concentration and conductivity, (expressed in terms of either cell number or fresh weight) However, with respect to dry weight, the corresponding linear relationship was not applicable during the stationary phase

The morphological characteristics of this cell line have been previously described by Kieran *et al* (1993) and chain and cell lengths have been found to follow log-normal distribution patterns In this work, a semi-automatic image analysis program was designed to facilitate more rapid analysis by including automatic segmentation of plant cell chains, into their constituent cells Processing time was reduced by approximately 66% by this improvement Although only preliminary data were collected, the designed program was successful and the morphological cell and chain length data were well described by log-normal distribution profiles Chain lengths were found to be marginally smaller than previously reported for same cell line, cultivated under nominally similar conditions

Production of extracellular polysaccharides and extracellular proteins was seen to be growth associated, with maximum concentrations of 1 9 g l^{-1} and 0 1 g l^{-1}, respectively The rheology of the cell-free broth displayed nominally Newtonian behaviour, with viscosity increasing over the course of the growth cycle from 1 1 to 5 5 1 mN s m^{-2} The study revealed that viscosity was strongly correlated with ECP concentration The

surface tension of the cell-free broth decreased very rapidly at the onset of significant protein production and remained relatively stable thereafter

The successful design of a bubble column, capable of generating reproducible and measurable stable foam heights, was a prelude to the characterisation of the foaming behaviour of *Morinda citrifolia* cell-free broths Ideally, a column design supporting reliable foam measurement over extended time periods was required However, the working life of successfully validated columns was no more than 6 months, which obviously limited the extent of the work achievable Foaminess studies in both cell-free broths and model solutions showed that smaller bubbles, generated using smaller sinter pores, enhance solution foaminess The foaming potential of the cell-free broth increased over the growth cycle in accordance with the examined metabolite profiles (ECPs and proteins)

In order to investigate the influence of broth ECPs and proteins on viscosity and surface tension, which are two of the physical parameters known to influence foaming, ideally these two components would be individually isolated However, attempts to achieve this separation were unsuccessful and, accordingly, the combined influences of extracted broth polysaccharides and proteins on viscosity, surface tension and foaming were assessed These studies revealed that, in addition to the influencing effect of these constituents, the culture medium played a key role Protein and polysaccharide extracts had little foaming potential when dissolved in deionised water However, in medium-based solutions, the foaminess exceeded measurable values in the available bubble column

One attempt to isolate broth ECPs and proteins from one other, to evaluate the effect of an individual constituent on foaming, focused on the use of a protease degradation technique Results revealed that the protease 'Pronase' was effective in degrading broth proteins However, the ECP was simultaneously degraded, confirming literature reports that ECPs contain a protein moiety The foaming potential of the degraded solution was negligible, suggesting that the protease destroyed the constituents responsible for foaming Attempts were also made to obtain a solution of proteins from suspension cells which was similar to the extracellular proteins found in the cell-free broth PAGE was performed to analyze the protein content of the two solutions However, it was shown

that most of the intracellular proteins were very different to those secreted by the cells into the suspending fluid

Since the isolation of either ECPs or proteins was not achieved, model studies were performed, using a polysaccharide (xanthan gum) to increase the viscosity, and a protein (BSA), to alter the surface tension, in an attempt to illustrate the general influence of these constituents on surface tension, viscosity and subsequently on foaming As expected, when the viscosity of a protein solution was increased, the foaming potential of the solution was exacerbated In concurrence with the results observed for the cell-free broth metabolites, the model protein solutions and the model protein-polysaccharide solutions displayed up to a 6 fold increased foaming potential in a medium based solution than in a water based solution Xanthan gum solutions in either water or medium demonstrated no foaming capacity on their own

An overall analysis of the effects of broth constituents on the foaming potential of *Morinda citrifolia* cell-free broths and in model systems indicates that proteins contribute greatly to foaminess and in the absence of proteins, the solutions will not foam However, the ability of broth ECPs to foam in isolation has not been established, but it is clear that xanthan gum has no foaming potential Therefore, polysaccharides, although not of great foaming potential in isolation, contribute greatly to the overall foaminess of a solution in the presence of a foaming agent They increase the viscosity of the solution which stabilises the foam

A preliminary study on the effect of a silicone antifoam (at a concentration of 100 ppm) on the growth and foaming potential of *Morinda citrifolia* suspension cultures illustrated that this antifoam was effective in controlling foaming in cell-free broths It is thought that the antifoam may degrade due to medium sterilisation or during culture growth, since 50 ppm of the same antifoam, when added directly to the cell-free broth immediately prior to foaming, inhibited foaming completely and had a greater reducing effect on surface tension Under the cultivation conditions investigated, this silicone antifoam did not significantly affect biomass growth or production of the investigated metabolites

Recommendations for further work are presented on the basis of specific issues arising from the studies reported in this thesis

- On-line application and validation of conductivity measurements in a bioreactor

- Optimisation of the image analysis program employed to further reduce processing time Validation of the designed program on each day of the culture cycle Investigation of the effect of shake flask conditions, specifically agitation rate and pitch and lighting conditions on chain length profiles

- Chemical analysis of the ECP constituents, over the course of the growth cycle, in terms of protein content and polysaccharide composition

- Separation of ECP and proteins in the broth, in order to achieve a relatively pure protein solution, for foaming analysis It should be noted that, however, large quantities of suspensions would be required for such studies

- Construction of a bubble column with a durable sintered disk, resistant to corrosion and abrasion, *e g* steel sinter, to allow foaming experimentation to be performed over an extended time period

- *Morinda citrifolia* suspensions should be cultivated at a larger scale to produce material for extended foaming studies and the investigation of a wider range of pH variations In this work, broth availability available was frequently a limiting factor

- Only cell-free broths were employed in foaming studies on this work Ideally, studies should be performed using whole broth, to establish the influence of the biomass, although this was not possible in the bubble column, due to settling effects

- Investigation of the effects of sterilisation on the silicone antifoam Studies should be performed, using this antifoam under sparged conditions, to evaluate the extent of foam suppression achieved under aerated conditions and the effective antifoam concentrations required

BIBLIOGRAPHY

Andou S , Yamagiwa K and Ohkawa A , 1996 Effect of gas sparger type on operational characteristics of a bubble column under mechanical foam control J Chem Tech Biotechnol Vol 66, 65-71

Anthony P , Davey M , Power J , Washington C and Lowe K , 1994 Image analysis assessments of perfluorocarbon- and surfactant-enhanced protoplast division Plant Cell Tissue and Organ Culture, Vol 38, No 1, 39-43

Bahr K , Weisser H and Schugerl K , 1991 Investigation on proteins excreted by the yeast *Hansenula polymorpha* and their influence on broth foaminess and cell recovery by floatation Enzyme and Microbial Technology, Vol 13, 747-754

Bahr K H and Schugerl K , 1992 Recovery of yeast from cultivation medium by continuous flotation and its dependence on cultivation conditions Chemical Engineering Science, Vol 47, No 1, 11-20

Bassetti L and Tramper J , 1994 Organic solvent toxicity in *Morinda citrifolia* cell suspensions Enzyme and Microbial Technology, Vol 16, August, 643-648

Bassetti L and Tramper J , 1995 Use of non-conventional media in *Morinda citrifolia* cell cultures Plant Cell, Tissue and Organ Culture, 43, 93-95

Bassetti L , Pijnenburg J and Tramper J , 1996 Silicone-stimulated anthraquinone production and release by *Morinda citrifolia* in a two-liquid-phase system Biotechnology Letters, Vol 18, No 4, 377-382

Bikerman J J , 1938 The unit of foaminess Trans Farad Soc , Vol 34, 634-638

Bikerman J J , 1973 Foams Springer-Verlag, New York

Blackhall L L and Marshall K C , 1989 The mechanism of stabilisation of actinomycete foams and the prevention of foaming under laboratory conditions Journal of Industrial Microbiology, Vol 4, No 3, 181- 187

Boyd J V , Mitchell J R , Irons L , Mussel , White P R and Sherman P J , 1973 Mechanical properties of milk protein films spread at the air-water interface J Colloid Interface Sci , Vol 45, 478

Bradford M M , 1976 A rapid and sensitive method for the quantitation of microgram quantities of protein utilising the principle of protein-dye binding Analytical Biochemistry, Vol 72, 248-254

Brown L , Narsimhan G and Wankat P C , 1990 Foam fractionation of globular proteins Biotechnology and Bioengineering, Vol 36, 947-959

Bumbullis W and Schugerl K , 1981 Foam behaviour of biological media, VI Foam stability Salt effects European Journal of Applied Microbiology and Biotechnology, 11, 106-109

Bumbullis W , Kalischewski K and Schugerl K , 1981 Foam behaviour of biological media, VII Surface Viscosity and Viscoelasticity European Journal of Applied Microbiology and Biotechnology, 11, 110-115

Cahoon R S , 1997 Biological process using foams US patent 5616493

Charles M and Wilson J , 1994 Fermenter Design In Lydersen B K *et al* (Eds), Bioprocess Engineering Systems, Equipment and Facilities, Wiley, New York, 19

Chisti Y , 1993 Animal cell culture in stirred bioreactors Observations on scale-up Process Biochemistry, Vol 28, 511-517

Cumper C W N , 1953 The stabilisation of foams by proteins Trans Faraday Soc , Vol 49, 1360

Curtin M E , 1983 Harvesting profitable products from plant tissue culture Bio/Technology, Vol 1, 649-657

Curtin F T , 1991 Shear stress effects on suspension cultures of *Morinda citrifolia* Ph D Thesis, University College Dublin, Ireland

Curtis W R and Emery A H , 1993 Plant cell suspension culture rheology Biotechnology and Bioengineering Vol 42, 520-526

De Alencar Ximenes J A , 1994 Electrical foam controller for fermentation processes BR patent 9204623

DiCosmo F and Misawa M , 1995 Plant cell and tissue culture alternatives for metabolite production Biotechnol Adv , Vol 13, 425-453

Doran Pauline M , 1993 Design of Reactors for plant cells and organs Advances in Biochemical Engineering and Biotechnology, Vol 48, 115-203

Dornenburg H and Knorr D , 1992 Release of intracellular stored anthraquinones by enzymatic permeabilization of viable plant cells Process Biochemistry, 27, 161-166

Dornenburg H and Knorr D , 1994 Effectiveness of plant-derived and microbial polysaccharides as elicitors for anthraquinone synthesis in *Morinda citrifolia* cultures J Agric Food Chem , Vol 42, 1048-1052

Edwards M , Eschenbruch R and Molan P C , 1982 Foaming in Winemaking, I A technique for the measurement of foaming in winemaking European Journal Applied Microbiology Biotechnology, 16, 105-109

Fett-Neto A G and DiCosmo F , 1996 Production of Paclitaxel and related Taxoids in cell cultures of *Taxus cuspidata* perspectives for industrial applications In DiCosmo F and Misawa M (Eds), Plant Cell Culture Secondary Metabolism-Toward Industrial Application CRC Press, Boca Raton, FL, 139-166

Fougias E and Forster C F , 1994 *Rhodococcus rubra* in relation to stable foams in activated sludge Process Biochemistry, Vol 29, 553-557

Fujita Y , 1988 Shikonin production by plant (*Lithospermum erythrorhizon*) cell cultures In Bajaj, TPS (Ed), Biotechnology in Agriculture and Forestry Medicinal and Aromatic Plants I, Vol 4, Springer-Verlag, Berlin, 225-236

Fukui H and Tanaka M , 1995 An envelope-shaped film culture vessel for plant cell suspension cultures and metabolite production without agitation Plant Cell, Tissue and Organ Culture, 41, 17-20

Gaff D F and Okong'o-ogola O , 1971 The use of non-permeating pigments for testing the survival of cells J Exp Bot , Vol 22, 756-758

Gallagher J O , 1987 The effect of shear on suspension cultures of *Morinda citrifolia* M Eng Sc Thesis, University College Dublin, Ireland

Gamborg OL , Miller R and Ojima K , 1968 Nutrient requirements of suspension cultures of Soybean Root Cells Exp Cell Res , Vol 50, 151-158

Gehle R D and Schugerl K , 1984 Penicillin recovery from aqueous solutions by continuous foam floatation Applied Microbiology and Biotechnology, 19, 373-375

Glicklis R , Mills D , Sitton D , Stortelder W and Merchuk J C , 1998 Polysaccharide production by plant cells in suspension Experiments and mathematical modeling Biotechnology and Bioengineering, Vol 57, 732-738

Grieves RB and Wang SL, 1966 Foam separation of *Escherichia coli* with a cationic surfactant Biotechnology and Bioengineering, Vol 8, 323-336

Hagendoorn M, van der Plas L and Segers G, 1994 Accumulation of anthraquinone in *Morinda citrifolia* cell suspensions Plant Cell, Tissue and Organ Culture, 38, 227-234

Hahlbrock K, 1975 Further studies on the relationship between the rates of nitrate uptake, growth and conductivity changes in the medium of plant cell suspension cultures Planta (Berl), 124, 311-318

Hall M J, Dickinson S D, Pritchard R and Evans J I, 1973 Foams and foam control in fermentation processes Progress in Industrial Microbiology, Vol 12, 171-231

Handa-Corrigan A, Emery A N and Spier R E, 1989 Effect of gas-liquid interfaces on the growth of suspended mammalian cells mechanisms of cell damage by bubbles Enzyme and Microbial Technology, Vol 11, April, 230-235

Harris E L V and Angal S, (Eds), 1989 Protein Purification Methods A practical approach IRL Press, Oxford University Press, USA

Hawke J G and Alexander A E, 1962 Retardation of evaporation by monolayers Academic Press 221-224

Hooker B S, Lee J M and An G, 1990 Cultivation of plant cells in a stirred vessel Effect of impeller design Biotechnology and Bioengineering, Vol 35, 296-304

Ishida M, Haga R, Nishimura N, Matuzaki H and Nakano R, 1990 High cell density suspension culture of mammalian anchorage independent cells Oxygen transfer by gas sparging and defoaming with a hydrophobic net Cytotechnology, Vol 4, 215-225

Jeanes A, Pittsley J E and Senti F R, 1961 Polysaccharide B-1459 A new hydrocolloid polyelectrolyte produced from glucose by bacterial fermentation Journal of Applied Polymer Science, Vol 5, No 17, 519- 526

Kalischewski K, Bumbulhs W and Schugerl K, 1979 Foam behaviour of biological media, I Protein foams European Journal of Applied Microbiology Biotechnology, 7, 21-31

Kato A, Kawazoe S and Soh Y, 1978 Viscosity of the broth of tobacco cells in suspension culture Journal of Fermentation Technology, Vol 56, 224-228

Kawase Y and Moo-Young M , 1990 The effect of antifoam agents on mass transfer in bioreactors Bioprocess Engineering, Vol 5, 169- 173

Kerley S and Forster C F , 1995 Extracellular polymers in activated sludge and stable foams Journal of Chemical Technology and Biotechnology, 62, 401-404

Kieran PM , 1993 An Investigation of the Hydrodynamic Shear Susceptibility of Suspension Cultures of *Morinda Citrifolia* Ph D Thesis, University College Dublin, Ireland

Kieran PM , Malone DM And MacLoughlin PF , 1993 Variation of aggregate size in plant cell suspension batch and semi-continuous cultures Food and bio-products processing Trans I Chem E , C, Vol 71, 40-46

Kieran PM , MacLoughlin PF and Malone, DM , 1997 Plant cell suspension cultures some engineering considerations Journal of Biotechnology, Vol 59, 39-52

Kim D I , Pedersen H and Chin C K , 1991 Cultivation of *Thalictrum rugosum* cell suspension in an improved airlift bioreactor Stimulatory effect of carbon dioxide and ethylene on alkaloid production Biotechnology and Bioengineering, Vol 38, 331-339

Kim J H , Shin J H, Lee H J , Chung I S and Lee H J , 1997 Effect of chitosan on indirubin production from suspension cultures of *Polygonum tinctorium* Journal of Fermentation and Bioengineering Vol 83, No 2, 206-208

Kitchener J A and Cooper C F 1959 Viscosities in Foaming solutions Quart Rev Chem Soc , Vol 13, 71-73

Koch V , Ruffer H M, Schugerl K , Innertsberger E , Menzel H and Weis J , 1995 Effect of antifoam agents on the medium and microbial cell properties and process performance in small and large reactors Process Biochemistry, Vol 30, No 5, 435-446

Konig B , Kalischewski K and Schugerl K, 1979 Foam behaviour of biological media, III *Penicillium chrysogenum* cultivation foam European Journal of Applied Microbiology and Biotechnology, 7, 251-258

Kotsaridu M , Gehle R and Schugerl K , 1983 Foam behaviour of biological media,
pH and salt effects European Journal of Applied Microbiology and Biotechnology, 18, 60-63

Kwok K H , Tsoulpha P and Doran P M , 1992 Limitations associated with conductivity measurement for monitoring growth in plant tissue culture Plant Cell, Tissue and organ culture, 29, 93-99

Lalchev Z , Dimitrova L , Tzvetkova P and Exerowa D , 1982 Foam separation of DNA and proteins from solutions Biotechnology and Bioengineering, Vol 24, No 10, 2253-2262

Lebrun L , Junter G A , Jouenne T and Mignot L , 1994 Exopolysaccharide production by free and immobilized microbial cultures Enzyme and Microbial Technology, Vol 16, December, 1048-1054

Lee J C, Salih M A , Sebai N N and Withey A , 1993 Control of foam in bioreactors- Action of antifoams In 3rd International Conference on Bioreactor and Bioprocess Fluid Dynamics, Cambridge UK Nienow A W (Ed), 275-287

Li G Q , Shin J H And Lee J M , 1995 Mineral oil addition as a means of foam control for plant cell cultures in stirred tank fermenters Biotechnology Techniques, Vol 9, 713-718

Liu H S , Chiung W and Wang Y C , 1994 Effect of Lard oil, olive oil and castor oil on oxygen transfer in an agitated fermentor Biotechnology Techniques, Vol 8, No 1, 17-20

Looby D and Griffiths J B , 1987 Comparison of oxygenation methods in a 39L stirred bioreactor Modern Approaches in Animal Cell Technology, 449-453

Mac Ritchie F , 1973 Effects of temperature on the dissolution and precipitation of proteins and amino acids J Macromol Sci Chem , Vol A4, 1169

Maniatis T , Fritsch E F and Sambrook J , 1989 Molecular Cloning A laboratory manual 2nd Ed , Cold Spring Harbor Laboratory Press, USA

Mita T , Nikai K , Hiraoka T , Matsuo S and Matsumoto H , 1976 Physiochemical studies on wheat protein foams Journal of Colloid and Interface Science, Vol 59, No 1, 172-178

Mohan S B and Lyddiatt A , 1994 Protein separation by differential drainage from foam Biotechnology and Bioengineering, Vol 44, 1261-1264

Molan P C , Edwards M and Eschenbruch,R , 1982 Foaming in Winemaking, II Separation and partial characterisation of foam-induced proteins excreted by a pure culture wine yeast European Journal Applied Microbiology Biotechnology, 16, 110-113

Moore T S , 1973 An extracellular macromolecule complex from the surface of soybean suspension cultures Plant Physiology, 51, 529-536

Moreno J , Vargas M A , Olivares H , Rivas J and Guerrero M G , 1998 Exopolysaccharide production by the cyanobacterium *Anabaena* sp ATCC 33047 in batch and continuous culture Journal of Biotechnology, Vol 60, 175-182

Murray C and O' Malley M , 1993 Segmentation of plant cell pictures Image and Vision Computing, Vol 11, No 3, 155-162

Murtagh J T , 1994 The effects of Hydrodynamic Shear Stress on Suspension Cultures of *Morinda citrifolia* using a Submerged, Turbulent Jet M Eng Sc Thesis, University College Dublin, Ireland

Nash DT and Davies ME , 1972 Some aspects of growth and metabolism of Pauls Scarlet rose cell suspensions J Exp Bot , Vol 23, 75-91

Noble I , Collins M , Porter N and Varley J , 1994 An investigation of the physico-chemical basis of foaming in fungal fermentations Biotechnology and Bioengineering, Vol 44, 801-807

Noble I , 1994 A study on foaming in microbiological fermentations Ph D Thesis, University of Reading, England

O'Donnell H , 1992 Capillary shear effects on suspensions of *Morinda citrifolia* M Eng Sc Thesis, University College Dublin, Ireland

Ohkawa A , Sakai N , Imai H and Endoh K , 1984a Foaming in an aerated stirred tank and its mechanical control Journal of Fermentation Technology, Vol 62, No 2, 179-187

Ohkawa A , Sakai N , Imai H and Endoh K , 1984b Mechanical control of foaming in a bubble column Biotechnology and Bioengineering, Vol 16, 702-713

Ohkawa A , Sugiyama K and Sakai N , 1984c Some characteristics of a sparged agitated vessel under foaming - mechanical control of foaming The Canadian Journal of Chemical Engineering, Vol 62, August, 507-510

Olivieri R , Forconi L , Bianciardi S and Rappuoli R , 1992 Foam formation and control in industrial production of modified diphtheria toxin by a mutant of *Corynebacterium diphtheriae* Chim Oggi , Vol 11, (1-2), 41-42

Olofsdotter M 1993 Image processing a non-destructive method for measuring growth in cell and tissue culture Plant Cell Rep Vol 12, 216-219

Olson A C, Evans J J, Frederick D P and Jansen E F, 1969 Plant suspension culture media macromolecules- pectic substances, proteins and peroxidase Plant Physiology, 44, 1594-1600

Onodera M, Nakaba H, Numata T, Nishibori H, and Kadota S and Ohkawa A, 1994 Cultivation of baker's yeast by a fermenter with a foam-breaker Biotechnology 1994, Second Conference on Advances in Biochemical Engineering

Otsuji K, Honda Y, Sugimura Y and Takei A, 1994 Production of polysaccharides in liquid cultures of *Polianthes tuberosa* cells Biotechnology Letters, Vol 16, No 9, 943-948

Panda AK, Saroj M, Bisaria VS And Bhojwani SS, 1989 Plant cell reactors a perspective Enzym and Microb Technology, Vol 11, 386-397

Pandit A B, 1994, ICHEME- Advances in Biochemical Engineering, Vol 44, 45-62

Parthasarathy S, Das T R, Kumar R and Gopalakrishman K S, 1988 Foam separation of microbial cells Biotechnology and Bioengineering, Vol 32, No 2, 174-183

Payne G F, Schuler M L And Brodelius P, 1987 Large scale plant cell culture In Lydersen BK (Ed), Large Scale Cell Culture Technology Hanser, Munich, 193-229

Payne G F, Payne N N and Shuler M L, 1988 Bioreactor considerations for secondary metabolite production from plant cell tissue culture Production of indole alkaloids from *Catharanthus roseus* Biotechnology and Bioengineering, Vol 30, 905-912

Phae C G and Shoda M, 1991 Investigation of optimal conditions for foam separation of Iturin, an antifungal peptide produced by *Bacillus subtilis* Journal of Fermentation and Bioengineering, Vol 71, No 2, 118-121

Phillips M C, Evans M T A and Hauser A, 1973 Proceedings of the sixth international congress on surface activity, Vol II, Part 1 381 Verlag Chemie, Weinheim m/Bergstrasse

Prins A and van't Riet K, 1987 Proteins and surface effects in fermentation foam, antifoam and mass transfer Trends in Biotechnology, Vol 5, 296-301

Proksch A and Wagner H, 1987 Structural analysis of 4-O-Methyl-glucuronoarabinoxylan with immuno-stimulating activity from *Echinacea purpurea* Phytochemistry Vol 26 No 7 1989-1993

Ramani M V, Kumar R and Gandhi K S, 1993 Drainage and separation factors for static foams containing agglomerates of microbial cells Chemical Engineering Science, Vol 48, No 10, 1819-1831

Ryu D Y , Lee S Q and Romani R J , 1990 Determination of growth rate for plant cell cultures comparative studies Biotechnology and Bioengineering, Vol 35, 305-311

Sahai O P and Shuler M L , 1984 Multistage continuous culture to examine secondary metabolite formation in plant cells Phenolics from *Nicotiana tabacum* Biotechnology and Bioengineering, Vol 16, 27-36

Sahai O and Knuth M , 1985 Commercializing plant tissue culture processes Economics, problems and prospects Biotechnology Progress, Vol 1, No 1, 1-9

Schopke C , Taylor N J , Carcamo R , Beachy R N and Fauquet C , 1997 Optimization of parameters for particle bombardment of embryogenic suspension cultures of cassava (*Manihot esculenta* Crantz) using image analysis *Plant Cell Reports, 16, 526-560*

Schweitzer PA , 1979 Handbook of separation techniques for chemical engineers McGraw-Hill, New York, USA

Scragg AH , 1987 Secondary products and cultured cells and organs II Large scale culture In Dixon RA and Gonzales RA (Eds), Plant Cell Culture, A practical approach 2nd ed , IRL Press at Oxford University Press, Oxford, 199-226

Sie T L and Schugerl K , 1983 Foam behaviour of biological media, XI Efficiency of antifoam agents with regard to their foam suppression effect on BSA solutions European Journal of Applied Microbiology and Biotechnology, 17, 221-226

Smart N J and Fowler M W , 1981 Effect of aeration on large-scale cultures of plant cells Biotechnology Letters, Vol 3, No 4, 117-176

Smith I H and Pace G W , 1982 Recovery of microbial polysaccharides Journal of Chemical Technology and Biotechnology, 32, 119-129

Smith M A L , Reid J F , Hansen A C and Madhavi D L , 1995 Non-destructive machine vision analysis of pigment-producing cell cultures Journal of Biotechnology, 40, 1-11

Snape J B , Thomas N H And Callow J A , 1989 How suspension cultures of *Catharanthus roseus* respond to oxygen limitation Small-scale tests with applications to large-scale cultures Biotechnology and Bioengineering, Vol 34, 1058-1062

Stafford A , Smith L and Fowler M W , 1985 Regulation of product synthesis in cell cultures of Catharanthus roseus (L) G Don, growth-related indole alkaloid accumulation in batch cultures Plant Cell Tissue and Organ Cultures, Vol 4, No 1, 83-94

Stafford A , Morris P and Fowler M W , 1986 Plant cell biotechnology a perspective Enzyme and Microbial Technology, Vol 8, 578-587

Stasinopoulos S J and Seviour R J , 1992 Exopolysaccharide production by *Acremonium persicinum* in stirred-tank and air-lift fermentors Applied Microbiology and Biotechnology, Vol 36, 465-468

Suzuki H and Matsumoto T , 1988 Anthraquinone production by plant cell culture In Bajaj YPS , (Ed), Biotechnology in Agriculture and Forestry Medicinal and Aromatic Plants I, Springer-Verlag, Berlin, Vol 4, 237-250

Szarka L and Magyar K , 1969 The foams of fermentation broths Biotechnology and Bioengineering, Vol 11, 701-710

Takeda M , Ishigami M ,, Shimada A , Matsuoka H and Nakamura I , 1994 Separation and preliminary characterisation of acidic polysaccharide produced by *Enterobacter* species Journal of Fermentation and Bioengineering, Vol 78, No 2, 140-144

Takesono S , Yasukawa M , Ondera M , Izawa K , Yamagiwa K and Ohkawa A , 1993a Performance characteristics of a tower fermenter with mechanical foam control Journal of Chemical Technology and Biotechnology, 56, 97-107

Takesono S , Ondera M , Yamagiwa K and Ohkawa A , 1993b Design and operation of rotating-disk foam-breaker fitted to Tower fermenters Journal of Chemical Technology and Biotechnology, 57, 237-246

Takesono S , Ondera M , Nagai J , Yamagiwa K , Mori A and Ohkawa A , 1993c Relation between mechanical foam breaking difficulty and the foaming characteristics of solutions Journal of Fermentation and Bioengineering, Vol 75, No 4, 314-318

Takesono S , Ondera M , Yamagiwa K , Mori A and Ohkawa A , 1994 Relationship between critical disk speed for foam-breaking of rotating-disk mechanical foam-breakers and foaming characteristics of solutions Journal of Fermentation and Bioengineering, Vol 77, No 2, 221-223

Takesono S , Ondera M , Yamagiwa K and Ohkawa A , 1995 Gas hold-up and volumetric mass transfer coefficient in bubble columns under foam control Journal of Chemical Technology and Biotechnology, 64, 188-194

Tanaka H , Nishijima F , Suwa M and Iwamoto T , 1983 Rotating drum fermenter for plant cell suspension cultures Biotechnology and Bioengineering, Vol 23, 1203-1218

Tanaka H , 1987 Large-scale cultivation of plant cells at high density A review Process Biochem , Vol 8, 106-113

Tanaka H , Semba H , Jitsufuchi T and Harada H , 1988 The effect of physical stress on plant cells in suspension cultures Biotech Lett , Vol 10, 485-490

Tanaka H , Aoyagi H and Jitsufuchi T , 1992 Turbidimetric measurement of cell biomass of plant cell suspensions Journal of Fermentation and Bioengineering, Vol 73, No 2, 130-134

Taya M , Hegglin M , Prenosil J E and Bourne J R , 1989 On-line monitoring of cell growth in plant tissue cultures by conductivity Enzyme and Microbial Technology, Vol 11, March, 170-176

Thomas A and Winkler M A , 1977 Foam separation of biological materials In Wiseman A , (Eds), Topics in enzyme and fermentation biotechnology, Ellis Horwood Ltd , Chichester, 43-71

Thorup J E , McDonald K A, Jackman A P , Bhatia N and Dandekar A M , 1994 Ribosome-inactivating protein production from *Trichosanthes kirilowii* plant cell cultures Biotechnology Progress, 10, 345-352

Tornkvist M , Larsson G and Enfors S O, 1996 Protein release and foaming in *Escherichia coli* cultures grown in minimal medium Bioprocess Engineering, 15, 231-237

Uchiyama T , Numata M , Terada S and Hosino T , 1993 Production and composition of extracellular polysaccharides from cell suspension cultures of *Mentha* Plant Cell, Tissue and Organ Culture, 32, 153-159

Uraizee F and Narsimhan G , 1990a Foam fractionation of proteins and enzymes I Applications Enzyme and Microbial Technology, Vol 12, March, 232-233

Uraizee F and Narsimhan G , 1990b Foam fractionation of proteins and enzymes II Performance and modeling Enzyme and Microbial Technology, Vol 12, April, 315-316

Uraizee F and Narsimhan G , 1996 Effects of kinetics of adsorption and coalescence on continuous foam concentration of proteins Comparison of experimental results with model predictions Biotechnology and Bioengineering, Vol 51, 384-398

Van't-Riet K , Prins A and Nieuwenhuijse J A , 1984 Some effects of foam control by dispersed natural oil on mass transfer in a bubble column European Congress of Biotechnology, 3 Meet Vol 3, 521-26

Van't-Riet K and Van Sonsbeek H M , 1992 Foaming, mass transfer and mixing Interrelations in large scale fermentors Harnessing Biotechnology 21th Century,189-192

Vardar- Sukan F , 1991 Effects of natural oil on foam collapse in bioprocesses Biotechnology Letters, Vol 13, No 2 107-112

Vardar-Sukan F , 1992 Foaming and its control in bioprocesses Recent Advances in Biotechnology, 113-146

Varley J , Kaul A and Ball S , 1996 Partition of protein from binary mixtures by a batch foaming process Biotechnology Techniques, Vol 10, No 2, 113-140

Vecht-Lifshitz S E and Ison A P , 1992 Biotechnological applications of image analysis present and future prospects Journal of Biotechnology, 23, 1-18

Viehweg H and Schugerl K , 1983 Cell recovery by continuous flotation European Journal of Applied Microbiology and Biotechnology, 17, 96-102

Viesturs U E , Kristapsons M Z and Levitans E S , 1982 Foam in Microbiological Processes In Fletcher A , (Ed), Advances in Biochemical Engineering, Springer-Verlag, Berlin, Vol 21, 169-224

Vogelmann H , Bischof A , Pape D , and Wagner F , 1978 Some aspects on mass cultivation In Alferman AW and Richard E , (Eds), Production of Natural Compounds by Cell Culture Methods GSF, Munich, 245-252

Wagner F and Vogelmann H , 1974 Cultivation of plant cell cultures in bioreactors and formation of secondary metabolites In Plant tissue culture and its biotechnological applications, Barz W *et al* (Ed), Springer-Verlag, New York, 245-252

Wagner H , Stuppner H , Schafer W and Zenk M , 1988 Immunologically active polysaccharides of *Echinacea purpurea* cell cultures Phytochemistry, Vol 27, No 1, 119-126

Wilson G , University College Dublin Personal Communication

Wolfes H and Schugerl K , 1983 Foam behaviour of biological media, VIII Surface properties European Journal of Applied Microbiology and Biotechnology, 17, 371-375

Wongsamuth R and Doran P M , 1994 Foaming and cell floatation in suspended plant cell cultures and the effect of chemical antifoams Biotechnology and Bioengineering, Vol 44, 481-488

Yagi H and Yoshida F , 1974 Oxygen absorption in fermenters - Effects of surfactants, antifoaming agents and sterilized cells Journal of Fermentation Technology, Vol 52, No 12, 905-916

Yasukawa M , Onodera M , Yamagiwa K and Ohkawa A , 1991a Performance characteristics of an aerated agitated vessel under mechanical foam control Journal of Chemical Engineering of Japan, Vol 24, No 2, 188-193

Yasukawa M , Onodera M , Yamagiwa K and Ohkawa A , 1991b Gas holdup, power consumption and oxygen absorption coefficient in a stirred-tank fermentor under foam control Biotechnology and Bioengineering, Vol 38, 629-636

Zenk M H , Shagi H and Schulte U , 1975 Anthraquinone production by cell suspension cultures of *Morinda citrifolia* Planta Medica Suppl , 79-101

Zhang S , Handa-Corrigan A and Spier R E , 1992 Foaming and media surfactant effects on the cultivation of animal cells in stirred and sparged bioreactors Journal of Biotechnology, Vol 25, 289-306

Zhong J J Seki T , Kinoshita S I and Yoshida T , 1992 Effect of surfactants on cell growth and pigment production in suspension cultures of *Perilla frutescens* World Journal of Microbiology and Biotechnology, Vol 8, No 2, 106-109

APPENDIX A

Image Analysis Program

```
Routine Header
   Number of fields 1
   Standard Frames
Setup Output Window  ( "Una's Results", Move to x 7, y 504, w 706, h 102 )
SETUP
For  ( BIN = 0 to 6, step 1 )
  BINEDOUT = BIN
  Binary Edit  ( Clear BINEDOUT )
Next  ( BIN )
DETLOWER = 250
DETCONTROL = 125
Input  ( NUMFIELDS )
Input  ( CHAINCOUNT )


START
1 AQUIRING OF IMAGES
Select Lens  ( Transmitted,  4 x, mag changer 1 0 x, 2 08731 microns per pixel )
Open File  ( C \DONAL\FILENAME DAT, channel #1 )
For  ( ACQIM = 1 to NUMFIELDS, step 1 )
  File Read  ( ACQFILE$, channel #1 )
  Live image  ( into Image0 )
  PauseText  ( "Select field of view" )
  Pause  ( No dialog )
  Acquire  ( into Image0 )
  Write image  ( from ACQOUTPUT into file ACQFILE$, type TIF )
Next  ( ACQIM )
Close File  ( channel #1 )


2 DETECTION AND ENHANCEMENT OF IMAGES
Open File  ( C \DONAL\BFILENAM DAT, channel #2 )
Open File  ( C \DONAL\FILENAME DAT, channel #1 )
For  ( DETIM = 1 to NUMFIELDS, step 1 )
  File Read  ( ACQFILE$, channel #1 )
  File Read  ( LOGFILE$, channel #2 )
  ACQOUTPUT = 0
  Read image  ( from file ACQFILE$ into ACQOUTPUT, type TIF )
  FERETS = 32
  LOGOUTPUT = 0
  Grey Transform  ( BSharpen from Image0 to Image1, cycles 3 )
  PauseText  ( "Alter detection level if neccessary" )
  DETIMAGE = 1
  Detect  [PAUSE]  ( blacker than DETLOWER, from DETIMAGE into DETBINARY  )
  MFEATINPUT = 0
  PauseText  ( "Keep chains of interest and make manual alterations if neccessary" )
  Binary Edit  [PAUSE]  ( Keep from Binary0 to Binary1, nib Fill, width 1 )
  LOGOUTPUT = 1
  Write binary image  ( from LOGOUTPUT into file LOGFILE$ )
  LOGOUTPUT = 0
```

```
Next  ( DETIM )
Close File  ( channel #1 )
Close File  ( channel #2 )
```

3 AUTOMATIC MEASUREMENT OF FEATURES

```
Open File  ( C \DONAL\FILENAME DAT, channel #1 )
Open File  ( C \DONAL\BFILENAM DAT, channel #2 )
XX = 0
For  ( MEASIM = 1 to NUMFIELDS, step 1 )
 File Read  ( ACQFILE$, channel #1 )
 File Read  ( LOGFILE$, channel #2 )
 LOGOUTPUT = 1
 MFEATINPUT = 1
 FERETS = 32
 Read image  ( from file ACQFILE$ into ACQOUTPUT, type TIF )
 Read binary image  ( from file LOGFILE$ into LOGOUTPUT )
 Feature Accept
   Area from 100  to 100000
 Measure feature  ( plane MFEATINPUT, FERETS ferets, minimum area  MINAREA, grey image
  FTRGREY IMAGE feature counts into FTRCOUNT(2), results into FTRRESULTS(count,1) )
   Selected parameters  Area
 TOTCNT = TOTCNT + FTRCOUNT(2)
 TOTALCNT = FTRCOUNT(2)
 For  ( LONGEST = 1 to TOTALCNT, step 1 )
  LENGTH = 0
  WIDTH = 0
  MAXREA = 0
  PIMAX = 0
  MINAREA = 0
  MFEATINPUT = 1
  Measure feature  ( plane MFEATINPUT, FERETS ferets, minimum area  MINAREA,  grey image
  FTRGREY IMAG feature counts into FTRCOUNT(2), results into FTRRESULTS(count,1) )
    Selected parameters  Area
  For  ( SORT = 1 to FTRCOUNT(2), step 1 )
   If  ( FTRRESULTS(SORT,1) > MAXREA )
    MAXREA = FTRRESULTS(SORT,1)
   Endif
  Next  ( SORT )
  PIMAX = MAXREA/4 3681
  MINAREA = PIMAX-1
  XX = XX+1
  Measure feature  ( plane MFEATINPUT, FERETS ferets, minimum area  MINAREA,  grey image
  FTRGREY IMAGE feature counts into FTRCOUNT(2), results into FTRRESULTS(count,1) )
    Selected parameters  Area
  Copy Accepted Features  ( from Binary1 into Binary0 )
  Binary Logical  ( C = A XOR B   C Binary1, A Binary1, B Binary0 )
  Binary Amend  ( Exh  Prune from Binary0 to Binary2, cycles 0, operator Octagon )
  Binary Identify  ( FillHoles from Binary2 to Binary2 )
  MFEATINPUT = 2
  Measure feature  ( plane MFEATINPUT, FERETS ferets, minimum area  MINAREA, grey image
  FTRGREY IMAGE feature counts into FTRCOUNT(2), results into FTRRESULTS(count,2) )
    Selected parameters  Area, Perimeter
  LENGTH = (FTRRESULTS(1,2)+(FTRRESULTS(1,2)^2-16*FTRRESULTS(1,1))^0 5)/4
  WIDTH = (FTRRESULTS(1,2)-(FTRRESULTS(1,2)^2-16*FTRRESULTS(1,1))^0 5)/4
  Display  ( LENGTH, field width  7, right justified, pad with spaces, 2 digits after ' ', tab follows )
  Display  ( WIDTH, field width  7, right justified, pad with spaces, 2 digits after ' ', tab follows )
  Binary Amend  ( Exh  Skeleton from Binary0 to Binary3, cycles 0, operator Octagon )
```

```
    Binary Amend  ( Exh  Prune from Binary3 to Binary3, cycles 0, operator Octagon )
    Binary Identify  ( FillHoles from Binary3 to Binary4 )
    Binary Logical  ( C = A XOR B   C Binary5, A Binary4, B Binary3 )
    MINAREA = 100
    FERETS = 32
    MFEATINPUT = 5
    Measure feature  ( plane MFEATINPUT, FERETS ferets, minimum area  MINAREA, grey image
     FTRGREY IMAGE feature counts into FTRCOUNT(2), results into FTRRESULTS(count,1) )
       Selected parameters  Length
    Display  ( FTRCOUNT(2), field width  7, right justified, pad with spaces, 2 digits after ' ', tab follows )
    Display  ( LENGTH/FTRCOUNT(2), field width  7, right justified, pad with spaces, 2 digits after ' ', tab
     follows )
    For  ( CELL = 1 to FTRCOUNT(2), step 1 )
     Display  ( FTRRESULTS(CELL,1), field width  7, right justified, pad with spaces, 2 digits after ' ', tab
     follows )
    Next  ( CELL )
    Display Line
   Next  ( LONGEST )
  Next  ( MEASIM )
  Close File  ( channel #1 )
  Close File  ( channel #2 )
  If  ( TOTCNT < CHAINCOUNT )
   PauseText  ( "Do you want to go to start (Y/N)" )
   Input  ( ANSWER )
   If  ( ANSWER =YES )
    Goto  START
   Endif
  END
```

Note commentary lines are highlighted in bold and italics

APPENDIX B

Raw data for Figure 3 4

Cell Length (Manual)	Cell Length (Auto)	Cell Length % Error	Cell Length (Manual)	Cell Length (Auto)	Cell Length % Error
72 000	73 000	1 389	124 020	118 000	-4 854
159 250	160 000	0 471	130 000	134 000	3 077
91 840	93 000	1 263	112 400	116 000	3 203
98 100	93 000	-5 199	100 970	98 000	-2 941
90 300	91 000	0 775	91 800	89 500	-2 505
80 000	85 000	6 250	155 300	156 000	0 451
55 150	52 000	-5 712	60 500	62 000	2 479
69 670	68 000	-2 397	84 400	85 000	0 711
46 350	45 000	-2 913	79 560	79 000	-0 704
53 220	52 000	-2 292	110 650	105 000	-5 106
48 500	50 000	3 093	80 300	81 000	0 872
37 600	38 000	1 064	65 500	62 000	-5 344
61 800	60 500	-2 104	153 410	152 000	-0 919
90 000	92 500	2 778	131 770	133 590	1 381
90 000	93 000	3 333	117 170	120 000	2 415
79 300	80 000	0 883	131 520	125 000	-4 957
84 100	80 000	-4 875	88 060	91 800	4 247
91 800	93 000	1 307	94 500	98 100	3 810
194 220	196 000	0 916	73 800	73 060	-1 003
93 800	96 000	2 345	66 300	68 000	2 564
102 770	104 000	1 197	285 000	290 000	1 754
96 800	96 000	-0 826	220 000	215 000	-2 273
94 020	93 000	-1 085	195 000	193 000	-1 026
100 230	104 000	3 761			
76 180	75 000	-1 549			
169 640	173 000	1 981			
170 290	169 000	-0 758			
138 410	137 000	-1 019			
171 880	175 000	1 815			
109 400	110 000	0 548			
112 900	112 000	-0 797			
93 900	98 000	4 366			
102 000	100 000	-1 961			
64 000	62 000	-3 125			
77 230	81 000	4 882			
83 000	83 000	0 000			
79 350	79 000	-0 441			
98 900	98 000	-0 910			
174 260	166 000	-4 740			
128 940	127 000	-1 505			
134 710	135 000	0 215			
157 120	150 000	-4 532			
136 940	141 000	2 965			
108 480	106 000	-2 286			
82 000	85 000	3 659			
106 530	112 000	5 135			
122 500	121 100	-1 143			

Raw data for Figure 3 5

Chain Length (Manual)	Chain Length (Auto)	Chain Length % Error
317 000	330 000	4 101
389 000	399 000	2 571
385 000	400 000	3 896
442 000	450 000	1 810
367 300	363 000	-1 171
700 000	723 000	3 286
418 090	438 000	4 762
300 000	312 000	4 000
557 700	573 000	2 743
322 700	330 000	2 262
550 000	555 000	0 909
420 000	420 000	0 000
555 000	555 000	0 000
630 000	630 000	0 000
540 000	540 000	0 000
550 000	565 000	2 727
670 000	685 000	2 239
500 000	520 000	4 000
925 000	900 000	-2 703
200 000	202 000	1 000
750 000	730 000	-2 667
850 000	845 000	-0 588
825 000	840 000	1 818
650 000	665 000	2 308

Raw data for Figure 3 6 All image analysis morphological raw data, throughout the growth cycle is presented in Appendix C

Raw data for Figure 3 8

BSA Standard Solution (mg ml ^{1})	Absorbance at 595 nm	BSA Standard Solution-duplicate	Absorbance at 595 nm
0	0	0	0
0 01	0 075	0 01	0 072
0 02	0 154	0 02	0 161
0 03	0 229	0 03	0 24
0 04	0 281	0 04	0 297
0 05	0 372	0 05	0 376
0 06	0 424	0 06	0 411
0 07	0 482	0 07	0 472
0 08	0 515	0 08	0 524
0 09	0 558	0 09	0 578
0 1	0 619	0 1	0 617

Raw data for Figure 3 10

Molecular Weight	Gel A Distance	Gel A R_f	Gel B Distance	Gel B R_f
200000 000	0 450	0 063	0 325	0 054
116300 000	1 100	0 139	0 750	0 125
97400 000	1 300	0 165	0 950	0 158
66300 000	1 950	0 253	1 450	0 242
36500 000	2 600	0 329	1 950	0 325
31000 000	4 000	0 506	3 000	0 500
21500 000	4 900	0 620	3 650	0 608
14400 000	6 650	0 842	5 100	0 850
6000 000	7 800	0 987	6 000	1 000

APPENDIX C

Raw data for Figure 4 1

DAY	DW1	DW2	DW3	DW4	DW5	DW6	DW AV	DW Dev	DW Err
0	1 41	2 25	1 102			1 005	1 442	0 566	0 231
1	1 08	2 25	1 8	2 085	1 83	2 115	1 860	0 420	0 171
2	2 155	2 28	2 675	3 02	2 29	3 125	2 591	0 413	0 169
3		3 38	3 3			4 08	3 587	0 429	0 175
4	3 53	3 86	4 45	6 065	4 56	5 075	4 590	0 904	0 369
5	4 4	5 865	6 05		6 33	8	6 129	1 285	0 525
6	6 7	7 675	7 63	11 2	9 58	10 65	8 906	1 831	0 748
7	10	8 49	10			13 08	10 393	1 928	0 787
8	10 83	11 2	11 22	13 58	12 96	12 8	12 098	1 150	0 470
9	12 27	11 77	12 46	13 14		11 32	12 192	0 692	0 282
10	10 32	12 28	12 62	12 5	11 76		11 896	0 941	0 384
11	11 1	13 49	13 25	12 36		10 92	12 224	1 187	0 485
12	11 47	13 07	12 64		12 07	11 08	12 066	0 816	0 333
13	11 67	13 11	12 75	11 93		12	12 292	0 609	0 249
14	11 25	12 99	13 2	12		13 2	12 528	0 870	0 355
15	10 95	12 04	13 5			12	12 123	1 048	0 428
16	10 23	11 87	13 11				11 737	1 445	0 590
17	10 3	11 3	12 33	11		10 5	11 086	0 800	0 327
18	10 38	10 98	11 16	11	10 99		10 902	0 301	0 123
19	10 16	10 37		10 92		10 2	10 413	0 350	0 143
20	9 98		11 35				10 665	0 969	0 395
21		10 25	11 2			9 78	10 410	0 723	0 295

DAY	FW1	FW2	FW3	FW4	FW5	FW6	FW AV	FW Dev	FW Err
0	34 88	25 12	27 00			32 6	29 900	4 680	1 9107
1	34 00	29 73	27 17	30 21	39 75	37 415	33 046	4 868	1 988
2	37 05	33 18	33 82	43 44	42 35	43 655	38 916	4 839	1 975
3		43 36	48 735			56 9	49 665	6 818	2 783
4	57 54	57 98	65 335	83 5	75 4	71 265	68 503	10 208	4 168
5	65 95	70 16	98 51		103 67	124 98	92 654	24 595	10 041
6	109 96	103 57	95 96	156 8	194 2	162 17	137 10	39 574	16 156
7	120 64	108 9	146 7			203 9	145 03	42 303	17 270
8	157 36	137 14	155 61	205 87	197 35	244 61	182 99	40 089	16 366
9	170 27	150 58	173 24	220 14		230 88	189 02	34 637	14 141
10	165 98	171 5	168 47	250	220	260	205 99	43 008	17 558
11	224 34	181 02	194 52	291 26		292 95	236 81	52 851	21 576
12	280 91	178 53	196 67		243 94	265	233 01	43 950	17 942
13	247 86	174	251 6	265 84		278 67	243 59	40 776	16 647
14	277 15	199 45	249 23			326 7	263 13	53 185	21 713
15		254 33				318 36	286 34	45 276	18 484
16	263 03	251 69	351			287 8	288 38	44 386	18 121
17			292 4			301 7	297 05	6 576	2 685
18	311 55	255 7	309 5	290 33	317 04		296 82	25 098	10 246
19	272 83	256 4	300	310 17	300	288 48	287 98	20 042	8 182
20	312 55		288				300 27	17 359	7 087
21	300	260	290	290	290	307 28	289 5	16 108	6 576

DW = Dry weight (g l^{-1}), FW = Fresh weight (g l^{-1}), AV = Average,
Dev = Standard deviation, Err = Standard error

Raw data for Figure 4.2

DAY	CELL	CELL2	CELL3	CELL AV	CELL Err	FW AV
0			0.44	0.43		29.900
1	0.41	0.46	0.36	0.40	0.023	33.046
2	0.52	0.56	0.33	0.43	0.059	38.916
3		0.64		0.64		49.665
4		0.73	0.89	0.81	0.059	68.503
5		1.15	0.63	0.89	0.152	92.654
6	1.75	1.48	1.01	1.31	0.219	137.109
7		2.18	1.17	1.68	0.357	145.035
8	3.31	3.44	1.31	2.34	0.570	182.990
9		4.10	2.86		0.506	189.022
10				3.43	0.000	205.992
11	4.40	4.35	3.50	3.94	0.242	236.818
12		4.80	4.27	4.53	0.190	233.011
13	4.70	5.15	4.29	4.60	0.252	243.594
14		4.90	4.96	4.75	0.076	263.133
15		4.86	4.63	4.90	0.103	286.345
16		4.86	4.68	4.77	0.064	288.380
17		4.95	4.83	4.89	0.042	297.050
18	4.86		5.00	4.93	0.049	296.824
19	4.85	5.23		5.04	0.133	287.980
20			4.95	4.95		300.275
21		5.00		4.88	0.062	289.547

CELL = Cell number (10^6 cells ml^{-1}).

Raw data for Figure 4.3

DAY	PH1	PH2	PH3	PH4	PH5	PH6	PH6	PH AV	PH Dev	PH Err
0	5.5	5.47	5.48	5.5	5.5	5.49	5.49	5.490	0.013	0.005
1	5.02	4.89	4.81	4.94	4.85	4.94	4.94	4.908	0.075	0.030
2	4.65		4.64	4.55	4.73	4.64	4.64	4.642	0.064	0.026
3	4.4	4.39	4.44	4.4	4.63	4.44	4.44	4.450	0.091	0.037
4	4.32	4.33	4.49	4.27	4.54	4.34	4.34	4.382	0.107	0.044
5	4.22	4.27	4.48		4.38	4.2	4.05	4.310	0.118	0.053
6	4.25	4.05	4.32	4.63	4.11	4.51	4.51	4.312	0.225	0.092
7		4.84	5.23			4.86	4.86	4.977	0.220	0.127
8	5	5.4	5.53	5.4	5.39	5.23	5.23	5.325	0.186	0.076
9	5.4	5.9	5.67	5.63		5.24	5.24	5.568	0.255	0.114
10	5.3	5.74	5.82	5.53	5.35			5.548	0.230	0.103
11	5.39	5.4	5.71	5.43		5.17	5.17	5.420	0.192	0.086
12	5.35	5.38	5.35	5.35	5.01	5.01	5.01	5.242	0.180	0.073
13	5.19	5.32	4.94	5.04		5.22	5.22	5.142	0.151	0.068
14	5.02	4.94	4.86	5.1		5.19	5.19	5.022	0.130	0.058
15	5	4.86	5	5.2		5.44	5.44	5.100	0.225	0.101
16	5.04	4.94	5.06	5.25		5.44	5.44	5.146	0.199	0.089
17	5	5	4.98	5.3		5.37	5.37	5.130	0.189	0.084
18	4.98	5.09	4.94	5.35	5.31	5.38		5.175	0.196	0.087
19	5.09	5.18	5	5.6	5.3	5.45	5.45	5.270	0.226	0.092
20	5.01		5.05	5.55	5.35	5.5		5.292	0.251	0.112
21	5.1	5.25	5.1	5.5	5.4	5.42	5.42	5.295	0.171	0.070

Raw data for Figures 4 4, 4 5 and 4 6

DAY	COND	DW	FW	CELL
0	3 960	1 587	32 000	0 430
1	3 910	1 710	34 000	0 397
2	3 820	2 370	37 050	0 434
3	3 760	3 340	48 000	
4	3 723	3 947	57 540	0 809
5	3 603	5 438	65 950	1 100
6	3 454	7 335	109 950	1 311
7	3 260	8 660	120 640	1 675
8	3 120	10 120	157 360	2 343
9	2 890	12 167	170 270	
10	2 750	12 350	185 000	3 430
11	2 500	12 613	224 340	3 938
12	2 337	12 393	250 000	4 533
13	2 313	12 510	267 000	4 604
14	2 240	12 730	277 000	4 750
15	2 170	12 040	280 000	4 900
16	2 150	12 490	290 000	4 770
17	2 120	12 230	300 000	4 890
18	2 093	11 160	311 000	4 930
19	2 070	10 265	300 000	5 038
20	2 020	10 500	312 000	4 950
21	1 960	10 700	301 230	4 875

COND = Conductivity (mS cm $^{-1}$)

Raw data for Figures 4 8 and 4 9

Day	Chain Width AV	Chain Width Dev	No of cells/chain	No of cells/chain Dev	Chain Length AV	Cell Length AV
0	35 524	8 210	4 510	1 950	379 850	81 83
3	37 500	6 590	3 680	2 090	430 380	111 67
5	36 120	9 850	2 734	1 332	355 310	119 64
7	37 400	7 840	3 510	1 620	375 300	103 26
10	38 330	8 350	4 380	1 766	421 260	91 36
12	39 590	6 663	4 226	1 890	381 060	89 93
14	37 300	5 960	4 150	1 850	347 010	83 64
17	37 870	9 380	4 790	2 160	429 980	84 63
21	38 520	8 210	4 510	1 950	379 850	81 83

Raw data for Figures 4 10 and 4 11

Morphological Data DAY 0

Chain Length (μm)	Chain Width (μm)	No of cells per chain	Cell Length (μm)	Chain Length (μm)	Chain Width (μm)	No of cells per chain	Cell Length (μm)
642 630	43 050	5 000	110 630	191 940	53 320	2 000	123 150
504 120	37 530	8 000	41 750	316 850	29 650	2 000	139 850
264 920	52 350	4 000	81 410	801 950	34 020	8 000	108 540
384 070	41 750	8 000	66 790	253 070	34 980	2 000	112 710
332 000	37 450	4 000	60 530	191 470	36 040	2 000	91 840
282 970	32 210	3 000	85 580	560 910	42 330	7 000	60 530
272 680	36 240	3 000	79 320	442 140	50 460	4 000	91 840
418 380	36 660	4 000	106 450	244 650	35 050	2 000	87 670
163 370	54 750	3 000	75 140	452 830	49 170	5 000	75 140
137 970	54 060	3 000	64 710	278 270	35 870	4 000	52 180
902 870	32 250	8 000	96 020	357 690	46 200	4 000	85 580
509 990	32 710	4 000	85 580	279 090	45 490	6 000	66 790
428 200	27 880	4 000	100 190	282 570	32 610	3 000	98 100
460 000	37 820	4 000	121 060	528 170	32 270	8 000	50 100
477 850	37 720	6 000	48 010	488 970	27 640	5 000	139 850
302 990	49 770	6 000	70 970	232 760	37 550	4 000	75 140
240 100	46 910	3 000	62 620	264 840	21 120	2 000	56 360
244 970	36 820	3 000	56 360	620 170	34 200	8 000	66 790
547 210	37 240	8 000	85 580	323 270	36 790	4 000	66 790
472 090	42 430	6 000	77 230	376 070	42 440	5 000	77 230
448 330	38 020	7 000	73 060	351 110	31 920	4 000	93 930
441 120	35 830	8 000	33 400	513 940	41 280	8 000	81 410
310 600	39 020	5 000	54 270	475 260	47 620	4 000	116 890
441 800	36 190	4 000	108 540	484 630	43 460	6 000	70 970
392 560	44 730	5 000	108 540	337 870	38 890	4 000	91 840
435 990	37 830	4 000	114 800	315 340	39 500	4 000	81 410
387 940	34 740	5 000	93 930	322 630	48 910	1 000	317 270
263 410	38 210	4 000	79 320	381 750	35 710	4 000	87 670
199 690	43 480	2 000	85 580	326 400	29 490	4 000	77 230
122 620	45 410	2 000	75 140	405 450	37 060	6 000	77 230
660 630	33 400	6 000	79 320	371 610	35 420	3 000	87 670
227 700	60 350	2 000	123 150	609 130	45 240	7 000	70 970
471 050	57 040	5 000	85 580	612 910	36 240	8 000	89 750
350 750	32 270	4 000	79 320	497 210	41 320	4 000	75 140
276 490	36 610	4 000	96 020	319 100	20 080	2 000	68 880
156 780	50 910	2 000	89 750	218 770	31 700	2 000	102 280
112 210	61 040	2 000	62 620	377 740	43 900	5 000	85 580
257 410	41 080	4 000	62 620	168 050	44 850	2 000	56 360
622 210	38 420	8 000	79 320	197 200	42 840	4 000	43 830
555 520	36 230	7 000	66 790	410 760	11 920	1 000	75 140
347 690	29 070	4 000	93 930	116 220	38 240	2 000	39 660
419 290	44 090	7 000	85 580	620 950	33 430	8 000	77 230
253 650	33 360	3 000	110 630	504 940	32 550	5 000	108 540
322 190	39 960	4 000	93 930	206 190	49 510	3 000	70 970
319 670	32 040	4 000	75 140	169 710	42 150	2 000	91 840
602 730	27 640	5 000	79 320	327 710	35 480	4 000	68 880
312 560	30 810	4 000	77 230	396 200	30 660	6 000	54 270
280 240	44 340	2 000	150 290	891 690	20 470	8 000	43 830
854 880	37 440	8 000	96 020	445 380	39 920	4 000	118 980
301 080	45 410	5 000	68 880	276 880	40 390	6 000	127 330
365 460	33 210	3 000	131 500	189 110	34 240	3 000	52 180

(DAY 0) CELL LENGTH *continued*						
85 580	121 060	60 530	56 360	66 790	60 530	89 750
98 100	77 230	60 530	68 800	79 320	68 880	64 710
68 880	70 970	70 970	64 700	127 330	43 830	114 800
56 360	66 790	70 970	64 700	87 670	83 490	75 140
58 440	60 530	64 710	83 710	68 880	48 010	43 830
58 440	79 320	60 530	118 980	100 190	81 410	70 970
166 980	85 580	96 020	70 970	56 360	39 660	114 800
68 880	54 270	62 620	85 580	48 010	104 370	58 440
45 920	123 150	64 710	60 560	75 140	83 490	35 480
45 920	102 280	64 710	56 300	79 320	100 190	100 190
37 570	106 450	64 710	54 270	50 100	85 580	50 100
62 620	81 410	60 530	75 140	89 750	68 880	70 970
62 620	56 360	68 880	60 530	81 410	118 980	137 760
114 800	73 060	96 020	66 790	41 750	62 620	106 450
56 360	127 330	56 360	75 140	83 490	254 650	106 450
70 970	87 670	87 670	116 890	75 140	87 670	52 180
50 100	68 880	54 270	93 900	146 110	50 100	125 240
56 360	54 270	102 280	66 700	131 500	75 140	60 530
89 750	93 930	121 060	110 300	110 630	48 010	62 620
66 790	70 970	58 440	56 400	68 880	73 060	66 790
73 060	81 410	50 100	60 600	87 670	70 970	104 370
144 020	48 010	150 290	78 000	75 140	73 060	60 530
81 410	79 320	106 450	64 000	79 320	60 530	81 410
68 880	79 320	100 190	77 230	150 290	62 620	96 020
108 540	118 980	66 790	50 100	73 060	85 580	56 360
91 840	62 620	77 230	64 700	64 710	48 010	43 830
79 320	104 370	43 830	73 060	114 800	70 970	127 330
108 540	64 710	112 710	73 000	70 970	64 710	141 940
52 180	98 100	112 710	56 000	43 830	62 620	56 360
62 620	85 580	75 140	64 700	91 840	41 750	70 970
77 230	112 710	87 670	79 320	73 060	75 140	70 970
54 270	79 320	64 710	150 290	93 930	125 240	70 970
106 450	85 580	37 570	106 450	83 490	93 930	43 830
66 790	75 140	85 580	70 970	56 360	68 880	123 150
73 060	45 920	100 190	58 440	52 180	98 100	87 670
110 630	79 320	52 180	81 410	89 750	68 880	114 800
83 490	68 880	100 190	123 150	73 060	70 000	75 140
79 320	48 010	58 440	45 920	77 230	148 200	48 010
85 580	60 530	62 620	73 060	60 530	129 410	62 620
77 230	75 140	68 880	108 540	60 530	112 710	164 900
125 240	100 190	100 190	81 410	60 530	89 750	93 930
56 360	73 060	60 530	60 530	185 770	106 450	104 370
66 790	83 490	66 790	75 140	77 230	118 980	118 980
52 180	96 020	81 410	83 490	66 790	146 110	106 450
104 370	62 620	81 410	89 750	41 750	87 670	77 230
45 920	93 930	123 150	50 100	68 880	62 620	
45 920	93 930	70 970	108 540	133 590	104 370	
45 920	75 140	81 410	106 450	83 490	54 270	
116 890	96 020	60 530	96 020	73 060	96 020	
68 880	60 530	87 670	48 010	60 530	60 530	
50 100	85 580	89 750	87 670	56 360	54 270	
48 010	87 670	100 190	64 710	87 670	64 710	
108 540	156 550	58 440	83 490	139 850	77 230	
121 060	89 750	112 710	43 830	79 320	77 230	

Morphological Data DAY 3

Chain Length (μm)	Chain Width (μm)	No of cells per chain	Cell Length (μm)	Chain Length (μm)	Chain Width (μm)	No of cells per chain	Cell Length (μm)
494 970	39 380	5 000	112 710	257 790	18 780	2 000	125 240
237 730	39 880	3 000	83 490	536 810	39 290	4 000	123 150
374 010	38 230	3 000	171 160	363 000	50 290	3 000	70 970
289 890	37 810	1 000	273 440	860 440	33 970	8 000	116 890
952 000	41 550	9 000	75 140	168 300	50 870	2 000	81 410
637 030	31 950	4 000	121 060	1051 700	30 570	8 000	154 460
107 580	44 790	1 000	108 540	640 230	33 970	6 000	96 020
565 750	36 440	4 000	150 290	406 720	37 880	2 000	137 760
544 610	31 490	7 000	98 100	261 040	36 400	3 000	93 930
221 250	38 620	2 000	102 280	147 740	39 070	2 000	68 880
154 700	43 600	2 000	75 140	539 580	39 650	4 000	125 240
120 790	42 020	1 000	123 150	427 970	39 590	4 000	141 940
510 360	43 820	5 000	118 980	373 490	49 190	3 000	73 060
169 010	37 640	2 000	75 140	400 120	36 130	3 000	137 760
553 460	35 160	7 000	79 320	389 310	38 590	3 000	93 930
499 970	32 300	4 000	118 980	428 650	38 910	4 000	79 320
224 290	38 710	1 000	196 210	213 810	43 970	2 000	91 840
227 020	35 980	1 000	206 640	128 290	43 910	1 000	129 410
558 600	41 500	7 000	83 490	367 250	31 430	2 000	154 460
279 010	40 350	3 000	118 980	199 460	44 760	2 000	87 670
256 290	30 720	2 000	125 240	942 680	33 140	8 000	133 590
216 990	30 360	2 000	87 670	600 570	33 970	3 000	281 790
783 640	34 590	5 000	137 760	578 800	47 390	5 000	116 890
841 670	30 830	8 000	75 140	754 670	28 070	5 000	164 900
825 380	31 460	5 000	194 120	166 980	44 880	2 000	89 750
491 940	42 410	5 000	83 490	679 080	35 820	8 000	79 320
291 900	32 670	3 000	133 590	651 840	32 800	6 000	148 200
140 430	49 520	2 000	85 580	952 410	36 980	10 000	102 280
233 070	38 280	2 000	104 370	550 760	33 690	5 000	129 410
219 260	39 560	2 000	106 450	687 540	31 540	5 000	77 230
141 720	39 870	1 000	127 330	629 240	33 480	4 000	156 550
606 680	25 770	5 000	116 890	277 620	40 690	3 000	66 790
552 770	33 770	4 000	108 540	655 860	29 820	5 000	139 850
194 020	34 540	2 000	79 320	661 820	25 940	3 000	160 720
170 900	36 790	2 000	96 020	533 270	36 570	4 000	98 100
466 960	42 340	5 000	56 360	327 000	37 240	4 000	62 620
501 480	39 130	4 000	162 810	603 850	39 040	4 000	162 810
685 700	18 760	3 000	104 370	476 310	39 260	8 000	60 530
417 060	34 840	3 000	183 680	282 780	40 750	3 000	93 930
282 280	32 910	2 000	137 760	266 980	38 810	3 000	96 020
148 270	31 240	1 000	129 410	944 760	34 190	4 000	271 350
91 750	43 920	2 000	50 100	291 930	55 610	3 000	87 670
267 440	38 350	3 000	98 100	201 130	59 790	1 000	202 470
246 450	33 250	2 000	100 190	626 930	45 190	6 000	164 900
279 520	31 490	1 000	256 740	345 860	42 380	3 000	150 290
223 820	32 920	2 000	100 190	248 590	54 070	2 000	135 680
220 350	33 260	2 000	110 630	637 280	34 830	4 000	64 710
169 200	37 440	1 000	164 900	516 300	36 830	4 000	102 280
416 150	35 750	4 000	116 890	176 330	49 090	2 000	77 230
457 520	38 210	4 000	112 710	205 300	39 960	2 000	64 710
366 640	37 250	4 000	100 190	446 320	27 500	4 000	91 840
969 710	39 500	8 000	116 890	817 100	34 530	8 000	123 150
695 880	35 730	6 000	52 180	717 000	30 260	6 000	64 710

(DAY 3) CELL LENGTH *continued*					
116.890	91.840	112.710	106.450	96.020	165.000
118.980	112.710	108.540	104.370	137.760	139.850
112.710	125.240	110.630	152.370	114.800	164.900
139.850	177.420	110.630	121.060	183.680	70.970
123.150	121.060	58.440	96.020	77.230	131.500
75.140	102.280	141.940	116.890	87.670	106.450
77.230	79.320	98.100	85.580	56.360	100.190
83.490	87.670	154.460	108.540	54.270	129.410
112.710	125.240	135.680	96.020	66.790	87.670
106.450	75.140	141.940	60.530	93.930	144.020
89.750	179.510	87.670	144.020	123.150	123.150
146.110	116.890	102.280	77.230	141.940	185.770
137.760	194.120	104.370	62.620	114.800	
158.640	102.280	148.200	121.060	98.100	
189.950	121.060	173.250	112.710	137.760	
141.940	181.600	93.930	146.110	112.710	
87.670	60.530	48.010	64.710	91.840	
123.150	104.370	118.980	152.370	79.320	
56.360	70.970	77.230	66.790	127.330	
98.100	96.020	154.460	35.480	89.750	
56.360	106.450	141.940	64.710	114.800	
202.470	73.060	83.490	125.240	93.930	
75.140	196.210	129.410	112.710	58.440	
156.550	129.410	75.140	125.240	83.490	
91.840	68.880	150.290	144.020	85.580	
96.020	81.410	60.530	96.020	60.530	
225.430	256.740	175.330	77.230	73.060	
139.850	141.940	64.710	106.450	89.750	
102.280	85.580	181.600	112.710	77.230	
133.590	146.110	123.150	179.510	100.190	
85.580	50.100	189.950	89.750	131.500	
77.230	83.490	108.540	127.330	75.140	
91.840	93.930	131.500	54.270	127.330	
106.450	229.600	125.240	108.540	81.410	
83.490	139.850	102.280	141.940	96.020	
154.460	141.940	54.270	110.630	73.060	
123.150	148.200	60.530	100.190	60.530	
75.140	79.320	105.000	102.280	166.980	
106.450	89.750	221.250	135.680	79.320	
77.230	58.440	50.100	91.840	110.630	
135.680	66.790	150.000	133.590	96.020	
93.930	64.710	114.800	81.410	85.580	
100.190	152.370	125.240	70.970	135.680	
123.150	131.500	77.230	100.190	87.670	
133.590	39.660	152.370	75.140	93.930	
166.980	66.790	79.320	87.670	56.360	
125.240	70.970	110.630	125.000	62.620	
70.970	83.490	104.370	131.500	144.020	
110.630	58.440	129.410	100.190	62.620	
160.000	112.710	156.550	108.540	87.670	
85.580	50.100	89.750	87.670	70.970	
85.580	170.000	152.370	106.450	85.580	
64.710	91.840	114.800	70.970	125.240	
125.240	150.000	100.190	227.520	129.410	
60.530	120.000	135.680	75.140	127.330	
125.240	93.930	114.800	77.230	89.750	

Morphological Data DAY 5

Chain Length (μm)	Chain Width (μm)	No. of cells per chain	Cell Length (μm)	Chain Length (μm)	Chain Width (μm)	No. of cells per chain	Cell Length (μm)
280.180	45.440	3.000	64.710	255.990	37.270	2.000	114.800
388.300	32.290	3.000	96.020	288.550	38.110	2.000	150.290
322.790	36.230	4.000	85.580	476.690	44.090	5.000	106.450
273.930	40.210	2.000	112.710	411.730	32.870	1.000	352.760
577.950	22.150	4.000	98.100	368.800	42.400	2.000	162.810
356.650	36.810	3.000	75.140	291.160	34.460	2.000	106.450
172.150	38.670	2.000	89.750	620.650	44.160	5.000	156.550
196.230	36.500	2.000	93.930	524.860	16.790	5.000	123.150
432.510	38.180	4.000	110.630	300.570	37.570	2.000	148.200
246.630	36.200	2.000	139.850	194.500	61.200	1.000	200.380
460.980	37.890	4.000	79.320	501.640	35.840	4.000	98.100
682.120	36.960	8.000	60.530	486.980	34.850	4.000	102.280
288.530	35.000	4.000	70.970	403.840	30.320	3.000	108.540
372.080	46.430	4.000	116.890	243.820	30.660	2.000	93.930
145.710	47.360	1.000	144.020	452.950	33.400	3.000	125.240
109.560	53.250	2.000	60.530	587.950	12.150	4.000	121.060
349.400	31.540	4.000	118.980	537.790	38.310	4.000	137.760
365.080	29.420	3.000	146.110	209.310	34.910	1.000	179.510
506.620	39.220	4.000	102.280	298.270	30.490	2.000	125.240
202.600	41.610	2.000	98.100	236.360	44.390	3.000	60.530
184.500	28.410	1.000	173.250	453.810	32.540	3.000	135.680
166.310	25.730	1.000	152.370	299.670	31.170	2.000	139.850
569.580	29.480	5.000	110.630	284.360	32.910	1.000	267.180
376.600	31.470	4.000	75.140	323.140	35.880	2.000	152.370
341.720	27.730	2.000	194.120	279.880	36.350	2.000	139.850
341.380	28.080	3.000	114.800	204.580	39.630	2.000	89.750
246.490	34.260	2.000	129.410	238.930	36.600	2.000	148.200
462.040	30.560	3.000	198.290	194.870	36.820	2.000	102.280
400.010	28.930	3.000	206.640	401.970	29.060	3.000	96.020
153.500	32.270	1.000	141.940	338.890	30.560	2.000	171.160
257.450	30.600	2.000	123.150	531.620	38.220	4.000	118.980
562.810	27.900	5.000	93.930	218.440	31.000	2.000	89.750
229.870	32.090	2.000	91.840	567.690	27.190	4.000	91.840
204.280	32.630	2.000	102.280	341.350	31.230	3.000	73.060
217.580	33.940	1.000	202.470	311.310	39.350	2.000	137.760
129.760	42.440	1.000	133.590	251.470	44.920	2.000	133.590
863.750	29.620	5.000	210.820	424.370	27.540	4.000	93.930
399.430	31.600	2.000	173.250	266.500	29.900	2.000	110.630
208.130	41.300	2.000	93.930	239.100	29.120	1.000	227.520
314.710	92.310	3.000	114.800	649.710	41.190	6.000	102.280
248.630	38.380	2.000	96.020	511.010	30.640	3.000	252.560
274.500	41.730	2.000	152.370	469.960	37.260	4.000	81.410
145.090	43.810	1.000	144.020	713.720	12.670	5.000	137.760
170.030	35.570	1.000	162.810	397.100	27.670	3.000	85.580
110.820	43.640	1.000	110.630	550.700	29.570	4.000	144.020
118.500	35.960	1.000	106.450	321.390	34.500	2.000	150.290
556.250	14.630	3.000	52.180	488.960	32.870	3.000	156.550
655.620	27.980	2.000	265.090	432.700	36.940	4.000	110.630
389.840	30.760	2.000	171.160	438.630	36.240	3.000	196.210
258.170	59.100	2.000	154.460	335.640	46.340	4.000	102.280
236.160	38.320	2.000	100.190	501.200	36.280	4.000	148.200
210.830	65.740	2.000	116.890	1007.050	13.650	1.000	277.610
224.390	37.570	2.000	83.490	506.170	34.440	4.000	125.240

Chain Length (μm)	Chain Width (μm)	No. of cells per chain	Cell Length (μm)				
481.060	30.330	4.000	108.540	451.130	35.210	4.000	152.370
532.670	42.390	5.000	162.810	324.490	35.570	2.000	166.980
282.180	39.260	2.000	156.550	230.770	35.360	1.000	219.170
301.960	37.230	3.000	148.200	112.710	104.370	183.680	66.790
264.040	36.530	3.000	125.240	98.100	123.150	154.460	79.320
239.700	38.950	2.000	110.630	114.800	156.550	100.190	120.000
176.480	49.990	2.000	75.140	81.410	154.460	93.930	102.000
138.110	62.270	2.000	93.930	158.640	100.190	125.240	129.410
191.570	42.210	1.000	152.370	204.560	100.190	73.060	100.000
630.150	36.740	5.000	93.930	73.060	89.750	100.000	231.690
257.980	42.590	2.000	121.060	112.710	79.320	75.140	89.750
259.830	41.790	2.000	127.330	144.020	110.630	127.330	160.000
635.610	38.590	6.000	131.500	106.450	102.280	154.460	110.630
			56.360	48.010	148.200	100.190	200.000
			89.750	344.410	112.710	114.800	116.890
			116.890	164.900	64.710	85.580	108.540
			62.620	106.450	125.240	179.510	83.490
			66.790	118.980	116.890	133.590	133.590
			83.490	108.540	96.020	77.230	125.000
			75.140	108.540	66.790	75.140	83.490
			116.980	141.940	93.930	105.000	85.580
			160.000	141.940	141.940	106.450	129.410
			200.000	123.150	125.240	106.450	56.360
			129.410	114.800	98.100	89.750	112.710
			114.800	137.760	116.890	93.930	135.680
			231.690	96.020	175.330	116.890	93.930
			89.750	200.380	85.580	139.850	118.980
			56.360	173.250	110.630	70.970	89.750
			43.830	141.940	181.600	100.190	137.760
			52.180	118.980	135.680	50.100	100.190
			66.790	152.370	127.330	148.200	100.190
			79.320	148.200	106.450	73.060	135.680
			102.280	118.980	52.180	91.840	202.470
			87.670	89.750	83.490	81.410	187.000
			81.410	121.060	104.370	190.000	116.890
			102.280	102.280	104.370	118.980	108.540
			43.830	100.000	131.500	56.360	139.850
			162.810	114.800	81.410	123.150	183.680
			118.980	166.980	102.280	83.490	
			70.970	64.710	148.200	100.000	
			83.490	152.370	104.370	93.930	
			96.020	129.410	75.140	87.670	
			89.750	148.200	98.100	140.000	
			102.280	129.410	112.710	139.850	
			116.890	114.800	85.580	135.680	
			70.970	90.000	79.320	137.760	
			70.970	89.750	96.020	118.980	
			87.670	93.930	85.580	83.490	
			73.060	146.110	70.970	125.240	
			70.970	141.940	116.890	196.000	
			96.020	114.800	81.410	123.150	
			123.150	89.750	135.680	110.630	
			100.190	87.670	154.460	66.790	
			89.750	156.550	183.680	77.230	

Morphological Data DAY 7

Chain Length (μm)	Chain Width (μm)	No. of cells per chain	Cell Length (μm)	Chain Length (μm)	Chain Width (μm)	No. of cells per chain	Cell Length (μm)
264.480	42.350	2.000	135.680	334.230	48.790	4.000	83.490
176.590	46.750	2.000	85.580	343.240	39.780	4.000	81.410
512.930	30.820	4.000	139.850	678.470	14.520	6.000	104.370
433.610	33.950	3.000	196.210	293.320	45.870	2.000	154.460
370.560	46.900	4.000	106.450	331.920	38.580	4.000	91.840
252.940	33.020	2.000	112.710	338.390	41.500	3.000	87.670
528.170	38.540	3.000	198.290	388.060	33.580	2.000	181.600
203.810	35.190	2.000	89.750	317.270	57.400	4.000	96.020
492.620	39.640	4.000	108.540	294.920	54.700	4.000	81.410
352.290	42.210	2.000	158.640	377.510	32.650	4.000	77.230
289.680	42.200	2.000	137.760	353.690	52.290	4.000	83.490
230.090	42.300	2.000	89.750	363.900	43.130	4.000	62.620
234.830	39.650	1.000	210.820	508.160	23.060	3.000	98.100
626.970	34.700	6.000	123.150	182.480	56.510	2.000	89.750
544.600	30.460	6.000	110.630	644.200	37.310	6.000	77.230
312.150	37.480	4.000	73.060	171.590	38.190	2.000	98.100
236.950	30.230	2.000	114.800	653.250	28.250	5.000	87.670
462.790	28.770	3.000	96.020	578.400	32.130	5.000	156.550
246.510	32.150	2.000	139.850	291.790	51.570	2.000	154.460
196.830	43.210	2.000	77.230	511.120	35.760	6.000	79.320
546.630	32.600	3.000	131.500	241.360	43.560	5.000	110.630
431.230	32.150	4.000	89.750	214.660	38.950	2.000	108.540
274.820	40.360	2.000	141.940	151.630	43.530	2.000	83.490
312.720	26.470	3.000	144.020	428.470	38.040	4.000	96.020
285.240	41.420	3.000	66.790	269.880	49.480	3.000	60.530
261.350	43.390	1.000	247.000	503.370	42.460	6.000	96.020
301.120	40.150	2.000	162.810	336.060	36.520	2.000	183.680
220.100	43.940	2.000	96.020	789.540	22.430	6.000	137.760
240.430	49.710	2.000	121.060	440.520	33.300	5.000	77.230
197.130	39.780	1.000	87.670	409.800	32.710	2.000	164.900
547.960	34.400	4.000	154.460	444.840	40.460	4.000	106.450
314.820	43.150	3.000	75.140	233.230	42.290	2.000	123.150
266.360	53.000	3.000	148.200	540.410	39.860	7.000	139.850
238.470	52.710	4.000	68.880	630.610	25.850	5.000	68.880
255.230	36.990	4.000	56.360	353.490	42.050	4.000	75.140
272.170	43.010	3.000	144.020	140.680	48.220	2.000	60.530
256.630	38.730	4.000	125.240	440.510	53.140	11.000	45.920
177.450	41.710	2.000	70.970	464.640	30.050	3.000	129.410
178.210	34.690	2.000	77.230	563.100	14.040	2.000	135.680
304.060	38.260	4.000	96.020	690.770	34.570	9.000	52.180
272.280	37.680	3.000	75.140	550.450	38.170	4.000	104.370
233.640	40.840	4.000	56.360	392.910	34.980	4.000	96.020
559.320	36.600	5.000	112.710	379.170	16.370	3.000	108.540
305.800	46.960	2.000	150.290	198.240	35.540	2.000	93.930
506.920	33.690	6.000	77.230	390.460	44.740	4.000	110.630
264.520	36.050	2.000	133.590	463.020	32.720	4.000	121.060
423.020	29.930	4.000	93.930	368.280	32.490	2.000	200.380
453.710	28.460	4.000	100.190	639.880	27.010	3.000	315.180
328.070	28.860	2.000	179.510	328.820	26.020	3.000	70.970
256.730	34.450	2.000	133.590	230.260	43.180	3.000	48.010
180.120	38.000	2.000	73.060	193.810	34.760	2.000	85.580
677.260	42.860	6.000	179.510	588.030	33.990	6.000	129.410
480.640	44.320	4.000	123.150	494.930	32.110	6.000	45.920

Chain Length (μm)	Chain Width (μm)	No. of cells per chain	Cell Length (μm)				
357.400	38.140	3.000	102.280	446.050	25.680	5.000	114.800
355.980	39.570	2.000	175.330	434.550	29.880	4.000	104.370
414.350	29.200	4.000	96.020	375.380	34.770	4.000	98.100
364.620	34.050	4.000	81.410	70.970	189.950	48.010	73.060
534.030	39.980	8.000	83.490	73.060	114.800	70.970	112.710
558.570	33.180	4.000	129.410	70.970	85.580	62.620	144.000
490.390	36.660	6.000	110.630	64.710	79.320	66.790	77.230
721.280	28.060	5.000	68.880	81.410	96.020	73.060	121.060
420.340	40.950	4.000	110.630	66.790	106.450	77.230	108.540
294.270	38.660	3.000	73.060	108.540	50.100	100.000	118.980
323.820	32.060	4.000	83.490	79.320	116.890	73.060	79.320
268.430	38.400	3.000	77.230	77.230	104.370	100.190	118.980
531.930	41.040	3.000	265.090	125.240	140.000	164.900	58.440
423.710	28.200	3.000	164.900	73.060	91.840	123.150	129.410
450.070	36.270	4.000	104.370	129.410	100.190	158.640	98.100
319.280	33.470	2.000	158.640	158.640	110.630	98.100	102.280
249.030	30.670	1.000	235.870	79.320	148.200	83.490	125.240
378.830	39.680	2.000	177.420	112.710	127.330	81.410	100.190
296.600	31.110	3.000	75.140	127.330	66.790	112.000	139.850
241.820	44.140	4.000	73.060	91.840	56.360	100.190	93.930
283.100	32.090	3.000	68.880	133.590	96.020	83.490	118.980
			54.200	114.800	81.410	177.420	73.060
			60.530	93.930	60.530	77.230	52.180
			64.700	68.880	35.480	81.410	127.330
			81.410	114.800	93.930	98.100	116.890
			89.750	93.930	89.750	96.020	106.450
			77.230	166.980	89.750	108.540	106.450
			41.700	106.450	60.530	91.840	66.790
			70.980	87.670	206.640	152.370	73.060
			85.580	77.230	106.450	135.680	45.920
			102.280	110.630	75.140	83.490	77.230
			70.790	131.500	87.670	62.620	87.670
			130.000	73.060	77.230	45.920	104.370
			93.930	70.970	79.320	93.930	93.930
			146.110	181.600	68.880	112.710	98.100
			81.410	75.140	139.850	64.710	104.370
			93.930	77.230	118.980	129.410	98.000
			127.330	96.020	118.980	58.440	81.410
			173.250	81.410	150.290	108.540	87.670
			93.930	87.670	181.600	89.750	79.320
			133.590	108.540	85.580	58.440	89.750
			173.250	106.450	64.710	50.100	102.280
			133.590	81.410	77.230	221.250	108.540
			129.410	68.880	110.630	106.450	60.530
			139.850	62.620	106.450	127.330	66.790
			81.410	121.060	87.670	93.930	116.890
			70.970	141.940	123.150	130.000	118.980
			108.540	70.970	123.150	96.020	148.200
			96.020	125.240	70.970	89.750	73.060
			102.280	89.750	112.710	148.200	64.710
			125.240	68.880	70.970	152.370	50.100
			187.860	100.190	148.200	135.680	136.000
			104.370	81.410	102.280	135.680	70.970
			129.410	131.500	58.440	79.320	73.060

(DAY 7) CELL LENGTH *continued*			
93 930	121 060	98 100	
70 970	108 540	58 440	
131 500	118 980	123 150	
75 140	79 320	129 410	
152 370	118 980	127 330	
102 280	58 440	129 410	
141 940	129 410	73 060	
50 100	98 100	112 710	
58 440	102 280	144 000	
89 750	125 240	77 230	
56 360	100 190	135 680	
148 200	139 850	79 320	
89 750	93 930	129 410	
127 330	118 980	81 410	
124 000	73 060	139 850	
133 590	52 180	91 840	
77 230	127 330	96 020	
148 200	116 890	136 000	
62 620	106 450	70 970	
110 630	106 450	73 060	
89 750	66 790	133 590	
145 000	73 060	116 890	
108 540	45 920	152 370	
52 180	77 230	64 710	
96 020	87 670	66 790	
33 400	104 370	66 790	
66 790	93 930	139 850	
62 620	98 100	91 840	
131 500	104 370	96 020	
108 540	98 000	121 060	
60 530	81 410	141 940	
56 360	87 670	114 800	
135 680	79 320	112 710	
87 670	73 060		
54 000	64 710		
81 410	50 100		
130 000	89 750		
118 980	102 280		
108 540	83 490		
70 970	112 710		
128 000	87 670		
35 480	87 670		
83 490	83 490		
85 580	73 060		
58 440	135 680		
106 450	79 320		
62 620	129 410		
77 230	81 410		
102 280	223 340		
108 540	110 630		
60 530	108 540		
66 790	106 450		
116 890	60 530		
118 980	85 580		
148 200	100 190		

Morphological Data DAY 10

Chain Length (μm)	Chain Width (μm)	No. of cells per chain	Cell Length (μm)	Chain Length (μm)	Chain Width (μm)	No. of cells per chain	Cell Length (μm)
413.790	42.280	7.000	75.140	632.050	39.020	7.000	81.410
1100.070	36.470	7.000	123.150	268.500	43.550	3.000	70.970
277.100	54.780	4.000	70.970	349.010	24.620	2.000	114.800
249.330	46.030	2.000	123.150	569.230	34.000	8.000	89.750
224.580	46.770	2.000	96.020	517.590	21.980	5.000	64.710
348.810	43.600	5.000	60.530	139.260	21.460	1.000	93.930
117.280	39.270	1.000	93.930	571.450	34.910	4.000	131.500
540.030	37.110	6.000	112.710	332.120	33.160	4.000	85.580
626.450	34.180	7.000	104.370	329.010	34.180	3.000	150.290
408.330	45.660	4.000	79.320	342.890	31.780	5.000	70.970
343.790	51.760	7.000	58.440	429.940	37.620	4.000	104.370
312.950	49.200	4.000	98.100	343.510	42.640	6.000	79.320
356.440	39.100	4.000	85.580	254.710	35.420	4.000	60.530
474.750	41.860	5.000	160.720	220.000	37.790	3.000	56.360
427.870	34.470	4.000	91.840	504.490	41.340	7.000	43.830
733.530	33.550	5.000	110.630	319.540	46.780	4.000	70.970
458.140	43.860	4.000	121.060	206.590	50.150	2.000	133.590
526.720	38.940	4.000	96.020	573.720	35.780	6.000	81.410
549.280	25.770	4.000	116.890	508.840	19.250	3.000	100.190
496.220	26.650	5.000	129.410	301.750	47.880	3.000	66.790
384.300	37.330	3.000	77.230	653.470	77.090	1.000	649.150
734.860	41.620	8.000	83.490	320.460	30.210	4.000	60.530
322.700	43.620	4.000	66.790	578.280	32.250	6.000	62.620
255.680	41.770	4.000	77.230	322.800	35.170	3.000	91.840
178.570	31.210	3.000	85.580	242.840	45.210	3.000	98.100
299.000	42.270	6.000	75.140	838.130	35.410	6.000	91.840
667.140	46.720	8.000	50.100	356.170	40.420	4.000	81.410
679.350	33.460	8.000	77.230	499.260	44.490	3.000	114.800
407.190	26.970	4.000	93.930	310.000	38.580	4.000	89.750
543.470	40.970	3.000	139.850	299.610	37.490	2.000	64.710
429.920	39.730	4.000	116.890	552.390	37.280	4.000	131.500
399.060	47.620	7.000	54.270	649.710	32.840	7.000	68.880
296.360	45.960	4.000	62.620	469.380	37.830	3.000	177.420
401.950	36.390	3.000	217.080	422.780	27.030	2.000	100.190
486.320	39.680	5.000	58.440	610.460	33.470	4.000	162.810
541.680	36.500	5.000	133.590	426.960	42.680	8.000	50.100
390.330	41.750	2.000	189.950				79.320
324.460	47.080	4.000	68.880				133.590
269.150	31.420	2.000	114.800				75.140
472.180	26.680	4.000	108.540				114.800
467.810	24.790	4.000	89.750				125.240
436.530	23.720	4.000	73.060				43.830
303.290	41.110	4.000	85.580				137.760
390.660	40.370	4.000	93.930				64.710
276.430	45.010	3.000	60.530				70.970
292.480	38.360	4.000	62.620				66.790
257.270	38.090	4.000	56.360				75.140
543.190	36.040	8.000	66.790				50.100
344.200	40.910	6.000	43.830				137.760
539.200	45.250	7.000	98.100				104.370
380.760	44.010	6.000	54.270				144.020
490.290	34.670	6.000	83.490				93.930
372.480	34.540	4.000	81.410				127.330

(DAY 10) CELL LENGTH *continued*							
446.000	29.900	6.000	50.100	135.680	91.840	133.590	116.890
327.890	47.820	3.000	118.980	48.010	110.630	81.410	75.140
408.770	30.610	4.000	77.230	41.750	121.060	100.190	83.490
311.180	48.880	3.000	68.880	50.100	96.020	66.790	93.930
274.220	28.440	2.000	116.890	70.970	116.890	649.150	77.230
123.150	129.410	110.630	43.830	93.930	129.410	60.530	112.710
81.410	83.490	106.450	39.660	75.140	77.230	62.620	85.580
93.930	104.370	70.970	75.140	70.970	83.490	91.840	43.830
114.800	83.490	64.710	83.490	52.180	66.790	98.100	79.320
106.450	75.140	81.410	98.100	100.190	77.230	91.840	64.710
133.590	85.580	98.100	102.280	66.790	85.580	81.410	73.060
204.560	62.620	68.880	118.980	81.410	75.140	114.800	75.140
150.290	89.750	70.970	73.060	77.230	50.100	89.750	58.440
43.830	85.580	79.320	83.490	104.370	77.230	64.710	52.180
64.710	104.370	66.790	91.840	45.920	93.930	131.500	66.790
254.650	41.750	83.490	104.370	112.710	139.850	68.880	66.790
77.230	60.530	85.580	64.710	85.580	116.890	177.420	81.410
64.710	64.710	98.100	177.420	43.830	54.270	100.190	60.530
68.880	41.750	89.750	79.320	79.320	62.620	162.810	89.750
77.230	87.670	60.530	100.190	64.710	217.080	50.100	133.590
118.980	104.370	104.370	75.140	73.060	58.440	79.320	77.230
54.270	87.670	89.750	106.450	75.140	133.590	133.590	181.600
77.230	83.490	66.790	48.010	58.440	189.950	75.140	64.710
50.100	79.320	68.880	73.060	52.180	68.880	114.800	50.100
60.530	127.330	210.820	104.370	66.790	114.800	125.240	89.750
112.710	64.710	81.410	89.750	66.790	108.540	43.830	54.270
85.580	62.620	37.570	89.750	81.410	89.750	137.760	110.630
121.060	256.740	102.280	54.270	60.530	73.060	64.710	60.530
131.500	83.490	64.710	64.710	89.750	85.580	70.970	85.580
144.020	221.250	62.620	58.440	73.060	93.930	66.790	62.620
66.790	60.530	66.790	89.750	181.600	60.530	75.140	106.450
212.910	169.070	66.790	52.180	133.590	62.620	50.100	160.720
79.320	83.490	121.060	77.230	110.630	56.360	137.760	100.190
89.750	104.370	87.670	93.930	60.530	66.790	104.370	129.410
56.360	125.240	154.460	98.100	85.580	43.830	144.020	85.580
45.920	41.750	64.710	123.150	62.620	98.100	93.930	133.590
64.710	41.750	108.540	116.890	31.310	54.270	127.330	204.560
52.180	135.680	75.140	116.890	98.100	83.490	116.890	150.290
70.970	77.230	89.750	137.760	127.330	81.410	75.140	43.830
108.540	77.230	106.450	87.670	68.880	50.100	83.490	64.710
269.260	77.230	62.620	100.190	70.970	118.980	93.930	254.650
100.190	96.020	64.710	68.880	171.160	77.230	77.230	77.230
79.320	118.980	139.850	77.230	96.020	68.880	77.230	64.710
93.930	75.140	131.500	39.660	85.580	116.890	43.830	68.880
81.410	85.580	54.270	89.750	89.750	81.410	39.660	77.230
79.320	169.070	70.970	79.320	64.710	70.970	75.140	118.980
60.530	66.790	87.670	75.140	75.140	114.800	83.490	54.270
85.580	106.450	58.440	52.180	123.150	89.750	98.100	58.440
144.020	192.030	91.840	100.190	70.970	64.710	102.280	89.750
133.590	110.630	137.760	56.360	123.150	93.930	118.980	52.180
60.530	156.550	85.580	64.710	96.020	131.500	73.060	77.230
77.230	110.630	62.620	87.670	60.530	85.580	83.490	93.930
108.540	108.540	77.230	112.710	93.930	150.290	91.840	98.100
102.280	87.670	68.880	91.840	112.710	70.970	104.370	123.150
64.710	87.670	77.230	75.140	104.370	104.370	64.710	116.890
68.880	54.270	108.540	98.100	79.320	79.320	177.420	116.890

(DAY 10) CELL LENGTH *continued*				
79.320	62.620	112.710	81.410	58.440
54.270	100.190	50.100	158.640	98.100
48.010	85.580	73.060	81.410	85.580
66.790	85.580	89.750	62.620	85.580
79.320	83.490	70.970	83.490	62.620
87.670	73.060	79.320	85.580	89.750
96.020	60.530	45.920	89.750	85.580
70.970	141.940	87.670	79.320	104.370
77.230	83.490	66.790	48.010	41.750
50.100	79.320	68.880	73.060	60.530
60.530	127.330	210.820	104.370	64.710
112.710	64.710	81.410	89.750	41.750
85.580	62.620	37.570	89.750	87.670
121.060	256.740	102.280	54.270	104.370
131.500	83.490	64.710	64.710	137.760
144.020	221.250	62.620	75.140	87.670
66.790	60.530	66.790	52.180	100.190
212.910	77.230	66.790	100.190	68.880
79.320	169.070	121.060	56.360	77.230
89.750	83.490	87.670	64.710	39.660
56.360	104.370	154.460	87.670	60.530
45.920	125.240	64.710	112.710	56.360
64.710	41.750	108.540	91.840	43.830
52.180	41.750	75.140	75.140	98.100
70.970	135.680	89.750	98.100	68.880
108.540	77.230	106.450	81.410	70.970
269.260	77.230	144.020	158.640	79.320
100.190	96.020	62.620	81.410	66.790
79.320	118.980	64.710	62.620	83.490
93.930	75.140	139.850	83.490	85.580
81.410	85.580	131.500	85.580	98.100
79.320	169.070	54.270	89.750	89.750
60.530	66.790	70.970	79.320	60.530
85.580	106.450	87.670	123.150	104.370
144.020	192.030	58.440	81.410	
133.590	110.630	91.840	93.930	
60.530	156.550	137.760	114.800	
77.230	110.630	85.580	106.450	
108.540	108.540	62.620	89.750	
102.280	87.670	77.230	87.670	
64.710	87.670	68.880	79.320	
68.880	54.270	77.230	100.190	
79.320	62.620	108.540	75.140	
54.270	100.190	112.710	50.100	
48.010	85.580	50.100	70.970	
66.790	85.580	73.060	93.930	
79.320	83.490	89.750	75.140	
87.670	73.060	70.970	70.970	
96.020	60.530	79.320	52.180	
70.970	141.940	100.190	100.190	
85.580	129.410	70.970	81.410	
129.410	110.630	87.670	66.790	
83.490	106.450	45.920	77.230	
104.370	70.970	135.680	104.370	
83.490	64.710	48.010	89.750	
75.140	81.410	41.750		

Morphological Data DAY 12

Chain Length (μm)	Chain Width (μm)	No of cells per chain	Cell Length (μm)	Chain Length (μm)	Chain Width (μm)	No of cells per chain	Cell Length (μm)
439 500	45 800	7 000	58 440	454 680	30 620	4 000	79 320
572 510	30 720	7 000	66 790	358 180	42 590	3 000	89 750
396 350	44 070	4 000	164 900	477 330	43 460	7 000	75 140
400 850	42 700	4 000	85 580	271 370	50 080	3 000	125 240
372 260	48 340	3 000	181 600	264 800	52 470	3 000	77 230
461 120	38 800	5 000	116 890	238 060	34 330	3 000	68 880
664 740	31 370	8 000	96 020	345 310	37 710	6 000	58 440
277 130	45 360	4 000	45 920	288 490	31 910	4 000	66 790
162 060	41 460	2 000	70 970	225 120	44 150	4 000	62 620
289 540	40 250	1 000	277 610	205 190	33 800	2 000	91 840
374 000	31 980	2 000	166 980	185 210	32 910	3 000	48 010
409 620	38 110	4 000	100 190	137 050	46 640	2 000	62 620
634 140	32 760	8 000	70 970	362 740	45 330	3 000	89 750
506 210	47 970	4 000	123 150	378 060	34 180	3 000	179 510
255 940	31 070	2 000	108 540	262 410	41 290	5 000	39 660
786 530	53 620	4 000	233 780	242 540	42 380	4 000	50 100
369 000	34 890	4 000	87 670	207 800	44 760	3 000	81 410
516 160	46 370	7 000	68 880	514 530	38 600	6 000	66 790
333 680	33 690	6 000	33 400	291 690	47 500	3 000	91 840
348 890	34 130	2 000	187 860	258 870	44 840	2 000	108 540
541 270	43 180	7 000	85 580	783 760	44 900	10 000	123 150
331 950	48 980	6 000	75 140	372 320	46 190	4 000	104 370
486 260	48 090	6 000	58 440	394 650	32 200	4 000	85 580
290 220	39 570	4 000	56 360	453 110	29 060	4 000	116 890
228 860	41 440	3 000	50 100	365 260	49 070	4 000	79 320
313 100	37 570	5 000	89 750	283 470	49 460	3 000	66 790
272 400	38 610	4 000	50 100	204 610	41 690	4 000	54 270
311 490	37 090	3 000	77 230	405 850	51 270	5 000	60 530
421 890	28 970	2 000	177 420	626 380	31 130	4 000	123 150
332 460	37 000	4 000	79 320	464 310	42 910	4 000	98 100
337 270	35 320	4 000	85 580	439 460	34 360	4 000	102 280
632 330	36 660	8 000	77 230	262 640	30 620	1 000	225 430
260 140	39 390	2 000	118 980	480 300	31 090	4 000	116 890
234 510	36 840	3 000	70 970	131 560	56 300	2 000	56 360
652 280	32 360	4 000	127 330	390 820	40 210	4 000	100 190
487 630	39 420	7 000	60 530	309 740	44 050	5 000	85 580
449 530	35 770	7 000	58 440	860 640	34 810	8 000	91 840
332 050	34 270	3 000	152 370	321 130	46 240	3 000	156 550
310 860	43 980	1 000	288 050	271 430	43 760	2 000	123 150
306 630	34 640	4 000	66 790	198 020	47 240	3 000	87 670
572 320	39 260	6 000	73 060	146 900	52 440	2 000	73 060
452 810	35 620	6 000	68 880	377 050	51 890	4 000	91 840
451 700	30 470	6 000	62 620	314 980	39 860	2 000	152 370
182 510	38 740	4 000	102 280	796 800	33 950	7 000	108 540
593 850	33 390	8 000	58 440	527 420	47 630	9 000	52 180
516 920	35 170	5 000	137 760	348 830	35 230	4 000	89 750
246 420	32 230	4 000	64 710	356 340	35 030	4 000	112 710
397 670	44 840	4 000	112 710	707 370	33 620	7 000	104 370
497 680	34 580	5 000	100 190	342 130	36 710	4 000	62 620
345 070	27 510	3 000	154 460	300 830	32 090	3 000	64 710
149 300	39 600	2 000	66 790				56 360
151 780	39 210	2 000	68 880				83 490

(DAY 12) CELL LENGTH *continued*					
56.360	60.530	112.710	75.140	73.060	64.710
102.280	127.330	77.230	116.890	102.280	91.840
50.100	79.320	60.530	125.240	87.670	43.830
70.970	121.060	98.100	79.320	96.020	156.550
98.100	60.530	112.710	96.020	52.180	81.410
93.930	79.320	83.490	83.490	75.140	52.180
43.830	70.970	77.230	81.410	171.160	79.320
66.790	91.840	66.790	173.250	156.550	68.880
75.140	70.970	110.630	106.450	98.100	83.490
100.190	102.280	87.670	64.710	135.680	81.410
75.140	79.320	135.680	133.590	91.840	91.840
146.110	166.980	68.880	135.680	62.620	100.190
54.270	68.880	66.790	144.020	135.680	70.970
85.580	66.790	102.280	89.750	87.670	75.140
96.020	77.230	100.190	89.750	96.020	70.970
87.670	79.320	98.100	50.100	54.270	100.190
112.710	64.710	75.140	135.680	79.320	43.830
85.580	83.490	79.320	68.880	56.360	54.270
62.620	125.240	106.450	85.580	81.410	77.230
66.790	104.370	79.320	64.710	102.280	64.710
141.940	62.620	116.890	81.410	62.620	68.880
79.320	118.980	212.910	60.530	60.530	62.620
123.150	35.480	85.580	70.970	77.230	81.410
91.840	58.440	70.970	66.790	75.140	83.490
93.930	141.940	52.180	154.460	87.670	70.970
85.580	100.190	79.320	225.430	48.010	102.280
81.410	148.200	48.010	73.060	68.880	87.670
87.670	175.330	73.060	75.140	81.410	91.840
89.750	73.060	81.410	77.230	64.710	87.670
146.110	60.530	39.660	131.500	110.630	48.010
58.440	96.020	70.970	79.320	77.230	152.370
91.840	102.280	75.140	129.410	64.710	85.580
102.280	64.710	93.930	75.140	93.930	81.410
156.550	79.320	85.580	54.270	148.200	79.320
127.330	66.790	169.070	85.580	62.620	75.140
64.710	85.580	64.710	68.880	41.750	89.750
89.750	183.680	56.360	73.060	70.970	81.410
110.630	93.930	83.490	79.320	60.530	66.790
91.840	56.360	50.100	60.530	64.710	52.180
79.320	81.410	64.710	75.140	56.360	56.360
87.670	60.530	85.580	54.270	45.920	70.970
70.970	87.670	83.490	121.060	125.240	
98.100	127.330	89.750	64.710	52.180	
43.830	70.970	68.880	121.060	162.810	
98.100	114.800	81.410	110.630	56.360	
79.320	91.840	106.450	64.710	131.500	
70.970	108.540	70.970	79.320	171.160	
77.230	77.230	112.710	77.230	66.790	
81.410	135.680	70.970	100.190	70.970	
89.750	45.920	41.750	87.670	56.360	
68.880	75.140	77.230	56.360	141.940	
133.590	146.110	60.530	83.490	93.930	
166.980	110.630	66.790	100.190	85.580	
102.280	93.930	60.530	56.360	135.680	
75.140	108.540	68.880	60.530	81.410	
50.100	108.540	62.620	58.440	96.020	

Morphological Data DAY 14

Chain Length (μm)	Chain Width (μm)	No. of cells per chain	Cell Length (μm)	Chain Length (μm)	Chain Width (μm)	No. of cells per chain	Cell Length (μm)
292.390	37.400	5.000	64.710	340.510	32.080	3.000	158.640
143.470	30.820	1.000	131.500	221.700	34.000	2.000	91.840
111.480	31.500	1.000	104.370	136.440	35.760	2.000	43.830
425.260	43.340	3.000	202.470	125.940	37.920	2.000	66.790
370.320	26.270	6.000	75.140	781.730	32.320	7.000	66.790
300.620	37.520	3.000	131.500	418.480	36.550	4.000	166.980
228.060	40.160	2.000	96.020	254.710	44.810	5.000	60.530
162.810	33.400	1.000	127.330	284.600	43.110	4.000	58.440
783.690	30.360	5.000	135.680	238.980	38.630	4.000	60.530
323.700	37.400	4.000	83.490	474.140	27.860	4.000	104.370
181.470	39.780	2.000	100.190	245.650	52.840	4.000	89.750
135.410	37.840	2.000	58.440	284.270	42.390	2.000	154.460
560.830	35.100	9.000	58.440	387.590	40.310	6.000	93.930
358.320	41.400	6.000	81.410	365.680	44.480	8.000	93.930
379.710	47.150	6.000	56.360	342.570	34.190	5.000	75.140
294.480	33.230	4.000	64.710	338.920	29.490	3.000	116.890
228.670	37.460	4.000	41.750	554.310	35.350	7.000	70.970
244.520	36.220	2.000	135.680	517.300	33.750	6.000	127.330
983.170	27.090	7.000	110.630	380.530	34.840	7.000	35.480
300.090	47.450	6.000	79.320	381.980	38.610	5.000	68.880
197.720	46.490	2.000	93.930	271.680	44.550	5.000	43.830
176.150	41.970	2.000	102.280	770.530	38.300	9.000	73.060
575.810	31.600	9.000	64.710	383.380	39.300	6.000	68.880
224.250	37.710	4.000	37.570	496.860	33.310	8.000	62.620
262.430	35.010	2.000	137.760	472.870	30.170	4.000	102.280
187.690	33.570	3.000	58.440	289.470	27.800	4.000	54.270
373.990	40.340	2.000	254.650	216.890	29.410	3.000	75.140
422.690	31.300	5.000	81.410	566.840	36.390	4.000	118.980
437.080	29.440	6.000	64.710	243.990	45.110	3.000	41.750
294.660	33.050	3.000	150.290	228.870	45.610	4.000	58.440
554.550	39.290	6.000	60.530	292.240	37.550	4.000	68.880
348.280	42.040	7.000	64.710	265.460	27.800	3.000	50.100
294.490	33.210	4.000	79.320	393.240	32.570	3.000	104.370
485.580	42.510	7.000	127.330	313.320	34.220	5.000	60.530
284.340	39.200	3.000	75.140	409.570	40.240	5.000	81.410
318.050	36.790	4.000	54.270	196.910	42.080	2.000	91.840
266.410	39.380	3.000	106.450	188.780	40.830	3.000	66.790
212.310	36.080	3.000	56.360	345.620	38.450	4.000	64.710
156.980	45.490	2.000	81.410	182.620	32.380	2.000	104.370
500.510	38.010	6.000	66.790	436.310	40.640	7.000	87.670
484.920	32.730	4.000	98.100	364.570	28.880	3.000	85.580
404.790	34.590	5.000	102.280	429.840	37.720	3.000	91.840
318.170	54.420	3.000	85.580	369.780	40.380	4.000	81.410
345.010	38.010	4.000	62.620	204.630	35.410	2.000	100.190
272.620	37.350	3.000	77.230	220.020	33.580	1.000	212.910
214.740	44.090	4.000	52.180	168.980	47.050	2.000	85.580
483.150	29.290	4.000	116.890	570.730	35.630	5.000	121.060
301.340	37.850	4.000	68.880	433.390	41.470	7.000	73.060
512.260	41.920	7.000	70.970	466.510	24.010	3.000	87.670
317.220	37.620	4.000	58.440	247.700	40.350	4.000	48.010
251.810	35.190	4.000	62.620	648.550	43.390	8.000	54.270
267.780	36.970	3.000	68.880	223.960	47.390	3.000	75.140
512.350	37.650	4.000	114.800	199.780	42.350	3.000	87.670

Chain Length (μm)	Chain Width (μm)	No. of cells per chain	Cell Length (μm)				
396.740	39.510	5.000	91.840	129.410	100.190	108.540	96.020
156.900	30.960	2.000	81.410	106.450	87.670	66.790	56.360
547.870	40.760	7.000	70.970	70.970	50.100	56.360	185.770
445.610	33.430	4.000	102.280	77.230	85.580	104.370	70.970
503.430	30.920	6.000	60.530	75.140	79.320	41.750	96.020
307.080	46.720	4.000	64.710	118.980	93.930	96.020	114.800
279.660	28.210	4.000	66.790	87.670	79.320	60.530	43.830
245.960	27.470	4.000	68.880	66.790	133.590	54.270	50.100
535.790	47.610	5.000	91.840	62.620	93.930	60.530	68.880
244.170	39.700	4.000	50.100	118.980	54.270	64.710	91.840
176.220	52.340	2.000	89.750	43.830	106.450	45.920	60.530
602.520	28.890	5.000	66.790	81.410	83.490	98.100	56.360
289.050	32.390	2.000	139.850	75.140	85.580	73.060	81.410
252.830	32.090	3.000	75.140	108.540	48.010	50.100	112.710
			66.790	60.530	79.320	118.980	102.280
			127.330	125.240	33.400	54.270	68.880
			35.480	79.320	60.530	68.880	89.750
			85.580	79.320	100.190	116.890	75.140
			127.330	56.360	64.710	96.020	48.010
			54.270	110.630	43.830	85.580	118.980
			73.060	62.620	85.580	93.930	45.920
			81.410	58.440	252.560	150.290	62.620
			73.060	50.100	64.710	135.680	102.280
			83.490	58.440	29.220	54.270	68.880
			108.540	58.440	43.830	62.620	39.660
			50.100	102.280	70.970	73.060	100.190
			98.100	60.530	100.190	98.100	77.230
			68.880	56.360	64.710	62.620	43.830
			106.450	89.750	85.580	154.460	85.580
			118.980	87.670	50.100	206.640	62.620
			64.710	68.880	29.220	81.410	133.590
			110.630	160.720	89.750	81.410	75.140
			73.060	108.540	106.450	64.710	96.020
			64.710	62.620	102.280	98.100	91.840
			66.790	75.140	70.970	89.750	70.970
			106.450	50.100	85.580	81.410	73.060
			31.310	104.370	70.970	116.890	70.970
			102.280	41.750	129.410	56.360	68.880
			89.750	93.930	39.660	121.060	96.020
			50.100	104.370	91.840	58.440	68.880
			73.060	54.270	104.370	75.140	54.270
			85.580	87.670	54.270	54.270	70.970
			50.100	64.710	81.410	56.360	70.970
			31.310	56.360	106.450	110.630	85.580
			56.360	106.450	81.410	73.060	60.530
			91.840	110.630	114.800	141.940	35.480
			110.630	93.930	81.410	208.730	83.490
			83.490	98.100	45.920	70.970	68.880
			70.970	89.750	125.240	75.140	56.360
			66.790	81.410	131.500	41.750	48.010
			43.830	89.750	64.710	50.100	68.880
			104.370	214.990	91.840	68.880	131.500
			91.840	77.230	87.670	77.230	77.230
			112.710	81.410	79.320	110.630	148.200

(DAY 14) CELL LENGTH *continued*							
60.530	37.570	54.270	98.100	43.830	56.360	48.010	70.970
54.270	137.760	75.140	135.680	66.790	58.440	70.970	81.410
150.290	58.440	118.980	62.620	121.060	85.580	77.230	102.280
93.930	254.650	41.750	112.710	89.750	29.220	81.410	158.640
102.280	81.410	58.440	70.970	87.670	89.750	81.410	64.710
75.140	64.710	68.880	79.320	68.880	106.450	64.710	85.580
79.320	150.290	50.100	85.580	160.720	102.280	98.100	62.620
135.680	60.530	104.370	73.060	108.540	70.970	89.750	89.750
64.710	64.710	60.530	75.140	62.620	85.580	81.410	54.270
81.410	79.320	81.410	64.710	75.140	70.970	116.890	64.710
93.930	127.330	91.840	66.790	50.100	129.410	56.360	98.100
131.500	75.140	66.790	106.450	104.370	39.660	121.060	54.270
131.500	54.270	64.710	31.310	41.750	91.840	58.440	148.200
54.270	106.450	104.370	102.280	93.930	104.370	75.140	73.060
114.800	56.360	87.670	89.750	104.370	54.270	54.270	227.520
85.580	81.410	85.580	50.100	54.270	81.410	56.360	39.660
85.580	66.790	91.840	73.060	87.670	106.450	110.630	41.750
50.100	98.100	81.410	85.580	64.710	81.410	73.060	131.500
66.790	102.280	100.190	50.100	56.360	114.800	54.270	118.980
114.800	85.580	212.910	31.310	106.450	81.410	141.940	43.830
56.360	62.620	85.580	56.360	110.630	45.920	79.320	75.140
114.800	77.230	121.060	91.840	93.930	125.240	43.830	131.500
146.110	52.180	73.060	110.630	98.100	131.500	208.730	96.020
137.760	116.890	87.670	83.490	89.750	64.710	70.970	127.330
87.670	68.880	48.010	70.970	81.410	91.840	75.140	135.680
85.580	70.970	54.270	66.790	89.750	87.670	41.750	83.490
54.270	58.440	75.140	43.830	214.990	79.320	50.100	100.190
52.180	62.620	87.670	104.370	77.230	56.360	68.880	58.440
118.980	68.880	102.280	91.840	81.410	58.440	77.230	58.440
52.180	114.800	60.530	112.710	43.830	85.580	110.630	81.410
102.280	91.840	64.710	98.100	66.790	50.100	48.010	56.360
41.750	81.410	66.790	135.680	121.060	108.540	98.100	64.710
125.240	70.970	68.880	62.620	60.530	66.790	89.750	41.750
75.140	158.640	91.840	112.710	100.190	56.360	70.970	135.680
89.750	91.840	50.100	70.970	87.670	104.370	77.230	110.630
64.710	43.830	89.750	79.320	50.100	41.750	75.140	79.320
50.100	66.790	66.790	85.580	85.580	96.020	48.010	93.930
83.490	66.790	139.850	73.060	79.320	60.530	118.980	102.280
73.060	166.980	75.140	75.140	93.930	54.270	45.920	64.710
43.830	60.530	66.790	129.410	79.320	60.530	62.620	93.930
79.320	58.440	127.330	106.450	133.590	64.710	102.280	114.800
116.890	60.530	35.480	70.970	93.930	45.920	68.880	56.360
81.410	104.370	85.580	77.230	54.270	98.100	39.660	114.800
98.100	89.750	127.330	75.140	85.580	73.060	100.190	146.110
81.410	154.460	54.270	118.980	48.010	50.100	77.230	137.760
96.020	93.930	73.060	87.670	79.320	118.980	43.830	87.670
185.770	93.930	81.410	66.790	106.450	54.270	85.580	85.580
114.800	75.140	73.060	62.620	83.490	68.880	62.620	54.270
70.970	116.890	83.490	118.980	33.400	116.890	133.590	52.180
56.360	70.970	108.540	43.830	60.530	96.020	75.140	118.980
96.020	127.330	50.100	81.410	100.190	85.580	96.020	52.180
43.830	35.480	98.100	75.140	64.710	93.930	91.840	70.970
50.100	68.880	68.880	108.540	43.830	150.290	70.970	58.440
56.360	43.830	106.450	60.530	85.580	135.680	73.060	102.280
81.410	73.060	118.980	125.240	252.560	54.270	70.970	41.750
85.580	68.880	64.710	79.320	64.710	62.620	68.880	125.240

(DAY 14) CELL LENGTH *continued*			
60 530	62 620		
35 480	96 020		
83 490	66 790		
68 880	70 970		
56 360	89 750		
48 010	64 710		
68 880	50 100		
131 500	83 490		
77 230	73 060		
148 200	116 890		
45 920	48 010		
56 360	81 410		
70 970	56 360		
81 410	79 320		
102 280	43 830		
104 370	110 630		
158 640	79 320		
64 710	56 360		
39 660	110 630		
89 750	62 620		
85 580	58 440		
62 620	50 100		
89 750	58 440		
54 270	58 440		
64 710	102 280		
98 100	60 530		
54 270	70 970		
148 200	100 190		
73 060	64 710		
227 520	85 580		
39 660	75 140		
41 750	62 620		
131 500	118 980		
118 980	58 440		
43 830	73 060		
60 530	98 100		
54 270	62 620		
150 290	154 460		
93 930	96 020		
102 280	68 880		
75 140	54 270		
79 320	70 970		
135 680			
50 100			
64 710			
81 410			
93 930			
131 500			
131 500			
54 270			
114 800			
85 580			
85 580			
50 100			
66 790			
60 530			

Morphological Data DAY 17

Chain Length (µm)	Chain Width (µm)	No of cells per chain	Cell Length (µm)	Chain Length (µm)	Chain Width (µm)	No of cells per chain	Cell Length (µm)
248 230	29 380	3 000	58 440	345 730	34 160	6 000	66 790
312 800	32 650	4 000	98 100	849 680	36 390	4 000	181 600
1009 570	26 780	8 000	87 670	398 160	34 960	6 000	50 100
435 400	32 160	4 000	139 850	501 430	24 570	3 000	93 930
442 460	23 010	3 000	75 140	368 350	35 540	4 000	104 370
329 660	35 620	4 000	68 880	616 030	33 130	6 000	83 490
426 720	41 880	5 000	139 850	383 630	41 130	4 000	75 140
412 520	40 430	5 000	93 930	317 570	37 280	4 000	81 410
548 860	26 200	5 000	89 750	304 190	39 170	4 000	79 320
373 600	26 120	3 000	106 450	263 020	35 470	3 000	81 410
523 000	35 350	8 000	45 920	571 390	36 010	7 000	81 410
591 720	38 650	9 000	64 710	504 780	37 920	4 000	81 410
605 240	37 650	8 000	70 970	300 380	47 150	7 000	60 530
412 470	38 390	7 000	54 270	446 810	38 490	1 000	421 640
471 920	35 290	6 000	108 540	402 540	35 790	4 000	73 060
429 200	28 960	5 000	83 490	244 960	51 440	2 000	112 710
351 000	35 150	4 000	91 840	486 860	40 190	8 000	70 970
690 830	33 470	8 000	75 140	391 680	46 650	5 000	56 360
292 510	49 810	4 000	83 490	506 240	36 470	4 000	116 890
387 360	31 140	4 000	75 140	676 060	39 890	8 000	85 580
748 130	45 050	7 000	93 930	390 390	35 420	4 000	98 100
840 740	25 490	6 000	125 240	327 280	34 860	4 000	83 490
391 390	31 290	4 000	77 230	235 510	47 320	2 000	123 150
338 400	34 180	4 000	87 670	384 980	32 480	2 000	200 380
251 690	31 140	2 000	133 590	214 620	50 470	4 000	60 530
236 470	31 740	3 000	83 490	268 030	32 540	4 000	75 140
345 870	41 330	4 000	108 540	661 280	34 830	8 000	83 490
437 180	47 080	5 000	98 100	345 470	40 680	4 000	152 370
212 070	56 150	3 000	114 800	386 980	35 700	6 000	70 970
189 090	42 600	2 000	102 280	295 670	50 820	3 000	102 280
206 410	30 500	2 000	83 490	255 330	35 850	4 000	48 010
397 180	36 980	6 000	60 530	462 760	36 110	7 000	48 010
308 970	51 090	4 000	104 370	390 180	40 850	5 000	64 710
597 640	33 780	4 000	123 150	372 850	50 880	4 000	68 880
197 440	37 380	4 000	54 270	407 160	41 620	4 000	91 840
627 540	43 530	10 000	52 180	433 540	31 930	4 000	110 630
301 460	29 380	4 000	56 360	442 880	43 460	6 000	75 140
302 780	52 060	2 000	152 370	467 170	37 960	4 000	81 410
284 440	45 350	2 000	144 020	346 630	55 180	4 000	114 800
618 740	38 760	7 000	66 790	225 150	38 900	3 000	70 970
236 280	35 070	4 000	58 440	638 500	37 790	9 000	50 100
201 350	34 510	3 000	75 140	365 160	33 520	4 000	91 840
586 770	38 380	12 000	50 100	740 720	37 850	8 000	62 620
489 450	37 590	6 000	60 530	507 990	32 630	3 000	137 760
397 160	39 090	6 000	73 060	387 370	41 570	6 000	89 750
244 510	32 060	3 000	100 190	297 310	42 920	4 000	60 530
293 910	31 710	4 000	64 710	691 840	34 540	5 000	156 550
223 940	34 880	3 000	98 100	466 930	54 890	6 000	89 750
240 060	31 290	4 000	33 400	461 090	34 650	7 000	66 790
645 480	41 250	5 000	148 200	756 340	11 790	1 000	89 750
413 690	24 640	3 000	96 020	483 880	23 340	3 000	114 800
295 130	35 710	4 000	68 880	306 110	39 340	5 000	62 620
297 150	34 730	4 000	73 060	694 090	38 550	13 000	62 620

Chain Length (μm)	Chain Width (μm)	No. of cells per chain	Cell Length (μm)				
294.520	32.150	2.000	64.710	89.750	64.710	79.320	93.930
169.570	80.910	2.000	118.980	141.940	85.580	85.580	114.800
111.970	89.460	2.000	77.230	135.680	91.840	68.880	89.750
426.430	29.650	3.000	204.560	68.880	75.140	81.410	121.060
630.960	30.720	6.000	77.230	62.620	114.800	68.880	125.240
520.890	46.860	6.000	73.060	66.790	68.880	70.970	56.360
477.600	30.660	3.000	108.540	68.880	79.320	181.600	58.440
653.590	46.700	9.000	79.320	68.880	162.810	35.480	96.020
529.030	37.680	8.000	48.010	85.580	68.880	54.270	70.970
382.900	43.960	4.000	112.710	77.230	54.270	79.320	66.790
336.980	34.560	4.000	81.410	85.580	87.670	139.850	91.840
566.430	30.540	2.000	254.650	77.230	87.670	50.100	73.060
316.290	42.730	4.000	83.490	85.580	58.440	50.100	50.100
435.410	25.890	2.000	110.630	171.160	79.320	68.880	85.580
656.980	39.140	8.000	70.970	118.980	83.490	89.750	50.100
381.190	43.580	5.000	81.410	60.530	79.320	58.440	93.930
314.150	48.000	5.000	77.230	70.970	221.250	45.920	114.800
350.850	33.220	4.000	68.880	70.970	62.620	62.620	91.840
915.430	23.860	8.000	73.060	100.190	75.140	43.830	37.570
494.950	41.490	8.000	50.100	89.750	89.750	56.360	98.100
860.820	35.680	8.000	108.540	83.490	70.970	85.580	83.490
479.030	34.450	5.000	64.710	196.210	281.790	81.410	89.750
418.300	35.690	5.000	50.100	52.180	66.790	87.670	50.100
374.210	39.070	3.000	160.720	85.580	89.750	83.490	64.710
			48.010	96.020	56.360	62.620	91.840
			33.400	73.060	48.010	250.480	116.890
			62.600	112.710	54.270	62.620	43.830
			70.970	77.230	100.190	106.450	139.850
			77.230	79.320	79.320	77.230	66.790
			116.890	68.880	54.270	137.760	104.370
			96.020	68.880	96.020	114.800	118.980
			79.320	81.410	60.530	75.140	60.530
			64.710	77.230	66.790	70.970	150.290
			54.270	87.670	91.840	89.750	100.190
			58.440	133.590	100.190	96.020	100.190
			73.060	45.920	62.620	68.880	104.370
			137.760	106.450	104.370	85.580	89.750
			50.100	123.150	85.580	62.620	129.410
			79.320	62.620	81.410	54.270	81.410
			77.230	85.580	87.670	127.330	50.100
			66.790	79.320	62.620	100.190	75.140
			75.140	118.980	75.140	85.580	54.270
			60.530	158.640	62.620	73.060	93.930
			87.670	62.620	102.280	56.360	102.280
			81.410	64.710	52.180	43.830	83.490
			56.360	68.880	52.180	50.100	81.410
			110.630	73.060	73.060	52.180	64.710
			123.150	79.320	70.970	56.360	79.320
			164.900	89.750	48.010	68.880	93.930
			110.630	66.790	54.270	75.140	116.890
			75.140	66.790	75.140	75.140	79.320
			100.190	93.930	77.230	73.060	81.410
			60.530	81.410	106.450	150.290	85.580
			77.230	135.680	100.190	125.240	114.800

(DAY 17) CELL LENGTH *continued*				
87 670	127 330	54 270	91 840	106 450
77 230	79 320	85 580	52 180	93 930
85 580	91 840	127 330	79 320	98 100
98 100	70 970	73 060	112 710	100 190
98 100	89 750	121 060	60 530	
58 440	73 060	100 190	70 970	
70 970	93 930	41 750	116 890	
114 800	104 370	77 230	56 360	
58 440	56 360	43 830	64 710	
70 970	64 710	60 530	62 620	
183 680	102 280	89 750	64 710	
93 930	60 530	64 710	62 620	
64 710	48 010	91 840	91 840	
98 100	100 190	96 020	66 790	
131 500	75 140	98 100	75 140	
121 060	100 190	96 020	114 800	
93 930	108 540	81 410	93 930	
89 750	83 490	131 500	70 970	
60 530	41 750	81 410	56 360	
70 970	73 060	87 670	108 540	
81 410	45 920	60 530	77 230	
98 100	77 230	79 320	64 710	
83 490	43 830	66 790	43 830	
125 240	104 370	43 830	144 020	
162 810	87 670	43 830	56 360	
85 580	81 410	41 750	79 320	
54 270	56 360	62 620	144 020	
68 880	45 920	35 480	77 230	
81 410	64 710	100 190	75 140	
50 100	81 410	52 180	79 320	
77 230	98 100	83 490	68 880	
45 920	135 680	60 530	81 410	
100 190	87 670	79 320	87 670	
83 490	160 720	83 490	125 240	
96 020	89 750	35 480	45 920	
77 230	58 440	62 620	75 140	
81 410	52 180	43 830	118 980	
45 920	39 660	58 440	118 980	
73 060	106 450	60 530	106 450	
56 360	62 620	50 100	77 230	
87 670	135 680	91 840	66 790	
77 230	81 410	62 620	75 140	
45 920	33 400	91 840	89 750	
108 540	139 850	73 060	66 790	
106 450	64 710	135 680	50 100	
48 010	85 580	93 930	50 100	
66 790	66 790	37 570	91 840	
85 580	50 100	52 180	70 970	
77 230	83 490	102 280	85 580	
68 880	114 800	60 530	93 930	
68 880	75 140	100 190	54 270	
114 800	87 670	108 540	87 670	
118 980	43 830	83 490	141 940	
50 100	39 660	60 530	102 280	
108 540	112 710	41 750	77 230	
91 840	96 020	66 790	137 760	

Raw data for Figure 4.12

DAY	Protein 1	Protein 2	Protein 3	Protein 4	Protein 5	Protein AV	Protein Dev	Protein Err
0	0.0105	0.0139	0.0084		0.0094	0.011	2.429e-3	1.214e-3
1	0.0092	0.0126			0.0106	0.011	1.724e-3	9.950e-4
2			0.01		0.0115	0.011	1.105e-3	7.810e-4
3	0.0142		0.0139	0.0152	0.0139	0.014	5.990e-4	3.000e-4
4		0.0173			0.0157	0.017	1.148e-3	8.120e-4
5	0.0173				0.0260	0.022	6.113e-3	4.323e-3
6		0.0396	0.0296	0.0443	0.0357	0.037	6.219e-3	3.109e-3
7	0.0310				0.0501	0.043	0.013	8.529e-3
8		0.0517	0.0551	0.0683	0.0753	0.063	0.011	5.529e-3
9				0.075	0.0774	0.076	1.720e-3	1.216e-3
10	0.0844	0.0702				0.080	0.010	5.765e-3
11			0.09	0.0814	0.0899	0.087	4.954e-3	2.860e-3
12	0.0984				0.0808	0.090	0.012	8.791e-3
13			0.094		0.0884	0.091	3.929e-3	2.778e-3
14	0.1024		0.0974	0.0864	0.0878	0.094	7.681e-3	3.841e-3
14	0.0990				0.0965	0.098	1.782e-3	1.260e-3
15	0.1031				0.0920	0.098	7.798e-3	5.514e-3
16	0.1				0.0907	0.095	6.557e-3	4.637e-3
17	0.0993		0.099			0.099	2.180e-4	1.260e-4
18				0.0992	0.0930	0.096	4.356e-3	3.080e-3
19	0.1047				0.095	0.100	6.870e-3	4.858e-3
	0.1042				0.0945	0.099	6.859e-3	4.850e-3
21	0.1065		0.1068		0.0975	0.099	5.306e-3	3.064e-3

Protein concentration (mg ml^{-1})

Raw data for Figure 4.13

DAY	ECP1	ECP2	ECP3	ECP4	ECP5	ECP AV	ECP Dev	ECP Err
0			0.14	0.3466		0.243	0.146	0.103
1		0.2475	0.26			0.254	0.083	0.062
2	0.405	0.3025	0.135			0.281	0.136	0.079
3			0.145	0.28	0.3766	0.267	0.116	0.067
4	0.4575		0.2175			0.338	0.170	0.120
5			0.3275		0.50	0.414	0.122	0.086
6		0.695	0.8028	0.626	0.7233	0.712	0.073	0.037
7	1.28		1.1333			1.207	0.104	0.073
8		1.40	1.45	1.224		1.358	0.119	0.069
9	1.4633		1.62			1.542	0.111	0.078
10	1.50		1.64			1.570	0.099	0.070
11	1.75		1.6833	1.70	1.50	1.658	0.109	0.055
12	1.80		1.67			1.735	0.092	0.065
13		1.65		1.72		1.685	0.049	0.035
14		1.7525	1.648	1.77	1.628	1.700	0.072	0.036
15			1.66	1.79	1.68	1.710	0.070	0.040
16	1.65		1.588	1.85		1.696	0.137	0.079
17			1.648	1.81		1.729	0.115	0.081
18	1.545	1.8966			1.78	1.741	0.179	0.103
19	1.733		1.592			1.700	0.100	0.071
20	1.65	1.85			1.74	1.747	0.100	0.058
21			1.656	1.78		1.718	0.088	0.062

ECP = extracellular polysaccharide concentration (g l^{-1})

Raw data for Figure 4 14

RPM	SR	SS Day 0	SS Day 3	SS Day 5	SS Day 7	SS Day 10	SS Day 12	SS Day 16	SS Day 20
60 00	450 00	0 531	0 553	0 612	0 842	1 971	1 449	1 526	1 494
30 00	225 00	0 261	0 281	0 306	0 434	1 055	0 736	0 817	0 785
12 00	90 00					0 473	0 318	0 352	0 349
6 00	45 00					0 245			
100 00	750 00	0 848	0 930	1 035	1 328			2 565	
50 00	375 00	0 420	0 473	0 514	0 705	1 665	1 245		1 271
20 00	150 00				0 281	0 750	0 540	0 566	0 540
10 00	75 00					0 391			0 292

SS= shear stress (N m ^{2}), SR = shear rate (s ^{1}) *Note apparent viscosity = SS/SR*

Raw data for Figure 4 15

DAY	VIS1	VIS2	VIS3	VIS4	VIS5	VIS AV	VIS Dev	VIS Err
0	1 106	1 213	1 1407	1 085	1 1204	1 133	0 049	0 028
1	1 115		1 189	1 256	1 10758	1 167	0 070	0 040
2	1 136			1 1907	1 1685	1 165	0 028	0 016
3	1 173	1 25	1 214			1 212	0 039	0 022
4	1 268			1 3841	1 2533	1 302	0 072	0 041
5	1 589		1 3732		1 41876	1 460	0 114	0 066
6	1 938	1 8285		2 1838	1 8029	1 938	0 174	0 100
7	2 783		1 817	3 9042		2 835	1 045	0 480
8	3 704	3 552		5 2671	4 023	4 137	0 779	0 450
9	3 749			5 3456	5 5	4 600	0 969	0 560
10		3 65	4 4567			4 053	0 570	0 329
11	2 736	3 857		5 7384		4 110	1 517	0 876
12	3 537		3 285		5 4	4 074	1 155	0 667
13	2 433			5	5 25	4 228	1 559	0 900
14	2 114		2 4635		5 5	3 600	1 862	0 800
15	3 6	3 6	2 5		5 02	3 680	1 033	0 596
16	2 538	3 4		4 5	5 2	3 700	1 177	0 679
17	2 503	3 498	2 434		4 9	3 500	1 152	0 665
18	2 6	3 6	3	4 6623	5 0053	3 774	1 038	0 600
19	2 6		3 5021	4 2	4 8	3 776	0 946	0 546
20	2 4		3 43		4 9	3 577	1 256	0 725
21	2 6		3 395	5	4 4	3 849	1 064	0 614

VIS= Newtonian viscosity (mN s m ^{2})

Raw data for Figure 4.16

Instantaneous surface tension data

Day	Inst ST 1	Inst ST 2	Inst ST 3	Inst ST 4	Inst ST 5	Inst ST 6	Inst ST AV	Inst ST Dev	Inst ST Err
0			0.07075		0.07		0.070375	0.00053	0.00037
1	0.0685				0.0695		0.069	0.000707	0.0005
2		0.0675			0.067		0.06725	0.000354	0.00025
3		0.066	0.0675		0.0645		0.0660	0.00109	0.00063
4		0.065			0.0605		0.06275	0.003182	0.00225
5	0.063	0.0645					0.06375	0.001061	0.00075
6	0.065	0.0635	0.0675	0.0665	0.061		0.0647	0.002564	0.00115
7		0.062			0.061		0.0615	0.000707	0.0005
8	0.057	0.058	0.066	0.065	0.0615		0.0615	0.004031	0.00180
9									
10	0.06				0.062		0.061	0.001414	0.001
11		0.057	0.061	0.0605			0.0595	0.002179	0.00126
12	0.062	0.059			0.05675		0.05925	0.002634	0.00152
13		0.059		0.063			0.061	0.002828	0.002
14	0.056	0.0545	0.053	0.0645		0.055	0.0566	0.004547	0.00203
15		0.06				0.057	0.0585	0.002121	0.0015
16		0.0565			0.062		0.05925	0.003889	0.00275
17		0.057	0.056		0.063	0.05825	0.058563	0.003098	0.00155
18	0.054	0.062		0.0645			0.060167	0.005485	0.00317
19					0.062	0.0635	0.06275	0.001061	0.00075
20									
21			0.0545		0.0645	0.06775	0.06225	0.006906	0.003987

Equilibrium surface tension data

DAY	EQ ST1	EQ ST2	EQ ST3	EQ ST4	EQ ST AV	EQ ST Dev	EQ ST Err
0	0.0665		0.0645		0.066	1.414e-3	1.000e-3
1	0.064		0.062		0.063	1.414e-3	1.000e-3
2							
3	0.0605	0.061			0.061	3.540e-4	2.500e-4
4	0.057		0.055		0.056	1.414e-3	1.000e-3
5							
6	0.0555	0.0555	0.055		0.055	2.890e-4	1.670e-4
7							
8	0.056	0.05	0.0555		0.054	3.329e-3	1.922e-3
9							
10	0.054		0.0545		0.054	3.540e-4	2.500e-4
11	0.0535	0.055			0.054	1.061e-3	7.500e-4
12		0.05	0.0535		0.052	2.475e-3	1.750e-3
13							
14	0.053	0.0555	0.0537	0.053	0.054	1.180e-3	5.900e-4
15							
16							
17	0.054		0.055	0.0542	0.054	5.290e-4	3.060e-4
18		0.056		0.0555	0.056	3.540e-4	2.500e-4
19			0.056	0.0565	0.056	3.540e-4	2.500e-4
20							
21	0.0535		0.056		0.055	1.768e-3	1.250e-3

ST= surface tension (N m^{-1})

Raw data for Figure 4 19

Shear Rate	SS Medium	SS 0 5 ECP*	SS 1 0 ECP	SS 1 5 ECP	SS 2 0 ECP
45 000	0 048	0 097	0 186	0 278	0 441
75 000	0 076	0 156	0 276	0 425	0 625
90 000	0 094	0 179	0 322	0 482	0 724
150 000	0 156	0 294	0 457	0 741	1 069
225 000	0 234	0 387	0 673	0 967	1 433
375 000	0 390	0 656	1 035	1 537	2 152
450 000	0 472	0 756	1 188	1 755	
750 000	0 765	1 267	1 912		

*ECP standard solutions (g l^{-1})

Raw data for Figure 4 20

ECP	k	n
0 00	1 072	0 994
0 50	3 104	0 903
1 00	7 800	0 825
1 50	13 430	0 787
2 00	24 930	0 750

k = fluid consistency index (mN s^n m^{-2})
n = flow behaviour index (-)
(derived from data illustrated for Figure 4 19)

Raw data for Figure 4 21

Standard ECP	VIS @ 225 s^{-1}	DAY	Broth ECP AV	Broth VIS AV
0 000	1 040	0 000	0 243	1 133
0 500	1 720	1 000	0 254	1 167
1 000	2 990	2 000	0 281	1 165
1 500	4 300	3 000	0 267	1 212
2 000	6 370	4 000	0 338	1 302
		5 000	0 414	1 460
		6 000	0 712	1 938
		7 000	1 207	2 835
		8 000	1 358	4 137
		9 000	1 542	4 865
		10 000	1 570	4 902
		11 000	1 658	4 733
		12 000	1 735	4 736
		13 000	1 685	4 811
		14 000	1 700	3 683
		15 000	1 710	3 433
		16 000	1 696	3 910
		17 000	1 729	3 334
		18 000	1 741	3 774
		19 000	1 700	4 526
		20 000	1 747	3 577
		21 000	1 718	3 849

VIS @ 225 s^{-1} = apparent viscosity (mN s m^{-2}) at a shear rate of 225 s^{-1}

Raw data for Figure 4.22

DAY	Protein AV	Inst. ST AV	EQ ST AV
0	0.011	0.070	0.066
1	0.011	0.069	0.063
2	0.011	0.067	
3	0.014	0.066	0.061
4	0.017	0.063	0.056
5	0.022	0.064	
6	0.037	0.065	0.055
7	0.043	0.062	
8	0.063	0.062	0.054
9	0.076		
10	0.080	0.061	0.054
11	0.087	0.060	0.054
12	0.090	0.059	0.052
13	0.091	0.061	
14	0.094	0.057	0.054
15	0.098	0.059	
16	0.095	0.059	
17	0.099	0.060	0.054
18	0.096	0.062	0.056
19	0.100	0.062	0.056
20	0.099	0.062	
21	0.100		0.055

Raw data for Figure 4.23

Standard ECP Conc	EQ ST	DAY	Broth EQ ST	Broth ECP AV
0.000	0.070	0.000	0.066	0.243
0.500	0.068	1.000	0.063	0.254
1.000	0.066	2.000		0.281
1.500	0.064	3.000	0.061	0.267
2.000	0.062	4.000	0.056	0.338
		5.000		0.414
		6.000	0.055	0.712
		7.000		1.207
		8.000	0.054	1.358
		9.000		1.542
		10.000	0.054	1.570
		11.000	0.054	1.658
		12.000	0.052	1.735
		13.000		1.685
		14.000	0.054	1.700
		15.000		1.710
		16.000		1.696
		17.000	0.054	1.729
		18.000	0.056	1.741
		19.000	0.056	1.700
		20.000		1.747
		21.000	0.055	1.718

Raw data for Figure 4 24

0 2 mg ml^{-1} BSA-XAN-WATER		XAN-WATER		XAN-MEDIUM	
XAN	VIS @ 225 s^{-1}	XAN	VIS @ 225 s^{-1}	XAN	VIS @ 225 s^{-1}
0 000	1 040	0 000	1 020	0 000	1 070
0 010	1 770	0 010	1 970	0 010	
0 015	2 440	0 015	2 340	0 015	2 070
0 020	2 700	0 020	2 880	0 020	2 420
0 030	3 580	0 030	3 610	0 030	3 500
0 040	4 050	0 040	4 080	0 040	3 850

XAN = xanthan gum concentration (% w/v)

Raw data for Figure 4 25

BSA mg ml^{-1}	EQ ST
0 000	0 072
0 0025	0 072
0 005	0 067
0 0075	0 065
0 010	0 060
0 020	0 059
0 050	0 060
0 075	0 058
0 100	0 059

Raw data for Figure 4.26

Air Flow Rate 3.3 ml s^{-1}		Air Flow Rate 8.33ml s^{-1}		Air Flow Rate 16.67 ml s^{-1}	
Minutes	Foam height (cm)	Minutes	Foam height (cm)	Minutes	Foam height (cm)
0.000	2.600	0.000	3.800	0.000	1.000
0.500	6.500	0.250	7.200	0.250	1.400
0.750	9.000	0.500	10.400	0.750	2.500
1.250	11.600	1.000	16.500	1.000	3.100
1.500	12.100	1.500	21.000	1.500	6.000
2.000	12.500	1.750	23.000	2.000	11.000
3.000	14.100	2.000	25.100	2.500	16.000
4.000	15.100	2.500	28.100	3.000	17.000
4.500	15.100	2.750	29.700	3.660	22.000
5.000	15.600	3.000	31.200	4.000	25.100
6.000	16.100	3.500	32.700	4.500	31.100
7.000	16.100	4.000	35.200	5.000	31.200
7.500	16.400	4.500	37.700	5.500	34.300
8.000	16.600	5.000	38.200	6.000	40.300
9.000	17.100	5.500	38.700	6.500	42.400
10.500	16.600	6.000	39.800	7.000	42.900
11.000	16.850	7.000	41.300	7.500	44.000
13.000	17.100	8.000	42.300	8.000	44.500
15.000	17.600	9.000	42.800	8.500	45.500
16.000	17.600	10.000	43.300	9.500	52.700
17.000	17.600	11.000	43.800	10.000	53.700
18.000	17.600	12.000	44.300	11.000	55.300
19.500	17.850	13.000	44.800	12.000	56.800
21.000	17.850	14.000	45.300	13.000	57.800
25.500	18.600	16.000	45.300	14.000	58.800
26.000		18.000	46.300	15.000	59.900
27.000		20.000	46.800	16.000	61.900
28.500		22.000	46.800	17.000	63.000
29.500		24.000	47.300	18.000	64.000
30.000		26.000	47.300	19.000	65.000
31.000		28.000	47.300	21.000	68.000
32.000		30.000	47.800	22.000	69.000
33.000		32.000	47.800	23.000	69.000
34.000		34.000	47.300	24.000	70.000
35.000		36.000	48.300	25.000	71.100
36.000		38.000	48.300	27.000	72.100
37.000		47.000	48.300	28.000	72.100
38.000		49.000	48.300	30.000	74.100
39.000				32.000	75.600
40.000				36.000	78.200
41.000				38.000	78.700
42.000				40.000	79.700
43.000				42.000	80.200
44.000				44.000	80.700
45.000				46.000	81.200
45.500				48.500	82.200
46.000				54.000	83.200
47.000				86.000	85.200
48.000				92.000	85.200
				119.00	86.200

Raw data for Figure 4 27

Air Flow Rate ml s^{-1}	0 5 mg ml^{-1} BSA		1 0 mg ml^{-1} BSA	
	DIM	BIK	DIM	BIK
3 330	3 14	73 21	5 00	135 23
8 330*	8 36	80 33	15 05	142 70
16 670	15 52	73 59		

*** Sample Bikerman Foaminess and Dimensionless Foam Volume Calculation**
From Figure 4 26, at a flow rate of 8 33 ml s^{-1}, the average foam height was 48 3 cm The diameter of the column was 4 2 cm and therefore, the cross sectional area ($\prod D^2/4$) = 13 854 cm^2

Bikerman foaminess BIK was calculated as follows

BIK = Foam Volume/ Aeration rate = (13 854 cm^2 x 48 3 cm)/ 8 33 ml s^{-1} = 80 33 s

Dimensionless foam volume DIM was calculated as follows

DIM = Volume of Foam / Sample Volume = (13 854 cm^2 x 48 3 cm)/80 ml = 8 36

Raw data for Figure 4 28

Air Flow Rate 1 2 ml s^{-1}		Air Flow Rate 2 6 ml s^{-1}		Air Flow Rate 3 6 ml s^{-1}	
Minutes	Foam height (cm)	Minutes	Foam height (cm)	Minutes	Foam height (cm)
0 000	0 000	0 000	0 000	0 000	0 000
0 500	2 000	0 500	5 600	0 500	6 300
1 000	4 600	1 000	11 300	1 000	14 000
1 500	7 600	1 500	16 850	1 500	21 100
2 000	9 600	2 000	21 900	2 000	28 100
2 500	11 600	2 500	26 900	2 500	35 100
3 000	13 600	3 000	31 400	3 000	41 600
3 500	15 600	3 500	34 900	3 500	48 100
4 000	17 100	4 000	40 900	4 000	52 600
4 500	18 600	4 500	42 900	4 500	58 100
5 000	19 600	5 000	46 900	5 000	65 100
5 500	20 600	5 500	49 900	5 500	69 100
6 000	21 100	6 000	54 200	6 000	74 100
6 500	22 600	6 500	54 900	6 500	78 100
7 000	22 600	7 000	55 900	7 000	80 100
7 500	23 600	7 500	56 900	7 500	79 100
8 000	24 600	8 000	55 900	8 000	78 100
8 500	24 600	8 500	56 900	9 000	79 100
9 000	23 600	9 000	55 900	10 000	78 100
9 500	24 600				
10 000	24 600				

Raw data for Figures 4 29 and 4 30

BSA 1 0 mgml^{-1}			BSA 0 5 mgml^{-1}			BSA 0 2 mgml^{-1}			BSA 0 1 mgml^{-1}		
Flow Rate	BIK	DIM	Flow Rate	BIK	DIM	Flow Rate	BIK	DIM	Flow Rate	BIK	DIM
1 28	417 0	6 687	1 042	293 5	3 821	1 000	209 0	2 651	1 150	119 4	2 239
1 98	404 1	10 01	1 800	251 5	5 742	1 243	216 6	3 366	1 908	159 6	3 806
2 53	374 9	11 86	2 006	261 4	6 652	1 425	230 5	3 950	3 000	153 6	5 761
			2 380	275 5	8 194	1 933	195 2	4 716			
			2 650	283 5	9 388	2 233	190 1	5 600			
			3 660	261 7	11 97	2 392	218 2	6 522			
						2 833	226 4	8 000			

Raw data for Figure 4 31

BSA (mg ml^{-1})	BIK AV	DIM (2 0 ml s^{-1})	DIM (1 0 ml s^{-1})
0 100	158 000	3 810	2 239
0 200	210 000	4 716	2 651
0 500	279 330	6 190	3 820
1 000	407 000	10 010	6 680

Raw data for Figure 4 32

80 ml (BSA 0 5 mg ml^{-1})			50 ml (BSA 0 5 mg ml^{-1})		
Flow Rate (ml s^{-1})	BIK	DIM	Flow Rate (ml s^{-1})	BIK	DIM
1 042	293 5	3 821	1 000	172 605	3 440
1 800	251 5	5 742	1 650	185 340	5 866
2 006	261 4	6 652	2 700	188 309	9 805
2 380	275 5	8 194	3 250	189 243	11 000
2 650	283 5	9 388			
3 660	261 7	11 97			

Raw data for Figure 4 33

DAY	BIK	DIM
0	56 923	0 988
3	62 071	1 084
6	188 966	3 484
8	373 528	7 975
11	535 000	10 822
14	584 000	12 536
17	543 000	11 700
21	555 250	11 894

Raw data for Figure 4 34

DAY	BIK 1	BIK 2	BIK AV	BIK Dev	BIK Err
0	56 92269	9 5568	33 23975	33 49274	23 68295
3	62 07142	10 7514	36 41141	36 28873	25 66001
6	188 966	78 43744	133 7017	78 1555	55 26428
8	373 5275	282 3557	327 9416	64 46825	45 58594
11	535	650 021	592 5	81 31728	57 5
14	584	625	604 5	28 99138	20 5
17	543	590	566 5	33 23402	23 5
18		477 84	514 26	51 50566	36 42
21	555 25	455	505 125	70 88745	50 125

Raw data for Figure 4 35

DAY 0		DAY 3		DAY 6		DAY 8		DAY 11		DAY 14		DAY 17	
BIK	PH	BIK	PH	BIK	PH	BIK	PH	BIK	PH	BIK	PH	BIK	PH
91 0	4 00	82 7	4 00	220	6 00	391	6 00	573	4 00	642	4 00	768	4 00
56 9	5 48	62 7	4 48	228	5 00	373	4 91	535	5 11	584	5 32	550	5 13
35 0	6 00	60 0	6 00	189	4 02	477	4 00	480	6 00	388	6 00		

Raw data for Figures 4 36, 4 37, 4 38 and 4 39

DAY	BIK1	Protein 1	ECP 1	VIS 1	ST 1	BIK 2	ST 2
0	56 923	0 008	0 347	1 213	0 067	9 557	0 065
3	62 071	0 014	0 348	1 250	0 061	10 751	0 061
6	188 96	0 030	0 626	1 829	0 056	78 437	0 0555
8	373 52	0 057	1 224	3 250	0 056	282 35	
11	535 00	0 089	1 662	3 857	0 054	650 00	0 055
14	584 00	0 097	1 770	3 900	0 053	625 00	0 056
17	543 00	0 099	1 810	3 750	0 054	590	
18						477 84	0 056
21	555 25	0 098	1 780	3 800	0 058	455	

Raw data for Figure 4 40

BSA-MEDIUM		BSA-WATER	
BSA	BIK	BSA	BIK
0 00	42 408	0 000	0 000
0 05	245 000	0 100	158 000
0 10	398 495	0 200	210 000
0 15	621 670	0 500	279 330
0 20	969 633	1 000	407 000
		2 000	606 000

Raw data for Figure 4 41

BSA-0 02% XAN-MEDIUM		BSA-0 02% XAN-WATER	
BSA	BIK	BSA	BIK
0 000	7 168	0 000	0 000
3 133	421 515	0 100	143 352
6 974	605 144	0 150	285 000
10 230	832 397	0 200	437 224

Raw data for Figure 4 42

BSA-WATER		BSA-0 02% XAN-WATER	
BSA	BIK	BSA	BIK
0 000	0 000	0 000	0 000
0 100	143 352	0 100	158 000
0 150	285 000	0 200	210 000
0 200	437 224	0 500	279 330
		1 000	407 000

Raw data for Figure 4 43

0 2 BSA-XAN-WATER		0 1 BSA-XAN-MEDIUM	
XAN	BIK	XAN	BIK
0 000	182 774	0 000	398 000
0 010	216 520	0 005	488 114
0 015	295 320	0 010	571 497
0 020	459 060	0 015	721 180
0 030	720 000	0 020	832 000
0 040	1000 000	0 030	1000 000

Raw data for Figures 4 43, 4 44, 4 45, 4 46 and 4 47

DAY	CULTURES WITHOUT ANTIFOAM					CULTURES WITH ANTIFOAM				
	BIK	FW	DW	ECP	PROT	BIK	FW	DW	ECP	PROT
0	9 55	41 00	2 00	0 300	0 015	0 00	40 0	2 10	0 270	0 015
3	10 75	64 000	4 11	0 376	0 015	1 19	62 0	4 00	0 300	0 016
6	78 43	181 00	12 20	0 723	0 044	33 62	186	12 35	0 890	0 043
8	282 35	271 68	12 70	1 260	0 068	133 0	274	12 80	1 400	0 067
11	650 00	309 90	11 26	1 493	0 081	73 11	312	11 30	1 550	0 084
14	625 00	308 48	10 90	1 628	0 086	39 77	342	10 56	1 720	0 093
18	477 84	332 18	9 96	1 784	0 099	26 22	353	10 22	1 860	0 100
21	500 00	320 00	10 00			25 00	340	10 10		